

Electronic Thesis and Dissertation Repository

4-16-2011 12:00 AM

Late Pleistocene climate and proboscidean paleoecology in North America: Insights from stable isotope compositions of skeletal remains

Jessica Z. Metcalfe
The University of Western Ontario

Supervisor
Fred Longstaffe
The University of Western Ontario

Graduate Program in Geology
A thesis submitted in partial fulfillment of the requirements for the degree in Doctor of Philosophy
© Jessica Z. Metcalfe 2011

Follow this and additional works at: <https://ir.lib.uwo.ca/etd>



Part of the [Biogeochemistry Commons](#)

Recommended Citation

Metcalfe, Jessica Z., "Late Pleistocene climate and proboscidean paleoecology in North America: Insights from stable isotope compositions of skeletal remains" (2011). *Electronic Thesis and Dissertation Repository*. 194.
<https://ir.lib.uwo.ca/etd/194>

This Dissertation/Thesis is brought to you for free and open access by Scholarship@Western. It has been accepted for inclusion in Electronic Thesis and Dissertation Repository by an authorized administrator of Scholarship@Western. For more information, please contact wlsadmin@uwo.ca.

LATE PLEISTOCENE CLIMATE AND PROBOSCIDEAN PALEOECOLOGY IN
NORTH AMERICA: INSIGHTS FROM STABLE ISOTOPE COMPOSITIONS OF
SKELETAL REMAINS

(Spine title: Late Pleistocene climate and proboscidean paleoecology)

(Thesis format: Integrated Article)

by

Jessica Z. Metcalfe

Graduate Program in Geology & Environmental Science

A thesis submitted in partial fulfillment
of the requirements for the degree of
Doctor of Philosophy

The School of Graduate and Postdoctoral Studies
The University of Western Ontario
London, Ontario, Canada

© Jessica Z. Metcalfe 2011

THE UNIVERSITY OF WESTERN ONTARIO
School of Graduate and Postdoctoral Studies

CERTIFICATE OF EXAMINATION

Supervisor

Examiners

Dr. Fred Longstaffe

Dr. Jisuo Jin

Supervisory Committee

Dr. Burns Cheadle

Dr. Elizabeth Webb

Dr. Lisa Hodgetts

Dr. Chris Ellis

Dr. Henry Schwarcz

The thesis by

Jessica Zoe Metcalf

entitled:

**Late Pleistocene climate and proboscidean paleoecology in
North America: Insights from stable isotope compositions of
skeletal remains**

is accepted in partial fulfillment of the
requirements for the degree of
Doctor of Philosophy

Date

Chair of the Thesis Examination Board

Abstract

This thesis uses the carbon, nitrogen, and oxygen isotope compositions of mammoth (*Mammuthus*) and mastodon (*Mammut*) skeletal remains to reconstruct paleoclimate and paleoecology in Late Pleistocene North America. Analytical methods, sampling strategies, environmental adaptations and seasonal behaviors of proboscideans were investigated.

Reliable and reproducible results are crucial for a study of this nature. A persistent methodological problem in the isotope analysis of structural carbonate in bioapatite was solved by reacting bioapatite under “sealed vessel” conditions.

Growth rate determinations are critical for designing sampling strategies and interpreting results. Histological and isotopic measurements demonstrated variations in enamel growth rates within and among teeth. Sequentially sampling through the enamel thickness can resolve shorter-term (weekly) isotopic variations, and sampling along the tooth height (especially on the inner enamel surface) can resolve longer-term (monthly or yearly) variations.

Proboscideans adapted to the conditions of their local environments. Clovis-age mammoths in Arizona sought out C₄ grasslands that “greened up” as a result of summer rainfall. In C₃-dominated environments (Great Lakes and Western Canada), seasonal variations were larger in mastodons than mammoths, possibly because the latter exploited a greater number of microhabitats, averaging plant and drinking water isotopic compositions. Mammoths and mastodons occupied different environmental niches, but both consumed a wide range of resources and regional differences were evident. Woolly mammoths in Old Crow delayed the initiation of weaning relative to modern elephants, perhaps as a defensive adaptation to the increased predation risk and decreased food quality/quantity during long hours of winter darkness at this high latitude location. Potential consequences of delayed weaning, such as longer inter-birth intervals and greater maternal energy investments, may have increased the population’s vulnerability to climatic stress or human hunting.

Isotope results for Clovis mammoths in the San Pedro Valley are consistent with a relatively warm and dry climate, but do not indicate severe drought. Regional differences

in $\delta^{13}\text{C}$ values of proboscideans from C_3 -dominated environments were minimal, but variations in $\delta^{15}\text{N}$ may be related to spruce abundances and/or aridity. Latitudinal variations in proboscidean $\delta^{18}\text{O}$ values correlate well with modern meteoric water isotope compositions, which indicates their potential for reconstructing past paleoclimatic conditions.

Keywords: stable isotopes, mammoth, mastodon, *Mammuthus*, *Mammut*, proboscidean, Pleistocene, enamel, bone, dentin, cementum, environmental niche, seasonality, paleoclimate, paleoecology, Arizona, San Pedro Valley, Great Lakes, Ontario, New York, Alberta, Yukon, British Columbia

Co-Authorship Statement

Chapter 2 of this thesis was co-authored by Dr. Fred Longstaffe and Dr. Christine White, who provided funding for the project, contributed valuable advice throughout the research process, and reviewed and edited the manuscript.

Chapter 3 of this thesis was co-authored by Dr. Fred Longstaffe and Dr. Grant Zazula. Fred provided funding for J.Z.M. to travel to Yukon and obtain samples for this study, as well as funding for analytical costs, advice, data checking, scientific reviewing, and editing. Grant provided access to samples and background information, assisted with size measurements needed to characterize specimens, prepared a map, and participated in very helpful discussions.

Chapter 5 of this thesis has been reviewed by Dr. Jesse Ballenger and Dr. C. Vance Haynes, who provided helpful comments and clarification.

Chapter 7 of this thesis has been reviewed by Dr. Grant Zazula, who provided additional references and constructive criticism.

Dedication

with love,

to Grandma and Dziadzia,
who passed away during the making of this thesis,

and to Henry,
who was born.

Acknowledgements

Over the last five years I have had the privilege of meeting so many wonderful people, who have helped me in many ways.

To my supervisor, Fred – thank you for suggesting this project and encouraging me to make it my own. Your support – financial, personal, and professional – has made it a true pleasure to work at Western. I am constantly inspired by your dedication to your students, your incredible work ethic, and your enthusiasm for science. You are the best example I can imagine of what a mentor should be. This is not the end of our collaboration, but the start of a new chapter.

To my advisory committee, Liz Webb and Chris Ellis – thanks for helping me develop this project. Liz – you were always ready with great advice and enthusiasm. Chris – you helped move my project in exciting directions, through your encyclopaedic knowledge of Paleoindian archaeology and your suggestion to contact Vance Haynes. Many thanks!

To my examining committee, Henry Schwarcz, Lisa Hodgetts, Jisuo Jin, and Burns Cheadle – your careful reading of this thesis and insightful comments were much appreciated.

Sample collection was a major part of this project, and I am indebted to numerous individuals and institutions for providing specimens:

Great Lakes Region

Steve Hicock and Aleksis Dreimanis (University of Western Ontario), Robert Pearce (Musuem of Ontario Archaeology), Kevin Seymour, David Evans, and Brian Iwama (Royal Ontario Museum), and Dick Laub (Buffalo Museum of Science) – thank you for providing access to specimens. Thanks also to Dick for inviting me to the Byron Dig (2006-2007), which allowed me to get my hands dirty.

Western Canada

Grant Zazula – thank you for access to the Yukon Government collections, and for making my visit to Whitehorse so enjoyable... even though it was November! Your enthusiasm for Pleistocene research and breadth of interests are inspiring, and I greatly value our collaboration – I hope we meet again soon. Thanks also to Grant’s family (Vicky and Roman) for putting up with my visit, and to John Bailey, Bob Bailey, and Greg Hare, who helped me get initially get in touch with Grant. Alwynne Beaudoin, Chris Jass, Peter Milot, and Jim Burns (Royal Alberta Museum) – thank you for access to your collections, which helped get my project off the ground. It was great to meet you, and I hope we will work together again some day. Grant Keddie – thank you for access to specimens from the Royal British Columbia Museum.

Arizona

Vance Haynes – it has been a pleasure and privilege to work with you. Thanks for trusting me with the San Pedro Valley specimens, assisting in sampling, and taking me to the Murray Springs site. Your dedication to research is inspiring. Everett Lindsay, Mike Jacobs, and Alan Ferg – thank you allowing me access to the specimens. Jesse Ballenger – you are following in the tradition of Haynes; thanks for providing samples and for many helpful discussions. Greg Hodgins – thank you for welcoming me to the AMS lab and being a truly wonderful host. I had a fantastic time in Tucson, and I greatly value your ongoing collaboration and friendship. Thanks to all the staff and students of the AMS lab, especially Becky Watson, Stephanie Castle, Lori Hewitt, Alex Leonard, Richard Cruz, Todd Lange, Lizzy Enriquez, and Susana Gonzalez – you made my time there so very enjoyable. Barney Pavao-Zuckerman – I will never forget our tour of the Murray Springs site. I hope we are all as strong as Vance Haynes when we are 80! Thanks also to Chris Eastoe and David Dettman for helpful discussions.

To the staff, students and faculty of the Laboratory for Stable Isotope Science, past and present – too many to name! Kim Law, Li Huang, and Grace Yau – thanks for supporting the transformation of a general scientist/anthropologist into a stable isotopist,

and for your friendship over the years; you taught me so much and I am very grateful. Ayumi Hyodo, my “work spouse” – you kept me sane and inspired me not to be afraid new methods, but to plunge in and figure them out; I hope we are friends for life. Karyn Olsen, Zoe Morris, Duane Petts, Reba Macdonald, Sam Russell, Erin Fraser, Zhenzhen Huang, Emily Webb, Rachel Schwartz-Narbonne, Nicolle Bellissimo, Nadine Wakabayashi, Deana Schwarz, Andrea Prentice, Ryan Hladyniuk, Natasha Bumstead, Joanne Potter, Ian Power, Bhairavi Shankar – you made my PhD years so enjoyable; I have enjoyed sharing the ideas and the beers. Thanks to Gord Wood and Alexis Dolphin for help with thin section preparation and microscopy; Nelson Cho all his time-series analysis tutorials; Avner Ayalon and Bettina Schilman, for their advice and friendship; and Chris White, for getting me involved in isotopic research and supporting my transition to Earth Sciences. Thanks also to the staff, students, and faculty of the Environment and Sustainability collaborative program – you enriched my academic experience. My research benefited greatly from discussions with Jeff Saunders, Chris Widga, and Wendy Dirks. My PhD was funded in part by an NSERC Canada Government Scholarship, and awards from the Centre for Environment and Sustainability and Department of Earth Sciences. Thanks also to Frédéric Lacomat for arranging funding for travel costs to the Mammoth Conference in France.

Finally, thank you to my family, to whom I owe everything. My grandparents influenced my life in so many ways, and I am grateful that my thesis work allowed me to be close to them for a number of years. Thanks to my parents, for always supporting my quest for knowledge. Thanks to my parents-in-law, for making me a part of your family. Most of all, thanks to Slade, the “super-dad” whose long stroller walks, “alouettes”, and baby-soothing techniques were instrumental in allowing me to finish this thesis. You make each day a treasure – I love you.

Table of Contents

Title page	i
Certificate of Examination	ii
Abstract	iii
Keywords	iv
Co-authorship Statement	v
Dedication	vi
Acknowledgements	vii
Table of Contents	x
List of Tables	xvi
List of Figures	xviii
Chapter 1: Introduction	1
1.1 Background and Objectives	1
1.2 Skeletal Tissues	2
1.3 Stable Isotope Analysis	3
1.3.1 Carbon	4
1.3.2 Nitrogen	6
1.3.3 Oxygen	7
1.4 Proboscidean Evolution and Environments	7
1.5 Previous Isotopic Studies of Mammoths and Mastodons	9
1.5.1 Carbon	9
1.5.2 Nitrogen	10
1.5.3 Oxygen	11
1.5.4 Seasonal Variations	12
1.6 Samples	14
1.7 Structure of the Thesis	14
1.8 References	17
Chapter 2: Method-dependent variations in stable isotope results for structural carbonate in bone bioapatite	26
2.1 Introduction	26
2.2 Sample	27
2.3 Methods	28
2.3.1 Pretreatments	28
2.3.2 Isotopic Analyses	28
2.3.2.1 C25 (Conventional 25°C) Method	28
2.3.2.2 GB50 (GasBench 50°C) Method	29
2.3.2.3 MP90 (MultiPrep 90°C) Method	29
2.3.2.4 MP50, MP50-S, MP90-S Method	29
2.3.2.5 Phosphate Oxygen	29
2.3.3 Mass Scans	30
2.3.4 Light Microscopy and Scanning Electron Microscopy (SEM)	30
2.3.5 Fourier Transform Infrared Spectroscopy (FTIR)	30

2.3.6	X-Ray Diffraction (XRD)	31
2.3.7	Thermogravimetric Analysis (TGA)	31
2.3.8	Total Inorganic Carbon / Total Organic Carbon (TIC/TOC)	31
2.3.9	Nitrogen Content	32
2.3.10	Inductively-Coupled Plasma Atomic Emission Spectroscopy (ICP-AES)	32
2.4	Results	32
2.4.1	Carbon Isotope Analyses	32
2.4.2	Oxygen Isotope Analyses (Structural Carbonate)	33
2.4.3	Pretreatment Effects	33
2.4.4	“Anomalous” Isotope Values	35
2.4.5	Contaminant Gas	35
2.4.6	Temperature Dependence	37
2.4.7	“Sealed” vs. “Open” Reaction Vessels	37
2.4.8	Gas Yields	37
2.4.9	Phosphate Oxygen Isotope Values	38
2.4.10	Light Microscopy and Scanning Electron Microscopy (SEM)	39
2.4.11	Fourier Transform Infrared Spectroscopy (FTIR)	41
2.4.12	X-Ray Diffraction (XRD)	43
2.4.13	Thermogravimetric Analysis (TGA)	45
2.4.14	Total Inorganic Carbon / Total Organic Carbon (TIC/TOC)	46
2.4.15	Nitrogen Content	46
2.4.16	Inductively-Coupled Plasma Atomic Emission Spectroscopy (ICP-AES)	47
2.5	Discussion	47
2.5.1	What Was the Contaminant Gas, and What Was its Relationship to Low $\delta^{18}\text{O}$ Values?	47
2.5.2	What Was Different about the “Anomalous” Bones?	50
2.5.3	Method-Dependent Differences for “Normal” Bones	51
2.6	Conclusions	51
2.7	References	53
Chapter 3: Nursing, weaning, and tooth development in woolly mammoths from Old Crow, Yukon, Canada: Implications for Pleistocene extinctions		56
3.1	Introduction	56
3.1.1	Elephant Nursing and Weaning	57
3.1.2	Stable Isotopes and Nursing/Weaning	58
3.1.2.1	Carbon	58
3.1.2.2	Nitrogen	60
3.1.2.2	Oxygen	61
3.1.3	Trace Elements and Nursing/Weaning	61
3.1.4	Elephant Tooth Formation	62
3.2	Materials and Methods	66
3.2.1	Study Area	66
3.2.2	Samples	66
3.2.3	Radiocarbon Dating	67

3.2.4	Stable Isotopes	67
3.2.4.1	Collagen	70
3.2.4.2	Carbonate	71
3.2.5	Trace/Major Elements	72
3.2.6	Statistics	73
3.3	Results and Interpretations	73
3.3.1	Carbon and Nitrogen in Collagen	73
3.3.2	Carbon and Oxygen in Structural Carbonate	77
3.3.3	Trace/Major Elements	79
3.4	Discussion	80
3.5	Conclusion	86
3.6	References	88
 Chapter 4: Mammoth tooth enamel growth rates inferred from stable isotope analysis and histology: Implications for sampling methodologies		 96
4.1	Introduction	96
4.2	Enamel Formation	98
4.3	Methods	100
4.3.1	Sampling from intact specimens	100
4.3.2	Histology	100
4.3.2.1	“Thin” Section Preparation	100
4.3.2.2	Extension Rate	101
4.3.2.2.1	Cross-Striation Interval (d)	102
4.3.2.2.2	Striae of Retzius – EDJ Angle (D)	102
4.3.2.2.3	Enamel Prism – EDJ Angle (I)	102
4.3.2.3	Enamel Thickness Growth Rate	103
4.3.3	Stable Isotope Analysis	103
4.3.3.1	Preparation and Sampling (IES and ET)	103
4.3.3.2	Analysis	105
4.3.3.3	Extension Rate Estimates	105
4.4	Results	105
4.4.1	Diagenesis	105
4.4.2	Inner Enamel Surface (IES)	106
4.4.2.1	Histology	106
4.4.2.2	Stable Isotopes	106
4.4.3	Enamel Thickness (ET)	108
4.4.3.1	Histology	108
4.4.3.2	Stable Isotopes	108
4.5	Discussion	108
4.5.1	Extension Rate (IES Sampling)	108
4.5.2	Enamel Thickness Growth Rate (ET Sampling)	109
4.6	Conclusions	110
4.7	References	111

Chapter 5: Stable isotope records of climate, diet, and seasonality from “bulk” and inner enamel “incremental” sampling of mammoth tooth enamel, San Pedro Valley, Arizona	115
5.1 Introduction	115
5.1.1 Study Area and Samples	116
5.1.2 Oxygen Isotopes and Climate	119
5.1.3 Carbon Isotopes and Vegetation	121
5.1.4 Seasonality and Elephant Behavior	123
5.1.5 Clovis Drought	124
5.2 Materials and Methods	125
5.2.1 Sampling	125
5.2.2 Carbonate Pretreatment and Stable Isotope Analysis	128
5.2.2.1 Open vs. Sealed Vessel Analyses	128
5.2.3 Diet $\delta^{13}\text{C}$ and $\%C_4$ Calculations	129
5.2.4 Drinking Water $\delta^{18}\text{O}$ Value Calculations	129
5.2.5 Incremental Samples: Data Transformations	130
5.3 Results	132
5.3.1 Diagenesis	132
5.3.2 Bulk Carbonate	133
5.3.3 Incremental Carbonate	133
5.4 Discussion	141
5.4.1 Comparison of “Bulk” and “Incremental” Stable Isotope Results	141
5.4.2 Bulk Carbonate	143
5.4.3 Incremental Carbonate	144
5.4.3.1 Clovis Mammoths	144
5.4.3.2 Pre-LGM Mammoths	148
5.4.4 Migration	149
5.4.5 Double Adobe	150
5.4.6 The Naco Mammoth: Escape from Lehner?	150
5.4.7 Eloise: The Last Mammoth at Murray Springs	150
5.4.8 Clovis Drought	151
5.4.9 Implications for Clovis Hunting and Extinction	152
5.5 Conclusions	153
5.6 References	155
Chapter 6: Isotopic paleoecology of mammoths and mastodons in the Great Lakes region (southern Ontario and western New York)	160
6.1 Introduction	160
6.2 Methods	161
6.3 Results and Discussion	166
6.3.1 Radiocarbon Dating	166
6.3.2 Structural Carbonate Analysis Pretreatment Effects	166
6.3.3 Diagenesis	166
6.3.4 Tissue Comparisons	167
6.3.5 Non-Local Individuals and Outliers	170

6.3.6	Isotopic Partitioning between Mammoths and Mastodons	172
6.3.6.1	Oxygen	172
6.3.6.2	Carbon	174
6.3.6.3	Nitrogen	175
6.3.7	Comparison of “Bulk” and “Serially-Sampled” Isotopic Results	177
6.3.8	Serially-Sampled Enamel: Regular Periodicity	183
6.3.9	Serially-Sampled Enamel: Isotopic Composition of Diet and Drinking Water	184
6.3.10	Serially-Sampled Enamel: Seasonal Patterns	184
6.3.11	Hypotheses: Seasonal Variations in Mammoth Diet and Drinking Water	190
6.4	Conclusions	190
6.5	References	193
Chapter 7: Paleoclimate and paleoenvironment of Pleistocene Western Canada (Yukon, Alberta, British Columbia) inferred from mammoth and mastodon skeletal remains		201
7.1	Introduction	201
7.1.1	Late Pleistocene Environments in Yukon, Alberta, and British Columbia	202
7.2	Materials and Methods	205
7.3	Results and Discussion	209
7.3.1	Radiocarbon Dating	209
7.3.2	Pretreatment Effects on Structural Carbonate Analysis	210
7.3.3	Diagenesis	211
7.3.4	Tissue Comparisons (Collagen)	218
7.3.5	Isotopic Partitioning between Mammoths and Mastodons: Paleoecological Implications	218
7.3.6	Nutritional Stress and $\delta^{15}\text{N}$ values	223
7.3.7	Regional Comparisons	224
7.3.8	Temporal Trends	230
7.3.9	Comparison of “Bulk” and “Incremental” Isotope Results	230
7.3.10	Serially-Sampled Enamel: Regular Periodicity	231
7.3.11	Serially-Sampled Enamel: Seasonal Patterns	240
7.3.12	Serially-Sampled Enamel: Isotopic Compositions of Diet and Drinking Water	240
7.3.13	Mammoth and Mastodon Seasonal Behaviour	243
7.3.14	Use of Isotopes for Geographic Sourcing and Taxonomic Determination	245
7.4	Conclusions	246
7.5	References	250
Chapter 8: General Discussion and Conclusions		260
8.1	Methodological Developments and Challenges	260
8.1.1	Analysis of Structural Carbonate in Bioapatite	260

8.1.2 Enamel Growth Rate	261
8.1.3 Incremental Sampling of Proboscidean Enamel	262
8.2 Mammoth and Mastodon Environmental Adaptations and Niche Partitioning	263
8.3 Seasonality of Proboscidean Drinking Water and Diet	265
8.4 Mammoths and Mastodons as Paleoenvironmental Proxies	266
8.5 Concluding Remarks	271
8.6 References	272
Appendix A: Copyright Release	274
Curriculum Vitae	275

List of Tables

2.1	Mean carbon and oxygen isotope results for archaeological bone after weak (WP) and strong pretreatments (SP) using analytical methods (C24, GB50, MP50, MP50-S, MP90-S, MP90-S*) described in the text	34
2.2	Total inorganic carbon (TIC), total organic carbon (TOC), calcium, phosphorus, and trace element contents of “anomalous” (B25, B21) and “normal” bones (B5, NK356)	46
2.3	Selected compounds with mass to charge ratios (m/z) of 44 or 47	48
3.1	Timing of tooth formation and wear in modern African elephants (<i>Loxodonta africana</i>), based on Laws (1966)	64
3.2	Sample information and tooth measurements for Old Crow mammoths	68
3.3	The isotopic composition of collagen (various tissues) and structural carbonate (enamel), and the trace/major element contents of enamel for Old Crow mammoths	76
Supp.	Details of sampling location for each specimen	87
5.1	Specimen information and context	118
5.2	Stable isotope results for “bulk” analyses, and their corresponding diet and drinking water compositions	127
5.3	Stable isotope results for “incremental” analyses, and their corresponding diet and drinking water compositions	134
5.4	Periods of the isotope curves for serially-sampled mammoth enamel	141
5.5	Summary of stable isotope results for “incremental” analyses, and corresponding diet and drinking water compositions	145
6.1	Sample information, including radiocarbon data	163
6.2	The isotopic compositions of collagen (various tissues) and structural carbonate in bioapatite (enamel) for Great Lakes mammoths and mastodons	164
6.3	Relationships between metabolic, vegetational, and climatic factors and the $\delta^{13}\text{C}$ values of animals living in C_3 -only environments	169
6.4	Relationships between metabolic, vegetational, and environmental factors and the $\delta^{15}\text{N}$ values of animals living in C_3 environments	176
6.5	Stable isotope compositions from serial sampling, and associated diet and drinking water compositions	178
6.6	Periods of the isotope curves for serially-sampled mastodon enamel	182
6.7	Histological measurements from photomicrographs of mastodon enamel from ON5	182
6.8	Summary of isotopic results for incrementally sampled Great Lakes mastodons	188
7.1	Sample information	207
7.2	The isotopic compositions of collagen (various tissues) and structural carbonate in bioapatite (enamel) for Western Canada mammoths and mastodons	212

7.3	Comparison of the “mean annual” and “seasonal extreme” isotopic compositions of drinking water (calculated from proboscidean enamel) with the weighted mean annual and seasonal extreme isotopic compositions of modern meteoric water at locations of similar latitude	227
7.4	Stable isotope compositions from “incremental” sampling, and their conversions to diet and drinking water compositions	232
7.5	Summary of isotopic results for incrementally sampled Western Canada mastodons and mammoths	239

List of Figures

2.1	Carbon and oxygen isotope results obtained from individual analyses of “anomalous” sample B21-WP, grouped by temperature of reaction	36
2.2	Mass scans of gas produced by reaction of specimen B21-WP with ortho-phosphoric acid using different methods	36
2.3	Oxygen isotope results obtained for phosphate and structural carbonate (C25 method) for Guatemala and Sudan bones using the weak pretreatment (WP)	38
2.4	Optical photomicrographs taken in transmitted light from transverse sections of bone, 70-100 μm thick (a-b), and SEM photomicrographs of bone surfaces (c-d)	40
2.5	FTIR spectra of “anomalous” bones B25-WP (1) and B21-WP (2), and “normal” bones B5-WP (3) and NK356-WP (4)	42
2.6	XRD patterns of “anomalous” bone samples B25-WP (1) and B21-WP (2), and “normal” bone samples B5-WP (3) and NK356-WP (4)	44
2.7	Thermogravimetric analysis of “anomalous” (B25-WP, B21-WP) and “normal” bones (B5-WP, NK356-WP)	45
3.1	Map of the Yukon Territory, including the location of specimen collection sites on the Old Crow River (asterisk)	65
3.2	Selected woolly mammoth teeth analyzed in this study	69
3.3	Comparison of the size of teeth used in this study (individual points) to the ranges reported in the literature (boxes)	70
3.4	(a) The collagen $\delta^{13}\text{C}$ and $\delta^{15}\text{N}$ values of individual Old Crow mammoths, organized by age category and tissue type. (b) The enamel structural carbonate $\delta^{13}\text{C}$ and $\delta^{18}\text{O}$ values of individual mammoths, organized by age category	74
3.5	Age category comparisons for stable isotope and trace/major element data	78
4.1	(a) Proboscidean tooth morphology. (b) Growth geometry of sectioned enamel	97
4.2	Thin section images for enamel from AZ1 (Eloise), taken in plane-polarized (a, c, d) and cross-polarized light (b)	101
4.3	Carbon and oxygen isotope results for AZ1 obtained using IES (a) and ET (b) sampling strategies, as described in the text	107
5.1	Map of the San Pedro Valley, showing the locations where mammoth specimens utilized in this study were found	117
5.2	“Incrementally sampled” specimens (a) AZ1 (Eloise), (b) AZ10 (Naco), (c) AZ5 (Lehner), (d) AZ11 (Murray Springs, Pre-LGM), (e) AZ14 (Moson Wash, Pre-LGM), (f) AZ13 (Horsethief Draw Loc. 129)	126
5.3	Carbon and oxygen isotope results obtained for “bulk” samples of SPV mammoth tooth enamel	132
5.4	Carbon and oxygen isotope results for “incremental” sampling of Clovis-age and pre-LGM mammoths from the SPV	140
5.5	Comparison of carbon and oxygen isotope results for “incremental” sampling of Clovis-age (a, b) and pre-LGM (c, d) mammoths from the SPV	146

5.6	Comparison of seasonal extremes in the $\delta^{18}\text{O}$ values of mammoth drinking water to the $\delta^{18}\text{O}$ values of seasonal precipitation in the modern SPV and Tucson, and the $\delta^{18}\text{O}$ values of modern SPV perennial water sources	147
6.1	The discovery locations of mastodon (closed circle) and mammoth (open square) specimens analyzed in the present study	162
6.2	Carbon and nitrogen isotope results obtained for collagen from various mammoth and mastodon tissues	168
6.3	Carbon and oxygen isotope results obtained for structural carbonate in enamel bioapatite from mammoths and mastodon	171
6.4	Carbon and oxygen isotope results for serial sampling of inner enamel from Great Lakes mastodons	181
6.5	Thin section images for enamel from ON5, taken in plane-polarized light	182
6.6	Comparison of carbon and oxygen isotope results for serial sampling of inner enamel from Great Lakes mastodons	189
7.1	Locations of origin for specimens discussed in this study	206
7.2	Carbon and nitrogen isotope results obtained for collagen from mammoths (open symbols) and mastodons (closed black symbols) from (a) British Columbia, (b) Alberta, (c) Klondike, (d) Old Crow, and (e) Herschel Island	216
7.3	Carbon and nitrogen isotope compositions of collagen for (a) mastodons and (b) mammoths from Western Canada	217
7.4	Carbon and oxygen isotope results obtained for structural carbonate in enamel bioapatite from mammoths (open symbols) and mastodons (closed symbols)	220
7.5	Comparison of the mean oxygen isotope compositions of Pleistocene drinking water and modern meteoric water at “nearby” locations (see text)	228
7.6	Temporal trends in isotopic compositions of Klondike proboscideans	229
7.7	Carbon and oxygen isotope results for serial sampling of inner enamel from Western Canada mastodons	237
7.8	Carbon and oxygen isotope results for serial sampling of inner enamel from Western Canada mammoths	238
7.9	Comparison of carbon and oxygen isotope results for serial sampling of inner enamel from Western Canada proboscideans	241
8.1	Carbon isotope compositions obtained from collagen (a) and structural carbonate (b) for mammoths and mastodons from the Great Lakes, Alberta, and Yukon Territory	267
8.2	Nitrogen isotope compositions obtained from collagen for mammoths and mastodons from the Great Lakes, Alberta, and Yukon Territory	268
8.3	Oxygen isotope compositions obtained from enamel structural carbonate for mammoths and mastodons from the Great Lakes, Alberta, and Yukon Territory	269
8.4	Comparison of the oxygen isotope compositions of Pleistocene drinking water calculated from proboscidean enamel and the weighted mean annual oxygen isotope compositions of precipitation from “nearby” locations	270

Chapter 1

Introduction

1.1 Background and Objectives

This thesis focuses on reconstructing Pleistocene paleoclimate and paleoecology using the carbon, nitrogen, and oxygen isotope compositions of proboscidean (mammoth, *Mammuthus*; and mastodon, *Mammut*) bone, enamel, dentin, and cementum. Mammoths and mastodons were once widespread in North America, but became extinct throughout most of the continent at the end of the Pleistocene (ca. 11,000-10,000 BP) (Agenbroad, 2005; Waters and Stafford, 2007). Explanations for Late Pleistocene megafaunal extinctions have been vigorously debated for decades. Most researchers argue that climate change and/or human hunting were the decisive factors, but there is still no general consensus (Barnosky et al., 2004; Haynes, 2009; Koch and Barnosky, 2006). Despite the importance of mammoths and mastodons in the debate, relatively little is known about differences in their diets and habitats within or among regions. The overall goals of this thesis are to improve our understanding of the isotopic records of paleoecological and paleoclimatic conditions preserved in proboscidean skeletal remains, and to use these records to investigate variability in Pleistocene environments and the paleoecology of mammoths and mastodons in North America. The specific goals of this research are to (1) ensure that reliable isotopic measurements can be obtained from skeletal tissues, (2) explore sampling strategies for reconstructing seasonal changes in proboscidean diet and drinking water, (3) reconstruct proboscidean diets, including short-term (seasonal) variations, long-term (“bulk” isotopic) averages, age-related shifts (i.e., as a result of nursing and weaning, or the timing of formation of different tissues), temporal variations, and geographical differences, (4) determine the isotopic composition of proboscidean drinking water, including seasonal changes and regional variations, and to explore their paleoclimatic implications, and (5) compare and contrast mammoth and mastodon palaeoecology within and among regions. This introductory chapter provides a brief background to the structure and chemistry of skeletal tissues (Section 1.2), stable carbon, nitrogen, and oxygen isotope analysis (Section 1.3), proboscidean evolution and environments (Section 1.4), and previous isotopic studies of mammoths and mastodons

(Section 1.5). It also provides an overview of the samples used (Section 1.6), and the structure of the thesis (Section 1.7).

1.2 Skeletal Tissues

Bone, enamel, and dentin are skeletal tissues comprised of organic and inorganic components. The ratio of organic to inorganic to water (by weight) in “fresh” tissues is 25:65:10 in bone, 2:96:2 in enamel, and 20:70:10 in dentin (LeGeros, 1991). The main inorganic component of bone, enamel, and dentin is biological apatite (bioapatite), which is a calcium phosphate mineral with a hexagonal unit cell (Posner, 1985). The composition of bioapatite differs within and among calcified tissues, and is not fully understood. In general, bioapatite is non-homogeneous, non-stoichiometric, nanocrystalline, and contains numerous minor and trace elements that are substituted into the structure, adsorbed onto the bioapatite surface, and/or present in inclusions of non-apatite phases (LeGeros, 1991; Wopenka and Pasteris, 2005). Bioapatite crystals are extremely small, resembling plates in bone and dentin, and long ribbons in enamel (Ten Cate and Nanci, 2003; Wopenka and Pasteris, 2005). Biological apatite is often “idealized” as hydroxyapatite [$\text{Ca}_{10}(\text{PO}_4)_6(\text{OH})_2$], but in reality has numerous ionic substitutions that are not present in pure hydroxyapatite (Elliott, 2002). The most important substitution for stable isotope studies is the carbonate ion (CO_3^{2-}), which comprises about 3.5% by weight in enamel, 5.6% in dentin, and 7.4% in bone (LeGeros, 1991). The majority of carbonate ions are substituted in the phosphate site (B-type substitution), but can also exist in the hydroxyl site (A-type substitution) or be adsorbed onto the crystal surface (Elliott, 2002). In stable isotope studies of carbonate in bioapatite, acid treatment is typically used to remove diagenetic carbonates, so that only structural carbonate is analyzed.

About 85% of bone organic material is type I collagen, and the rest is non-collagenous structural matrix proteins (Nanci et al., 2003). Collagen fibrils provide a structure with holes, pores, and surfaces for the deposition of bioapatite crystals (Ten Cate and Nanci, 2003). In bone, the organic and inorganic components are intimately associated, and both are continually remodelled by specialized cells that destroy and re-

form them as part of normal maintenance. Consequently, bone provides an isotopic record corresponding to the last several years of an individual's life (Manolagas, 2000).

Dentin is similar to bone in both structure and composition, but is slightly harder. Like bone, most of the organic phase of dentin is type I collagen, and the collagen fibrils provide a matrix for bioapatite deposition. Dentin is permeated by dentinal tubules, which contain the odontoblast processes that originally formed the dentin, and can diffuse nutrients and deposit new dentin in response to injury (Nanci, 2003a). The organic matrix is deposited in increments at a rate of about 4 μ m per day, and bioapatite deposition occurs after a slight delay (Nanci, 2003a). Unlike bone, dentin is not continuously remodelled (Ten Cate and Nanci, 2003), so its isotopic composition reflects conditions during the time of tooth formation.

Unlike bone and dentin, the organic component of mature enamel is entirely non-collagenous, primarily amelogenins (Ten Cate and Nanci, 2003), and is such a minor component that isotopic studies have not been attempted. Enamel formation is a two-step process. First, an organic-rich, partially (~30%) mineralized enamel is deposited. Second, additional mineral is deposited while organic material and water are simultaneously removed, producing a mature tissue comprised of 97% bioapatite by weight (Nanci, 2003b). The second step involves three stages, which result in a vertical (occlusal to basal) and horizontal (enamel-dentin junction to outer surface) gradient in enamel mineralization (Kohn et al., 2002; Suga, 1982; Zazzo et al., 2005). These patterns facilitate micro-sampling to obtain a record of isotopic changes over time (Zazzo et al., 2006).

1.3 Stable Isotope Analysis

Isotopes are atoms with the same number of protons and electrons but different numbers of neutrons, and therefore different atomic weights. The mass differences between isotopes of the same element cause them to have slightly different bond energies and reaction kinetics. As a result, isotopes fractionate (i.e. separate into different fractions) in predictable ways. Fractionation can occur under equilibrium conditions (e.g. high temperature or long-term processes) or under non-equilibrium conditions (e.g. diffusion, evaporation, kinetic effects, metabolic effects) (Criss, 1999). In both cases,

light isotopes of a given element generally react faster than the heavy isotopes of that element, causing the latter to remain in the more stable phase.

Stable isotopes do not decay over time, and thus the isotopic composition of a substance (e.g., bone) provides information about conditions that existed when the substance formed, as long as isotopic alteration has not occurred. Isotopic compositions are calculated using the measured ratio of heavy to light isotopes in the sample relative to the ratio of heavy to light isotopes in a universally accepted standard reference material. This is expressed as a delta (δ) value, in units of permil (‰, parts per thousand) according to the formula given by McKinney et al. (1950):

$$\delta (\text{‰}) = [(R_{\text{sample}}/ R_{\text{standard}}) - 1] \times 1000, \quad [\text{Equation 1.1}]$$

where R = heavy/light isotope of a given element.

1.3.1 Carbon

The $\delta^{13}\text{C}$ values of animal tissues are derived from the $\delta^{13}\text{C}$ values of the foods consumed by the animal. Plants are located at the base of the food chain, and discriminate against ^{13}C in favour of ^{12}C , so their $\delta^{13}\text{C}$ values are lower than those of their carbon source. Most terrestrial plants use photosynthesis to fix atmospheric CO_2 , which had a $\delta^{13}\text{C}$ value of about -8‰ in 1989, and is currently decreasing as a result of fossil fuel combustion (Marino and McElroy, 1991). The degree to which photosynthetic plants discriminate against ^{13}C depends on their photosynthetic pathway: C_3 (Calvin Cycle), C_4 (Hatch-Slack Cycle), or CAM (Crassulacean Acid Metabolism). C_3 plants (most trees and shrubs) produce a 3-carbon molecule in photosynthesis and discriminate the most against ^{13}C , such that their mean $\delta^{13}\text{C}$ value is -26.5‰ (O'Leary, 1988; Smith and Epstein, 1971). C_4 plants (most tropical grasses) produce a 4-carbon molecule in photosynthesis and have a mean $\delta^{13}\text{C}$ value of -12.5‰ (O'Leary, 1988; Smith and Epstein, 1971). Terrestrial C_3 and C_4 plants do not have overlapping $\delta^{13}\text{C}$ values. CAM plants (cacti and succulents) have a wide range of $\delta^{13}\text{C}$ values that overlaps those of both C_3 and C_4 plants, but they are typically restricted to tropical deserts and are not likely to be a major food source for proboscideans in North America.

Small variations in the $\delta^{13}\text{C}$ values of plants can be caused by variations in water availability, salinity, light levels, and degree of canopy cover (Kohn and Cerling, 2002).

Specifically, ^{13}C depletion is associated with lower levels of light, more canopy cover, and lower salinity (Farquhar et al., 1989). Drought conditions tend to cause ^{13}C enrichment, although the effects can be large (e.g., some succulents can change their metabolic pathway from C_3 to CAM, resulting in a ^{13}C enrichment of up to 15‰) (Farquhar et al., 1989) or small (e.g., the leaves, roots, and stems of European beech seedlings exposed to an experimentally-induced 3-week drought were enriched in ^{13}C by less than 1‰ relative to control samples) (Peuke et al., 2006; Peuke et al., 2002).

There is a fractionation between the $\delta^{13}\text{C}$ value of the food an organism consumes and its tissues. Structural carbonate (sc) $\delta^{13}\text{C}$ values reflect the total macronutrient content of the diet. The enrichment of $\delta^{13}\text{C}_{\text{sc}}$ relative to $\delta^{13}\text{C}_{\text{diet}}$ ($\Delta^{13}\text{C}_{\text{sc-diet}} = \delta^{13}\text{C}_{\text{sc}} - \delta^{13}\text{C}_{\text{diet}}$) ranges from about 9 to 14‰, and may be species-dependent (Ambrose and Norr, 1993; Cerling and Harris, 1999; Tieszen and Fagre, 1993). Cerling et al. (1997) reported $\alpha_{\text{enamel-diet}}$ values of 1.0143 to 1.0148 [where $\alpha = (1000 + \delta^{13}\text{C}_{\text{enamel}})/(1000 + \delta^{13}\text{C}_{\text{diet}})$] for wild and captive large mammals (mostly ruminants, but including two elephants). Subsequently, Cerling and Harris (1999) reported a ^{13}C enrichment factor [$\epsilon^* = 1 - \alpha^*$] of $14.1 \pm 0.5\%$, or an $\alpha_{\text{enamel-diet}}$ of 1.0141 for large-bodied ungulates. In a controlled feeding study, Passey et al. (2005) found that ϵ^* values varied by more than 5% among species, with the largest values in steers ($14.6 \pm 0.3\%$) and pigs ($13.3 \pm 0.3\%$), and the smallest values in mice ($9.1 \pm 1.6\%$).

The difference between collagen and diet $\delta^{13}\text{C}$ values ($\Delta^{13}\text{C}_{\text{col-diet}}$) can also vary considerably (Ambrose and Norr, 1993; Tieszen and Fagre, 1993). In part, this is because a large proportion of carbon in collagen is derived directly from the protein component of the diet rather than the whole diet (Howland et al., 2003; Schwarcz, 2000). Ambrose and Norr (1993) reviewed the $\Delta^{13}\text{C}_{\text{col-diet}}$ values obtained in numerous studies and concluded that they are higher in large wild mammals than in small mammals. Large herbivorous mammals that consume predominantly C_3 or C_4 diets (including elephants) have $\Delta^{13}\text{C}_{\text{col-diet}}$ values of a relatively constant 5.5‰ (Sullivan and Krueger, 1981; van der Merwe, 1989; Vogel et al., 1990). Since the fractionations between tissues and dietary components can be estimated, the $\delta^{13}\text{C}$ values in collagen and bioapatite can be used to identify large changes in vegetation (C_3 to C_4), changes in the diet of the animal, and/or smaller variations in local climate.

1.3.2 Nitrogen

Most plants obtain nitrogen from dissolved nitrates (NO_3^-), ammonia (NH_3), and ammonium (NH_4^+) in soil water, freshwater, or the ocean. Terrestrial plant $\delta^{15}\text{N}$ values typically range from -5 to $+2\text{‰}$ (Fry, 1991). However, plants that have symbiotic relationships with nitrogen-fixing bacteria obtain nitrogen directly from atmospheric or dissolved N_2 , and are depleted of ^{15}N relative to other plants (Koch et al., 1994). In addition, different components of plants (e.g. leaves, seeds) can have large difference in $\delta^{15}\text{N}$ values (Hedges et al., 2004).

Animals obtain nitrogen from their diet. Bone collagen is enriched in ^{15}N relative to plants and is further enriched with each step up the food chain (or trophic level) within a given ecosystem. The average trophic-level enrichment is about 3‰ , but can vary with species and diet (Bocherens and Drucker, 2003; Koch et al., 1994; Sponheimer et al., 2003a). Variations in mammalian $\delta^{15}\text{N}$ values can also be caused by stress, pathology, metabolism, infant feeding, and climate (Ambrose, 1993; Sare et al., 2005; Sponheimer et al., 2003b; White and Armelagos, 1997; Williams et al., 2005). The significant differences in nitrogen metabolism among species require that comparisons of temporal or geographical changes be species-specific (Grocke et al., 1997).

Climate also causes variations in $\delta^{15}\text{N}$ values. In general, hotter, drier, more saline soils produce plants with higher $\delta^{15}\text{N}$ values than cooler, wetter, less saline soils (Ambrose, 1993). However, experimental studies on beech trees and barley plants have not shown such increases in response to drought stress (Peuke et al., 2006; Robinson et al., 2000), which suggests that drought response depends on the plant species. Nevertheless, animals living in hot, dry environments (where less water is available) tend to have higher $\delta^{15}\text{N}$ values than the same animals living in cooler, drier environments (Ambrose, 1993; Schwarcz et al., 1999). This likely results from both metabolic changes in response to changes in water availability (e.g. changes in nitrogen cycling and urea concentration) and changes in the nitrogen isotope composition of individual plants (Ambrose, 1993; Hedges et al., 2004).

1.3.3 Oxygen

Stable oxygen isotope compositions of skeletal materials can be measured using either the phosphate or structural carbonate component of bioapatite. In thermoregulating terrestrial vertebrates (i.e., animals with constant body temperatures), bone and enamel phosphate oxygen ($\delta^{18}\text{O}_p$) is in isotopic equilibrium with body water oxygen (Longinelli, 1984; Luz et al., 1984). In well-preserved bone and enamel the stable oxygen isotope composition of structural carbonate ($\delta^{18}\text{O}_{sc}$) is correlated with $\delta^{18}\text{O}_p$ (Bryant et al., 1996; Iacumin et al., 1996), which indicates that structural carbonate oxygen is also in isotopic equilibrium with body water. The $\delta^{18}\text{O}$ value of an animal's body water is determined by its physiological balance of oxygen inputs (i.e., drinking water, liquid water in plants, metabolic oxygen derived from food, and atmospheric oxygen) and outputs (i.e., liquid – urine, fecal water, sweat; transcutaneous water vapour; and expired CO_2), whose proportions may differ among species (Bryant and Froelich, 1995; Kohn and Cerling, 2002). Despite these many variables, body water $\delta^{18}\text{O}$ values are linearly related to drinking water $\delta^{18}\text{O}$ values (Ayliffe et al., 1992; Longinelli, 1984; Luz et al., 1984). If drinking water is primarily derived from precipitation, bioapatite $\delta^{18}\text{O}$ values can be used to reconstruct meteoric water $\delta^{18}\text{O}$ values. Large-bodied obligate drinkers, such as elephants, record the $\delta^{18}\text{O}$ values of surface (meteoric) waters much better than smaller or drought-tolerant animals (Bryant and Froelich, 1995; Levin et al., 2006). Meteoric water $\delta^{18}\text{O}$ values ($\delta^{18}\text{O}_{mw}$) vary geographically as a result of latitude, altitude, distance from the coast, amount of precipitation, and surface air temperature (Dansgaard, 1964). The best correlations between $\delta^{18}\text{O}_{mw}$ and temperature occur in mid- to high-latitude continental regions (Hoefs, 2004).

1.4 Proboscidean Evolution and Environments

The Mammutidae (mastodon family) and Elephantidae (modern elephant and mammoth family) diverged at the end of the Oligocene or the beginning of the Miocene (ca. 27-23 Ma) (Agenbroad, 2005). Early members of the family Mammutidae entered North America from Eurasia during the middle Miocene (ca. 15.5 Ma) (Saunders, 1996). The American mastodon (*Mammut americanum*) evolved in North America, and the earliest known specimen is from south-central Washington, ca. 3.75 Ma (Dudley, 1996;

Webb, 1992). Mastodon remains have been found throughout North America, but are most common in the east, particularly in the Great Lakes region at the end of the Pleistocene (Dreimanis, 1968; Haynes, 1991; Saunders, 1996). Mastodon remains are associated with coniferous forests, particularly those dominated by spruce, as well as bogs, ponds, and marshes (Haynes, 1991; Newsom and Mithlacher, 2006; Saunders, 1996). In combination with evidence from tooth morphology, tooth enamel isotopic compositions, enamel microwear, and gut/fecal contents, this suggests that mastodons were primarily browsers that inhabited relatively wet, forested environments (Green et al., 2005; Harington and Ashworth, 1986; Koch et al., 1998; Lepper et al., 1991; MacFadden and Cerling, 1996; Newsom and Mithlacher, 2006). However, tooth enamel isotopic analysis and phytoliths in dental calculus also suggest that mastodons consumed some grasses (Gobet and Bozarth, 2001; Koch et al., 1998).

Although there is some taxonomic confusion, most researchers agree that the first mammoths in North America (*Mammuthus trogontherii* or *Mammuthus meridionalis*) entered via Beringia around 2 million years ago (Agenbroad, 2005; Debruyne et al., 2008; Dudley, 1996). Woolly mammoths (*Mammuthus primigenius*) are thought to have evolved in Siberia and entered North America around 200,000 BP, but interaction between the populations continued intermittently throughout the Pleistocene, including a replacement or succession of western Beringian populations during the Terminal Pleistocene by populations originating in North America (Debruyne et al., 2008; Lister et al., 2005). Woolly mammoth remains are typically found at northern latitudes, but have been discovered as far as 200 km south of the Wisconsin ice sheets in North America (Agenbroad, 2005). They are associated with cold, arid, open steppe-tundra environments, and were primarily grazers, though they also consumed woody plants and mosses (Guthrie, 2001; Haynes, 1991; van Geel et al., 2008).

Columbian mammoths (*Mammuthus columbi*) evolved in North America, and were common throughout the continental United States, especially in temperate grassland areas (Agenbroad, 2005). However, specimens have also been discovered as far north as Alberta and Eastern Beringia (Burns, 2010). Some researchers recognize an additional species, *Mammuthus jeffersoni* (Kurten and Anderson, 1980; Saunders et al., 2010), but others do not consider it to be separate from *M. columbi* (Agenbroad, 2005; Maglio,

1973). Studies of tooth enamel isotopic compositions (Feranec, 2004; Hoppe, 2004; Koch et al., 1998), enamel microwear (Green et al., 2005), fecal remains (Mead et al., 1986), and tooth phytoliths (Cummings and Albert, 2007) indicate that Columbian mammoths were predominantly grazers, but also consumed a variety of forbs, shrubs, and woody plants (Haynes, 1991).

Like mammoths, modern elephants (*Elephas* and *Loxodonta*) have teeth that are adapted for grazing, and stable isotope studies suggest that their ancestors were C₄ grazers (Cerling et al., 1999). However, most elephants today are mixed feeders (i.e., they consume both browse and graze) in a variety of different environments (Cerling et al., 1999; Codron et al., 2006; Sukumar, 1989), which suggests that their tooth morphology may permit grazing, but does not require it (Haynes, 1991). Like modern elephants, mammoths and mastodons were apparently capable of significant dietary flexibility. Reconstruction of mammoth and mastodon diets and environmental niches in a variety of geographic locations is important, since vegetational shifts are a key component of many climate-change theories of megafaunal extinction (e.g., Graham and Lundelius, 1984; Guthrie, 1984; Kuzmin, 2010).

1.5 Previous Isotopic Studies of Mammoth and Mastodons

1.5.1 Carbon

The use of stable isotopes to quantify the proportion of grass versus browse in the diets of animals living in mixed C₃-C₄ environments is well-established. For example, mammoths from the southern and central United States (New Mexico, Colorado, Texas, and Florida) consumed diets that were predominantly C₄ (grasses), but contained variable amounts of C₃ plants (trees and shrubs) (Feranec, 2004; Hoppe, 2004; Koch et al., 2004; MacFadden and Cerling, 1996). In one of the only studies to directly compare mammoth and mastodon diets, Koch et al. (1998) found that Florida mastodons consumed more C₃ plants, whereas mammoths consumed more C₄ plants (grasses) and had more variable diets. Numerous studies have shown that in more northern areas (e.g., the northern United States, Switzerland, Belgium, Finland, Sweden, the Russian Plains, Siberia, Alaska, and Yukon) mammoths and/or mastodons had $\delta^{13}\text{C}$ values that indicate pure C₃ plant

consumption, which reflects the lack of C₄ plants in these environments (Arppe and Karhu, 2006; Bocherens et al., 1996, 1997; Coltrain et al., 2004; Fisher and Fox, 2003; France et al., 2007; Hoyle et al., 2004; Iacumin et al., 2000, 2005, 2006; Koch, 1991; Saunders et al., 2010; Szpak et al., 2010; Tutken et al., 2007; Ukkonen et al., 2007). In C₃ environments, mammoths sometimes have lower $\delta^{13}\text{C}$ values than co-existing herbivores, which has been attributed to the metabolism of stored fats (Bocherens, 2003; Bocherens et al., 1996, 1997; Iacumin et al., 2000). However, not all studies have reported such a difference (Fox-Dobbs et al., 2008; France et al., 2007). Mastodon $\delta^{13}\text{C}$ values in C₃-dominated environments are not consistently different from those of mammoths or other co-existing herbivores (Coltrain et al., 2004; France et al., 2007; Koch, 1991).

Carbon isotope compositions of mammoth tissues have also been used to infer temporal and geographical changes in climate and vegetation. For example, Koch et al. (2004) compared %C₄ values derived from herbivore (including mammoth) tooth enamel to the predictions for %C₄ made using a global climate model, and concluded that low atmospheric CO₂ levels were partially responsible for the persistence of C₄ plants in Texas throughout most of the Quaternary. Iacumin et al. (2005) inferred from mammoth hair that the mean plant $\delta^{13}\text{C}$ values in Siberia around 40,000 to 50,000 years ago were about 2‰ higher than modern values, indicating environmental change. Szpak et al. (2010) suggest that lower $\delta^{13}\text{C}_{\text{col}}$ values in mammoths from eastern than western Beringia, particularly during the Last Glacial Maximum, were related to increased metabolism of stored fats in very cold and dry environments. In Europe, Arppe et al. (in press) found that mammoth $\delta^{13}\text{C}_{\text{sc}}$ values decreased from southwest to northeast, arguably because of colder and wetter conditions in the latter region. However, because there are many climatic, vegetational, and physiological factors that can change the $\delta^{13}\text{C}$ values of animals living in C₃ environments, these interpretations are far from straightforward.

1.5.2 Nitrogen

Early studies from Alaska, Alberta, and Russia found that mammoth $\delta^{15}\text{N}$ values were so much higher than those of contemporary herbivores (i.e., 6 to 12‰) that they actually resembled those of carnivores (Bocherens et al., 1994, 1996). Subsequent studies have confirmed that mammoths typically have high $\delta^{15}\text{N}$ values: 4.5 to 12‰ in Russia

(Iacumin et al., 2000, 2010), 4.4 to 9.7‰ in Alaska-Yukon (Bocherens, 2003; Fox-Dobbs et al., 2008; Szpak et al., 2010), 7.5 to 11.4‰ in Siberia (Bocherens, 2003; Szpak et al., 2010), 8.3 to 9.4‰ in Belgium (Bocherens et al., 1997) and 7.6 ± 0.9 ‰ in Michigan, Ohio, Indiana, and New York (Koch, 1991). The $\delta^{15}\text{N}$ values of mammoths in Russia tend to increase from the southwest to the northeast, which could result from regional differences in climate, plant consumption, and plant availability (Iacumin et al., 2000). Regional variations in mammoth $\delta^{15}\text{N}$ values may be attributable primarily to climatic differences, with higher $\delta^{15}\text{N}$ values in more arid locations and time periods (Iacumin et al., 2006; Szpak et al., 2010). Although the sample sizes are small, several studies have shown that mammoth $\delta^{15}\text{N}$ values decreased during or just after the LGM (Iacumin et al., 2000, 2010; Szpak et al., 2010), perhaps as a result of the changing climate. In contrast to the relatively high $\delta^{15}\text{N}$ values of mammoth tissues, mastodon bone and dentin tend to have lower $\delta^{15}\text{N}$ values: 1.0 to 4.5‰ at the Hiscock site in New York (Fisher and Fox, 2003), 3.9 ± 1.0 ‰ in Michigan, Ohio, Indiana, and New York (Koch, 1991), 4.2 to 5.1‰ at Rancho La Brea, California (Coltrain et al., 2004), and 2.5 to 3.6 in Virginia (France et al., 2007). These lower values are typically attributed to consumption of nitrogen-fixing plant taxa.

1.5.3 Oxygen

Ayliffe et al. (1992, 1994) were the first to demonstrate that the $\delta^{18}\text{O}$ values of proboscidean tooth enamel were lower during glacial than interglacial periods, as expected based on meteoric water $\delta^{18}\text{O}$ values. Moreover, they showed that the $\delta^{18}\text{O}$ values of ancient drinking water can potentially be determined by applying the modern $\delta^{18}\text{O}_p - \delta^{18}\text{O}_{\text{mw}}$ relationship derived for elephants to extinct proboscideans. Since then, this approach has been used to reconstruct drinking water $\delta^{18}\text{O}$ values for mammoths in Sweden, Finland, Switzerland, Ukraine, Russia, and Siberia (Arppe and Karhu, 2006, 2010; Genoni et al., 1998; Iacumin et al., 2010; Tutken et al., 2007; Ukkonen et al., 2007). Some studies have also used modern relationships between meteoric water and ambient temperature to estimate Pleistocene temperatures (Arppe and Karhu, 2006, 2010; Tutken et al., 2007; Ukkonen et al., 2007). However, even assuming that mammoths drank primarily meteoric water, the relationship between temperature and $\delta^{18}\text{O}_{\text{mw}}$ is not

always straightforward. For example, Iacumin et al. (2010) found that $\delta^{18}\text{O}_{\text{mw}}$ values calculated from mammoth bones were higher during a stadial than during an interstadial period, contrary to expectations based on temperature alone; they suggest that aridity may have been to blame.

Recently, geographical variations in the $\delta^{18}\text{O}$ values of meteoric water have also been examined using mammoth skeletal remains. Fox et al. (2007) found that the longitudinal gradient of $\delta^{18}\text{O}$ values from woolly mammoth tusks in northern Russia is similar to the modern meteoric water $\delta^{18}\text{O}$ gradient, which indicates that moisture transport across the continent, and its effect on meteoric water $\delta^{18}\text{O}$ values, was similar during the Pleistocene and today. Arppe and Karhu (2010) reconstructed the $\delta^{18}\text{O}$ values of precipitation across Europe at 52,000 - 24,000 BP using mammoth tooth enamel and paleogroundwater data. They also concluded that atmospheric circulation patterns were similar to modern, but that $\delta^{18}\text{O}_{\text{mw}}$ values and temperatures were lower than at present. Taking a different approach, Kohn and McKay (2010) showed that the $\delta^{18}\text{O}$ values of large mammals (including mammoths) from the southern United States validate global circulation models that predict an increased proportion of winter precipitation (low $\delta^{18}\text{O}$) in the central United States, and increased summer precipitation (high $\delta^{18}\text{O}$) in the southern United States, during the LGM.

1.5.4 Seasonal Variations

Several studies have investigated seasonal variations in mammoth and mastodon diet and drinking water using stable isotopes. Most studies to date have used dentin, which has the advantage of containing both bioapatite and collagen, but the disadvantage of poorer bioapatite preservation relative to enamel (Ayliffe et al., 1994). In their pioneering study, Koch et al. (1989) found regular periodic variations in the $\delta^{18}\text{O}_{\text{sc}}$ values of proboscidean tusk dentin, with ^{18}O -depletions of 5-9‰ in slow-growth areas. This was interpreted as a winter (temperature-related) lowering of the $\delta^{18}\text{O}$ values of ingested precipitation. A sinusoidal pattern for $\delta^{18}\text{O}$ values was also observed in a woolly mammoth tusk from Maine (Hoyle et al., 2004) and Columbian mammoth tusks and molar dentin from Colorado (Fisher and Fox, 2007). However, in a study of four mastodon tusks from New York, some of the samples showed the pattern of seasonal

variation expected for meteoric water (higher $\delta^{18}\text{O}$ values in summer, lower in winter), but others showed the opposite trend (Fisher and Fox, 2003). In addition, patterns for $\delta^{13}\text{C}_{\text{sc}}$, $\delta^{13}\text{C}_{\text{col}}$, and $\delta^{15}\text{N}$ values from the same tusks did not correspond to consistent seasons either within or among individuals. Fox et al. (2007) found that proboscidean tusks from the Taimyr Peninsula in northern Russia did not exhibit coherent patterns of seasonal variation in $\delta^{18}\text{O}$ values. Tusks from Chukotka tended to have the highest $\delta^{18}\text{O}$ values during later winter (the opposite of the typical seasonal pattern for meteoric water $\delta^{18}\text{O}$), and Holocene tusks from Wrangel Island followed two patterns, (1) somewhat irregular variations with high values typically occurring during summer but with occasional low values obscuring the seasonal pattern, and (2) the same “inverse” pattern as in the Chukotka specimens (Fox et al., 2007). Fox et al. (2007) argue that the latter pattern for Chukotka and Wrangel Island specimens resulted from (1) the contribution of high- ^{18}O northern Pacific and Arctic moisture sources to winter precipitation, and (2) the effects of low- ^{18}O winter snow melt and increased surface evaporation during summer, which would yield recycled moisture with relatively low $\delta^{18}\text{O}$ values.

Studies of seasonal variations in $\delta^{13}\text{C}$ and $\delta^{15}\text{N}$ values have also been conducted using mammoth hair. Iacumin et al. (2005) found an inverse relationship between $\delta^{13}\text{C}$ and $\delta^{15}\text{N}$ values in mammoth hair from northern Siberia, and hypothesized that high $\delta^{15}\text{N}$ and low $\delta^{13}\text{C}$ values represent winter growth (based on the lower $\delta^{13}\text{C}$ values of modern plants during winter, and the slower growth rate for regions of the hair with low $\delta^{13}\text{C}$ values). For additional northern Siberian samples, Iacumin et al. (2006) report “quasi-sinusoidal” patterns with a lack of correlation between $\delta^{13}\text{C}$ and $\delta^{15}\text{N}$, but the relationship is difficult to interpret since the results from each individual are not plotted together. In contrast, Rountrey et al. (2007) found that the peaks and valleys for $\delta^{13}\text{C}_{\text{col}}$ and $\delta^{15}\text{N}$ coincided in a juvenile woolly mammoth tusk from Wrangel Island. They argued that the pattern reflected changes in the relative proportion of plant proteins to milk in the diet, with more plant consumption (and lower δ -values) occurring during the growing season.

Few studies have examined seasonal variations in proboscidean molar tooth enamel. Koch et al. (1998) found that low $\delta^{18}\text{O}_{\text{sc}}$ values in a Florida mammoth specimen corresponded to slow-growth periods, and probably represented winter growth. In addition, there was a trend towards increasing $\delta^{18}\text{O}$ values later in the animal’s life, but

virtually no variation in $\delta^{13}\text{C}_{\text{sc}}$ values. Feranec and MacFadden (2000) serially sampled four mammoth tooth enamel specimens (as well as horse and bison) from Florida. For all species, there appeared to be a generally positive relationship between $\delta^{13}\text{C}_{\text{sc}}$ and $\delta^{18}\text{O}_{\text{sc}}$ values. Although the authors discuss their results primarily in relation to niche partitioning, the data may also indicate an increase in C_4 grasses in the diet during summers and/or warmer years. To our knowledge, no studies of serially-sampled proboscidean enamel from C_3 -dominated environments have been published.

1.6 Samples

Specimens used for the methodological study of bone bioapatite (Chapter 2) were obtained from archaeological sites in Sudan and Guatemala as part of the research program of Dr. Christine White (Anthropology, The University of Western Ontario), and were incorporated into this study because the methodological problems associated with their analysis had been observed in a variety of other specimens, including mammoths and mastodons. Specimens used for the remainder of the research are proboscidean skeletal remains (bone, enamel, dentin, and cementum) that were collected by the author from various North American museums and universities, between 2006 and 2009 (see Chapters 3 to 7 for details). These specimens represent individuals from five regions of North America: Arizona, the Great Lakes (Ontario and New York), Alberta, British Columbia, and Yukon. The time periods represented range from before the Last Glacial Maximum (most Alberta, British Columbia, and Yukon specimens) to the Terminal Pleistocene, just prior to mammoth and mastodon extinction (Arizona and Great Lakes specimens).

All dates in this thesis are reported as conventional radiocarbon years before AD 1950, in the form “17,000 \pm 100 BP” (mean \pm 1 SD), except when citing literature that reported only calibrated (“cal”) dates. In the latter cases, the dates are reported in the form “17,000 cal BP.”

1.7 Structure of the Thesis

This work is divided into six “results” chapters, written as independent research articles intended for publication (or already published) in peer-reviewed journals. As

such, each chapter includes a description of the samples studied, methods used, and interpretive considerations, as well as results, interpretations, and conclusions.

Chapter 2, published in the *Journal of Archaeological Science* (Metcalf et al., 2009), addresses a methodological problem in the C- and O-isotope analysis of structural carbonate in bone bioapatite. Although this study utilized human bone samples, the results presented in subsequent chapters indicate that a similar problem also occurs when analyzing mammoth and mastodon bone, dentin, and even some enamel samples. Thus, solving this problem was critical for producing the reliable and reproducible results necessary for making paleoenvironmental interpretations in subsequent chapters.

Chapter 3, published in *Palaeogeography, Palaeoclimatology, Palaeoecology* (Metcalf et al., 2010) investigates evidence for the timing of nursing and weaning in woolly mammoths using C-, N- and O- isotopes and Sr/Ca and Ba/Ca ratios. Nursing and weaning are important ecological behaviours that influence the health, growth, and survival of infants, and hence, of populations. We constrain the timing of nursing and weaning in a population of woolly mammoths that lived north of the Arctic Circle, and suggest hypotheses to explain why delayed weaning may have been adaptive, but may also have had implications for mammoth extinction.

Chapter 4 investigates the duration and rate of formation of proboscidean molar tooth enamel in two dimensions, using a combination of stable C- and O- isotope analysis and histological measurements. Growth rate estimates obtained from this study were used to structure sampling methodologies for the rest of the thesis, and aided in interpreting the isotope values obtained from serially-sampled tooth enamel.

Chapter 5 investigates the climate, diet, and seasonality of Columbian mammoths in the San Pedro Valley, Arizona using C- and O- isotope compositions of enamel bioapatite. The mammoths included in this study lived in a mixed C₃-C₄ environment, and some of them were certainly hunted or scavenged by Clovis people around 10,900 BP. The study compares the isotopic compositions of Clovis-associated mammoths, “Clovis-age” mammoths, and pre-Clovis mammoths, to provide insights into mammoth and Clovis ecology and foraging behaviour.

Chapter 6 compares mammoth and mastodon environmental niche partitioning in the Great Lakes region (southern Ontario and western New York) using C-, N-, and O-

isotope compositions of bones and teeth (collagen and bioapatite). These proboscideans lived in C₃-dominated environments during the postglacial period (ca. 15,500 to 10,000 BP), a time of rapid environmental change. This chapter investigates similarities and differences in the isotopic compositions of mammoths and mastodons in relation to their diet, drinking water, metabolism, and seasonal behaviour, and explores the use of stable isotope compositions to identify non-local individuals in museum collections.

Chapter 7 investigates mammoth and mastodon paleoecology, regional variations, and temporal trends for Western Canada (Alberta, British Columbia, and Yukon) using C-, N-, and O-isotope compositions of bones and teeth (collagen and bioapatite). The specimens used in this study lived in C₃-dominated environments and pre-date the Last Glacial Maximum (i.e., >17,000 BP). Isotopic analyses presented in this study provide unique insights into environmental conditions, including short-term variations (i.e., monthly, yearly) which are difficult to resolve using more “traditional” environmental proxies.

Chapter 8 provides a summary of the results presented in the preceding chapters, and discusses their broader implications.

1.8 References

- Agenbroad, L.D., 2005. North American proboscideans: Mammoths - the state of knowledge, 2003. *Quaternary International*, 126-28: 73-92.
- Ambrose, S.H., 1993. Isotopic analysis of paleodiets: methodological and interpretive considerations. In: M.K. Sandford (Editor), *Investigations of Ancient Human Tissue: Chemical Analyses in Anthropology*. Gordon and Breach Science Publishers, Langhorne, PA, pp. 59-130.
- Ambrose, S.H. and Norr, L., 1993. Experimental evidence for the relationship of the carbon isotope ratios of whole diet and dietary protein to those of bone collagen and carbonate. In: J.B. Lambert and G. Grupe (Editors), *Prehistoric Human Bone: Archaeology at the Molecular Level*. Springer-Verlag, Berlin, pp. 1-37.
- Arppe, L., Aaris-Sørensen, K., Daugnora, L., Lõugas, L., Wojtal, P. and Zupins, I., in press. The palaeoenvironmental $\delta^{13}\text{C}$ record in European woolly mammoth tooth enamel. *Quaternary International*, In Press, Corrected Proof.
- Arppe, L. and Karhu, J.A., 2006. Implications for the Late Pleistocene climate in Finland and adjacent areas from the isotopic composition of mammoth skeletal remains. *Palaeogeography Palaeoclimatology Palaeoecology*, 231(3-4): 322-330.
- Arppe, L. and Karhu, J.A., 2010. Oxygen isotope values of precipitation and the thermal climate in Europe during the middle to late Weichselian ice age. *Quaternary Science Reviews*, 29(9-10): 1263-1275.
- Ayliffe, L.K., Chivas, A.R. and Leakey, M.G., 1994. The retention of primary oxygen-isotope compositions of fossil elephant skeletal phosphate. *Geochimica et Cosmochimica Acta*, 58(23): 5291-5298.
- Ayliffe, L.K., Lister, A.M. and Chivas, A.R., 1992. The preservation of glacial-interglacial climatic signatures in the oxygen isotopes of elephant skeletal phosphate. *Palaeogeography Palaeoclimatology Palaeoecology*, 99(3-4): 179-191.
- Barnosky, A.D., Koch, P.L., Feranec, R.S., Wing, S.L. and Shabel, A.B., 2004. Assessing the causes of Late Pleistocene extinctions on the continents. *Science*, 306(5693): 70-75.
- Bocherens, H., 2003. Isotopic biogeochemistry and the paleoecology of the mammoth steppe fauna. *Deinsea*, 9: 57-71.
- Bocherens, H., Billiou, D., Patou-Mathis, M., Bonjean, D., Otte, M. and Mariotti, A., 1997. Paleobiological implications of the isotopic signatures (^{13}C , ^{15}N) of fossil mammal collagen in Scladina cave (Sclayn, Belgium). *Quaternary Research*, 48(3): 370-380.
- Bocherens, H. and Drucker, D., 2003. Trophic level isotopic enrichment of carbon and nitrogen in bone collagen: Case studies from recent and ancient terrestrial ecosystems. *International Journal of Osteoarchaeology*, 13(1-2): 46-53.
- Bocherens, H., Fizet, M., Mariotti, A., Gangloff, R.A. and Burns, J.A., 1994. Contribution of isotopic biogeochemistry (^{13}C , ^{15}N , ^{18}O) to the paleoecology of mammoths (*Mammuthus primigenius*). *Historical Biology*, 7(3): 187-202.
- Bocherens, H., Pacaud, G., Lazarev, P.A. and Mariotti, A., 1996. Stable isotope abundances (^{13}C , ^{15}N) in collagen and soft tissues from Pleistocene mammals from Yakutia: Implications for the palaeobiology of the Mammoth Steppe. *Palaeogeography Palaeoclimatology Palaeoecology*, 126(1-2): 31-44.

- Bryant, J.D. and Froelich, P.N., 1995. A model of oxygen-isotope fractionation in body-water of large mammals. *Geochimica et Cosmochimica Acta*, 59(21): 4523-4537.
- Bryant, J.D., Koch, P., Froelich, P.N., Showers, W.J. and Genna, B.J., 1996. Oxygen isotope partitioning between phosphate and carbonate in mammalian apatite. *Geochimica et Cosmochimica Acta*, 60(24): 5145-5148.
- Burns, J.A., 2010. Mammalian faunal dynamics in Late Pleistocene Alberta, Canada. *Quaternary International*, 217(1-2): 37-42.
- Cerling, T.E. and Harris, J.M., 1999. Carbon isotope fractionation between diet and bioapatite in ungulate mammals and implications for ecological and paleoecological studies. *Oecologia*, 120(3): 347-363.
- Cerling, T.E., Harris, J.M. and Leakey, M.G., 1999. Browsing and grazing in elephants: the isotope record of modern and fossil proboscideans. *Oecologia*, 120: 364-374.
- Cerling, T.E., Harris, J.M., MacFadden, B.J., Leakey, M.G., Quade, J., Eisenmann, V. and Ehleringer, J.R., 1997. Global vegetation change through the Miocene/Pliocene boundary. *Nature*, 389(6647): 153-158.
- Codron, J., Lee-Thorp, J.A., Sponheimer, M., Codron, D., Grant, R.C. and de Ruiter, D.J., 2006. Elephant (*Loxodonta africana*) diets in Kruger National Park, South Africa: spatial and landscape differences. *Journal of Mammalogy*, 87(1): 27-34.
- Coltrain, J.B., Harris, J.M., Cerling, T.E., Ehleringer, J.R., Dearing, M.D., Ward, J. and Allen, J., 2004. Rancho La Brea stable isotope biogeochemistry and its implications for the palaeoecology of late Pleistocene, coastal southern California. *Palaeogeography Palaeoclimatology Palaeoecology*, 205(3-4): 199-219.
- Criss, R.E., 1999. *Principles of Stable Isotope Distribution*. Oxford University Press, New York, 254 pp.
- Cummings, L.S. and Albert, R.M., 2007. Phytolith and starch analysis of Dent site mammoth teeth calculus: new evidence for Late Pleistocene mammoth diets and environments. In: R.H. Brunswig and B.L. Pitblado (Editors), *Frontiers in Colorado Paleoindian Archaeology: From the Dent Site to the Rocky Mountains*. University Press of Colorado, Boulder, pp. 185-192.
- Dansgaard, W., 1964. Stable isotopes in precipitation. *Tellus*, 16: 436-468.
- Debruyne, R., Chu, G., King, C.E., Bos, K., Kuch, M., Schwarz, C., Szpak, P., Grocke, D.R., Matheus, P., Zazula, G., Guthrie, D., Froese, D., Buigues, B., de Marliave, C., Flemming, C., Poinar, D., Fisher, D., Southon, J., Tikhonov, A.N., MacPhee, R.D.E. and Poinar, H.N., 2008. Out of America: Ancient DNA evidence for a New World origin of Late Quaternary woolly mammoths. *Current Biology*, 18(17): 1320-1326.
- Dreimanis, A., 1968. Extinction of mastodons in eastern North America: testing a new climatic-environmental hypothesis. *The Ohio Journal of Science*, 68(6): 337-352.
- Dudley, J.P., 1996. Mammoths, gomphotheres, and the Great American Faunal Interchange. In: J. Shoshani and P. Tassy (Editors), *The Proboscidea: Evolution and Palaeoecology of Elephants and their Relatives*. Oxford University Press, Oxford, pp. 289-295.
- Elliott, J.C., 2002. Calcium phosphate biominerals. In: M.J. Kohn, J. Rakovan and J.M. Hughes (Editors), *Phosphates: Geochemical, Geobiological, and Materials Importance*. Reviews in Mineralogy and Geochemistry. Mineralogical Society of America, Washington, D.C., pp. 427-453.

- Farquhar, G.D., Ehleringer, J.R. and Hubick, K.T., 1989. Carbon isotope discrimination and photosynthesis. *Annual Review of Plant Physiology and Plant Molecular Biology*, 40: 503-537.
- Feranec, R.S., 2004. Geographic variation in the diet of hypsodont herbivores from the Rancholabrean of Florida. *Palaeogeography Palaeoclimatology Palaeoecology*, 207(3-4): 359-369.
- Feranec, R.S. and MacFadden, K.B.J., 2000. Evolution of the grazing niche in Pleistocene mammals from Florida: evidence from stable isotopes. *Palaeogeography Palaeoclimatology Palaeoecology*, 162(1-2): 155-169.
- Fisher, D.C. and Fox, D.L., 2003. Season of death and terminal growth histories of Hiscock mastodons. In: R.S. Laub (Editor), *The Hiscock Site: Late Pleistocene and Holocene Paleoecology and Archaeology of Western New York State: Proceedings of the Second Smith Symposium, held at the Buffalo Museum of Science, October 14-15, 2001*. Buffalo Society of Natural Sciences, Buffalo, pp. 83-101.
- Fisher, D.C. and Fox, D.L., 2007. Season of death of the Dent mammoths: Distinguishing single from multiple mortality events. In: R.H. Brunswig and B.L. Pitblado (Editors), *Frontiers in Colorado Paleoindian archaeology: From the Dent site to the Rocky Mountains*. University Press of Colorado, Boulder, pp. 123-153.
- Fox-Dobbs, K., Leonard, J.A. and Koch, P.L., 2008. Pleistocene megafauna from eastern Beringia: Paleoecological and paleoenvironmental interpretations of stable carbon and nitrogen isotope and radiocarbon records. *Palaeogeography Palaeoclimatology Palaeoecology*, 261(1-2): 30-46.
- Fox, D.L., Fisher, D.C., Vartanyan, S., Tikhonov, A.N., Mol, D. and Buigues, B., 2007. Paleoclimatic implications of oxygen isotopic variation in late Pleistocene and Holocene tusks of *Mammuthus primigenius* from northern Eurasia. *Quaternary International*, 169: 154-165.
- France, C.A.M., Zelanko, P.M., Kaufman, A.J. and Holtz, T.R., 2007. Carbon and nitrogen isotopic analysis of Pleistocene mammals from the Saltville Quarry (Virginia, USA): Implications for trophic relationships. *Palaeogeography Palaeoclimatology Palaeoecology*, 249(3-4): 271-282.
- Fry, B., 1991. Stable isotope diagrams of fresh-water food webs. *Ecology*, 72(6): 2293-2297.
- Genoni, L., Iacumin, P., Nikolaev, V., Gribchenko, Y. and Longinelli, A., 1998. Oxygen isotope measurements of mammoth and reindeer skeletal remains: an archive of Late Pleistocene environmental conditions in Eurasian Arctic. *Earth and Planetary Science Letters*, 160(3-4): 587-592.
- Gobetz, K.E. and Bozarth, S.R., 2001. Implications for late Pleistocene mastodon diet from opal phytoliths in tooth calculus. *Quaternary Research*, 55(2): 115-122.
- Graham, R.W. and Lundelius, E.L.J., 1984. Coevolutionary disequilibrium and Pleistocene extinctions. In: P.S. Martin and R.G. Klein (Editors), *Quaternary extinctions: A prehistoric revolution*. University of Arizona Press, Tucson, pp. 211-222.
- Green, J.L., Semprebon, G.M. and Solounias, N., 2005. Reconstructing the palaeodiet of Florida *Mammot americanum* via low-magnification stereomicroscopy. *Palaeogeography Palaeoclimatology Palaeoecology*, 223(1-2): 34-48.

- Grocke, D.R., Bocherens, H. and Mariotti, A., 1997. Annual rainfall and nitrogen-isotope correlation in macropod collagen: application as a palaeoprecipitation indicator. *Earth and Planetary Science Letters*, 153(3-4): 279-285.
- Guthrie, R.D., 1984. Mosaics, alleochemicals, and nutrients: An ecological theory of late Pleistocene megafaunal extinctions. In: P.S. Martin and R.G. Klein (Editors), *Quaternary extinctions: A prehistoric revolution*. University of Arizona Press, Tucson, pp. 259-298.
- Guthrie, R.D., 2001. Origin and causes of the mammoth steppe: a story of cloud cover, woolly mammal tooth pits, buckles, and inside-out Beringia. *Quaternary Science Reviews*, 20(1-3): 549-574.
- Harington, C.R. and Ashworth, A.C., 1986. A mammoth (*Mammuthus primigenius*) tooth from Late Wisconsin deposits near Embden, North-Dakota, and comments on the distribution of woolly mammoths south of the Wisconsin ice sheets. *Canadian Journal of Earth Sciences*, 23(7): 909-918.
- Haynes, G., 1991. *Mammoths, mastodonts, and elephants: biology, behavior, and the fossil record*. Cambridge University Press, Cambridge New York, 413 pp.
- Haynes, G., 2009. Introduction to the volume. In: G. Haynes (Editor), *American megafaunal extinctions at the end of the Pleistocene*. Vertebrate Paleobiology and Paleoanthropology Series. Springer, Netherlands, pp. 1-20.
- Hedges, R.E.M., Stevens, R.E. and Richards, M.P., 2004. Bone as a stable isotope archive for local climatic information. *Quaternary Science Reviews*, 23(7-8): 959-965.
- Hoefs, J., 2004. *Stable Isotope Geochemistry*. Springer, Berlin ; New York, 244 pp.
- Hoppe, K.A., 2004. Late Pleistocene mammoth herd structure, migration patterns, and Clovis hunting strategies inferred from isotopic analyses of multiple death assemblages. *Paleobiology*, 30(1): 129-145.
- Howland, M.R., Corr, L.T., Young, S.M.M., Jones, V., Jim, S., Van der Merwe, N.J., Mitchell, A.D. and Evershed, R.P., 2003. Expression of the dietary isotope signal in the compound-specific $\delta^{13}\text{C}$ values of pig bone lipids and amino acids. *International Journal of Osteoarchaeology*, 13(1-2): 54-65.
- Hoyle, B.G., Fisher, D.C., Borns, H.W., Churchill-Dickson, L.L., Dorion, C.C. and Weddle, T.K., 2004. Late Pleistocene mammoth remains from Coastal Maine, USA. *Quaternary Research*, 61(3): 277-288.
- Iacumin, P., Bocherens, H., Mariotti, A. and Longinelli, A., 1996. Oxygen isotope analyses of co-existing carbonate and phosphate in biogenic apatite: a way to monitor diagenetic alteration of bone phosphate? *Earth and Planetary Science Letters*, 142: 1-6.
- Iacumin, P., Davanzo, S. and Nikolaev, V., 2005. Short-term climatic changes recorded by mammoth hair in the Arctic environment. *Palaeogeography Palaeoclimatology Palaeoecology*, 218(3-4): 317-324.
- Iacumin, P., Davanzo, S. and Nikolaev, V., 2006. Spatial and temporal variations in the $^{13}\text{C}/^{12}\text{C}$ and $^{15}\text{N}/^{14}\text{N}$ ratios of mammoth hairs: Palaeodiet and palaeoclimatic implications. *Chemical Geology*, 231(1-2): 16-25.
- Iacumin, P., Di Matteo, A., Nikolaev, V. and Kuznetsova, T.V., 2010. Climate information from C, N and O stable isotope analyses of mammoth bones from northern Siberia. *Quaternary International*, 212(2): 206-212.
- Iacumin, P., Nikolaev, V. and Ramigni, M., 2000. C and N stable isotope measurements on Eurasian fossil mammals, 40 000 to 10 000 years BP: Herbivore physiologies

- and palaeoenvironmental reconstruction. *Palaeogeography Palaeoclimatology Palaeoecology*, 163(1-2): 33-47.
- Koch, P.L., 1991. The isotopic ecology of Pleistocene proboscideans. *Journal of Vertebrate Paleontology*, 11(Suppl. 3): 40A.
- Koch, P.L. and Barnosky, A.D., 2006. Late Quaternary extinctions: State of the debate. *Annual Review of Ecology Evolution and Systematics*, 37: 215-250.
- Koch, P.L., Diffenbaugh, N.S. and Hoppe, K.A., 2004. The effects of late Quaternary climate and pCO₂ change on C₄ plant abundance in the south-central United States. *Palaeogeography Palaeoclimatology Palaeoecology*, 207(3-4): 331-357.
- Koch, P.L., Fisher, D.C. and Dettman, D., 1989. Oxygen isotope variation in the tusks of extinct proboscideans: a measure of season of death and seasonality. *Geology*, 17: 515-519.
- Koch, P.L., Fogel, M.L. and Tuross, N., 1994. Tracing the diets of fossil animals using stable isotopes. In: K. Lathja and R.H. Michener (Editors), *Stable Isotopes in Ecology and Environmental Science*. Blackwell Scientific Publications, Oxford, pp. 63-92.
- Koch, P.L., Hoppe, K.A. and Webb, S.D., 1998. The isotopic ecology of late Pleistocene mammals in North America - Part 1. Florida. *Chemical Geology*, 152(1-2): 119-138.
- Kohn, M.J. and Cerling, T.E., 2002. Stable isotope compositions of biological apatite. In: M.J. Kohn, J. Rakovan and J.M. Hughes (Editors), *Phosphates: Geochemical, Geobiological, and Materials Importance*. Reviews in Mineralogy and Geochemistry. Mineralogical Society of America, Washington, D.C., pp. 455-488.
- Kohn, M.J. and McKay, M., 2010. Stable isotopes of fossil teeth corroborate key general circulation model predictions for the Last Glacial Maximum in North America. *Geophysical Research Letters*, 37(22): L22702.
- Kohn, M.J., Miselis, J.L. and Fremd, T.J., 2002. Oxygen isotope evidence for progressive uplift of the Cascade Range, Oregon. *Earth and Planetary Science Letters*, 204(1-2): 151-165.
- Kurten, B. and Anderson, E., 1980. *Pleistocene mammals of North America*. Columbia University Press, New York, 442 pp.
- Kuzmin, Y.V., 2010. Extinction of the woolly mammoth (*Mammuthus primigenius*) and woolly rhinoceros (*Coelodonta antiquitatis*) in Eurasia: Review of chronological and environmental issues. *Boreas*, 39(2): 247-261.
- LeGeros, R.Z., 1991. *Calcium Phosphates in Oral Biology and Medicine*. Monographs in Oral Science, 15. Karger, New York.
- Lepper, B.T., Frolking, T.A., Fisher, D.C., Goldstein, G., Sanger, J.E., Wymer, D.A., Ogden, J.G. and Hooge, P.E., 1991. Intestinal contents of a Late Pleistocene mastodont from midcontinental North America. *Quaternary Research*, 36(1): 120-125.
- Levin, N.E., Cerling, T.E., Passey, B.H., Harris, J.M. and Ehleringer, J.R., 2006. A stable isotope aridity index for terrestrial environments. *Proceedings of the National Academy of Sciences of the United States of America*, 103(30): 11201-11205.
- Lister, A.M., Sher, A.V., van Essen, H. and Wei, G.B., 2005. The pattern and process of mammoth evolution in Eurasia. *Quaternary International*, 126-28: 49-64.

- Longinelli, A., 1984. Oxygen isotopes in mammal bone phosphate: a new tool for paleohydrological and paleoclimatological research? *Geochimica et Cosmochimica Acta*, 48: 385-390.
- Luz, B., Kolodny, Y. and Horowitz, M., 1984. Fractionation of oxygen isotopes between mammalian bone phosphate and environmental drinking water. *Geochimica et Cosmochimica Acta*, 48(8): 1689-1693.
- MacFadden, B.J. and Cerling, T.E., 1996. Mammalian herbivore communities, ancient feeding ecology, and carbon isotopes: A 10 million-year sequence from the Neogene of Florida. *Journal of Vertebrate Paleontology*, 16(1): 103-115.
- Maglio, 1973. Origin and evolution of the Elephantidae. *Transactions of the American Philosophical Society, New Series*, 63(3): 1-149.
- Manolagas, S.C., 2000. Birth and death of bone cells: Basic regulatory mechanisms and implications for the pathogenesis and treatment of osteoporosis. *Endocrine Reviews*, 21(2): 115-137.
- Marino, B.D. and McElroy, M.B., 1991. Isotopic composition of atmospheric CO₂ inferred from carbon in C₄ plant cellulose. *Nature*, 349: 127-131.
- McKinney, A.R., McCrae, J.M., Epstein, S., Allen, H.A. and Urey, H.C., 1950. Improvements in mass spectrometry for the measurement of small differences in isotope abundance ratios. *Revue of Scientific Instruments*, 21: 724-730.
- Mead, J.I., Agenbroad, L.D., Davis, O.K. and Martin, P.S., 1986. Dung of *Mammuthus* in the arid southwest, North America. *Quaternary Research*, 25(1): 121-127.
- Metcalfe, J.Z., Longstaffe, F.J. and White, C.D., 2009. Method-dependent variations in stable isotope results for structural carbonate in bone bioapatite. *Journal of Archaeological Science*, 36(1): 110-121.
- Metcalfe, J.Z., Longstaffe, F.J. and Zazula, G.D., 2010. Nursing, weaning, and tooth development in woolly mammoths from Old Crow, Yukon, Canada: Implications for Pleistocene extinctions. *Palaeogeography Palaeoclimatology Palaeoecology*, 298: 257-270.
- Nanci, A., 2003a. Dentin-pulp complex. In: A. Nanci (Editor), *Ten Cate's Oral Histology: Development, Structure, and Function*. Mosby, St. Louis, pp. 192-239.
- Nanci, A., 2003b. Enamel: composition, formation, and structure. In: A. Nanci (Editor), *Ten Cate's Oral Histology: Development, Structure, and Function*. Mosby, St. Louis, pp. 145-191.
- Nanci, A., Whitson, S.W. and Bianco, P., 2003. Bone. In: A. Nanci (Editor), *Ten Cate's Oral histology: Development, Structure, and Function*. Mosby, St. Louis, pp. 111-144.
- Newsom, L.A. and Muhlbachler, M.C., 2006. Mastodons (*Mammuth americanum*) diet foraging patterns based on analysis of dung deposits. In: S.D. Webb (Editor), *First Floridians and Last Mastodons: The Page-Ladson site in the Aucilla River*. Springer, pp. 263-331.
- O'Leary, M., 1988. Carbon isotopes in photosynthesis. *Bioscience*, 38: 328-336.
- Passey, B.H., Robinson, T.F., Ayliffe, L.K., Cerling, T.E., Sponheimer, M., Dearing, M.D., Roeder, B.L. and Ehleringer, J.R., 2005. Carbon isotope fractionation between diet, breath CO₂, and bioapatite in different mammals. *Journal of Archaeological Science*, 32(10): 1459-1470.

- Peuke, A.D., Gessler, A. and Rennenberg, H., 2006. The effect of drought on C and N stable isotopes in different fractions of leaves, stems and roots of sensitive and tolerant beech ecotypes. *Plant Cell and Environment*, 29(5): 823-835.
- Peuke, A.D., Schraml, C., Hartung, W. and Rennenberg, H., 2002. Identification of drought-sensitive beech ecotypes by physiological parameters. *New Phytologist*, 154(2): 373-387.
- Posner, A.S., 1985. The mineral of bone. *Clinical Orthopaedics and Related Research*, 200: 87-99.
- Robinson, D., Handley, L.L., Scrimgeour, C.M., Gordon, D.C., Forster, B.P. and Ellis, R.P., 2000. Using stable isotope natural abundances ($\delta^{15}\text{N}$ and $\delta^{13}\text{C}$) to integrate the stress responses of wild barley (*Hordeum spontaneum*, C. Koch.) genotypes. *Journal of Experimental Botany*, 51(342): 41-50.
- Rountrey, A.N., Fisher, D.C., Vartanyan, S. and Fox, D.L., 2007. Carbon and nitrogen isotope analyses of a juvenile woolly mammoth tusk: Evidence of weaning. *Quaternary International*, 169: 166-173.
- Sare, D.T.J., Millar, J.S. and Longstaffe, F.J., 2005. Nitrogen- and carbon-isotope fractionation between mothers and offspring in red-backed voles (*Clethrionomys gapperi*). *Canadian Journal of Zoology-Revue Canadienne De Zoologie*, 83(5): 712-716.
- Saunders, J.J., 1996. North American Mammutidae. In: J. Shoshani and P. Tassy (Editors), *The Proboscidea: evolution and palaeoecology of elephants and their relatives*. Oxford University Press, New York, pp. 271-279.
- Saunders, J.J., Grimm, E.C., Widga, C.C., Campbell, G.D., Curry, B.B., Grimley, D.A., Hanson, P.R., McCullum, J.P., Oliver, J.S. and Treworgy, J.D., 2010. Paradigms and proboscideans in the southern Great Lakes region, USA. *Quaternary International*, 217(1-2): 175-187.
- Schwarcz, H.P., 2000. Some biochemical aspects of carbon isotopic paleodiet studies. In: S.H. Ambrose and M.A. Katzenberg (Editors), *Biogeochemical Approaches to Paleodietary Analysis*. Kluwer Academic, New York, pp. 189-209.
- Schwarcz, H.P., Dupras, T.L. and Fairgrieve, S.I., 1999. ^{15}N enrichment in the Sahara: In search of a global relationship. *Journal of Archaeological Science*, 26(6): 629-636.
- Smith, B.N. and Epstein, S., 1971. Two categories of $^{13}\text{C}/^{12}\text{C}$ ratios for higher plants. *Plant Physiology*, 47: 380-384.
- Sponheimer, M., Robinson, T., Ayliffe, L., Roeder, B., Hammer, J., Passey, B., West, A., Cerling, T., Dearing, D. and Ehleringer, J., 2003a. Nitrogen isotopes in mammalian herbivores: Hair $\delta\text{N-15}$ values from a controlled feeding study. *International Journal of Osteoarchaeology*, 13(1-2): 80-87.
- Sponheimer, M., Robinson, T.F., Roeder, B.L., Passey, B.H., Ayliffe, L.K., Cerling, T.E., Dearing, M.D. and Ehleringer, J.R., 2003b. An experimental study of nitrogen flux in llamas: is ^{14}N preferentially excreted? *Journal of Archaeological Science*, 30(12): 1649-1655.
- Suga, S., 1982. Progressive mineralization pattern of developing enamel during the maturation stage. *Journal of Dental Research*: 1532-1542.
- Sukumar, R., 1989. *The Asian elephant: ecology and management*. Cambridge studies in applied ecology and resource management. Cambridge University Press, Cambridge, 251 pp.

- Sullivan, C.H. and Krueger, H.W., 1981. Carbon isotope analysis of separate chemical phases in modern and fossil bone. *Nature*, 292(5821): 333-335.
- Szpak, P., Grocke, D.R., Debruyne, R., MacPhee, R.D.E., Guthrie, R.D., Froese, D., Zazula, G.D., Patterson, W.P. and Poinar, H.N., 2010. Regional differences in bone collagen $\delta^{13}\text{C}$ and $\delta^{15}\text{N}$ of Pleistocene mammoths: Implications for paleoecology of the mammoth steppe. *Palaeogeography Palaeoclimatology Palaeoecology*, 286(1-2): 88-96.
- Ten Cate, A.R. and Nanci, A., 2003. Structure of the oral tissues. In: A. Nanci (Editor), *Ten Cate's Oral Histology: Development, Structure, and Function*. Mosby, St. Louis, pp. 1-16.
- Tieszen, L.L. and Fagre, T., 1993. Effect of diet quality and composition on the isotopic composition of respiratory CO_2 , bone collagen, bioapatite, and soft tissues. In: J.B. Lambert and G. Grupe (Editors), *Prehistoric Human Bone: Archaeology at the Molecular Level*. Springer-Verlag, Berlin, pp. 121-155.
- Tutken, T., Furrer, H. and Vennemann, T.W., 2007. Stable isotope compositions of mammoth teeth from Niederweningen, Switzerland: Implications for the Late Pleistocene climate, environment, and diet. *Quaternary International*, 164-65: 139-150.
- Ukkonen, P., Arppe, L., Houmark-Nielsen, M., Kjaer, K.H. and Karhu, J.A., 2007. MIS 3 mammoth remains from Sweden: implications for faunal history, palaeoclimate and glaciation chronology. *Quaternary Science Reviews*, 26(25-28): 3081-3098.
- van der Merwe, N.J., 1989. Natural variations in ^{13}C concentration and its effect on environmental reconstruction using $^{13}\text{C}/^{12}\text{C}$ ratios in animal bones. In: T.D. Price (Editor), *The Chemistry of Prehistoric Human Bone*. Cambridge University Press, Cambridge, pp. 105-125.
- van Geel, B., Aptroot, A., Baittinger, C., Birks, H.H., Bull, I.D., Cross, H.B., Evershed, R.P., Gravendeel, B., Kompanje, E.J.O., Kuperus, P., Mol, D., Nierop, K.G.J., Pals, J.P., Tikhonov, A.N., van Reenen, G. and van Tienderen, P.H., 2008. The ecological implications of a Yakutian mammoth's last meal. *Quaternary Research*, 69(3): 361-376.
- Vogel, J.C., Talma, A.S., Hallmartin, A.J. and Viljoen, P.J., 1990. Carbon and nitrogen isotopes in elephants. *South African Journal of Science*, 86(3): 147-150.
- Waters, M.R. and Stafford, T.W., 2007. Redefining the age of Clovis: Implications for the peopling of the Americas. *Science*, 315(5815): 1122-1126.
- Webb, S.D., 1992. A brief history of New World Proboscidea with emphasis on their adaptations and interactions with man. In: J.W. Fox, C.B. Smith and K.T. Wilkins (Editors), *Proboscidean and paleoindian interactions*. Baylor University Press, Waco, Texas, pp. 15-34.
- White, C.D. and Armelagos, G.J., 1997. Osteopenia and stable isotope ratios in bone collagen of Nubian female mummies. *American Journal of Physical Anthropology*, 103: 185-199.
- Williams, J.S., White, C.D. and Longstaffe, F.J., 2005. Trophic level and macronutrient shift effects associated with the weaning process in the Postclassic Maya. *American Journal of Physical Anthropology*, 128(4): 781-790.
- Wopenka, B. and Pasteris, J.D., 2005. A mineralogical perspective on the apatite in bone. *Materials Science & Engineering C: Biomimetic and Supramolecular Systems*, 25(2): 131-143.

- Zazzo, A., Balasse, M. and Patterson, W.P., 2006. The reconstruction of mammal individual history: refining high-resolution isotope record in bovine tooth dentine. *Journal of Archaeological Science*, 33(8): 1177-1187.
- Zazzo, A., Balasse, M., Patterson, W.P. and Patterson, P., 2005. High-resolution $\delta^{13}\text{C}$ intratooth profiles in bovine enamel: Implications for mineralization pattern and isotopic attenuation. *Geochimica et Cosmochimica Acta*, 69(14): 3631-3642.

Chapter 2

Method-dependent variations in stable isotope results for structural carbonate in bone bioapatite ¹

2.1 Introduction

Bone is a composite of organic (collagen) and inorganic (bioapatite) components. Bioapatite is an impure calcium phosphate mineral that resembles hydroxyapatite, $\text{Ca}_{10}(\text{PO}_4)_6(\text{OH})_2$. In its normal state, bioapatite is affected by numerous minor and trace element substitutions and adsorptions (LeGeros, 1991; Wopenka and Pasteris, 2005). Most importantly for isotopic studies, the carbonate anionic complex (CO_3) can be substituted into both phosphate (B-type substitution) and hydroxyl sites (A-type substitution) within bioapatite (Elliott, 2002).

The stable carbon and oxygen isotope compositions ($\delta^{13}\text{C}$, $\delta^{18}\text{O}$) of carbonate in skeletal materials have been used to study topics as diverse as ancient climate, diet, physiology, and migration (e.g., Bocherens et al., 1995; Dupras and Schwarcz, 2001; Hoppe, 2004). In some cases, the studies are based on the premise that the original isotopic composition of bioapatite is preserved (e.g., Koch et al., 1998), and in other cases, that the sample has been altered to reflect conditions present in the soil after the animal's death (e.g., Kohn and Law, 2006). Regardless, interpretations depend on reliable analysis of $\delta^{13}\text{C}$ and $\delta^{18}\text{O}$ values for the sample.

Prior to analysis of carbonate isotope compositions, bone samples are commonly treated with bleach (to remove organic matter) and acid (to remove secondary and adsorbed minerals) (Koch et al., 1997). Samples are then reacted with ortho-phosphoric acid to produce the CO_2 gas from which stable isotope values are obtained:



In the past, carbonate samples were typically reacted at 25°C in a sealed evacuated vessel, and CO_2 was cryogenically isolated prior to being transferred to an isotope ratio mass spectrometer (IRMS) (McCrea, 1950). However, many researchers now use

¹ A version of this chapter has been published:
Metcalf, J.Z., Longstaffe, F.J. and White, C.D., 2009. Method-dependent variations in stable isotope results for structural carbonate in bone bioapatite. *Journal of Archaeological Science*, 36(1): 110-121.

automated reaction devices (e.g., Isocarb, GasBench, and MultiPrep devices), which are directly interfaced with mass spectrometers. Results can be obtained more quickly using these methods but higher reaction temperatures are generally utilized. Using these methods, CO₂ may be produced in a sealed reaction vessel or in a vessel that remains open to cryogenic traps during CO₂ evolution, allowing the gaseous reaction products to be removed as the reaction proceeds (Swart et al., 1991). In addition, water may be removed from the reaction products using cryogenic or Nafion trapping, gases may be separated using gas chromatography, and isotopic measurements of the purified CO₂ may be obtained using either continuous-flow or dual-inlet IRMS. Our aims in this study were (1) to determine whether different methods produce comparable results when archaeological bone bioapatite samples are analyzed, and (2) to ascertain the causes of any differences in isotope compositions among methods.

2.2 Sample

Archaeological human bone samples were obtained from two regions: the Nile desert in Sudan (Hambukol site, n=14) and the Pacific coast of Guatemala (Balberta, Los Chatos, and Manantial sites, n=15).

The Guatemala sites date to AD 250-400 and are located in an area of high rainfall (1500 to 2000 mm/year), with annual flooding and a high water table. The mean temperature at >25 cm depth is approximately 30°C. Soils are derived from volcanic deposits. Present river drainage, runoff, and groundwater are heavily contaminated with chemicals and human waste. Burials were placed directly in mound fill or in ceramic vessels (F. Bove, personal communication, April 2007).

The Sudan site dates to AD 600-1300 and is located at the southern end of the Letti Basin, in an island-like area between the Nile River and an extinct river channel. The region is hyper-arid (13 mm rainfall/year) and warm (mean monthly temperature = 18 to 34°C) (Elagib and Mansell, 2000). Burials were placed in dry, sandy earth.

All of the above samples were used in the comparison of stable isotope analytical methods. All samples were also characterized using Fourier Transform Infrared Spectroscopy. Four samples were chosen for more detailed structural and chemical analyses: NK356 from the Sudan site and B5, B21, and B25 from the Guatemala sites.

2.3 Methods

2.3.1 Pretreatments

Bones were cleaned with a wire brush, ground with a mortar and pestle, treated with bleach to remove organic matter, rinsed with de-ionized water, treated with acetic acid to remove adsorbed and diagenetic carbonates, rinsed, and dried. An aliquot of each bone was subjected to (a) a strong pretreatment (SP) of 4% bleach for 24 hours and 1.0 M acetic acid for 1 hour, and (b) a weak pretreatment (WP) of 2% bleach for 72 hours and 0.1 M acetic acid for 4 hours. These two approaches are reasonably representative of the spectrum of commonly employed pretreatment methods for isotopic analysis of carbonate in mammalian bioapatite (Garvie-Lok et al., 2004; Koch et al., 1997).

2.3.2 Isotopic Analyses

Stable isotope results are presented in standard delta (δ) notation relative to VSMOW (oxygen) and VPDB (carbon), following Coplen (1994). Anhydrous orthophosphoric acid (H_3PO_4) was prepared and de-gassed prior to use. The same acid was used for all reactions. Calcite standards of known composition were analyzed with each batch of samples at the same temperature and using the same methodology. For the C25 method (described below), the oxygen isotope values were calculated using the known fractionation between calcite and CO_2 at 25°C ($\alpha = 1.01025$) (Friedman and O'Neil, 1977). For the GB and MP methods (described below), NBS-19, NBS-18, and Suprapur standards were used to form a calibration curve. A separate laboratory calcite standard (WS-1) was used in all methods to monitor accuracy and precision.

2.3.2.1 C25 (Conventional 25°C) Method

Approximately 50 mg of sample was reacted with an excess of H_3PO_4 in a sealed vessel under vacuum for three days at 25°C. Gases were transferred cryogenically using liquid nitrogen traps (-200°C), and water was removed using a nitrogen-ethanol slurry (-75°C). The CO_2 yield was measured manometrically using a pressure transducer attached

to a panel meter. The gas remaining after these steps was analyzed using a VG Optima dual-inlet IRMS.

2.3.2.2 *GB50 (GasBench 50°C) Method*

Approximately 5 mg of sample was loaded into a reaction vessel, the vessel was sealed and purged with helium, and the sample was reacted with an excess of H_3PO_4 at 50°C for two hours. The gas produced was then processed using a Finnigan GasBench II automated sampling system coupled to a Thermo-Finnigan Delta^{Plus}XL IRMS in continuous flow mode. Nafion traps were used to remove water vapour and a PoraPLOT Q GC column was employed to separate CO_2 from other molecular species before it entered the mass spectrometer.

2.3.2.3 *MP90 (MultiPrep 90°C) Method*

Approximately 0.9 mg of sample was reacted with an excess of H_3PO_4 under vacuum at 90°C for 25 minutes, using a Micromass MultiPrep autosampling device. In contrast to the methodologies described earlier, the gaseous reaction products were removed as soon as they were produced, using a cryogenic trap (-170°C). Water vapour was removed cryogenically (-70°C), and the remaining gas was analyzed using a VG Optima dual-inlet IRMS. Gas yields were monitored for each sample using a pressure transducer in the mass spectrometer.

2.3.2.4 *MP50, MP50-S, MP90-S Methods*

Selected samples were analyzed using the MP90 method (above) with the following modifications: reaction at 50°C for two hours (MP50 method), reaction at 50°C for two hours with the valve to the cryogenic traps closed, simulating a “sealed vessel” reaction (MP50-S), and reaction at 90°C with the valve to the cryogenic traps closed (MP90-S, 25 minute reaction; MP90-S*, 3.5 hour reaction).

2.3.2.5 *Phosphate Oxygen*

The oxygen isotope composition of the phosphate anionic complex within bioapatite was also measured. Silver phosphate (Ag_3PO_4) was precipitated from bone

samples following the method of Stuart-Williams (1996). Oxygen was liberated from Ag_3PO_4 by reaction with bromine pentafluoride (BrF_5) at 600°C for 18 hours, and converted to CO_2 by reaction with hot graphite. The $\delta^{18}\text{O}_p$ value of the CO_2 was measured using a VG Optima dual-inlet IRMS. Replicate analyses of a silver phosphate reference material were normally within $\pm 0.3\%$.

2.3.3 Mass Scans

Mass scans of the gases introduced into the mass spectrometer were performed to characterize the molecular composition of gases produced and purified using the methods described above. The sample gas was introduced into the ion source of a VG Optima dual-inlet IRMS, and the magnetic current was gradually increased from 1.5 to 5.0 A, using a step size of 0.0025 A. The spectrum of all gas peaks (approximate mass/charge (m/z) ratios 18 to 60) for each sample or standard was recorded.

2.3.4 Light Microscopy and Scanning Electron Microscopy (SEM)

Microscopy was used to examine the physical integrity of samples. Whole bone samples were embedded in epoxy and transverse sections were cut using an Ingram cut-off saw. Sections were mounted on glass slides and polished with diamond powder to a thickness of 70-100 μm . Thin sections were examined under transmitted light using a Jenapol petrographic microscope. Periosteal and endosteal surfaces of bone were sputter-coated with gold and examined using a Hitachi S4500 field emission scanning electron microscope.

2.3.5 Fourier Transform Infrared Spectroscopy (FTIR)

FTIR was used to examine the molecular structure of samples. Approximately 2 mg of pretreated (WP or SP) bone was mixed with 200 mg of KBr and compressed with a hydraulic press at 10 tons for 10 minutes to create a 12 mm pellet. Absorbance spectra were obtained using a Bruker Vector 22 FTIR Spectrometer, scanning 16 times from 400 to 4000 cm^{-1} , with a resolution of 4 cm^{-1} . Spectra were compared to those obtained in previous studies for bone, enamel, and synthetic hydroxyapatite (Bigi et al., 1997; Boyar et al., 2004; LeGeros, 1991; Puceat et al., 2004; Wright and Schwarcz, 1996) to determine

whether any unusual phases were present. Crystallinity Indices (CI values) were calculated following Weiner and Bar-Yosef (1990). Carbonate/phosphate ratios (C/P values) were obtained following Puc at et al. (2004). Precision was better than ± 0.06 for CI values and ± 0.05 for C/P values. Fourier self-deconvolution, a computational method used to resolve overlapping bands by decreasing the bandwidths of the individual components (Kauppinen et al., 1981), was used to identify some IR peaks. The self-deconvolution program used a Lorentzian curve shape, a band width of 1.47, and a resolution enhancement factor of 2.5.

2.3.6 X-Ray Diffraction (XRD)

XRD analyses were used to identify the crystalline components of samples. Randomly-oriented powdered samples were mounted on glass slides and scanned using a Rigaku diffractometer (45 mA, 160 kV), equipped with Co-K α radiation. Samples were scanned from 2 $^\circ$ to 82 $^\circ$ 2 Θ , using a step size of 0.02 $^\circ$ 2 Θ , and a scan rate of 10 $^\circ$ 2 Θ /min; and from 28 $^\circ$ to 44 $^\circ$ 2 Θ , using a step size of 0.01 $^\circ$ 2 Θ , and a scan rate of 1 $^\circ$ 2 Θ /min.

2.3.7 Thermogravimetric Analysis (TGA)

TGA was conducted to determine whether samples reacted differently from one another when heated. Approximately 10 mg of sample and Al₂O₃ reference material were heated to 950 $^\circ$ C at 10 $^\circ$ C/min in air using a Linseis Thermobalance L81. Weight loss and temperature change were recorded simultaneously and TG curves were derived for each sample.

2.3.8 Total Inorganic Carbon / Total Organic Carbon (TIC/TOC)

TIC/TOC analyses were conducted to determine whether samples differed in their amount and forms of carbon. Reaction vessels were manually purged with helium and 2-3 mg of sample was reacted with an excess of H₃PO₄ at 25 $^\circ$ C for seven days. The resulting gas (CO₂ derived from inorganic material) was analyzed using a Finnigan GasBench II automated sampling system coupled to a Delta^{plus}XL IRMS in continuous flow mode. TIC (weight %) was derived from the height of the curve relative to the weight of the sample, calibrated using a calcite standard of known composition. After this analysis,

approximately 300 μL of sodium persulfate (Na_2SO_4) was added to the sample and the reaction vessel was sparged with helium to remove any residual CO_2 . The liquid was then heated at 100°C to promote the oxidation of organic matter to CO_2 , and the resulting gas analyzed as described earlier.

2.3.9 Nitrogen Content

Nitrogen contents (weight %N) were obtained using a Fisons Instruments EA 1108 elemental analyzer, to determine whether samples differed in their preservation of collagen and/or degree of nitrogen contamination. Approximately 30 mg of sample or standard was placed in an 8.5 by 5.0 mm tin cup and combusted at 1020°C in a Cr_2O_3 oxidation tube. The resulting gas was carried by He through a 650°C reduction tube and a 40°C GC column. A thermal conductivity detector was used to measure the amount of N_2 gas evolved, allowing the nitrogen contents of the samples to be calculated based on calibration curves for standards of known nitrogen content.

2.3.10 Inductively-Coupled Plasma Atomic Emission Spectroscopy (ICP-AES)

ICP-AES was used to determine the chemical composition of samples. Approximately 50 mg of pretreated (WP or SP) bone sample was dissolved in 4 ml of 3:1 HCl/HNO_3 and diluted to 50 ml. Aliquots (10 ml) were analyzed using a Perkin-Elmer Optima 3300 DV system and the average of three measurements for each sample was reported.

2.4 Results

2.4.1 Carbon Isotope Analyses

The mean measured $\delta^{13}\text{C}$ values ($\pm 1\sigma$) for laboratory standard WS-1 calcite were $0.7 \pm 0.1\text{‰}$ (C25 method; $n=10$), $0.7 \pm 0.1\text{‰}$ (GB50 method; $n=11$), and $0.8 \pm 0.03\text{‰}$ (MP90 method; $n=12$), which compare well with its accepted value of 0.8‰ . The isotopic results for bone samples are listed in Table 2.1. The precision of sample analyses reported in this and the following section consider results for both SP and WP, but treat them as separate samples. Replicate $\delta^{13}\text{C}$ analyses of the same sample averaged $\pm 0.04\text{‰}$ (C25

method; n=2 pairs), $\pm 0.1\%$ (GB50 method; n=12 pairs), and $\pm 0.3\%$ (MP90 method; n=26 samples, each of which was analyzed two to four times). The $\delta^{13}\text{C}$ values obtained for a given sample using the C25 and GB50 methods were, on average, within $\pm 0.1\%$ for both Guatemala and Sudan samples. The average $\delta^{13}\text{C}$ values measured using the MP90 method were generally within $\pm 0.1\%$ of those measured using the C25 and GB50 methods for the Sudan samples, and within $\pm 0.3\%$ for the Guatemala samples.

2.4.2 Oxygen Isotope Analyses (Structural Carbonate)

The mean $\delta^{18}\text{O}$ values ($\pm 1\sigma$) for WS-1 were $26.1 \pm 0.2\%$ (C25 method, n=10), $26.2 \pm 0.3\%$ (GB50 method, n=11), and $26.3 \pm 0.1\%$ (MP90 method, n=12), which compare well with its accepted value of 26.2% . The reproducibility of $\delta^{18}\text{O}$ values for the bone samples averaged $\pm 0.2\%$ (C25 method, n=2), $\pm 0.3\%$ (GB50 method, n=12), and $\pm 2.9\%$ (MP90 method, n=26). The average $\delta^{18}\text{O}$ values obtained for a given sample (Sudan or Guatemala) using the C25 and GB50 methods generally agreed within $\pm 0.5\%$. For Sudan samples, $\delta^{18}\text{O}$ values obtained using the MP90 method were on average within $\pm 0.7\%$ of $\delta^{18}\text{O}$ values obtained using the C25 and GB50 methods, but this difference was much larger ($\pm 3.9\%$) for Guatemala samples. Some of the Guatemala samples were characterized by extremely low $\delta^{18}\text{O}$ values when analyzed using the MP90 method (see below).

2.4.3 Pretreatment Effects

Anomalously low $\delta^{18}\text{O}$ values were obtained for some bone samples regardless of pretreatment method. Hence, it appears that some feature of the original bone sample was responsible for the tendency to produce the contaminant gas and the attendant low $\delta^{18}\text{O}$ values. That said, lower (more anomalous) $\delta^{18}\text{O}$ values and poorer reproducibility among methods was more typical of weakly pretreated (WP) than strongly pretreated (SP) samples (Table 2.1). Since the stronger pretreatment was associated with more “normal” results, it is unlikely that the pretreatment caused formation of a new contaminant phase. However, the strong pretreatment may have removed relatively more of some contaminant, or stripped away reactive surfaces more completely than the weak pretreatment.

2.4.4 “Anomalous” Isotope Values

Whenever the oxygen isotope results for the various methods differed by more than $\pm 0.4\%$, the MP90 $\delta^{18}\text{O}$ values were lower than C25 and GB50 $\delta^{18}\text{O}$ values (Table 2.1). In the most extreme case (B25-WP), one MP90 $\delta^{18}\text{O}$ measurement was 45‰ lower than the average $\delta^{18}\text{O}$ value obtained using the C25 or GB50 methods. In all cases of low $\delta^{18}\text{O}$ values, the corresponding $\delta^{13}\text{C}$ value was only slightly higher than that obtained using other methods (Table 2.1, Figure 2.1).

To investigate potential differences among the bone samples that could be related to the production of anomalously low $\delta^{18}\text{O}$ values, four representative specimens were chosen for more detailed analyses: NK356 from the Sudan site and B5, B21, and B25 from the Guatemala sites. The $\delta^{18}\text{O}$ values obtained for the first two specimens were within $\pm 0.6\%$ or better among methods (“normal” bones) whereas the latter two samples had anomalously low MP90 $\delta^{18}\text{O}$ values (“anomalous” bones). The “normal” bone from Guatemala (B5) was intended to “control” for differences among Sudan and Guatemala bones that were unrelated to production of the “anomalous” $\delta^{18}\text{O}$ values.

2.4.5 Contaminant gas

Mass scans of gas produced from the “normal” bone samples and standard reference materials showed the expected CO_2 peaks at m/z 44, 45, and 46, and only negligible peaks at higher masses, regardless of the analytical method used. “Anomalous” bones were characterized by additional large peaks at m/z 47, 48, and 49 when processed using the MP50 and MP90 methods. This result indicated that a contaminant gas was produced during the reaction of these samples and was introduced into the mass spectrometer along with CO_2 (Figure 2.2). Moreover, the m/z 47 peak was larger when lower $\delta^{18}\text{O}$ values were obtained (Figure 2.2). The presence of the contaminant gas was directly related to the occurrence of low $\delta^{18}\text{O}$ values. “Normal” values were obtained for the same samples when they were processed using the C25 or GB50 methods, for which the mass scans showed only the expected CO_2 peaks at m/z 44, 45, and 46.

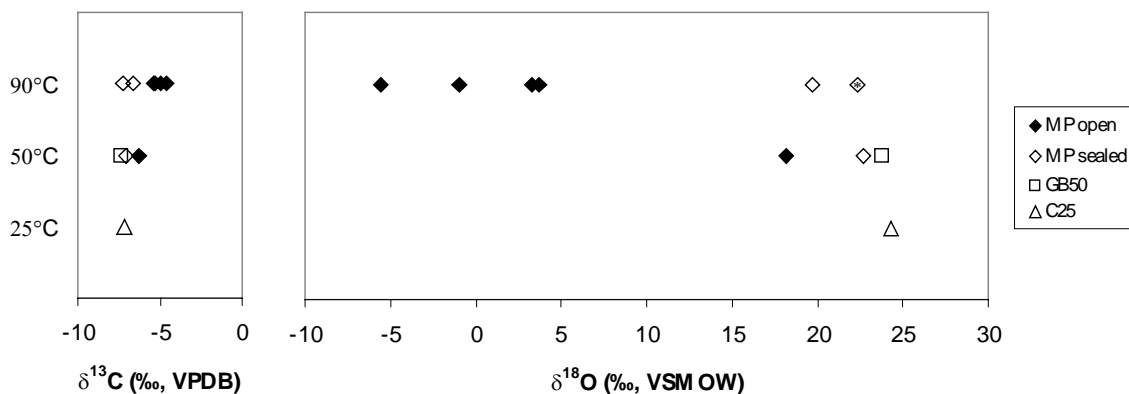


Figure 2.1 Carbon and oxygen isotope results obtained from individual analyses of "anomalous" sample B21-WP, grouped by temperature of reaction. Open symbols represent reactions in "sealed" systems and closed symbols represent reactions that occurred while condensable reaction products were simultaneously being removed cryogenically. The diamond enclosing an asterisk represents the MP90-S* method in which the reaction time was increased to 3.5 hours.

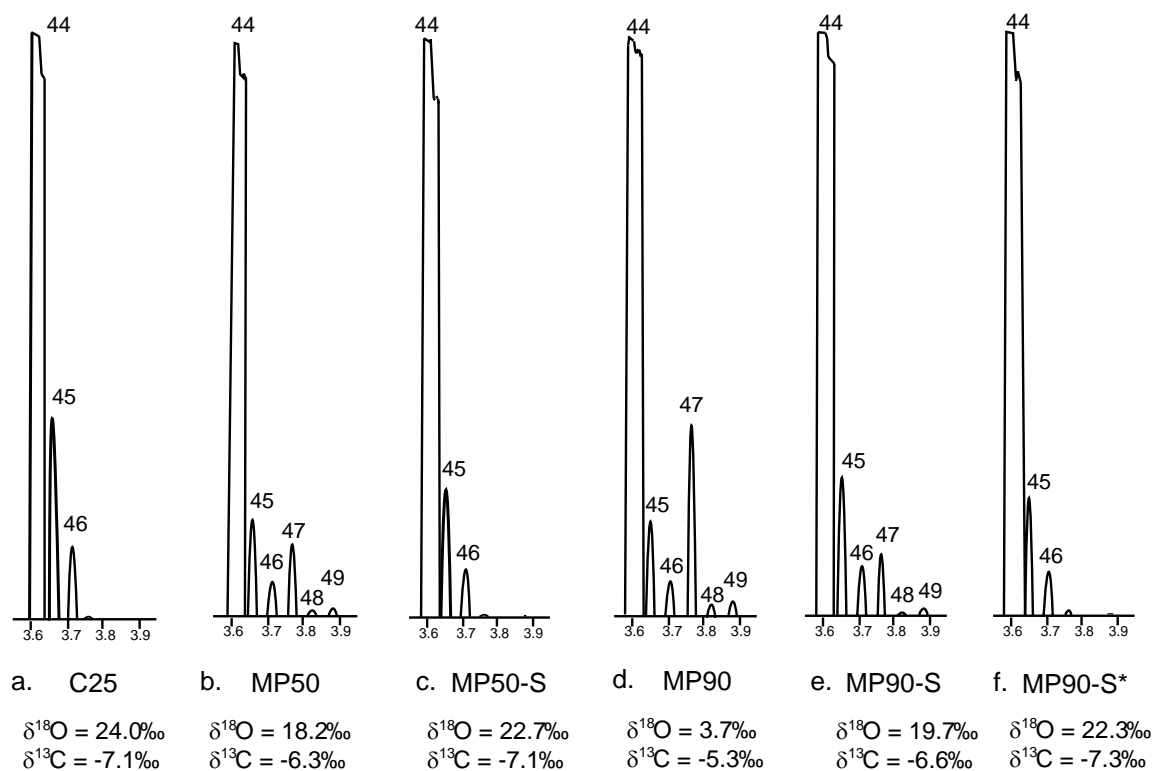


Figure 2.2 Mass scans of gas produced by reaction of specimen B21-WP with orthophosphoric acid using different methods. The horizontal axis shows magnetic current (in Amperes) and numbers above peaks indicate mass/charge (m/z) ratios. The $\delta^{18}\text{O}$ and $\delta^{13}\text{C}$ values listed were obtained from the same aliquot of gas as that used for mass scanning.

2.4.6 Temperature Dependence

The MP90 and MP50 methods were identical except in reaction time and temperature. For “anomalous” bones, both methods produced low $\delta^{18}\text{O}$ values, but those obtained using the MP90 method were systematically lower than those obtained using the MP50 method (Table 2.1, Figure 2.1). This suggests that a temperature-dependent reaction occurs between some bones and phosphoric acid, which ultimately results in anomalously low $\delta^{18}\text{O}$ values.

2.4.7 “Sealed” vs. “Open” Reaction Vessels

When “anomalous” sample B21-WP was reacted using the MP50 method, a contaminant gas was produced and a low $\delta^{18}\text{O}$ value was obtained (Figure 2.2b). When the same sample was reacted under identical conditions but with the valve to the cryogenic traps closed during the reaction (MP50-S method), no contaminant gas was detected and the resulting $\delta^{18}\text{O}$ value was within $\pm 0.7\%$ of the $\delta^{18}\text{O}$ value obtained using the C25 method. (Figure 2.2c). Using the MP90 method, this sample was characterized by an extremely low $\delta^{18}\text{O}$ value and large m/z 47 peak (Figure 2.2d). However, using the MP90-S method the m/z 47 peak was significantly reduced and the $\delta^{18}\text{O}$ value obtained was closer to “normal” (Figure 2.2e). When the sample was allowed to react in a sealed system at 90°C for a longer period of time, the contaminant gas peak disappeared completely and the $\delta^{18}\text{O}$ value obtained was within $\pm 0.9\%$ of its expected $\delta^{18}\text{O}$ value (i.e., that produced using the C25 method) (Figure 2.2f).

2.4.8 Gas Yields

There were no correlations between transducer readings (which reflect gas yields) or carbonate contents (calculated from transducer readings and sample weights, calibrated using calcite standards) and $\delta^{18}\text{O}$ values obtained using the MP90 method. There was also no correlation between gas yields obtained using the C25 method and the reproducibility of $\delta^{18}\text{O}$ values.

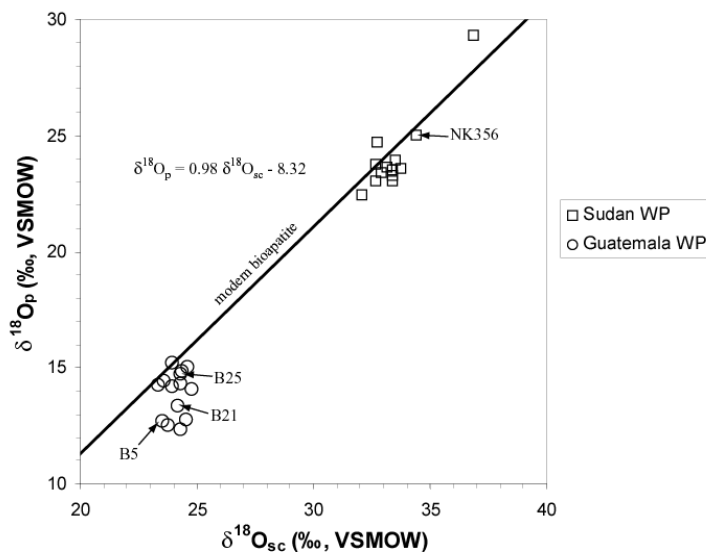


Figure 2.3 Oxygen isotope results obtained for phosphate and structural carbonate (C25 method) for Guatemala and Sudan bones using the weak pretreatment (WP). The trendline and equation for modern bioapatite (Bryant et al., 1996; Iacumin et al., 1996) and individual data points for the "normal" (NK356, B5) and "anomalous" (B21, B25) bone samples selected for detailed study are also indicated.

2.4.9 Phosphate Oxygen Isotope Values

There is a linear relationship between structural carbonate and phosphate oxygen isotope values ($\delta^{18}\text{O}_{\text{sc}}$, $\delta^{18}\text{O}_{\text{p}}$) for modern bioapatite (Bryant et al., 1996; Iacumin et al., 1996). For the Sudan samples the $\delta^{18}\text{O}_{\text{p}}$ values were significantly correlated with the $\delta^{18}\text{O}_{\text{sc}}$ values obtained using all three structural carbonate analytical methods, but the correlations obtained using the C25 and GB50 methods ($r = 0.91$, $df = 11$, $p < 0.001$; $r = 0.91$, $df = 12$, $p < 0.001$, respectively) were better than that obtained using the MP90 method ($r = 0.71$, $df = 12$, $p < 0.01$). For the Guatemala samples there were no significant correlations ($p < 0.05$) between the $\delta^{18}\text{O}_{\text{p}}$ values and the $\delta^{18}\text{O}_{\text{sc}}$ values obtained using any of the structural carbonate analytical methods.

The relationship between $\delta^{18}\text{O}_{\text{sc}}$ and $\delta^{18}\text{O}_{\text{p}}$ values in modern bioapatite (Bryant et al., 1996; Iacumin et al., 1996) is illustrated in Figure 2.3, along with $\delta^{18}\text{O}_{\text{p}}$ and $\delta^{18}\text{O}_{\text{sc}}$ (C25 method) results obtained for samples from Guatemala and Sudan. Well-preserved archaeological samples should plot close to the modern bioapatite line, while samples that have undergone post-mortem alteration should plot further away from the line (Iacumin et

al., 1996). Assuming that the oxygen isotope composition of carbonate in the sample (whether of biogenic or diagenetic origin) was measured accurately using the C25 method, the relationship between $\delta^{18}\text{O}_p$ and $\delta^{18}\text{O}_{sc}$ (C25 method) can provide information on the nature and degree of post-mortem alteration. Results for the Sudan samples fell close to the modern bioapatite line (Figure 2.3). Results for some of the Guatemala samples plotted near the modern line, but many fell well beneath it (Figure 2.3), which suggests that the $\delta^{18}\text{O}_{sc}$ and/or $\delta^{18}\text{O}_p$ values were affected by post-mortem alteration. However, the “anomalous” bones were not necessarily furthest from the modern line (Figure 2.3), indicating that contaminant gas production cannot be predicted based on the overall degree of post-mortem alteration.

2.4.10 Light Microscopy and Scanning Electron Microscopy (SEM)

Preservation of the bone samples, as indicated by microscopic observations, was highly variable. Original bone microstructures (haversian canals, lacunae, and canaliculi) were visible in both “normal” and “anomalous” samples (Figure 2.4a). All three Guatemala bones contained areas in which a cloudy black/brown substance obscured the histological structure (Figure 2.4a). B21 was the most poorly preserved specimen: aside from small areas of lamellar bone near the periosteal surface, the original bone microstructure was completely replaced by the cloudy black/brown substance and by a granular material that likely resulted from microbial tunnelling (Figure 2.4b) (Piepenbrink, 1989). The other “anomalous” bone from Guatemala (B25) had a comparable degree of histological preservation to the “normal” bone from Guatemala (B5).

The periosteal surfaces of “normal” bones contained small holes/pits (about 20-30 μm diameter) and a few larger holes (about 90 μm diameter), while the “anomalous” bone surfaces contained no holes of any size (Figures 2.4c-d). These holes were likely sites of blood vessel entry and Sharpey’s fiber attachment. Their absence in “anomalous” bones suggests greater post-mortem alteration, including the possibility of recrystallization of apatite and/or precipitation of new minerals in pore spaces.

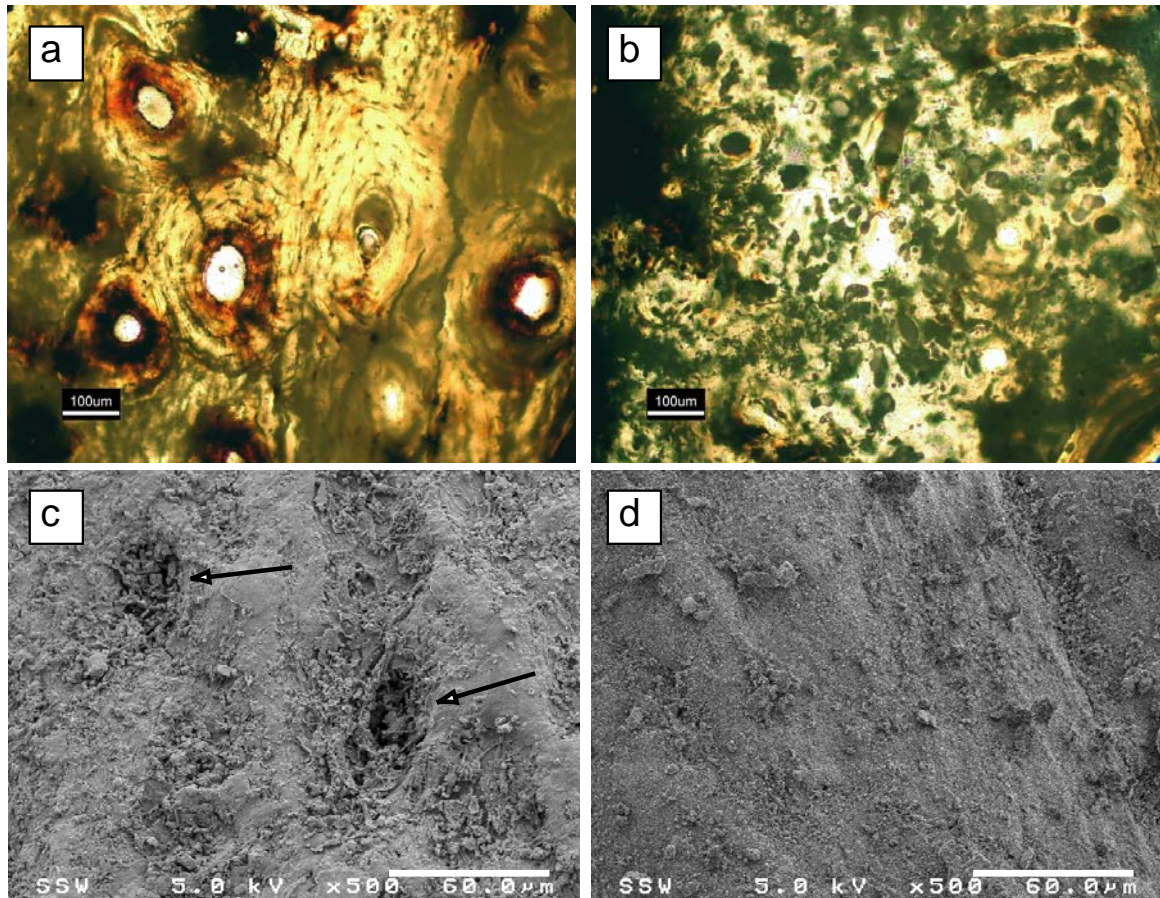


Figure 2.4 Optical photomicrographs taken in transmitted light from transverse sections of bone, 70-100 μm thick (a-b), and SEM photomicrographs of bone surfaces (c-d). (a) Relatively well-preserved bone with intact osteons ("normal" specimen B5). A cloudy black-brown substance and iron staining (red) cover parts of the sample. (b) Replacement of original bone microstructure by the black-brown substance and a granular material ("anomalous" specimen B21). (c) Periosteal surface of "normal" specimen NK356, showing holes/pits (arrows). (d) Periosteal surface of "anomalous" specimen B25, lacking pits.

2.4.11 Fourier Transform Infrared Spectroscopy (FTIR)

All of the FTIR peaks could be assigned to phases normally found in bone (e.g., Puceat et al., 2004; Sponheimer and Lee-Thorp, 1999), including phosphate, carbonate, and hydroxyl ions and organic moieties (Figure 2.5a). No unusual phases were identified. The fluorapatite peak at 1096 cm^{-1} (Shemesh, 1990) was nearly absent in some samples and distinct in others, but occurred as a weak shoulder in the majority of samples. Guatemala samples had stronger fluorapatite peaks, significantly higher CI values (for WP, independent samples $t = 4.4$, $df = 27$, $p < 0.0005$; for SP, $t = 2.3$, $df = 27$, $p < 0.05$) and lower C/P values (for WP, $t = 2.7$, $df = 26$, $p < 0.05$) than Sudan samples (Table 2.1), which suggests that more post-mortem alteration occurred at the Guatemala sites. However, there was no correlation between the reproducibility of $\delta^{18}\text{O}$ values and fluorapatite peak strength, CI, or C/P values.

An OH^- peak at 3564 cm^{-1} is normally present in geologic and synthetic hydroxyapatites, but not in bone (Pasteris et al., 2004; Rey et al., 1995). Its presence in the FTIR spectra of many bones in the present study suggests post-mortem recrystallization of the apatite (Figure 2.5b).

Very weak CH_3 and CH_2 stretching peaks (2800 to 3000 cm^{-1}), indicative of organic compounds, were present in the FTIR spectra of both “normal” and “anomalous” bones. Comparison of this region after local baseline correction suggests that in “anomalous” samples the 2875 cm^{-1} peak was diminished or lost compared to that of “normal” bones (Figure 2.5c), which may indicate that the former contained less collagen (Boyar et al., 2004).

FTIR peaks in the ν_3 carbonate region (1400 to 1550 cm^{-1}) are sometimes attributed to A- and B-type CO_3 substitution (e.g., Rink and Schwarcz, 1995), but the different positions of these peaks in bioapatite relative to synthetic A- and B-type apatite (Elliott, 1994) and the overlapping peaks from organic matter in bone (Boyar et al., 2004) make this interpretation problematic. In the present study, the ν_3 carbonate peak at approximately 1420 cm^{-1} was shifted to higher wavenumbers (up to 1428 cm^{-1}) in the “anomalous” bones (Figure 2.5d). “Anomalous” bones also lacked a peak or shoulder at about 1474 cm^{-1} , which was present in “normal” bones. This could indicate a change in the carbonate environment or it may be a result of the amide II band (C-N stretch, N-H

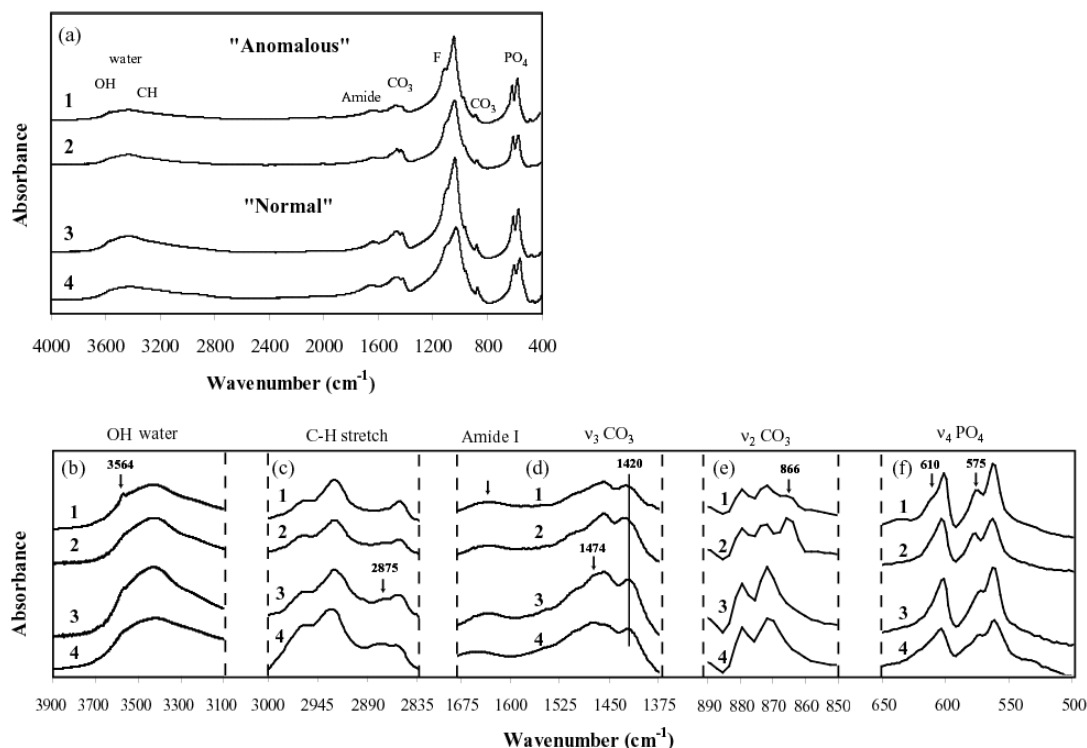


Figure 2.5 FTIR spectra of "anomalous" bones B25-WP (1) and B21-WP (2), and "normal" bones B5-WP (3) and NK356-WP (4). (a) Whole spectrum, (b) hydroxyl region, (c) C-H stretching region, (d) amide and ν_3 carbonate region, (e) ν_2 carbonate region, deconvoluted, and (f) ν_4 phosphate region, deconvoluted.

bend combination) that occurs around 1550 cm^{-1} in collagen (Boyar et al., 2004). The amide I peak (1600 to 1700 cm^{-1}) in the "normal" bone from Sudan (NK356-WP) was shifted towards higher wavenumbers relative to the other samples (Figure 2.5d), which may reflect the higher organic content of this sample (see TGA and TOC results). Such a shift was not observed for the other "normal" bone sample

The ν_2 carbonate peak of the "anomalous" bones was broader than that of the "normal" bones. Deconvolution of the ν_2 carbonate domain revealed a clear difference: "normal" bones had two sub-peaks at approximately 879 and 872 cm^{-1} , attributable to A- and B-site carbonate, respectively, while "anomalous" bones had an additional sub-peak or shoulder at 866 cm^{-1} (Figure 2.5e). Rey et al. (1989) first reported the 866 cm^{-1} sub-peak as a weak shoulder in the deconvoluted FTIR spectra of some bones, and observed

that the 866 cm^{-1} sub-peak (1) is also present in synthetic fluoridated apatites, (2) occurs in the same location as a broad band typical of amorphous calcium phosphate carbonate, and (3) is present in modern bones with low fluoride and amorphous carbonate content and is attributable to a labile, disordered domain related to early stages of apatite crystal formation. In the present study, every specimen was examined for the presence of this sub-peak. In the Sudan samples, the 866 cm^{-1} peak was either absent or present as a very weak shoulder. In contrast, the 866 cm^{-1} peak was present in the majority of the Guatemala samples, occurring as a distinct peak (as opposed to a shoulder) in about half of the samples. In two of the most “anomalous” samples (B4-WP and B21-WP), the 866 cm^{-1} peak was the largest of the three $\nu_2\text{ CO}_3$ peaks (e.g., Figure 2.5e2). In addition, the relative size of the 872 cm^{-1} peak decreased, which could indicate diminished substitution of CO_3 for PO_4 in “anomalous” bones relative to “normal” bones.

No differences were obvious in the ν_4 phosphate domain of “normal” versus “anomalous” bones before deconvolution. Deconvolution, however, showed that the 575 cm^{-1} peak/shoulder was shifted to higher wavenumbers in “anomalous” samples (Figure 2.5f). Further, there was a slight shoulder at 610 cm^{-1} in B25-WP and possibly B21-WP, which Rey et al. (1990) assigned to a labile PO_4 environment.

2.4.12 X-Ray Diffraction (XRD)

All of the peaks in the XRD spectra were characteristic of apatite, and no unusual phases (e.g., brushite, $\text{CaHPO}_4\cdot 2\text{H}_2\text{O}$) were detected in any of the samples analyzed (Figure 2.6a). Based on the separation of the [211], [112], [300], and [202] peaks, B5, B21, and B25 (both SP and WP) had greater long-range order (larger crystal sizes) than NK356, indicating greater post-mortem recrystallization of apatite.

After heating the bone samples to 950°C , the XRD spectra of “normal” bones contained both hydroxyapatite and β -TCP (whitlockite; $\beta\text{-Ca}_3\text{PO}_4$) peaks, while those of “anomalous” bones contained only hydroxyapatite peaks (Figure 2.6b). The lack of β -TCP peaks in the heat-treated “anomalous” samples may indicate that the original specimens contained relatively less HPO_4 , and different amounts of other ionic substituents, than “normal” bones (Elliott, 2002). For example Mg and Sr substitution in synthetic apatites facilitates the simultaneous incorporation of HPO_4 and promotes the

formation of β -TCP along with hydroxyapatite in heat-treated samples. In contrast, F and CO_3 substitution inhibit HPO_4 substitution and the formation of β -TCP during heating (LeGeros, 1991). That said, the “normal” and “anomalous” bones did not differ in Mg or Sr contents (Table 2.2), nor were there consistent differences in fluorine content (as represented by the peak at 1096 cm^{-1} of the FTIR spectra), or in carbonate content as measured by C/P ratios and gas yields. However, it is possible that the additional CO_3 environment detected in the ν_2 domain of the FTIR spectra of “anomalous” bones played a role in inhibiting β -TCP formation. It is also possible that HPO_4 was absent in the “anomalous” bones, and that the 866 cm^{-1} peak reflected the presence of CO_3 in sites that otherwise would have been filled by HPO_4 . Elliott (1994) reported that synthetically precipitated apatites produced pyrophosphate (a precursor to β -TCP, formed at lower temperatures) upon heating, while biological apatites did not. Thus, the XRD patterns obtained for “anomalous” bones may indicate a greater amount of apatite that precipitated during post-mortem processes.

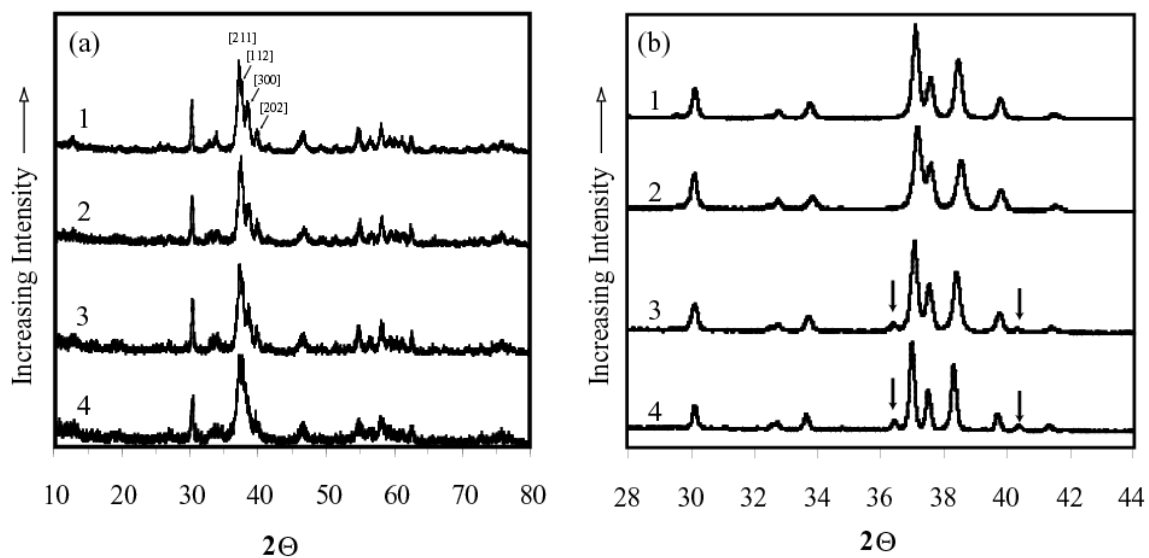


Figure 2.6 (a) XRD patterns of “anomalous” bone samples B25-WP (1) and B21-WP (2), and “normal” bone samples B5-WP (3) and NK356-WP (4). (b) XRD patterns of the same bone samples after heating to 950°C . Arrows indicate β -TCP peaks.

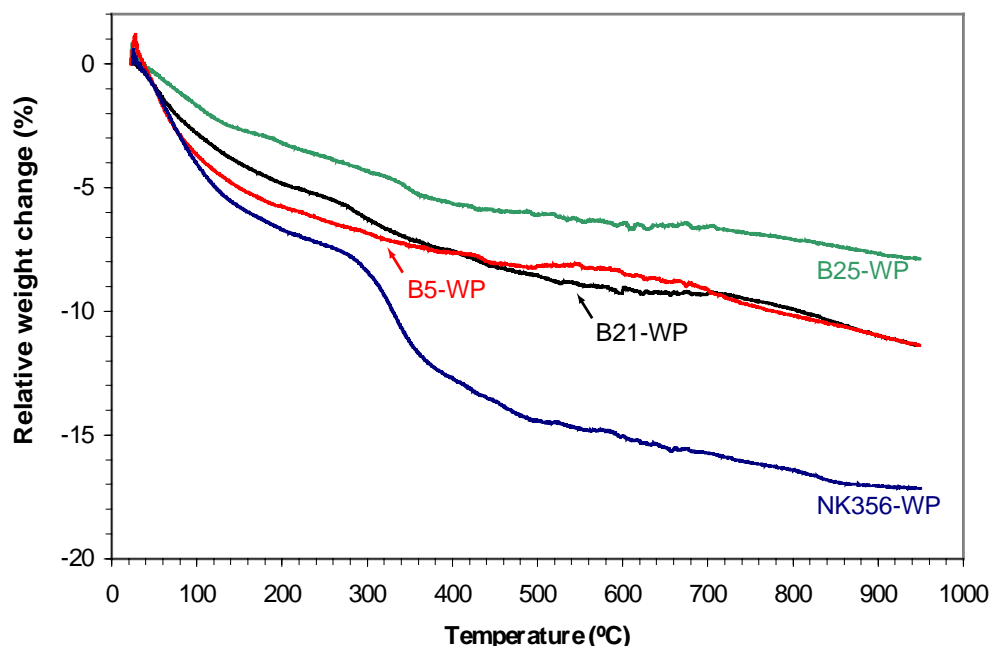


Figure 2.7 Thermogravimetric analysis of "anomalous" (B25-WP, B21-WP) and "normal" bones (B5-WP, NK356-WP).

2.4.13 Thermogravimetric Analysis (TGA)

The Sudan sample (NK356-WP) lost 17.2% of its weight after heating to 950°C, and its weight loss curve was characterized by steps, indicating loss of volatile components at discrete temperature intervals (Figure 2.7). In contrast, the Guatemala samples lost weight gradually and continuously, and experienced less total weight loss (7.9 to 11.4%) than the Sudan sample (Figure 2.7). Between 25 and ~250°C the two "anomalous" bones experienced less weight loss and lower rates of weight change than the "normal bones", probably because the former contained less water (Mkukuma et al., 2004; Peters et al., 2000). Between 250 and ~600°C, weight loss occurred primarily because of combustion of organic matter (Peters et al., 2000). During this interval, all of the samples from Guatemala ("normal" and "anomalous") exhibited similar weight losses, whereas the "normal" bone sample from Sudan (NK356-WP) exhibited a much greater change (Figure 2.7).

Table 2.2 Total inorganic carbon (TIC), total organic carbon (TOC), calcium, phosphorus, and trace element contents of "anomalous" (B25, B21) and "normal" bones (B5, NK356).

Sample	TIC (%)		TOC (%)		Ca (%)	P (%)	N (%)	Al (%)	B (%)	Ba (%)	Cu (%)	Fe (%)	K (%)	Mg (%)	Mn (%)	Na (%)	S (%)	Si (%)	Sr (%)	Zn (%)
	WP	SP	WP	SP																
B25	0.9	0.9	0.6	0.8	22.6	11.4	0.04	0.22	0.01	0.00	0.01	0.11	0.00	0.04	0.03	0.18	0.03	0.12	0.02	0.03
B21	1.5	1.7	0.7	0.7	22.9	11.4	0.03	0.23	0.01	0.00	0.01	0.11	0.00	0.04	0.03	0.18	0.03	0.11	0.02	0.03
B5	1.3	1.4	0.3	0.6	21.5	11.3	0.03	0.13	0.01	0.04	0.00	0.95	0.00	0.07	0.29	0.29	0.03	0.02	0.04	0.02
NK356	1.4	1.7	2.2	0.4	22.8	12.1	0.03	0.02	0.01	0.00	0.00	0.06	0.01	0.12	0.00	0.56	0.07	0.02	0.00	0.02

Ca, P, and trace element contents were measured following the strong pretreatment (SP).

2.4.14 Total Inorganic Carbon / Total Organic Carbon (TIC/TOC)

TIC values for all samples were slightly higher for SP than WP (Table 2.2). Given that the stronger acid should have dissolved more carbonate, it is possible that a proportion of dissolved carbonate recrystallized during the procedure. Treatment with 1 M acetic acid can cause bioapatite to recrystallize to brushite (Koch et al., 1997; Lee-Thorp and van der Merwe, 1991; Sillen and Sealy, 1995), but there was no evidence of brushite in the XRD spectra. Moreover, since SP samples were less "anomalous" than WP samples, putative addition of inorganic carbon cannot be responsible for the "anomalous" isotope results. Finally, the two "anomalous" samples had both the highest and the lowest TIC values, which further indicates that TIC is not related to the unusually low $\delta^{18}\text{O}$ values.

The "normal" Sudan bone (NK356) had the highest TOC of the WP samples but the lowest TOC of the SP samples (Table 2.2), likely because more collagen was removed during the strong pretreatment. In contrast, the TOC contents of the Guatemala samples were not diminished by the strong pretreatment. This might reflect the presence of highly stable, non-collagenous organic matter. For the Guatemala samples, TOC contents after either pretreatment were higher in the "anomalous" samples than in the "normal" sample.

2.4.15 Nitrogen Content

All samples had very low nitrogen contents (0.03 to 0.04%), and there was no systematic difference between "normal" and "anomalous" samples (Table 2.2).

2.4.16 Inductively-Coupled Plasma Atomic Emission Spectroscopy (ICP-AES)

All samples were predominantly composed of Ca and P (Table 2.2). “Anomalous” bones had slightly higher Al and Si contents, and lower Na contents, than “normal bones”, but there were no other systematic differences (Table 2.2).

2.5 Discussion

2.5.1 What Was the Contaminant Gas, and What Was its Relationship to Low $\delta^{18}\text{O}$ Values?

When some bones were reacted with ortho-phosphoric acid at high temperatures, and the gases produced by the reaction were simultaneously captured using cryogenic traps, a contaminant gas was subsequently transferred to the mass spectrometer along with CO_2 . The contribution of the contaminant gas to the m/z 44 through 49 signals resulted in apparently low $\delta^{18}\text{O}$ values.

The C25, GB50, MP50-S, and MP90-S methods resulted in “normal” $\delta^{18}\text{O}$ values because the samples were reacted in a sealed system, allowing the contaminant gas (if produced) to back-react or recombine with other compounds present during the reaction (i.e., phosphoric acid, phosphate polymers in solution, water produced when carbonate was converted to CO_2 , trace ions from dissolved bone samples, or non-condensable gases). In contrast, the MP-50 and MP-90 methods led to the measurement of “anomalous” $\delta^{18}\text{O}$ values because the samples were reacted in a system that cryogenically removed the contaminant gas (along with CO_2) as soon as it was produced, preventing any back-reaction with other compounds in the reaction vessel. In support of the hypothesis that the back-reaction involves compounds that remain in the reaction vessel, an aliquot of CO_2 and the contaminant gas were cryogenically removed from the reaction vessel and left in a second sealed vessel at room temperature overnight, after which the contaminant gas was still present. Greater quantities of contaminant gas, leading to still lower $\delta^{18}\text{O}$ values, were produced at 90°C than at 50°C . At higher temperatures, the reaction between the bone sample and phosphoric acid occurred more rapidly, allowing

less time for back-reaction before the contaminant gas was isolated from the reaction vessel.

Table 2.3 Selected compounds with mass to charge ratios (m/z) of 44 or 47. Minor masses (m/z) associated with these compounds are discussed in the text.

m/z	Mass (m)	Charge (z)	Compound
44	44	1+	N ₂ O, H ₂ N ₃ , CH ₂ NO, CH ₄ N ₂ , C ₂ H ₄ O, C ₂ H ₆ N, C ₂ HF, C ₃ H ₈ , CS
	88	2+	N ₄ O ₂ , CN ₂ O ₃ , CH ₂ N ₃ O ₂ , CH ₄ N ₄ O, C ₂ O ₄ , C ₂ H ₄ N ₂ O ₂ , C ₄ H ₈ O ₂
47	47	1+	HNO ₂ , H ₃ N ₂ O, H ₅ N ₃ , CH ₃ O ₂ , CH ₅ NO, COF, SNH, CCl, PO
	94	2+	H ₂ N ₂ O ₄ , H ₄ N ₃ O ₃ , H ₆ N ₄ O ₂ , CH ₄ NO ₄ , CH ₆ N ₂ O ₃ , C ₂ H ₆ O ₄ , C ₃ N ₃ O, C ₃ H ₂ N ₄ , C ₄ NO ₂ , C ₄ H ₂ N ₂ O, C ₄ H ₄ N ₃ , C ₅ H ₂ O ₂ , C ₅ H ₄ NO, C ₅ H ₆ N ₂ , C ₆ H ₆ O, C ₆ H ₈ N, C ₇ H ₁₀

Note: Minor masses (m/z) associated with these compounds are discussed in the text.

The contaminant gas included ionized compounds with m/z 47, 48, and 49. The clustering of a large peak (m/z 47) along with two much smaller peaks (m/z 48 and 49) (Figure 2.2) suggests that they are isotopologues of the same molecule. Compounds with a major mass of 47 or 94 (which would produce a peak at m/z 47 if they had a 2+ charge) are listed in Table 2.3 (Elliott et al., 2005; Hoffmann et al., 1996). In mass scans of “anomalous” bones, the m/z 49 peak intensity was greater than that of the m/z 48 peak. Of the molecules listed in Table 2.3, only SNH, CCl, and PO have this pattern of intensities. However, HNO₂ and H₂N₂O₄ have an m/z 48 peak that is only slightly more intense than the m/z 49 peak, and a slight increase in peak intensity of m/z 49 might result from overlap with minor isotopologues of another compound.

We have considered two ways that the contaminant gas could cause large decreases in $\delta^{18}\text{O}$ values (46/44 ratios) and slight increases in $\delta^{13}\text{C}$ values (45/44 ratios). The first possibility is that the contaminant gas simultaneously contributed to the m/z 44 and 45 signals, but not the 46 signal. This scenario does not require the contaminant gas to contain oxygen, nor does it require a change in the oxygen or carbon isotope composition of CO₂. Mucciarone and Williams (1990) describe an analogous situation where NO₂ gas (m/z 46) was released from ammonium-bearing minerals and interfered with CO₂ peaks, producing anomalously *high* $\delta^{18}\text{O}$ values. There are numerous

compounds with major masses at 44 or 88, which might increase the m/z 44 signal, causing the apparent $\delta^{18}\text{O}$ value to decrease (Table 2.3) (Epstein et al., 1951; Hoffmann et al., 1996). Of these, CS has an m/z 46 peak intensity that is greater than that of the m/z 45, which would cause apparent $\delta^{18}\text{O}$ values to decrease less than $\delta^{13}\text{C}$ values, contrary to our observations. The remaining compounds all have isotopologues with abundances decreasing from m/z 44 to 46, which suggests that they could have caused the observed changes in 46/44 and 45/44 ratios. That said, it seems that no single compound can explain both the change in 46/44 ratios and the presence of m/z 47-49 peaks. However, it is possible that two different compounds were produced during reaction with phosphoric acid, or that a single molecule was fragmented in the ionization chamber of the mass spectrometer.

The second possibility is that the presence of the contaminant gas was linked to a decreased m/z 46 but relatively constant 44 and 45 signals. Oxygen isotope fractionation would change the 46/44 ratio with minimal effect on the 45/44 ratio, as long as carbon isotope fractionation did not occur as well. The only oxygen-bearing compound with the observed pattern of m/z 47, 48, and 49 peak intensities is PO^- . PO^- could be derived from the ortho-phosphoric acid, which contains various phosphate polymers ($\text{H}_{(2+n)}\text{P}_n\text{O}_{(3n+1)}$) with unknown oxygen isotope fractionations (Swart et al., 1991). However, since the same phosphoric acid was used for all reactions, the acid alone could not be responsible for the putative PO^- production. A more likely explanation is that PO^- was derived from an oxyphosphorus compound in the bone itself. The production and volatilization of PO^- or its precursor appears to be reversible, given that reaction in a sealed system prior to cryogenic separation was characterized by “normal” oxygen isotope values and no contaminant gas. Morris and Viggiano (1998) demonstrated PO^- formation from dimethyl phosphate in an electron impact ion source. An analogous reaction may have occurred in the ion source of the IRMS. Regardless of its origin, PO^- on its own would not affect the ratios of masses 44-46, since it does not contain masses in that range. However, a reaction between CO_2 derived from carbonate in bone and PO^- derived from phosphate polymers dissolved in acid could explain the anomalous $\delta^{18}\text{O}$ values and the presence of the contaminant gas. PO^- has been shown to scavenge oxygen from CO_2 (Morris and

Viggiano, 1998), which almost certainly would change the oxygen isotope composition of the remaining CO₂.

2.5.2 What Was Different about the “Anomalous” Bones?

What was different about “anomalous” bone samples that caused the formation of the contaminant gas? There is no evidence that the pretreatment methods produced a new phase; on the contrary, more “anomalous” results were obtained using the weak pretreatment, suggesting that (1) a contaminant was already present in the bone, and/or (2) structural-chemical changes to the bone occurred during post-mortem alteration.

The greater extent of post-mortem alteration in the Guatemala samples relative to the Sudan samples was evident from the phosphate-carbonate $\delta^{18}\text{O}$ comparisons (Figure 2.3), CI values (Table 2.1), histology (Figure 2.4), XRD patterns (Figure 2.6), and TGA curves (Figure 2.7). However, “anomalous” and “normal” Guatemala samples did not differ systematically in their phosphate oxygen isotope compositions, overall crystallinities, carbonate to phosphate ratios, or total gas yields (measured for the C25 and MP90 methods). XRD and FTIR spectra of all samples were characteristic of apatite, with no evidence for significant organic or inorganic contamination. Nevertheless, it remains possible that a contaminant was present in such small quantities that it was not detectable using these methods. Based on the m/z values and peak intensities (Table 2.3), this contaminant phase conceivably could have been an organic compound or a nitrogen oxide. The slightly higher TOC contents of the “anomalous” Guatemala samples relative to the “normal” Guatemala samples (Table 2.2) could be indicative of an organic contaminant, but the higher TOC values of SP relative to WP samples were not correlated with the most “anomalous” $\delta^{18}\text{O}$ values, which were obtained for the WP samples. Alternatively, the slightly higher Al and Si contents of “anomalous” bones relative to “normal” bones (Table 2.2) could reflect aluminosilicate contaminants, which might have contained ammonium in their interlayer sites (Mucciarone and Williams, 1990). The ammonium could have been released during higher temperature reactions with orthophosphoric acid and then reacted to form N₂O (causing the observed large change in 46/44 and smaller change in 45/44 ratios) and HNO₂ (producing the m/z 47, 48, and 49 peaks). However, there was no difference in nitrogen content between “normal” and

“anomalous” bones. That said, this may have been a result of greater collagen preservation in “normal” bones offset by greater organic contamination in “anomalous” bones.

The two most striking differences between “normal” and “anomalous” bones were that the latter (1) contained an unusual structural carbonate environment, indicated by the peak at 866 cm^{-1} in the deconvoluted FTIR spectra, and (2) lacked β -TCP peaks in their post-heating XRD spectra, which may indicate an absence of HPO_4 in the original specimens. These differences suggest that changes to the structural state of the CO_3 and PO_4 groups originally present in bone influenced the production of the contaminant gas. These changes likely caused PO^- or a larger “precursor” molecule to be volatilized during the reaction between bone and ortho-phosphoric acid.

2.5.3 Method-Dependent Differences for “Normal” Bones

The $\delta^{18}\text{O}$ values obtained using higher temperature methods tended to be lower than those obtained using lower temperature methods, even for “normal” bones (Table 2.1). Although these differences were much smaller than the method-dependent differences observed in the “anomalous” bones, they could significantly affect reconstructions of paleoclimate or inferences about migration. For example, the average difference in $\delta^{18}\text{O}$ values between the MP-90 method and C25/GB50 methods for “normal” Sudan bone samples was 1.4‰, which corresponds to an error of about 2°C in a mean annual temperature estimate calculated using the apparent oxygen isotope fractionation between structural carbonate in bioapatite and body water (Bryant et al., 1996) and the modern relationship between the $\delta^{18}\text{O}$ value of meteoric water and mean annual temperature (Dansgaard, 1964).

2.6 Conclusions

The contaminant gas has not been conclusively identified. However, the lack of physical or chemical evidence for a contaminant phase, the changes to the structural environment of carbonate and phosphate groups in “anomalous” bones, and the relative intensities of the contaminant m/z 47, 48, and 49 peaks suggest that PO^- (or a molecule that contains PO^-) was produced when “anomalous” bones reacted with phosphoric acid,

and that low oxygen isotope values resulted from oxygen isotope fractionation during this process. Lower reaction temperatures diminished the amount of contaminant gas produced, but did not prevent its formation altogether. The contaminant gas was “removed” (and “anomalous” $\delta^{18}\text{O}$ measurements avoided) by reacting the sample in a sealed vessel, which allowed the contaminant gas to back-react with other compounds (likely phosphate polymers in acid).

In this study, measures commonly used as diagenetic indicators (e.g., $\delta^{18}\text{O}_p$ vs $\delta^{18}\text{O}_{sc}$ plots, FTIR crystallinity indices and C/P values, XRD patterns, thin section histology) were not useful in predicting which bones would produce “anomalous” $\delta^{18}\text{O}$ values. The most consistent predictor of low $\delta^{18}\text{O}$ values was the presence of the 866 cm^{-1} peak/shoulder in the deconvoluted $\nu_2\text{ CO}_3$ domain of the FTIR spectrum, which indicated the presence of a unique CO_3 environment, possibly amorphous or fluorine-associated CO_3 .

Significant error may be introduced to studies of past environments and behaviours if comparisons are made among $\delta^{18}\text{O}$ values that were obtained using different analytical methods, even if the bones did not produce a contaminant gas. Further investigation is needed to determine whether the method-dependent variations among “normal” bones resulted from a difference between the temperature-dependent fractionation of CO_2 during the structural carbonate (bioapatite) vs. calcite reactions with orthophosphoric acid.

2.7 References

- Bigi, A., Cojazzi, G., Panzavolta, S., Ripamonti, A., Roveri, N., Romanello, M., Suarez, K.N. and Moro, L., 1997. Chemical and structural characterization of the mineral phase from cortical and trabecular bone. *Journal of Inorganic Biochemistry*, 68(1): 45-51.
- Bocherens, H., Fogel, M.L., Tuross, N. and Zeder, M., 1995. Trophic structure and climatic information from isotopic signatures in Pleistocene cave fauna of Southern England. *Journal of Archaeological Science*, 22(2): 327-340.
- Boyar, H., Zorlu, F., Mut, M. and Severcan, F., 2004. The effects of chronic hypoperfusion on rat cranial bone mineral and organic matrix: A Fourier Transform Infrared spectroscopy study. *Analytical and Bioanalytical Chemistry*, 379(3): 433-438.
- Bryant, J.D., Koch, P., Froelich, P.N., Showers, W.J. and Genna, B.J., 1996. Oxygen isotope partitioning between phosphate and carbonate in mammalian apatite. *Geochimica et Cosmochimica Acta*, 60(24): 5145-5148.
- Coplen, T.B., 1994. Reporting stable hydrogen, carbon, and oxygen isotopic abundances. *Pure and Applied Chemistry*, 66: 271-276.
- Dansgaard, W., 1964. Stable isotopes in precipitation. *Tellus*, 16: 436-468.
- Dupras, T.L. and Schwarcz, H.P., 2001. Strangers in a strange land: Stable isotope evidence for human migration in the Dakhleh Oasis, Egypt. *Journal of Archaeological Science*, 28(11): 1199-1208.
- Elagib, N.A. and Mansell, M.G., 2000. Recent trends and anomalies in mean seasonal and annual temperatures over Sudan. *Journal of Arid Environments*, 45(3): 263-288.
- Elliott, J.C., 1994. Structure and Chemistry of the Apatites and other Calcium Orthophosphates. *Studies in Inorganic Chemistry*, 18. Elsevier Science, Amsterdam.
- Elliott, J.C., 2002. Calcium phosphate biominerals. In: M.J. Kohn, J. Rakovan and J.M. Hughes (Editors), *Phosphates: Geochemical, Geobiological, and Materials Importance. Reviews in Mineralogy and Geochemistry*. Mineralogical Society of America, Washington, D.C., pp. 427-453.
- Elliott, V.L., McLeod, C.W. and Marshall, P.S., 2005. Combination of gel electrophoresis and ICP-mass spectrometry: novel strategies for phosphoprotein measurement. *Analytical and Bioanalytical Chemistry*, 383(3): 416-423.
- Epstein, S., Buchsbaum, R., Lowenstam, H. and Urey, H.C., 1951. Carbonate-water isotopic temperature scale. *Bulletin of the Geological Society of America*, 62: 417-426.
- Friedman, I. and O'Neil, J.R., 1977. Compilation of stable isotope fractionation factors of geochemical interest. In: M. Fleischer (Editor), *Data of Geochemistry 6th Edition*. Government Printing Office, Washington, D.C.
- Garvie-Lok, S.J., Varney, T.L. and Katzenberg, M.A., 2004. Preparation of bone carbonate for stable isotope analysis: the effects of treatment time and acid concentration. *Journal of Archaeological Science*, 31(6): 763-776.
- Hoffmann, E.d., Charette, J.J. and Stroobant, V., 1996. *Mass Spectrometry: Principles and Applications*. John Wiley & Sons, New York, xii, 340 p. pp.

- Hoppe, K.A., 2004. Late Pleistocene mammoth herd structure, migration patterns, and Clovis hunting strategies inferred from isotopic analyses of multiple death assemblages. *Paleobiology*, 30(1): 129-145.
- Iacumin, P., Bocherens, H., Mariotti, A. and Longinelli, A., 1996. Oxygen isotope analyses of co-existing carbonate and phosphate in biogenic apatite: a way to monitor diagenetic alteration of bone phosphate? *Earth and Planetary Science Letters*, 142: 1-6.
- Kauppinen, J.K., Moffatt, D.J., Mantsch, H.H. and Cameron, D.G., 1981. Fourier self-deconvolution: a method for resolving intrinsically overlapped bands. *Applied Spectroscopy*, 35(3): 271-276.
- Koch, P.L., Hoppe, K.A. and Webb, S.D., 1998. The isotopic ecology of late Pleistocene mammals in North America - Part 1. Florida. *Chemical Geology*, 152(1-2): 119-138.
- Koch, P.L., Tuross, N. and Fogel, M.L., 1997. The effects of sample treatment and diagenesis on the isotopic integrity of carbonate in biogenic hydroxylapatite. *Journal of Archaeological Science*, 24(5): 417-429.
- Kohn, M.J. and Law, J.M., 2006. Stable isotope chemistry of fossil bone as a new paleoclimate indicator. *Geochimica et Cosmochimica Acta*, 70(4): 931-946.
- Lee-Thorp, J.A. and van der Merwe, N.J., 1991. Aspects of the chemistry of modern and fossil biological apatites. *Journal of Archaeological Science*, 18: 343-354.
- LeGeros, R.Z., 1991. *Calcium Phosphates in Oral Biology and Medicine*. Monographs in Oral Science, 15. Karger, New York.
- McCrea, J.M., 1950. On the isotopic chemistry of carbonates and a paleotemperature scale. *Journal of Chemical Physics*, 18: 849-857.
- Mkukuma, L.D., Skakle, J.M.S., Gibson, I.R., Imrie, C.T., Aspden, R.M. and Hukins, D.W.L., 2004. Effect of the proportion of organic material in bone on thermal decomposition of bone mineral: an investigation of a variety of bones from different species using thermogravimetric analysis coupled to mass spectrometry, high-temperature X-ray diffraction, and Fourier transform infrared spectroscopy. *Calcified Tissue International*, 75(4): 321-328.
- Morris, R.A. and Viggiano, A.A., 1998. Chemistry of PO⁻, PO²⁻, and PO³⁻ in the gas phase. *Journal of Chemical Physics*, 109(10): 4126-4127.
- Mucciarone, D.A. and Williams, D.F., 1990. Stable isotope analyses of carbonate complicated by nitrogen-oxide contamination: a Delaware Basin example. *Journal of Sedimentary Petrology*, 60(4): 608-614.
- Pasteris, J.D., Wopenka, B., Freeman, J.J., Rogers, K., Valsami-Jones, E., van der Houwen, J.A.M. and Silva, M.J., 2004. Lack of OH in nanocrystalline apatite as a function of degree of atomic order: implications for bone and biomaterials. *Biomaterials*, 25(2): 229-238.
- Peters, F., Schwarz, K. and Epple, M., 2000. The structure of bone studied with synchrotron X-ray diffraction, X-ray absorption spectroscopy and thermal analysis. *Thermochimica Acta*, 361(1-2): 131-138.
- Piepenbrink, H., 1989. Examples of chemical changes during fossilisation. *Applied Geochemistry*, 4: 273-280.
- Puceat, E., Reynard, B. and Lecuyer, C., 2004. Can crystallinity be used to determine the degree of chemical alteration of biogenic apatites? *Chemical Geology*, 205(1-2): 83-97.

- Rey, C., Collins, B., Goehl, T., Dickson, I.R. and Glimcher, M.J., 1989. The carbonate environment in bone mineral: a resolution-enhanced Fourier Transform Infrared spectroscopy study. *Calcified Tissue International*, 45(3): 157-164.
- Rey, C., Miquel, J.L., Facchini, L., Legrand, A.P. and Glimcher, M.J., 1995. Hydroxyl groups in bone mineral. *Bone*, 16(5): 583-586.
- Rey, C., Shimizu, M., Collins, B. and Glimcher, M.J., 1990. Resolution-enhanced Fourier-Transform Infrared spectroscopy study of the environment of phosphate ions in the early deposits of a solid phase of calcium-phosphate in bone and enamel, and their evolution with age. I: Investigations in the ν_4 PO₄ domain. *Calcified Tissue International*, 46(6): 384-394.
- Rink, W.J. and Schwarcz, H.P., 1995. Tests for diagenesis in tooth enamel: ESR dating signals and carbonate contents. *Journal of Archaeological Science*, 22(2): 251-255.
- Shemesh, A., 1990. Crystallinity and diagenesis of sedimentary apatites. *Geochimica et Cosmochimica Acta*, 54(9): 2433-2438.
- Sillen, A. and Sealy, J.C., 1995. Diagenesis of Strontium in Fossil Bone: a Reconsideration of Nelson et al. (1986). *Journal of Archaeological Science*, 22(2): 313-320.
- Sponheimer, M. and Lee-Thorp, J.A., 1999. Alteration of enamel carbonate environments during fossilization. *Journal of Archaeological Science*, 26(2): 143-150.
- Stuart-Williams, H.L., 1996. Analysis of the Variation of Oxygen Isotopic Composition of Mammalian Bone Phosphate. Ph.D. Thesis, McMaster University, Hamilton.
- Swart, P.K., Burns, S.J. and Leder, J.J., 1991. Fractionation of the stable isotopes of oxygen and carbon in carbon dioxide during the reaction of calcite with phosphoric acid as a function of temperature and technique. *Chemical Geology*, 86: 89-96.
- Weiner, S. and Bar-Yosef, O., 1990. States of preservation of bones from prehistoric sites in the Near East: a survey. *Journal of Archaeological Science*, 17: 187-196.
- Wopenka, B. and Pasteris, J.D., 2005. A mineralogical perspective on the apatite in bone. *Materials Science & Engineering C: Biomimetic and Supramolecular Systems*, 25(2): 131-143.
- Wright, L.E. and Schwarcz, H.P., 1996. Infrared and isotopic evidence for diagenesis of bone apatite at Dos Pilas, Guatemala: paleodietary implications. *Journal of Archaeological Science*, 23: 933-944.

Chapter 3

Nursing, weaning, and tooth development in woolly mammoths from Old Crow, Yukon, Canada: Implications for Pleistocene extinctions¹**3.1 Introduction**

Nursing has important immunological benefits and influences infant health, growth and survival (Katzenberg et al., 1996; Knodel and Kintner, 1977; Main et al., 2004; Stumpf and Welsch, 2004). Weaning, the introduction and gradual increase in consumption of non-milk foods, can vary greatly in timing and duration even within a species. The timing of weaning can be related to environmental stressors. For example, the duration of nursing among modern elephants is shorter under favourable environmental conditions, since mothers have subsequent offspring sooner than they do under harsher conditions (Lee and Moss, 1986). Furthermore, lactation is a substantial metabolic investment for females (Vaughan et al., 2000), and in very dry environments can be affected by water availability (Jenness, 1974). An understanding of species-specific nursing and weaning behaviours can thus provide insights into the degree of environmental stress experienced by animals. For extinct taxa such as woolly mammoths (*Mammuthus primigenius*), this could improve our understanding of the population dynamics that preceded their extinction during the Terminal Pleistocene/Early Holocene (Barnosky et al., 2004; Fisher, 1996, 2009; Koch and Barnosky, 2006).

The stable isotope and trace element compositions of skeletal remains can provide important information about the duration of nursing and timing of weaning. General trends (e.g., high $\delta^{15}\text{N}$ values in nursing infants and high Sr/Ca ratios in infants undergoing weaning) have been previously identified for several species (e.g., Humphrey et al., 2008b; Jenkins et al., 2001). However, relatively little is known about species-specific effects of weaning on trace element ratios (especially Ba/Ca ratios). Furthermore, substantial variations in the effects of nursing and weaning on $\delta^{13}\text{C}$ and $\delta^{15}\text{N}$ values have been observed, both among and within species (e.g., Jenkins et al., 2001). Thus, it is

¹ A version of this chapter has been published:

Metcalfe, J.Z., Longstaffe, F.J. and Zazula, G.D., 2010. Nursing, weaning, and tooth development in woolly mammoths from Old Crow, Yukon, Canada: Implications for Pleistocene extinctions. *Palaeogeography Palaeoclimatology Palaeoecology*, 298: 257-270.

necessary to determine species-, diet- and environment-specific relationships between mothers and offspring in order to make inferences about weaning from stable isotope compositions.

To our knowledge only one isotopic study of modern elephants has focused on age-related changes, and its results are complicated by mixed C₃-C₄ diets, and did not include nitrogen isotope analysis (Sukumar and Ramesh, 1992). One other study has paved the way for studies of nursing and weaning in woolly mammoths by using the isotopic composition of a serially-sampled juvenile tusk to reconstruct the timing of weaning (Rountrey et al., 2007). This approach provided detailed information about changes within the lifetime of one individual (an “intra-individual” approach), but as these authors pointed out, analysis of many individuals is needed to identify general age-related trends. The effects of nursing and weaning on mammoth stable isotope compositions have not previously been explored using groups of multiple individuals (an “inter-individual”, or population approach). Together, these two approaches can provide a more complete picture of woolly mammoth behavioral ecology.

The present study investigates the carbon, nitrogen, and oxygen isotope compositions, and trace element contents, of juvenile and adult woolly mammoth (*Mammuthus primigenius*) skeletal remains from Old Crow, Yukon, using a population approach. Teeth, which form during particular stages of an animal’s life, were sampled so that defined age categories could be compared. We aim to determine the nature and magnitude of changes in stable isotope compositions and trace element contents that result from nursing and weaning, and to identify general trends in the timing of nursing and weaning in woolly mammoths.

3.1.1 Elephant Nursing and Weaning

The social behaviour of modern elephants (*Loxodonta and Elephas*) is a useful reference for understanding the behaviour of extinct proboscideans (Haynes, 1991). Newborn African elephants nurse exclusively until about 3 months of age, after which they begin consuming vegetation (Lee and Moss, 1986; Owen-Smith, 1988). Weaning is very gradual. Juveniles can survive without milk by about 2 years of age, but typically continue to nurse until the birth of the mother’s next offspring, after about 3 to 6 years

(Lee and Moss, 1986; Owen-Smith, 1988; Sukumar, 2003). The duration of inter-birth intervals are related to food availability (mean = 3.5 in years of high food availability and 5.6 in years of low food availability) (Lee and Moss, 1986). About 15% of juveniles continue to nurse even after their sibling is born, for up to 8 years (Lee and Moss, 1986).

3.1.2 Stable Isotopes and Nursing/Weaning

3.1.2.1 Carbon

The isotopic composition of infant tissues is dependent on the isotopic composition of infant diets (milk and any supplemental foods) and the tissue-specific isotopic fractionations relative to diet. The isotopic composition of the macromolecules in milk is equal to those in the lactating female's diet, plus any metabolic isotopic fractionation that occurs during milk production. Milk fats tend to have lower $\delta^{13}\text{C}$ values than carbohydrates, whereas the $\delta^{13}\text{C}$ values of proteins are higher (Camin et al., 2008; Wilson et al., 1988). Because it is relatively high in fat, milk is typically depleted of ^{13}C relative to diet (Boutton et al., 1988; Jenkins et al., 2001; Knobbe et al., 2006; Miller et al., 2008). Although different species have different digestive pathways (e.g., ruminant vs. nonruminant) and relative abundances of milk macronutrients (Jenness, 1974), studies of multiple species (e.g., bear, moose, caribou, cow, and mice) have reported an average 1-2‰ depletion of ^{13}C in milk relative to diet (Boutton et al., 1988; Jenkins et al., 2001; Knobbe et al., 2006; Miller et al., 2008). Some studies have found $\delta^{13}\text{C}$ values for milk that were higher than those of the diet (e.g., Camin et al., 2008; Knobbe et al., 2006; Masud et al., 1999; Metges et al., 1990). However, those studies involved switches between C_4 and C_3 diets followed by relatively short dietary equilibration times, which likely led to a difference between the $\delta^{13}\text{C}$ values of previously-formed body tissues (e.g., stored fat) and newly-formed milk. Since the metabolism of body tissues is important in milk production (Wilson et al., 1988), and lipids have a longer and more complex metabolic pathway than carbohydrates (Masud et al., 1999), milk formed after a dietary switch may be comprised partly of lipids derived from the earlier diet. That said, no such dramatic dietary shifts should have affected Yukon mammoths, since C_4 plants were

essentially absent from Beringia during the Pleistocene (Wooller et al., 2007; Zazula and Wooller, 2008).

All else being equal, we would expect infant tissues that form before birth to have $\delta^{13}\text{C}$ values equivalent to those of the mother, and tissues that form during nursing to have $\delta^{13}\text{C}$ values 1-2‰ lower than the mother, because of the ^{13}C -depletion of milk. However, this model does not take into account the “routing” of certain macromolecules in the diet to specific body tissues (Schwarcz, 2000). Collagen is primarily constructed from proteins in the diet, while structural carbonate in bioapatite is formed from the bulk metabolic carbon pool, derived from the whole diet (Ambrose and Norr, 1993; Tieszen and Fagre, 1993). Thus, we expect the $\delta^{13}\text{C}_{\text{sc}}$ values of nursing infants to be lower than those of their mothers, and the $\delta^{13}\text{C}_{\text{col}}$ values of nursing infants to be more similar to those of their mothers.

Some studies support the hypothesis that $\delta^{13}\text{C}_{\text{sc}}$ values of teeth that develop during nursing are lower than those of teeth that develop after weaning (e.g., Wright and Schwarcz, 1998), while others have found no age-related differences in $\delta^{13}\text{C}_{\text{sc}}$ values (e.g., Williams et al., 2005). Numerous archaeological and modern studies have shown that human infants have collagen and keratin $\delta^{13}\text{C}$ values that are ~1‰ higher than those of adults (Fogel et al., 1989; Fuller et al., 2006; Fuller et al., 2003; Katzenberg et al., 1993; Williams et al., 2005), which has been attributed to a trophic level effect. However, studies of other species have shown depletions of ^{13}C in infant collagen relative to adults (e.g., Witt and Ayliffe, 2001), which was attributed to rapid growth rate. Still other studies have observed no differences between $\delta^{13}\text{C}$ values of mothers and nursing offspring (Ducatez et al., 2008; Newsome et al., 2006). In a controlled study of a variety of species, Jenkins et al. (2001) found no difference between the $\delta^{13}\text{C}$ values of plasma from mothers and those of their nursing offspring. Their research showed that the ^{13}C -depletion of milk relative to mother’s plasma was offset by the trophic enrichment between milk and offspring plasma. In summary, comparisons of $\delta^{13}\text{C}$ values between infants and mothers/adults have yielded a range of results, some of which may be species-specific.

3.1.2.2 Nitrogen

Animal tissues are typically enriched in ^{15}N relative to the diet (Minagawa and Wada, 1984). Milk is enriched in ^{15}N relative to the lactating female's diet by about 2-3‰ for cows (Camin et al., 2008; Knobbe et al., 2006; Masud et al., 1999), mice (Miller et al., 2008), moose, caribou, bears, deer, coyotes, rabbits, sheep, pigs, and cats (Jenkins et al., 2001), so healthy nursing infants should have higher $\delta^{15}\text{N}$ values than their mothers. Enrichment in ^{15}N of infant tissues has been demonstrated for species as diverse as voles (Sare et al., 2005), polar bears (Polischuk et al., 2001), seals and sea lions (Ducatez et al., 2008; Newsome et al., 2006; York et al., 2008), meerkats (Dalerum et al., 2007), and humans (Fogel et al., 1989; Fuller et al., 2006; Fuller et al., 2003; Williams et al., 2005).

The magnitude of ^{15}N enrichment during nursing depends on the tissue and on the physiology and metabolism of the animal. For example, during the first 2 months of nursing, caribou and grizzly bear offspring had plasma $\delta^{15}\text{N}$ values about 2‰ higher than their mothers, but there was no difference between offspring and mothers for moose (Jenkins et al., 2001). Fogel et al. (1989) found a 2.4‰ enrichment in ^{15}N for human infant nail clippings relative to those of their mothers. In a more recent study of modern human mother-infant pairs, Fuller et al. (2006) found ^{15}N -enrichments of 2-3‰ in nails and hair of exclusively breastfed infants (relative to mothers), reduced enrichments in infants fed both breast milk and formula, and no enrichment in infants fed exclusively on formula. Numerous archaeological studies have also found ^{15}N -enrichment in infants, and have interpreted the age at which infant $\delta^{15}\text{N}$ values become equivalent to those of adults as the age of weaning. However, Balasse et al. (2001) caution that for herbivores (who consume low-protein plants), protein from milk may continue to make the largest amino acid contribution to collagen, even when relatively small amounts of milk are consumed. In addition, the gradual formation of collagen and the averaging that occurs during sampling could cause a "nursing" signal to be retained for some time after most nursing has ceased. Fuller et al. (2006) found that even during human infant weaning, $\delta^{15}\text{N}$ values did not decrease to maternal levels as quickly as $\delta^{13}\text{C}$ values. Thus, $\delta^{15}\text{N}$ values of infants are most useful for identifying the duration of nursing, but not necessarily the initiation of weaning.

3.1.2.3 Oxygen

Most of the oxygen in milk occurs as water, and is derived from drinking water and plant water in the diet. Cow milk is enriched in ^{18}O relative to drinking water by about 1 to 6‰ (Camin et al., 2008; Renou et al., 2004). The degree of enrichment depends largely on the water content and isotopic composition of the diet. Camin et al. (2008) found that dietary plant-water $\delta^{18}\text{O}$ values were 5-6‰ higher than those of environmental water, as a result of evapotranspiration that takes place in the leaves of plants. In addition, the amount of water in plant tissues varies greatly (e.g., grass contains up to 85% water, as opposed to only 15% in hay) (Renou et al., 2004), so grass diets produce higher milk $\delta^{18}\text{O}$ values than hay diets when drinking water $\delta^{18}\text{O}$ values are the same. Although not well studied, physiological factors may also contribute to ^{18}O enrichment in milk.

Animal tissues that form prior to birth should have $\delta^{18}\text{O}$ values similar to those of the mother's tissues, since both are formed from the same pool of body water. Nursing infants should have higher $\delta^{18}\text{O}$ values than their mothers because of the ^{18}O -enrichment of milk. Feeding on leafy plants while nursing would also increase juvenile $\delta^{18}\text{O}$ values, but drinking environmental waters should decrease $\delta^{18}\text{O}$ values towards the level of the mother.

3.1.3 Trace Elements and Nursing/Weaning

Enamel is primarily composed of bioapatite, a calcium phosphate that incorporates - among other elements - small amounts of barium and strontium into its structure during formation. Since Ba and Sr contents of bioapatite are proportional to their abundance in the animal's diet, Ba and Sr contents of skeletal remains can be used to reconstruct an animal's geographic origin (Burton et al., 2003). During digestion, mammals discriminate against Ba and Sr in favour of Ca (Burton et al., 1999; Comar et al., 1957), so Ba/Ca and Sr/Ca ratios can also be used to reconstruct trophic level, at least in animals living on the same geological substrate. Soils tend to have the highest Sr/Ca and Ba/Ca ratios, while plants, herbivores, and carnivores have progressively lower values (Burton et al., 1999; Sponheimer and Lee-Thorp, 2006).

Research on humans has shown that in addition to the discrimination against Sr that occurs during digestion, active transfer of Ca (as opposed to concentration gradient transfer of Sr) occurs within the mammary gland and placenta (Krachler et al., 1999; Rossipal et al., 2000). This process causes unborn and exclusively nursing infants to have lower Sr/Ca ratios than their mothers. However, the immature digestive tracts of human infants only gradually develop the ability to discriminate against strontium (Lough et al., 1963). As a result, the Sr/Ca ratios of juveniles increase dramatically during weaning, and can reach levels higher than those of their mothers if infants are weaned before their ability to discriminate against Sr is developed. Since barium undergoes more “biopurification” than Sr because of the former’s larger atomic radius (Burton et al., 1999), differences in Ba/Ca ratios among unborn, nursing, and weaned offspring are expected to be even greater than differences in Sr/Ca ratios. However, Ba concentrations in modern humans are highly variable (Krachler et al., 1999), which might obscure age-related differences.

Sillen and Smith (1984) used modern and ancient human bone to demonstrate that Sr/Ca ratios increased when supplemental foods were introduced during weaning, then decreased as the ability to discriminate against dietary Sr developed. More recently, Humphrey et al. (2008a) found that enamel formed after birth had low Sr/Ca ratios when (human) infants were exclusively breastfed, but higher Sr/Ca ratios when exclusively fed on formula. Few studies have investigated the effects of nursing and weaning on Sr/Ca and Ba/Ca ratios in non-human species. Humphrey et al. (2008b) found that tooth enamel from anubis baboons showed decreases in Sr/Ca ratios after birth consistent with exclusive suckling, followed by gradual increases in Sr/Ca ratios during the period of prolonged weaning, and subsequent decreases attributable to the increasing ability of the infant digestive system to discriminate against strontium.

3.1.4 Elephant Tooth Formation

Mammoths, like modern elephants, normally had six molariform teeth develop in each quadrant of their mouth during a lifetime, or 24 teeth in all (Laws, 1966). Unlike the teeth of many mammals, which are replaced from beneath, elephant teeth grow successively forwards from the back of the jaw (Shoshani, 1996). As an earlier tooth

becomes worn, a new tooth comes in from behind to replace it, and the remnant of the earlier tooth eventually falls out (Laws, 1966). There are never more than two teeth in use simultaneously in each quadrant of the jaw (Laws, 1966). Evolutionarily, the first three teeth are deciduous premolars (Shoshani, 1996), dp2, dp3, and dp4, and the last three teeth are molars, M1, M2, and M3. However, Laws (1966) points out that in elephants all the teeth are technically deciduous (i.e., they fall out) and suggests referring to them simply as M1 to M6, which is the nomenclature adopted in the present study.

The timing and rate of tooth replacement is essentially equal for both African and Asian elephants (Shoshani, 1996), and a similar progression occurred in mammoths (Haynes, 1991). Laws (1966) and Haynes (1991) summarized the chronology for African elephant teeth, focussing on eruption and degree of wear, which can be used to estimate the animal's age at death. However, neither researcher specifically addressed the age at which the teeth *formed*, which is the crucial information needed to interpret isotopic compositions and trace element contents. Large elephant teeth grow over a period of years to decades, and some parts of a tooth can be in wear while other parts are still developing. Furthermore, different tissues develop at different times. For all teeth except M1, plates are formed in sequence from anterior to posterior (Maschenko, 2002). The first tissue formed is the crown dentin of the most anterior plate, followed by the enamel that covers it. Next, cementum fills the gaps between plates. Cementum continues forming while the tooth is in wear (Maschenko, 2002). Root formation begins after all the crown lamellae are present but before crown cementum is completely formed, and continues to form for some time after crown formation is complete (Maschenko, 2002). Further research into proboscidean tooth enamel, dentin, and cementum growth and maturation is needed to precisely determine the timing of formation and the applicability of an elephant model to mammoths. Nevertheless, the detailed figures and notes provided by Laws (1966) can be used to define a broad age range over which each individual proboscidean tooth crown forms. We estimated the period of growth of elephant tooth crowns by noting the stage (date) at which each tooth's formation begins (as noted in Laws' text or illustrations), the stage at which lamellae are visible (which indicates that enamel formation is underway), and the stage at which full size is attained (maximum number of lamellae depicted in illustrations, including those not in wear) (Table 3.1). Ages are

expressed as African Elephant Years (AEY), based on Laws' (1966) calibration of tooth stage to true age, and only approximate the true ages of mammoth teeth at corresponding stages.

There is some published evidence to suggest that the eruption and wear of woolly mammoth teeth occurred earlier than those of modern *Elephas maximus* (Maschenko, 2002), and presumably also of *Loxodonta africana*. Indeed, photos in Maschenko (2002) suggest that crown formation of woolly mammoth upper M2s began well before 1 month of age and may have been completed by 10-11 months (Maschenko's Photos 4 & 5), whereas the upper M3 crown formed almost entirely after birth and was probably complete by 2 years of age (Maschenko's Photos 4,7). However, Maschenko's photographs do not conclusively demonstrate whether or not the full thickness of enamel has been deposited, or whether enamel maturation is complete. Moreover, although the age estimates in Maschenko (2002) were based on a complex of morphological features, he notes that it is difficult to judge their reliability without new and more complete data. For simplicity, we rely primarily on African elephant tooth formation estimates derived from Laws (1966) (Table 3.1), but also discuss the implications of possible earlier development times.

Table 3.1 Timing of tooth formation and wear in modern African elephants (*Loxodonta africana*), based on Laws (1966). Tooth nomenclature is as described in the text. Full size attainment was determined by counting the number of lamellae depicted in the figures presented in Laws (1966). Roman numerals are Laws stages. True ages in African Elephant Years, calibrated by Laws (1966), are given in parentheses.

	M1 (dp2)	M2 (dp3)	M3 (dp4)	M4 (M1)	M5 (M2)	M6 (M3)
Formation begins	0 (prenatal)	0 (prenatal)	0 (prenatal)	V (3 yrs)	X-XI (13-15 yrs)	XVI-XVII (26-28 yrs)
Lamellae present	I (birth)	I (birth)	II-III (0.5-1 yr)	VI (4 yrs)	XI (15 yrs)	XVII (28 yrs)
Full size attained	I (birth)	IV (2 yrs)	V (3 yrs)	XI (15 yrs)	XVII (28 yrs)	XXIII (43 yrs)
Crown formation ^a	0 (prenatal)	0-IV (prenatal-2 yrs)	0-V (prenatal-3 years)	V-XI (3-15 yrs)	X-XVII (13-28 yrs)	XVI-XXIII (26-43 yrs)
Lamellae in wear	I-III (0-1 yr)	II-VI (0.5-4 yrs)*	IV-X (2-13 yrs)	VIII-XVI (8-26 yrs)	XII-XXII (18-39 yrs)	XIX-XXX (32-60 yrs)
Tooth lost	IV (2 yrs)	VI-VII (4-6 yrs)	XI (15 yrs)	XVII (28 yrs)	XXII-XXIII (39-43 yrs)	Death

^a The period of root growth begins after the beginning of crown formation and continues after crown formation is complete.

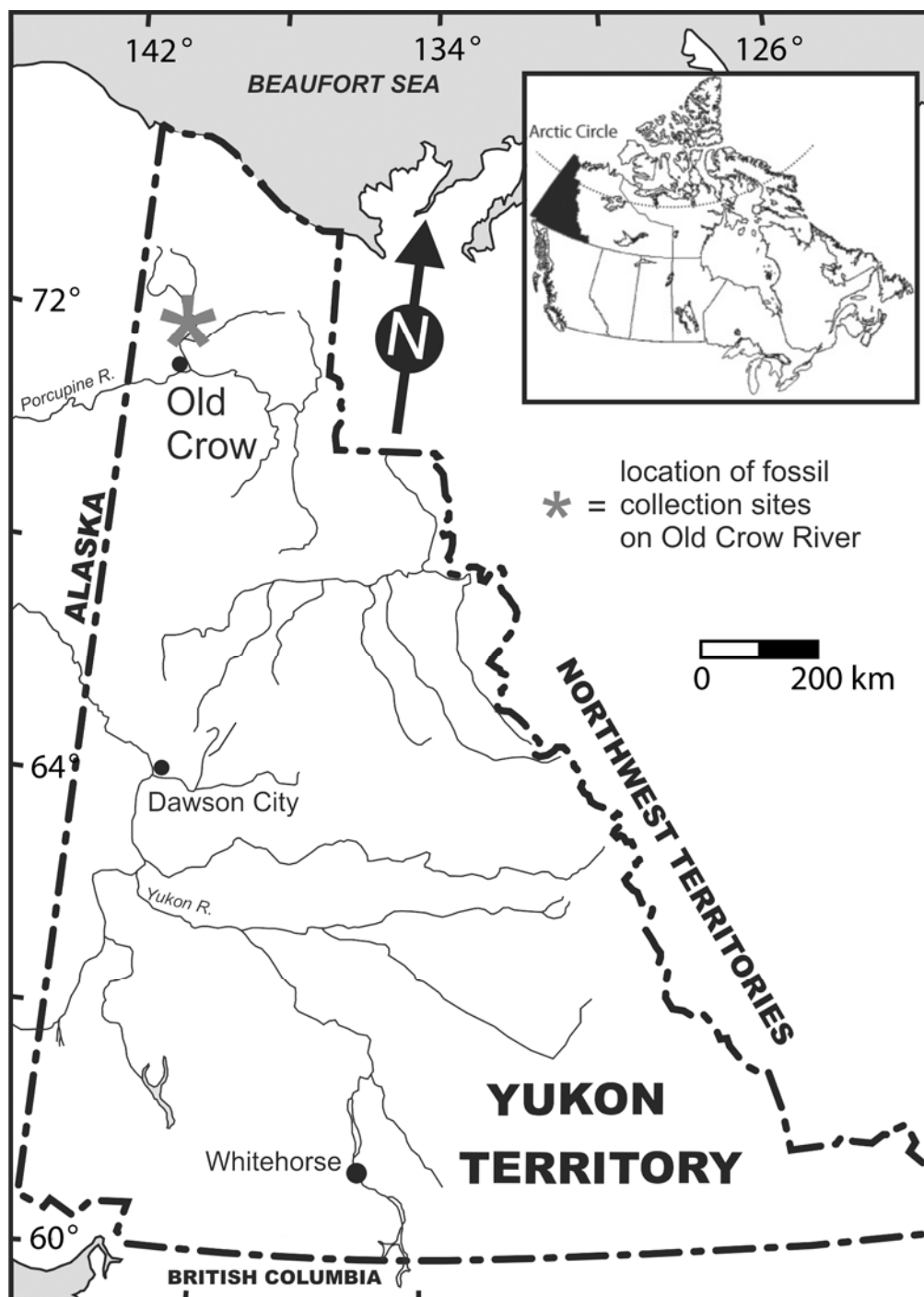


Figure 3.1 Map of the Yukon Territory, including the location of specimen collection sites on the Old Crow River (asterisk). Inset map shows the location of the Yukon Territory within Canada.

3.2 Materials and Methods

3.2.1 Study Area

Woolly mammoth tooth and bone samples were obtained from the Old Crow region of northern Yukon (Figure 3.1). The Old Crow Basin is a large intermontane sedimentary basin that contains Canada's richest and most diverse Quaternary vertebrate fossil record (Harington, 1977). Most faunal remains are recovered on the surface of modern alluvial point bars, having been eroded and re-transported from primary sediments exposed along the Old Crow River. Nearly a half century of systematic palaeontological investigation has resulted in a proboscidean fossil record dominated by the Late Pleistocene woolly mammoth (*Mammuthus primigenius*), though rare specimens of the Early Pleistocene mammoths (*M. meridionalis* and/or *M. trogontherii*) and American mastodon (*Mammut americanum*) have also been recovered (Harington, 1977; Harington, 2002; Morlan, 2003).

3.2.2 Samples

Mammoth teeth that develop during infancy (M2 crown: before birth to 2 AEY, M3 crown: before birth to 3 AEY) and during adulthood (M6 crown: 26-43 AEY) were selected for analysis (Table 3.2, Figure 3.2). Teeth were identified as M2, M3, or M6 based primarily on number of lamellae, length and width, in comparison with literature values for *Mammuthus primigenius* (Table 3.2, Figure 3.3) (Baryshnikov, 2003; Germonpre, 1993; Harington, 1977; Maglio, 1973; Zherekhova, 1977). Additional measurements (height, lamellar frequency, and enamel thickness) (after Maglio, 1973) were obtained to provide a complete characterization of the teeth, and as a reference for future studies (Table 3.2). Although many of the teeth were fragmentary, in most cases the measurements were sufficient to make a confident designation. However, in two cases it was not possible to determine whether the tooth was M3 vs. M4 (YT23) or M5 vs. M6 (YT5). These teeth were included in the analyses as M3 and M6, respectively. Enamel and dentin samples were removed from teeth using a Dremel tool with a diamond cutting wheel. The exact cutting locations were selected on a tooth-by-tooth basis, for ease of sampling and to minimize damage to the specimen (see Supplementary Table).

Root dentin was used for collagen extraction and C- and N-isotope analysis of most samples, including all M2 and M3 samples. At least half the thickness of the root (typically >1 cm) was sampled and homogenized. This should represent more than one year of growth, even in juvenile teeth (Fisher and Fox, 2007). When possible, the ventral half of the anterior root was sampled, which should have formed about midway through the root's development time. For some adult specimens, bone, crown cementum, or crown dentin were used, depending on ease of sampling. Enamel was used for structural carbonate C- and O-isotope analysis and trace element analysis, because of its greater resistance to diagenetic alteration (Sponheimer et al., 2005). Pieces of enamel comprising the entire enamel thickness and at least several mm in the dorsal-ventral direction were sampled and homogenized, and aliquots were taken for isotopic and elemental analysis. These samples should represent at minimum several months, and up to several years, of growth (Ferretti, 2003). For M2s and M3s, enamel was sampled near the cervix and, when possible, from posterior lamellae. This enamel should have formed near the end of the crown development time.

3.2.3 Radiocarbon Dating

Eight specimens (including at least one from each age category) were radiocarbon dated at the University of Arizona Accelerator Mass Spectrometry (AMS) Laboratory, after collagen extraction (see Section 3.2.4.1) (Hajdas et al., 2007; Longin, 1971), combustion, and graphitization. All eight samples yielded ages greater than 40,000 years BP (Table 3.2). Although precise dates for the samples were unavailable, there is no contextual evidence to suggest systematic differences in dates for the juvenile versus adult teeth.

3.2.4 Stable Isotopes

Stable isotope compositions are presented in standard delta (δ) notation, in units of per mil (‰) relative to VPDB (carbon), AIR (nitrogen), and VSMOW (oxygen) (Coplen, 1994; Coplen et al., 2006; Mariotti, 1983).

Table 3.2 Sample information and tooth measurements.

Specimen LSIS #	YG #	Latitude	Longitude	Radiocarbon		Tissue used for			Tooth Measurements						Comments
				Age	Lab number	Collagen	SC &TE*	Tooth	L	W	P	H	LF	ET	
YT12	286.15	68°02.750' N	139°35.603' W			RD	E	L M2	37+	31	5+	16	15	1.1 (0.8-1.4)	portion missing
YT13	236.65	68°02'12" N	139°34'40" W			RD	E	U M2	38+	40	3+	38	10	1.5 (1.3-1.9)	portion missing
YT14	236.378	68°02'12" N	139°34'40" W	>41,100	AA84990	RD	E	L M2	52	32	6	27	12	0.9 (0.1-1.1)	
YT17	318.140	67°49'10" N	139°54'15" W			RD	RD**	U M2	33	28	0				enamel completely worn
YT18	236.519	68°02'12" N	139°34'40" W			RD	E	L M2	43+	34	4+	27	15	1.1 (0.9-1.4)	portion missing
YT20	236.375	68°02'12" N	139°34'40" W			RD	RD**	LL M2	53+	42	5+	38	10	1.4 (1.1-1.7)	relatively little wear
YT21	237.17	67°49'10" N	139°54'15" W			RD	E	L M2	55	31	7	33	14	0.9 (0.7-1.1)	
YT22	237.18	67°49'10" N	139°54'15" W			RD	E	U M2	65	34	8	40	12	1.3 (1.0-1.5)	little wear
YT15	123.2	68°02'55" N	139°39'25" W	>41,100	AA84991	RD	E	LR M3	65+	54	8+	19	12	1.5 (1.3-1.8)	portion missing
YT16	238.18	67°49'29" N	139°50'11" W			RD	E	U M3	64	58	7	26	12	1.3 (0.9-1.6)	crown highly worn
YT19	237.23	67°49'10" N	139°54'15" W			RD	E	LR M3	78	48	7	36	12	1.4 (1.2-1.7)	
YT23	221.38	67°49'10" N	139°54'15" W	>41,100	AA84993	RD	E	UL M3 ^a	97+	56	10+	38	12	1.2 (1.1-1.7)	portion missing
YT5	60.2	68°08'44" N	139°58'12" W			RD	E	LR M6 ^b	194+	83	12+	77	7-8	2.6 (2.2-2.9)	large portion missing
YT1	291.1	67°58.166' N	139°33.689' W	>41,100	AA84987	RD	E	LR M6	287	91	20	123	7-9	2.2 (1.7-2.7)	
YT2	122.2	68°03'33" N	139°46'07" W	>41,100	AA84992	RD	E	UL M6	257	99	18	125	6-8	2.3 (2.0-2.7)	
YT3	173.5	67°29'00" N	139°55'00" W			D	E	U M6	215	76	16	142	7-8	1.9 (1.5-2.2)	not highly worn
YT4	285.1	67°55.1' N	139°40.7' W	>39,100	AA85002	B	E	LR M6	312	89	21	115	8-9	1.7 (1.3-2.4)	in mandible
YT6	57.1	68°11'19" N	140°32'04" W			C	E	LR M6	205+	75	19+	112	10-13	1.7 (1.5-1.9)	portion missing
YT7	325.22	67°51.892' N	139°48.075' W	>40,100	AA84984	B	E	UL M6	195	72	21	153	9-10	1.7 (1.4-2.2)	in maxilla
YT9	284.4	67°49'29" N	139°50'11" W			C	E	UL M6	240	97	21	153	7-10	1.9 (1.5-2.1)	
YT10	252.2	68°01'46" N	139°34'15" W	>40,000	AA85001	RD	E	LL M6	283	90	19	90	7-9	2.1 (2.0-3.0)	
YT11	173.1	67°29'00" N	139°55'00" W			RD, C	E	U M6	117+	106	9+	122	8	2.0 (1.5-2.3)	portion missing

Specimens: LSIS# was assigned for laboratory processing; YG# is the Yukon Government catalogue number.

Materials: RD = root dentin, D = crown dentin, B= bone, C = cementum, E = enamel

* Structural carbonate and trace element analysis

** Dentin was used for trace/major element analysis because no enamel was available. Results were excluded from consideration because of diagenetic alteration.

No structural carbonate isotope analyses were performed.

^a possibly M4

^b possibly M5

Tooth designations: U or L = upper or lower, L or R = left or right

Tooth measurements: L = Length (mm), W = Width (mm), P = Number of Plates, H = Height (mm), LF = Lamellar Frequency, ET = Enamel Thickness.

Enamel thickness: average of 10 measurements and range

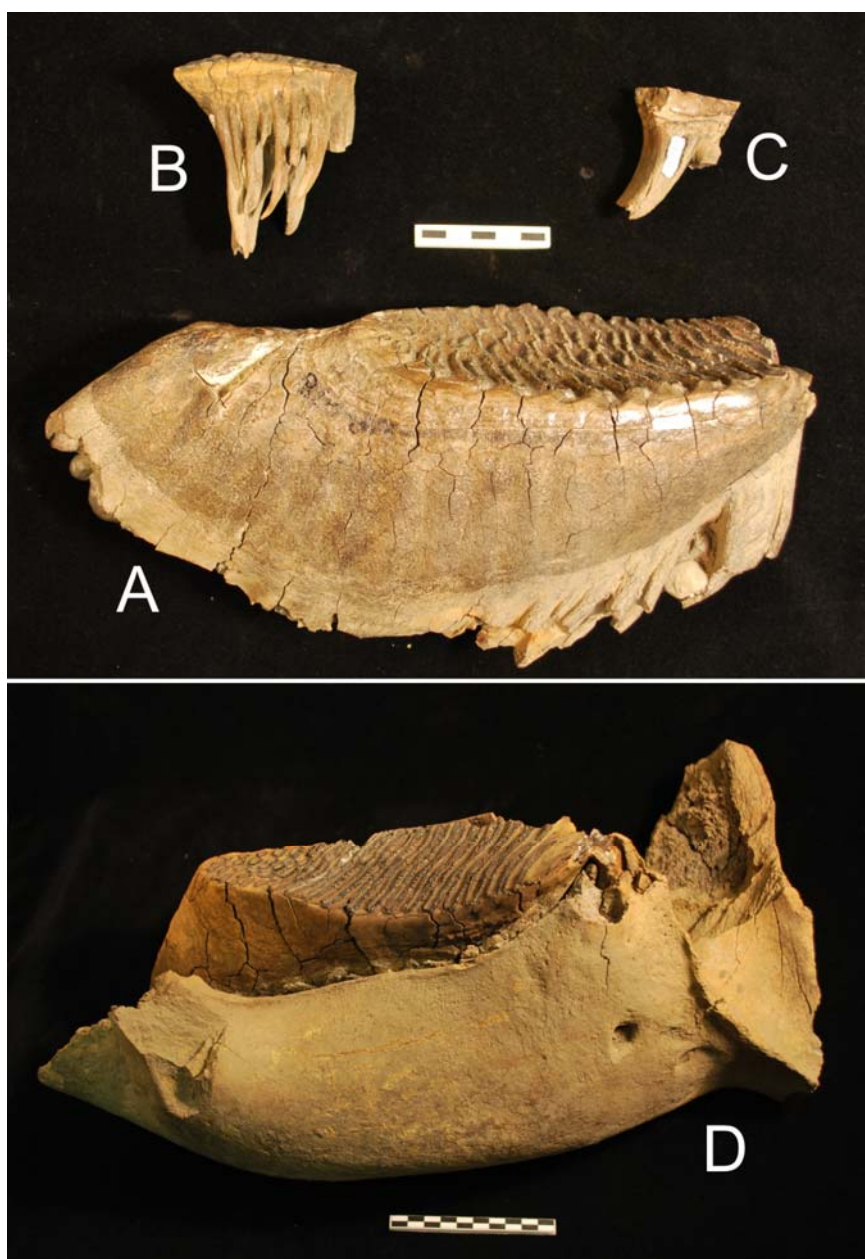


Figure 3.2 Selected woolly mammoth teeth analyzed in this study. Scale bar is in centimeters. A) M6 molar (YT10); B) M3 molar (YT15); C) M2 molar (YT12); D) partial mandible with M6 molar (YT4).

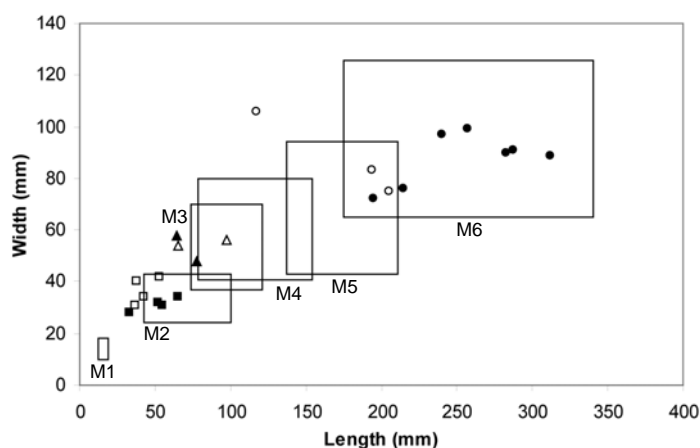


Figure 3.3 Comparison of the size of teeth used in this study (individual points) to the ranges reported in the literature (boxes). Closed symbols represent complete specimens and open symbols represent incomplete specimens. Teeth were designated M2 (squares), M3 (triangles), or M6 (circles) based on size and number of lamellae (see text).

3.2.4.1 Collagen

The surfaces of bone, dentin, and cementum samples were removed with a diamond or carbide burr Dremel tool attachment, and specimens were sonicated in de-ionized water. Samples were demineralised in 0.25 to 0.5 M HCl at room temperature, with frequent acid changes. When the samples were soft to gummy, they were rinsed with de-ionized water, and then treated with 0.1 M NaOH to remove humic substances and lipids. This procedure was conducted both using an automated flow-cell system at the AMS Laboratory, and manually at the Laboratory for Stable Isotope Science (LSIS). After rinsing to neutrality, collagen was solubilized in 10^{-3} M HCl at 75°C (AMS lab) or 90°C (LSIS). Collagen from the same specimens extracted independently at the two laboratories (not included in this study) had $\delta^{13}\text{C}$ and $\delta^{15}\text{N}$ values that differed by a maximum of $\pm 0.15\%$ for carbon and $\pm 0.25\%$ for nitrogen, which are similar to the typical intra-laboratory analytical error.

Carbon and nitrogen isotope ratios were obtained using a Costech elemental combustion system (ECS 4010) coupled to a Thermo-Finnigan Delta^{Plus}XL stable isotope ratio mass spectrometer (IRMS), operated in continuous-flow mode. The $\delta^{13}\text{C}$ values were calibrated to VPDB using ANU-Sucrose and NBS-22 (accepted values = -10.5‰

and -30.0‰, respectively), which yield the accepted value of 1.95‰ for NBS-19 (Coplen, 1994; Coplen et al., 2006). The $\delta^{15}\text{N}$ values were calibrated relative to AIR using IAEA N-1 and IAEA N-2 (accepted values = 0.4 and 20.3‰, respectively). Carbon and nitrogen contents were also calibrated using accepted values for the above standards, and were used to calculate atomic C/N ratios. An internal standard (keratin) was included in each run to monitor the accuracy and precision of measurements ($\delta^{13}\text{C}$ measured = $-24.0 \pm 0.2\%$ (mean \pm 1 SD), accepted = -24.0‰; $\delta^{15}\text{N}$ measured = $6.3 \pm 0.2\%$, accepted = 6.4‰; C/N measured = 3.68 ± 0.06 ; n = 23). Duplicate analyses of individual collagen samples were within 0.1‰ for $\delta^{13}\text{C}$, 0.2‰ for $\delta^{15}\text{N}$, and 0.1 for C/N.

3.2.4.2 Carbonate

Pieces of enamel were mechanically cleaned of adhering dirt, dentin and cementum using tweezers and dental tools and/or a Dremel tool with diamond/carbide burr attachments. Samples were then sonicated in distilled or Millipore water 2-3 times (minimum), and dried at room temperature. All samples were examined under an optical microscope prior to being ground to a powder using a mortar and pestle.

Approximately 5-15 mg of enamel was treated with ~2.5% NaOCl at room temperature for ~21 hours, rinsed 5 times with de-ionized water, reacted with 0.1M acetic acid for 4 hours, rinsed as above, and freeze-dried. About 0.5 to 1 mg of sample was reacted with ortho-phosphoric acid using a MultiPrep automated sampling device coupled with a VG Optima IRMS in dual-inlet mode. The $\delta^{13}\text{C}$ values were calibrated relative to VPDB using NBS-19 and Suprapur, and $\delta^{18}\text{O}$ values were calibrated relative to VSMOW using NBS-19 and NBS-18. The mean (\pm 1 SD) $\delta^{13}\text{C}$ values of NBS-18 ($-5.0 \pm 0.1\%$, n=14) and internal laboratory standard WS-1 ($0.8 \pm 0.1\%$, n=4) were in good agreement with their accepted values (-5.0 and 0.8‰, respectively). The mean (\pm 1 SD) $\delta^{18}\text{O}$ values of Suprapur ($13.1 \pm 0.2\%$, n=14) and WS-1 ($26.4 \pm 0.2\%$, n=4) were also in good agreement with their accepted values (13.2 and 26.2‰, respectively). The amount of carbonate in the samples (weight %) was determined using a calibration curve derived from the intensity of the mass 44 beam and the carbonate content of calcite standards. Duplicate analyses of samples (n=3 pairs) resulted in carbonate contents within $\pm 0.2\%$ on average (“sealed vessel” analyses only; see below).

Some enamel carbonate samples analyzed in the present study had low $\delta^{18}\text{O}$ values and very poor reproducibility when analyzed using the standard “open valve” MultiPrep configuration. (In this configuration, the CO_2 produced during reaction with phosphoric acid is frozen in a cryogenic trap immediately after it is produced, because a valve between the reaction vessel and cryogenic trap remains open while the reaction takes place.) A similar problem has been reported previously for bone, and was resolved by reacting the sample in a sealed system (i.e., closing the valve between the reaction vessel and cryogenic trap), and allowing the gas to be transferred to the trap only after the reaction was complete (Metcalf et al., 2009). Consequently, the MultiPrep analytical procedure was modified to use a “sealed vessel” reaction method, and all samples were re-analyzed. For many of the specimens ($n=12$), the δ -values obtained using both methods were within analytical error. For other specimens ($n=8$), the $\delta^{18}\text{O}$ values obtained using the sealed vessel method were 1-9‰ higher than those obtained using the open valve method. Duplicate “sealed vessel” analyses of the samples with the largest differences between open and sealed vessel methods resulted in precisions better than $\pm 0.2\%$ for $\delta^{18}\text{O}$ and $\pm 0.1\%$ for $\delta^{13}\text{C}$. Hence, only results obtained using the sealed vessel method are reported here. One sample (YT19E) did not have sufficient pretreated enamel to re-analyze using the sealed vessel method. Consequently, several tiny pieces of untreated enamel were identified under binocular microscope and analyzed untreated. The resulting δ -values lie within the range of other Old Crow samples.

3.2.5 Trace/Major Elements

Trace/major element analyses were conducted at Activation Laboratories in Ancaster, Ontario. Enamel samples were digested with aqua regia for 2 hours at 95°C , cooled and diluted with deionized water, and analyzed using a Spectro CirOS axial ICP. Detection limits were 1 ppm for Sr, 50 ppm for Ba, 0.01% for Ca, and 0.001% for P. Duplicate analyses of one sample (YT20RD) were within ± 9 ppm for Sr, ± 55 ppm for Ba, $\pm 0.2\%$ for Ca, and $\pm 0.1\%$ for P.

Following convention, this paper presents Sr/Ca and Ba/Ca as ratios (in identical units) multiplied by 1000 (e.g., Gilbert et al., 1994; Sponheimer and Lee-Thorp, 2006). Logarithmic transforms of these data are often obtained prior to statistical comparison

(e.g., Burton et al., 1999). However, we found no differences in the statistical results with or without the use of log transforms. Consequently, the untransformed data have been used throughout this paper.

3.2.6 Statistics

Statistical analyses were conducted using Microsoft Excel 2002 (correlations) and SPSS Statistics 17.0 (comparisons of means). For comparisons of variables that met the homogeneity of variance assumption (according to the Levene test), ANOVA and Tukey post-hoc tests were used. For comparisons of variables with unequal variance, Dunnett T3 tests were used.

3.3 Results and Interpretations

3.3.1 Carbon and Nitrogen in Collagen

In general, well-preserved collagen has a collagen extraction yield >1%, C/N ratio between 2.9 and 3.6, carbon content of 30 to 43%, and nitrogen content of 11 to 16% (Ambrose, 1990; DeNiro, 1985; van Klinken, 1999). The Old Crow collagen is well-preserved by all of these measures (collagen yield = $10 \pm 4\%$ (mean \pm 1 SD), C/N = 3.2 ± 0.1 , %C = $42 \pm 3\%$, %N = $15 \pm 1\%$) (Table 3.3).

The $\delta^{13}\text{C}$ and $\delta^{15}\text{N}$ values of adult Old Crow woolly mammoths (means = -21.5‰ and 8.8‰ , respectively) are intermediate to values previously obtained for mammoths from Alaska/Yukon and Siberia ($\delta^{13}\text{C}$ means = -20.7 and -21.9‰ , respectively; $\delta^{15}\text{N}$ means = 7.2 and 9.3 , respectively) (Szpak et al., 2010). If the interpretations of Szpak et al. (2010) regarding Beringian mammoth carbon and nitrogen isotope compositions are correct, the new data suggest that Old Crow was colder and drier than the central Alaska/Yukon sites (i.e., Klondike and Fairbanks), but warmer and wetter than the Siberian sites. This inference is consistent with the higher latitude of Old Crow relative to the central Alaska/Yukon sites studied by Szpak et al. (2010). Heightened aridity further north in Pleistocene Alaska/Yukon has also been inferred from the observation that the more northerly faunas are dominated by horse (*Equus*) fossils, whereas bison (*Bison priscus*) dominates the fauna of the interior (Guthrie and Stoker, 1990; Zazula et al.,

2009). Assuming a $\Delta^{13}\text{C}_{\text{col-diet}}$ value of about 5‰ for large herbivores (Ambrose and Norr, 1993; Koch, 1998), which is only a rough approximation (Caut et al., 2009), adults were consuming an entirely C_3 diet, with an average $\delta^{13}\text{C}$ value of about -26.5‰.

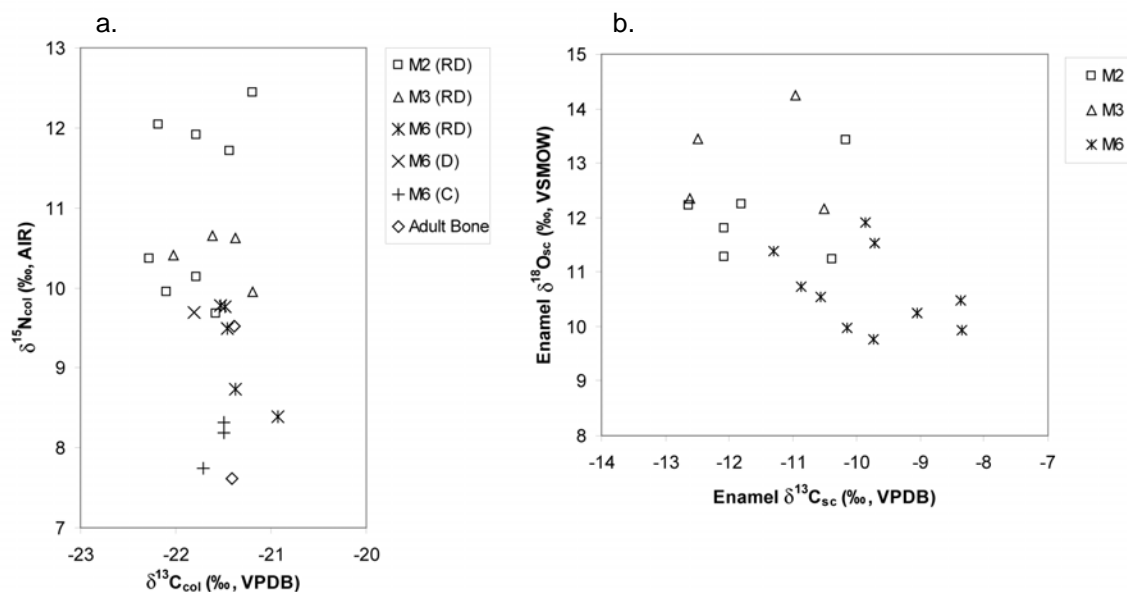


Figure 3.4 (a) The collagen $\delta^{13}\text{C}$ and $\delta^{15}\text{N}$ values of individual Old Crow mammoths, organized by age category and tissue type. RD = root dentin, D = crown dentin, C = cementum. (b) The enamel structural carbonate $\delta^{13}\text{C}$ and $\delta^{18}\text{O}$ values of individual mammoths, organized by age category.

Prior to analysis it was assumed that there would be no systematic offsets in stable isotope compositions of different adult tissues. In this sample set, M6 dentin ($n=6$) has only slightly higher $\delta^{13}\text{C}_{\text{col}}$ values than M6 cementum ($n=3$) (mean difference = 0.2‰). However, all M6 dentin samples have substantially higher $\delta^{15}\text{N}$ values than M6 cementum samples ($n=3$) (mean difference = 1.2‰), including one dentin-cementum pair from the same tooth (Figure 3.4a, Table 3.3). Previous studies have shown that dentin from various species tends to have higher $\delta^{15}\text{N}$ values than bone (Bocherens et al., 1994, 1995, 1997; Bocherens and Mariotti, 1997; Fizet et al., 1995), which has been attributed to the effects of nursing on teeth that develop during infancy. The mammoth M6s used in this study, however, developed entirely after the age of 26 AEY (Table 3.1), so nursing cannot have been a contributing factor. No consistent offsets were found for dentin-

cementum pairs from Alberta mammoths (Metcalf, unpublished data), but the Alberta data were obtained from crown dentin whereas the Yukon data were mostly from root dentin, which form at different times, especially in high-crowned herbivores like mammoths (Hillson, 2005; Maschenko, 2002). It is possible that there is an age-related shift in mammoth $\delta^{15}\text{N}$ values, which might be related to growth rate, metabolic changes, or age-related changes in diet, but further isotope data and improved age-of-formation estimates are needed to investigate this possibility. We note that the isotopic compositions of cementum have seldom been studied, because few animals besides proboscideans have enough to make collagen extraction possible.

Our results show that teeth that developed during infancy had higher $\delta^{15}\text{N}$ values than teeth or bones that developed during adulthood (Figure 3.5). This suggests that juveniles were consuming milk during the formation of M2 and M3, from birth to at least 3 AEY, and probably longer (since root dentin formation continues after crown formation is complete) (Table 3.1 and Section 3.1.4). The mean $\delta^{15}\text{N}$ value of M2 root dentin was 2.2‰ higher than that of adult tissues (or 1.7‰ if adult bone and cementum are excluded because of the tissue-related differences described above). This is comparable to the ~2‰ enrichment of offspring over mothers observed previously for humans (Fogel et al., 1989; Fuller et al., 2006), grizzly bears, and caribou (Jenkins et al., 2001). A one-way ANOVA and Dunnett's T3 test showed that the differences between adult and infant dentin (both M2 and M3) were statistically significant ($F(2,15) = 7.2$, $p = 0.006$).

The differences between the $\delta^{13}\text{C}_{\text{col}}$ values of Old Crow juvenile and adult woolly mammoth teeth were small (0.4‰ for M2 versus M6 dentin and 0.2‰ for M3 versus M6 dentin) and not statistically significant ($F(2,15) = 1.9$, $p = 0.19$) (Figure 3.5). This is similar to the results of Jenkins et al. (2001), who found no differences between the plasma $\delta^{13}\text{C}$ values of mothers and nursing offspring, but different from the ^{13}C -enrichment of collagen that normally occurs in human infants (e.g., Fuller et al., 2006). These data support the call for species-specific investigations of nursing effects on stable isotope values.

Table 3.3 The isotopic compositions of collagen (various tissues) and structural carbonate (enamel), and the trace/major element contents of enamel for Old Crow mammoths.

	Collagen							Structural carbonate				Trace/Major Elements									
	Tissue	C (%)	$\delta^{13}\text{C}$ (‰)	N (%)	$\delta^{15}\text{N}$ (‰)	C/N (Atomic)	Col Yield (%)	Tissue	$\delta^{13}\text{C}$ (‰)	$\delta^{18}\text{O}$ (‰)	CO_3 (%)	Tissue	Ca (%)	P (%)	Sr (ppm)	Ba (ppm)	Ca/P (molar)	Sr/Ca *1000	Ba/Ca *1000	Sr/Ba	
M2																					
YT12	RD	40.3	-21.8	15.2	11.9	3.1	6.9	E	-10.4	11.2	5.1	E	35.7	21.8	148	330	1.27	0.41	0.92	0.45	
YT13	RD	40.6	-21.2	14.7	12.4	3.2	6.0	E	-12.6	12.2	5.5	E	32.1	13.8	180	120	1.80	0.56	0.37	1.50	
YT14	RD	42.2	-21.4	15.7	11.7	3.1	11.9	E	-12.1	11.8	5.3	E	32.1	14.4	153	180	1.72	0.48	0.56	0.85	
YT18	RD	42.5	-22.1	15.5	9.9	3.2	7.1	E	-11.8	12.2	4.8	E	33.4	14.9	164	160	1.73	0.49	0.48	1.03	
YT21	RD	35.5	-22.2	12.6	12.0	3.3	2.2	E	-10.2	13.4	5.1	E	34.8	15.3	197	280	1.76	0.57	0.80	0.70	
YT22	RD	41.4	-21.6	15.0	9.7	3.2	8.1	E	-12.1	11.3	4.9	E	34.0	15.2	148	260	1.73	0.44	0.76	0.57	
YT17	RD	40.5	-21.8	14.8	10.1	3.2	8.6	no enamel present			<i>RD**</i>	21.5	9.3	616	1730	1.79	2.87	8.05	0.36		
YT20	RD	38.9	-22.3	14.3	10.4	3.2	8.6	no enamel available			<i>RD**</i>	19.4	8.1	489	1770	1.86	2.52	9.12	0.28		
Mean		40.2	-21.8	14.7	11.0	3.2			-11.5	12.0	5.1		33.7	15.9	165	222	1.67	0.49	0.65	0.85	
SD		2.2	0.4	1.0	1.1	0.1			1.0	0.8	0.3		1.4	2.9	20	81	0.20	0.06	0.21	0.38	
M3																					
YT15	RD	43.0	-21.4	16.1	10.6	3.1	12.1	E	-11.0	14.3	4.7	E	32.5	13.3	311	260	1.89	0.96	0.80	1.20	
YT16	RD	39.5	-21.2	14.4	10.0	3.2	5.5	E	-10.5	12.2	4.9	E	33.3	14.9	309	360	1.73	0.93	1.08	0.86	
YT19	RD	45.9	-22.0	17.1	10.4	3.1	10.2	E	-12.5	13.4	6.2*	E	52.4	21.8	616	750	1.86	1.18	1.43	0.82	
YT23	RD	40.9	-21.6	15.3	10.6	3.1	11.9	E	-12.6	12.3	5.1	E	33.7	14.9	285	310	1.75	0.85	0.92	0.92	
Mean		42.3	-21.6	15.7	10.4	3.1			-11.6	13.0	4.9		38.0	16.2	380	420	1.81	0.98	1.06	0.95	
SD		2.8	0.4	1.2	0.3	0.0			1.1	1.0	0.2		9.6	3.8	158	224	0.08	0.14	0.27	0.17	
Adult (M6)																					
YT5	RD	42.9	-21.5	15.5	9.8	3.2	11.2	E	-8.4	10.5	5.1	E	34.1	15.5	180	120	1.70	0.53	0.35	1.50	
YT1	RD	41.6	-21.4	15.6	8.7	3.1	14.4	E	-11.3	11.4	n.d.	E	33.2	16.3	159	<50	1.57	0.48	<0.2	>3.2	
YT2	RD	39.2	-20.9	14.6	8.4	3.1	11.0	E	-8.3	9.9	5.3	E	33.9	15.5	258	170	1.69	0.76	0.50	1.52	
YT3	D	44.0	-21.8	16.4	9.7	3.1	>6.7	E	-10.1	10.0	5.5	E	32.7	13.4	211	150	1.89	0.65	0.46	1.41	
YT4	B	41.1	-21.4	15.2	9.5	3.1	13.1	E	-9.7	11.5	5.1	E	35.4	16.2	268	210	1.69	0.76	0.59	1.28	
YT6	C	42.5	-21.7	15.2	7.7	3.3	10.1	E	-9.7	9.8	4.6	E	36.1	16.1	148	50	1.73	0.41	0.14	2.96	
YT7	B	42.3	-21.4	15.8	7.6	3.1	15.7	E	-9.1	10.2	5.3	E	35.2	16	225	160	1.70	0.64	0.45	1.41	
YT9	C	41.4	-21.5	15.0	8.2	3.2	7.1	E	-9.9	11.9	5.0	E	35.8	15.9	227	100	1.74	0.63	0.28	2.27	
YT10	RD	38.9	-21.5	14.4	9.8	3.2	11.4	E	-10.9	10.7	5.3	E	37.1	16.5	245	90	1.74	0.66	0.24	2.72	
YT11	C	44.1	-21.5	15.9	8.3	3.2	18.2	E	-10.6	10.5	5.1	E	34.8	16.1	185	130	1.67	0.53	0.37	1.42	
	RD	47.2	-21.5	17.6	9.5	3.1	14.3														
Mean		42.3	-21.5	15.6	8.8	3.2			-9.8	10.6	5.1		34.8	15.8	211	131	1.71	0.60	0.38	1.83	
SD		2.3	0.2	0.9	0.8	0.1			1.0	0.7	0.3		1.4	0.9	41	48	0.08	0.12	0.14	0.64	

Tissue: RD = root dentin, D = crown dentin, B = bone, C = cementum, E = enamel

Sr/Ca and Ba/Ca ratios have been multiplied by 1000, as described in text

* This sample was not pretreated prior to structural carbonate analysis (see text)

** Not included in mean of trace/major element results

Values in **bold** are the means of duplicate analyses.

3.3.2 Carbon and Oxygen in Structural Carbonate

The carbonate content of the Old Crow woolly mammoth enamel samples ($5.1 \pm 0.3\%$) is close to that typical of mature enamel (2.7 to 5.0%, Hillson et al. 1996), and there is no correlation between carbonate contents and $\delta^{13}\text{C}_{\text{sc}}$ or $\delta^{18}\text{O}_{\text{sc}}$ values. Given a $\Delta^{13}\text{C}_{\text{sc-diet}}$ value of about 14‰ for large-bodied herbivores (Cerling and Harris, 1999), the adult mammoths were consuming an entirely C_3 diet with an average $\delta^{13}\text{C}$ value of about -24‰. The difference between this estimate and that obtained from collagen (-26.5, see Section 3.3.1) may partially result from error in the assumed tissue-diet fractionations (Caut et al., 2009). However, since collagen is preferentially formed from protein in the diet whereas structural carbonate is formed from the whole diet (Ambrose and Norr, 1993; Tieszen and Fagre, 1993), and plant proteins have lower $\delta^{13}\text{C}$ values than the whole plant (Tieszen, 1991), lower diet $\delta^{13}\text{C}$ estimates from collagen likely reflect lower $\delta^{13}\text{C}$ values of dietary proteins in adult mammoth diets.

The $\delta^{13}\text{C}_{\text{sc}}$ values of M2 and M3 enamel are significantly lower than those of adult enamel ($F(2,17) = 7.7$, $p = 0.004$; Tukey HSD), consistent with a diet of ^{13}C -depleted milk. Although the trends are similar, the magnitude of the juvenile-adult difference for $\delta^{13}\text{C}_{\text{sc}}$ is much greater than that for $\delta^{13}\text{C}_{\text{col}}$, consistent with a whole-diet (lipid-rich, lower- $\delta^{13}\text{C}$) milk carbon source for structural carbonate, and a dietary protein (higher $\delta^{13}\text{C}$) carbon source for collagen (Figure 3.5). The range of $\delta^{13}\text{C}_{\text{sc}}$ values is much larger than that of the $\delta^{13}\text{C}_{\text{col}}$ values. This is probably a result of several factors, including (i) less isotopic averaging in the carbonate because smaller sample sizes were used, and (ii) dietary variations in the proportion of carbohydrate, protein and lipids, or milk versus plants, which would affect a “whole diet” proxy (bioapatite) more than a “protein component” proxy (collagen).

The $\delta^{18}\text{O}_{\text{sc}}$ values of M2 and M3 enamel are significantly higher than those of adult enamel ($F(2,17) = 14.6$, $p < 0.001$; Tukey HSD), consistent with infants drinking ^{18}O -enriched milk rather than environmental water (Figure 3.5). The $\delta^{18}\text{O}_{\text{sc}}$ values of M3 enamel are slightly higher than those of M2 enamel, which is consistent with consumption of grass during weaning and reliance on milk as a liquid water source, both of which would increase $\delta^{18}\text{O}$ values relative to animals drinking environmental water. Statistically significant negative correlations between $\delta^{18}\text{O}_{\text{sc}}$ and $\delta^{13}\text{C}_{\text{sc}}$ (Pearson's r

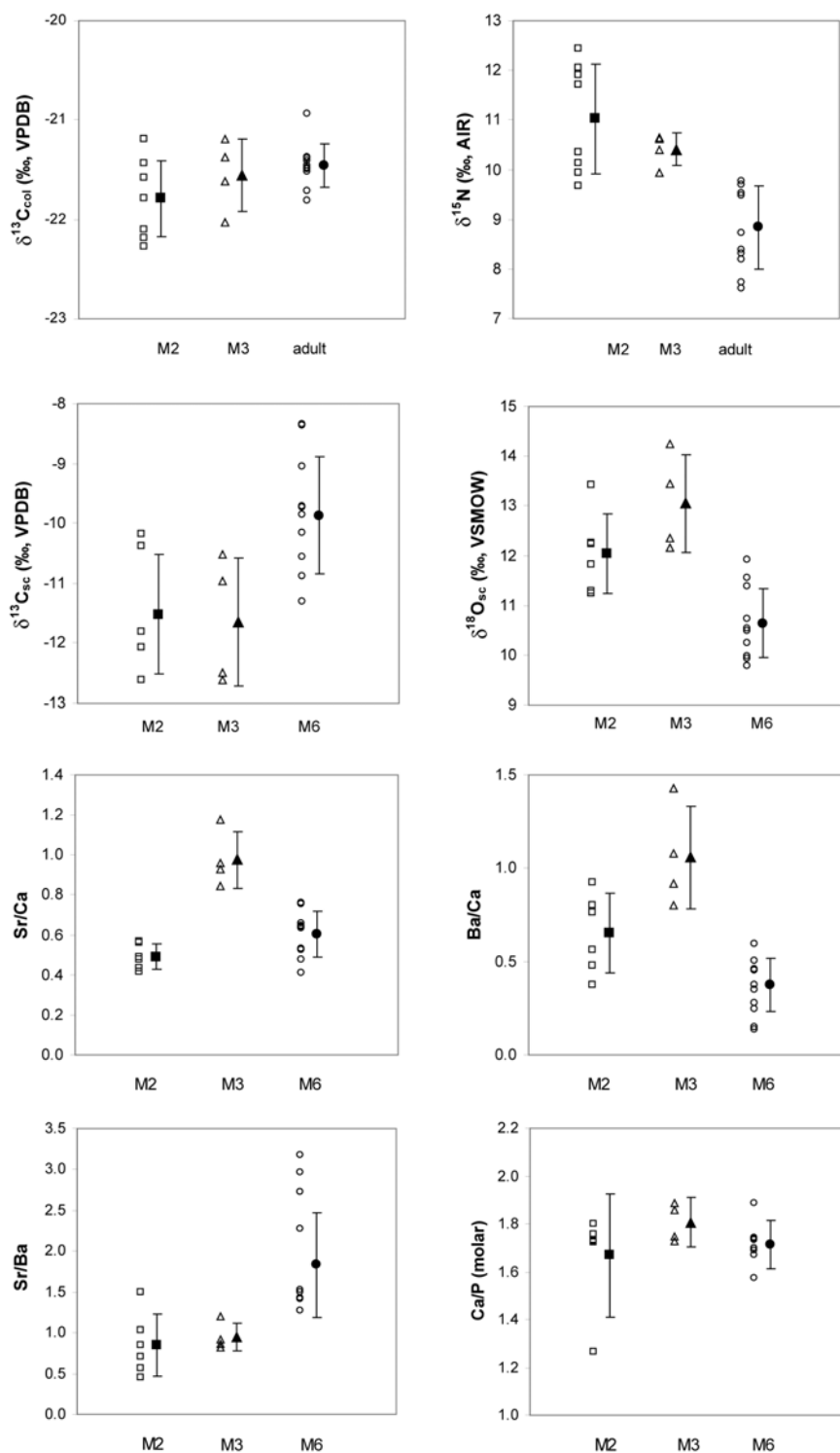


Figure 3.5 Age category comparisons for stable isotope and trace/major element data. Solid symbols are means and error bars represent one standard deviation. Open symbols are results for individual specimens.

= -0.55, $df = 18$, $p < 0.02$), and between $\delta^{13}C_{sc}$ and $\delta^{15}N_{col}$ (Pearson's $r = -0.49$, $df = 19$, $p < 0.05$), can also be explained by the contribution of milk to the diet (Figure 3.4b).

3.3.3 Trace/Major Elements

Enamel was used for trace/major element analysis because its greater density and larger crystal size (and hence, lower surface area and solubility) cause it to remain better preserved than bone or dentin (Sponheimer and Lee-Thorp, 2006; Trueman and Tuross, 2002). Indeed, some authors argue that trace element compositions of ancient bone can never be reliably used to reconstruct paleodiet (e.g., Trueman and Tuross, 2002). The Sr and Ba contents, and Sr/Ca and Ba/Ca ratios, of Old Crow mammoth enamel samples are within the range previously reported for modern bone and enamel (Burton et al., 1999; Sponheimer and Lee-Thorp, 2006; Trueman and Tuross, 2002). In contrast, two Old Crow mammoth tooth dentin samples analyzed for comparison had much higher Sr/Ca ratios, Ba contents, and Ba/Ca ratios than any of those obtained for enamel (Table 3.3), which suggests that the original trace element contents of dentin were not preserved. The Ca/P molar ratios of enamel (mean = 1.72 ± 0.13) are slightly higher than those previously reported for modern enamel (1.59, 1.63) (Elliott, 2002; LeGeros, 1991), which may indicate post-mortem alteration (but note that the latter values were obtained from ashed samples). However, there were no significant differences in Ca/P ratios among age groups ($F(2,17) = 1.5$, $p = 0.255$), which suggests no differences in the extent of alteration. In addition, there were no statistically significant correlations between Ca/P ratios and Ba or Sr contents. In total, these data suggest that diagenetic alteration of trace element ratios was not significant in the enamel samples analyzed here.

One enamel sample (YT19) had higher Ca, P, Sr, and Ba contents than all other samples, though its Ca/P ratio did not differ. Because its Sr/Ca and Ba/Ca ratios were not substantially different from other M3s, and because its inclusion did not significantly alter interpretations, this sample's results have been retained within the dataset.

The Sr/Ca and Ba/Ca ratios of M2 and adult teeth are similar (Table 3.3, Figure 3.5), which is consistent with a lack of plant foods in the diet during the formation of M2 enamel (i.e., formation before birth or while exclusively nursing). In contrast, the Sr/Ca

and Ba/Ca ratios of M3s are significantly higher than those of adults and/or M2s (Table 3.3, Figure 3.5) (Sr/Ca: $F(2,17) = 25.8$, $p < 0.001$; Ba/Ca: $F(2,17) = 19.2$, $p < 0.001$; Tukey's HSD), which is consistent with plant food consumption prior to the development of digestive discrimination against Sr and Ba. These results suggest that plant foods were consumed during the development of M3s (<3 AEY) but not M2s (<2 AEY) (Table 3.1).

Because of progressively greater discrimination against Ba relative to Sr or Ca, Sr/Ba ratios tend to increase with trophic level (Sponheimer and Lee-Thorp, 2006). The M3 group has lower Sr/Ba ratios than adults (Figure 3.5), which is consistent with the explanation that they were consuming plants but had not yet developed the ability to discriminate against Sr and Ba (i.e., their "apparent trophic level" would be lower than those of adults). However, the M2 group, whose Sr/Ca and Ba/Ca ratios did not indicate plant consumption, had similarly low Sr/Ba ratios. These data could indicate diagenetic alteration of Ba and Sr contents in the juvenile teeth. However, they may instead be a result of differential Ba and Sr discrimination across the mammary gland, placental membrane, and/or immature infant digestive tract, and thus require further investigation.

3.4 Discussion

The significantly higher $\delta^{15}\text{N}$ values of juveniles relative to adults is similar to the trend previously reported for many species, and almost certainly reflects milk consumption. However, does it follow that the higher the $\delta^{15}\text{N}$ value of an individual, the more milk that individual consumed? Four of the M2 samples had $\delta^{15}\text{N}$ values that were considerably higher than those of the other four M2s (means = 12 versus 10‰, respectively) (Figure 3.4). There were no differences between the two groups in tissue analyzed, site location, or size of tooth. If the different $\delta^{15}\text{N}$ values were primarily a result of different amounts of milk consumption, we would expect individuals with higher $\delta^{15}\text{N}$ values to have lower $\delta^{13}\text{C}_{\text{sc}}$ values, higher $\delta^{18}\text{O}_{\text{sc}}$, and/or lower Sr/Ca and Ba/Ca ratios. However, there are no differences between the two groups for any of these variables. Rather than consuming different amounts of milk, these individuals could have experienced metabolic differences (e.g., stress), or had mothers with very different $\delta^{15}\text{N}$ values because of differences in climate, diet, or metabolic stress. For example, the type of plant consumed (e.g., grass, shrub), part of plant consumed (e.g., leaf, stem, root), and

environmental conditions of growth (e.g., temperature, precipitation) can all affect plant $\delta^{15}\text{N}$ values, and hence, herbivore $\delta^{15}\text{N}$ values (Amundson et al., 2003; Bocherens, 2003; Handley and Raven, 1992). The possibility of stress influencing $\delta^{15}\text{N}$ values is especially important to consider, since individuals that died young may have experienced disease or stress atypical of healthy individuals, a situation known as the “osteological paradox” (Wood et al., 1992). Although this possibility can never be completely ruled out, it could be investigated by examining enamel, dentin and cementum for signs of arrested growth, and/or by searching for evidence of skeletal pathology.

Rountrey et al. (2007) found that $\delta^{15}\text{N}$ and $\delta^{13}\text{C}_{\text{col}}$ values in a serially-sampled juvenile mammoth tusk followed similar patterns (i.e., peaks and valleys for the two curves occurred at about the same locations). They argued that low $\delta^{15}\text{N}$ values correspond to a decreased proportion of milk in the diet during the early summer growing season, and concurrently low $\delta^{13}\text{C}_{\text{col}}$ values indicate that in summer relatively more carbon was derived from plant proteins than from milk proteins, the former being depleted of ^{13}C . The hypothesis that both $\delta^{13}\text{C}$ and $\delta^{15}\text{N}$ values are high when relatively more milk is consumed implies that the ^{13}C -depleted lipids in milk have little effect on collagen $\delta^{13}\text{C}$ values. The data reported here support this assumption. The Old Crow data also demonstrate a means of testing the assumption that seasonal variations in $\delta^{15}\text{N}$ values are related to changes in the degree of milk consumption. An alternative explanation of the data obtained by Rountrey et al. (2007) is that the seasonal changes in $\delta^{15}\text{N}$ values of the juvenile tusk are a result of seasonal changes in the $\delta^{15}\text{N}$ values of the mother (as a result of dietary or climatic changes, or metabolic stress) rather than a decreased proportion of milk in the diet of the juvenile. Determining the $\delta^{13}\text{C}_{\text{sc}}$, $\delta^{18}\text{O}_{\text{sc}}$, and trace element contents could provide valuable alternative lines of evidence for nursing and weaning in future intra-tusk studies, at least in situations where dentin is very well-preserved (e.g., burial in permafrost).

The combined isotopic and trace element evidence paints a coherent picture of nursing and weaning among Pleistocene woolly mammoths of the Old Crow region. In juvenile mammoths, the higher $\delta^{15}\text{N}$ values (from the “trophic level” effect), higher $\delta^{18}\text{O}_{\text{sc}}$ values (from consuming ^{18}O -enriched milk and smaller amounts of ^{18}O -enriched plant water), and lower $\delta^{13}\text{C}_{\text{sc}}$ values (from ^{13}C -depleted lipids in milk) all indicate that

mammoths were consuming milk during the development of both M2 and M3; that is, until the age of 3 AEY or later (given that roots continue to form after crown formation is complete). Woolly mammoth juveniles appear to have spent at least 3 years nursing, as do modern elephants. Sr/Ca and Ba/Ca ratios suggest that plants were being consumed during the formation of enamel from M3 but not M2. Based on our assumption that the enamel samples average several months to years of development during the latter stages of crown formation (see Section 3.2.2), we suggest that plants were consumed between the ages of 2 and 3 AEY, but not in significant quantities before 2 AEY. We emphasize that the timing of formation for these teeth is still not particularly well-known and requires further study. However, even if we assume that mammoth tooth formation occurs earlier than African elephant tooth formation (e.g., Maschenko (2002) suggests that M2 enamel formation may be complete by 10-11 months of age and M3 by 2 years of age), the isotopic evidence suggests that the enamel of both M2 and M3 analyzed in this study formed primarily after birth. Based on these considerations, we could revise our estimate for the introduction of plant foods to between 10 months and 2 years of age. Either way, these data suggest the possibility that unlike African elephant infants, who begin consuming plants at the age of 3 months (Owen-Smith, 1988), Old Crow woolly mammoth infants delayed plant consumption. Why might mammoths delay weaning? We propose that delayed weaning in Old Crow mammoths was a behavioural adaptation to increased predation risk and poor food quality/quantity during winter months, ultimately related to the long hours of darkness that occur at high latitudes north of the Arctic Circle.

Lactation imposes serious metabolic demands on females, including increased food requirements (Laws et al., 1975). As the body masses of infants increase, the energy demands placed on their mothers further increase. Moreover, delayed weaning incurs a short-term demographic cost by promoting longer interbirth intervals (Sukumar, 2003). Consequently, for the greater maternal investment associated with delayed weaning to be adaptive, it must significantly increase infant survival. Prolonged nursing could diminish the risk of several causes of infant mortality, including accident (by ensuring close proximity to the mother), malnutrition, and infection (because of the superior nutritional value and immunological benefits provided by milk). In addition, a significant proportion of juvenile elephant deaths in modern populations result from predation, mainly by

African lions (*Panthera leo*) (Sukumar, 2003). The age of greatest vulnerability to predation is between 4 and 7 years; that is, recently weaned individuals who begin to wander away from their mothers (Joubert, 2006; Power and Compion, 2009). Lions are unable to kill healthy, full-grown elephants (Owen-Smith, 1988), so staying in very close proximity to the mother is an infant's best defense against predation. Delayed weaning would likely delay exploratory behaviour associated with plant consumption, ensuring that infants remained close to their mothers at all times.

Most elephant hunting by African lions occurs at night, and the most successful hunts occur on dark (rather than moonlit) evenings (Joubert, 2006; Power and Compion, 2009; Schaller, 1972). Lions have excellent visual abilities at night, which gives them an advantage in the darkness over prey such as African buffalo and elephants, which have relatively poor eyesight (Sukumar, 2003; Turner, 1997). Areas north of the Arctic Circle experience 24 hours of darkness in mid-December, and shorter days than nights from September to March. We suggest that this would have been a time of increased predation risk for Pleistocene woolly mammoths in the Old Crow region. At least two species of large felids were present in the region during the Pleistocene, *Panthera spelaea vereschagini* (Beringian lion) and *Homotherium serum* (scimitar cat) (Barnett et al., 2009; Harington, 1996a, b). Both groups were likely quite capable of hunting juvenile mammoths, and would have posed the greatest threat to woolly mammoths of any carnivore in Beringia. Pleistocene Beringian lions were similar in size to modern lions, at least as fast, and are known to have hunted other megaherbivores (e.g., the famous Pleistocene bison, Blue Babe) (Guthrie, 1990; Harington, 1996a). Scimitar cats had large fangs that could be used to slash the throats of their prey, and their remains have been found in association with large numbers of juvenile mammoths in Friesenhahn Cave, Texas (Harington, 1996b; Turner, 1997). Furthermore, scimitar cats had enlarged orbits and visual cortices relative to other felids, which suggests they had truly exceptional visual acuity, particularly at night (Turner, 1997).

Among modern elephants in environments with highly seasonal patterns of rainfall, most births occur 1-2 months prior to the season of greatest productivity (Sukumar, 2003). Guthrie (1990) argues that woolly mammoth births would similarly have been timed to coincide with the growth of protein-rich plants in early spring, which

would help the mother recover from winter and nurture her young, and maximize the weight gain of both mother and calf, thus improving their chances of surviving the following winter. If Old Crow woolly mammoth calves were born in spring (May-June), they would be 6-7 months old in December, when the hours of darkness reach a maximum. Modern elephants of similar age incorporate significant quantities of plants into their diet, without substantially decreasing the amount of time spent nursing (Sukumar, 2003). However, the relatively poor quantity and quality of plant food available on the mammoth steppe during winter, combined with the greater predation risk attributable to short daylight hours, would have made it advantageous for woolly mammoth infants to rely solely on milk throughout this period, and to delay plant food consumption until later in life.

Fox-Dobbs et al. (2008) concluded, based on isotopic mixing models, that felids in the vicinity of Fairbanks, Alaska were not mammoth specialists. However, the isotopic compositions of some of the samples they analyzed, especially the scimitar cats, certainly do not preclude mammoth consumption (maximum scimitar cat $\delta^{15}\text{N}$ and $\delta^{13}\text{C} = 9.7\text{‰}$ and -18.3‰ , respectively, in comparison to mean mammoth $\delta^{15}\text{N}$ and $\delta^{13}\text{C} = 7.2\text{‰}$ and -20.7‰ from Fairbanks/Klondike) (Bocherens and Drucker, 2003; Fox-Dobbs et al., 2008; Szpak et al., 2010). Furthermore, Fairbanks is further south than Old Crow, so mammoth hunting might have been less important in the former region.

Our hypothesis of the relationship between daylight hours and timing of weaning should be tested in populations of woolly mammoths from various latitudes, and by detailed “life-history” studies of individuals from similar locations. Further evidence could be gleaned from non-destructive studies of tooth wear. If mammoths were not eating solid foods prior to age two, teeth that are “in wear” before age 2 (i.e., M1s) should show minimal abrasion and reduction in crown height, though some might result from masticatory movements that abrade teeth in advance of plant consumption. M2s, by comparison, develop before 2 AEY, but are *in wear* from about 0.5 to 4 AEY, so their degree of wear is uninformative about plant consumption during the earliest years of life. Since no M1s were identified in the Yukon Government collection, we do not currently have the material required to address this question. Woolly mammoth M1s from Sevs, Russia do show significant wear (Maschenko, 2002). However, our hypothesis suggests

that mammoths living at this lower latitude (approximately 52°N) would not have needed to delay weaning for as long as those living in the Old Crow region. Other implications of our hypothesis are also testable. For example, did other large herbivore species living at high latitudes (e.g., horse, steppe bison) delay weaning? Did carnivores have greater success at capturing mammoths during winter than summer, and at higher latitudes than lower latitudes? Fisher (2009) has shown that the patterns of variation in dentin laminations are related to circadian rhythms, such that mammoths living above the Arctic Circle have patterns that differ from those living at lower latitudes. However, the impact of extreme seasonal variations in the number of daylight hours in high latitude regions on Pleistocene animals' behavioral adaptations, predator-prey relationships, population dynamics, or demographic variables remains to be fully investigated.

The possibility of delayed weaning in Old Crow mammoths may have further significance for understanding mammoth life histories and extinction. Today, a leading cause of infant elephant deaths in Myanmar is insufficient maternal milk production (Saragusty et al., 2009). Woolly mammoths may have been more vulnerable to the effects of climate change and human hunting than modern elephants not only because of their harsher environment, but also because of the metabolic demands of lactation and prolonged nursing, especially during the long winter months.

Our interpretations of stable isotope compositions and trace/major element contents involve two major assumptions. First, we have assumed there were no systematic differences in the environmental conditions (e.g., temperature, rainfall amounts, vegetation availability) experienced by adults versus juveniles, since these could confound any interpretations of age-related differences. Second, we have assumed that disease or metabolic stress did not systematically alter the isotopic and elemental compositions of adults versus juveniles. There is no evidence that these assumptions are incorrect, but that possibility cannot be ruled out completely. Finally, as noted earlier, our interpretations are based on presently incomplete knowledge of the timing of individual mammoth tooth and tissue formation. Re-evaluation may be in order once further studies of tooth formation times become available.

3.5 Conclusion

The data presented here provide a baseline for recognizing mammoth nursing and weaning patterns. Nursing in mammoths is associated with minimal decreases in collagen $\delta^{13}\text{C}$ ($\sim 0.2\%$), large decreases in enamel structural carbonate $\delta^{13}\text{C}$ ($\sim 1.5\%$), and large increases in collagen $\delta^{15}\text{N}$ ($\sim 2\%$) and structural carbonate $\delta^{18}\text{O}$ values ($\sim 2\%$). Weaning in mammoths is associated with increased Sr/Ca and Ba/Ca ratios, as shown previously for other species. Similar trends were observed in all members of an age group. Given this “population” approach, alternative explanations of the isotope and trace element data (e.g., stress, climate differences, idiosyncratic life-history events) are much less likely.

This study suggests that mammoths nursed for prolonged periods of time, like African elephants, but may not have begun to consume plants as early as their modern relatives. We estimate that mammoth weaning began by the age of 2 AEY, and was not yet complete by 3 AEY. We suggest that delayed weaning would have been an effective behavioral adaptation to the long hours of winter darkness, and the increased predation risk and poor quality/quantity of forage, that occur at high latitude locations. That said, our present estimates for tooth formation times rely on the developmental stages of African elephant rather than mammoth teeth, and we currently lack data for the precise timing of enamel, cementum, and dentin formation within each tooth. Detailed study of tooth incremental growth features and chemical studies of bioapatite mineralization could provide more accurate estimates for the timing of development, and would greatly aid in assigning absolute dates to these significant life-history events. The study of mammoth M4s, which develop from 3-15 years of age, would also be beneficial for determining the age at which weaning is complete.

We have shown that the combination of stable carbon, nitrogen, and oxygen isotope and trace element analysis of skeletal remains from multiple individuals of varying age can significantly contribute to our understanding of the timing and duration of nursing and weaning in mammoths. This combination of multiple lines of evidence offers great promise for the study of other species.

Supplementary table. Details of sampling location for each specimen.

Tissue for collagen (dentin, bone, or cementum)				Enamel
M2				
YT12	286.15	RD	anterior-most root, tip, entire thickness (16.6 to 7.6 mm)	posterior-most end (5th loop from anterior end), entire height but worn (H=16mm) therefore near cervix
YT13	236.65	RD	second from anterior root, tip, half thickness (9.7 mm)	posterior half of tooth (but probably middle of tooth if other half present) - 4th plate from anterior end, near cervix
YT14	236.38	RD	posterior root, mid to tip, entire thickness (16.3 mm)	posterior (5th loop from anterior), near cervix
YT18	236.52	RD	anterior root, entire thickness (but highly worn or reabsorbed) (18.3 to 8.7 mm)	posterior plates from broken end (5th loop from anterior), near occlusal surface
YT21	237.17	RD	anterior-most root, base (near cervix), whole thickness (but hollow pulp cavity) (5.7 mm)	3rd loop from anterior end (~8 loops total), occlusal to halfway down
YT22	237.18	RD	anterior root, middle, entire thickness (4.7 mm)	2nd or 3rd from posterior loop, cervical
YT17	318.140	RD	anterior root, tip, whole thickness (11.4 mm)	<i>no enamel available (completely worn)</i>
YT20	236.38	RD	posterior root, mid to tip, not whole thickness but fused root (10.3 mm)	<i>did not sample</i>
M3				
YT15	123.2	RD	anterior-most root, tip, whole thickness (12.8 to 18.5 mm)	posterior-most end (9th loop from anterior end), cuspal, but tooth quite worn (H<2cm), so near cervix
YT16	238.18	RD	middle-anterior root, middle, entire thickness (8.8 to 28.6 mm)	anterior most end (7th loop from posterior end), near cervix because highly worn
YT19	237.23	RD	anterior root, middle, half thickness (17.0 mm)	posterior loop (8th loop from anterior end), cuspal, but "near" cervix b/c relatively worn (within 2-3 cm)
YT23	221.38	RD	middle root, tip, not whole thickness (10.6 mm)	posterior loop, cuspal, but tooth quite worn (max height = 37mm so less than that)
Adult (M6)				
YT5	60.2	RD	anterior root, base (near cervix), not entire thickness	anterior end (fractured) - 13th loop from posterior, cuspal
YT1	291.1	RD	anterior root, tip, whole thickness (21.7 to 8.5 mm)	6th loop from anterior, cervical
YT2	122.2	RD	posterior root, tip, whole thickness (7.1 to 18.7 mm)	last or 2nd to last plate (not in wear), 15th loop from anterior, cervical
YT3	173.5	D	crown dentin from cone unfused cone	3rd to last cone (~16th loop from anterior) (not yet fused)
YT4	285.1	B	bone = mandible	midway anterior-posterior (12th loop from anterior), occlusal surface to about 4 cm down
YT6	57.1	C	anterior root, tip (33.2 to 20.9 mm)	anterior loop (20th loop from posterior end), includes occlusal surface
YT7	325.22	B	maxilla bone	Last cone (posterior)
YT9	284.4	C	cementum from near cervix, loop not yet in wear	Not yet in wear (posterior) - 17th from anterior, cervical
YT10	252.2	RD	middle root, tip, whole thickness (11.5mm)	17th loop from anterior, not yet in wear (posterior), cervical
YT11	173.1	C	mechanically broke off crown cementum from middle of the tooth	8th loop from anterior end (photo), occlusal
	173.1	RD	middle of the tooth root - 2 med/lg pieces from root already fractured	n/a

3.6 References

- Ambrose, S.H., 1990. Preparation and characterization of bone and tooth collagen for isotopic analysis. *Journal of Archaeological Science*, 17(4): 431-451.
- Ambrose, S.H. and Norr, L., 1993. Experimental evidence for the relationship of the carbon isotope ratios of whole diet and dietary protein to those of bone collagen and carbonate. In: J.B. Lambert and G. Grupe (Editors), *Prehistoric Human Bone: Archaeology at the Molecular Level*. Springer-Verlag, Berlin, pp. 1-37.
- Amundson, R., Austin, A.T., Schuur, E.A.G., Yoo, K., Matzek, V., Kendall, C., Uebersax, A., Brenner, D. and Baisden, W.T., 2003. Global patterns of the isotopic composition of soil and plant nitrogen. *Global Biogeochemical Cycles*, 17(1): 1031, doi:10.1029/2002GB001903.
- Balasse, M., Bocherens, H., Mariotti, A. and Ambrose, S.H., 2001. Detection of dietary changes by intra-tooth carbon and nitrogen isotopic analysis: an experimental study of dentine collagen of cattle (*Bos taurus*). *Journal of Archaeological Science*, 28(3): 235-245.
- Barnett, R., Shapiro, B., Barnes, I., Ho, S.Y.W., Burger, J., Yamaguchi, N., Higham, T.F.G., Wheeler, H.T., Rosendahl, W., Sher, A.V., Sotnikova, M., Kuznetsova, T., Baryshnikov, G.F., Martin, L.D., Harington, C.R., Burns, J.A. and Cooper, A., 2009. Phylogeography of lions (*Panthera leo* ssp.) reveals three distinct taxa and a late Pleistocene reduction in genetic diversity. *Molecular Ecology*, 18(8): 1668-1677.
- Barnosky, A.D., Koch, P.L., Feranec, R.S., Wing, S.L. and Shabel, A.B., 2004. Assessing the causes of Late Pleistocene extinctions on the continents. *Science*, 306(5693): 70-75.
- Baryshnikov, G., 2003. *Mammuthus primigenius* from the Crimea and the Caucasus. *Deinsea*, 9: 41-56.
- Bocherens, H., 2003. Isotopic biogeochemistry and the paleoecology of the mammoth steppe fauna. *Deinsea*, 9: 57-71.
- Bocherens, H., Billiou, D., Patou-Mathis, M., Bonjean, D., Otte, M. and Mariotti, A., 1997. Paleobiological implications of the isotopic signatures (¹³C, ¹⁵N) of fossil mammal collagen in Scladina cave (Sclayn, Belgium). *Quaternary Research*, 48(3): 370-380.
- Bocherens, H. and Drucker, D., 2003. Trophic level isotopic enrichment of carbon and nitrogen in bone collagen: Case studies from recent and ancient terrestrial ecosystems. *International Journal of Osteoarchaeology*, 13(1-2): 46-53.
- Bocherens, H., Fizet, M. and Mariotti, A., 1994. Diet, physiology and ecology of fossil mammals as inferred from stable carbon and nitrogen isotope biogeochemistry: Implications for Pleistocene bears. *Palaeogeography Palaeoclimatology Palaeoecology*, 107(3-4): 213-225.
- Bocherens, H., Fogel, M.L., Tuross, N. and Zeder, M., 1995. Trophic structure and climatic information from isotopic signatures in Pleistocene cave fauna of Southern England. *Journal of Archaeological Science*, 22(2): 327-340.
- Bocherens, H. and Mariotti, A., 1997. Comments on: Diet, physiology and ecology of fossil mammals as inferred from stable carbon and nitrogen isotope biogeochemistry: Implications for Pleistocene bears by Bocherens et al. - Reply. *Palaeogeography Palaeoclimatology Palaeoecology*, 128: 362-364.

- Boutton, T.W., Tyrrell, H.F., Patterson, B.W., Varga, G.A. and Klein, P.D., 1988. Carbon kinetics of milk formation in Holstein cows in late lactation. *Journal of Animal Science*, 66(10): 2636-2645.
- Burton, J.H., Price, T.D., Cahue, L. and Wright, L.E., 2003. The use of barium and strontium abundances in human skeletal tissues to determine their geographic origins. *International Journal of Osteoarchaeology*, 13(1-2): 88-95.
- Burton, J.H., Price, T.D. and Middleton, W.D., 1999. Correlation of bone Ba/Ca and Sr/Ca due to biological purification of calcium. *Journal of Archaeological Science*, 26(6): 609-616.
- Camin, F., Perini, M., Colombari, G., Bontempo, L. and Versini, G., 2008. Influence of dietary composition on the carbon, nitrogen, oxygen and hydrogen stable isotope ratios of milk. *Rapid Communications in Mass Spectrometry*, 22(11): 1690-1696.
- Caut, S., Angulo, E. and Courchamp, F., 2009. Variation in discrimination factors ($\delta^{15}\text{N}$ and $\delta^{13}\text{C}$): the effect of diet isotopic values and applications for diet reconstruction. *Journal of Applied Ecology*, 46(2): 443-453.
- Cerling, T.E. and Harris, J.M., 1999. Carbon isotope fractionation between diet and bioapatite in ungulate mammals and implications for ecological and paleoecological studies. *Oecologia*, 120(3): 347-363.
- Comar, C.L., Russell, R.S. and Wasserman, R.H., 1957. Strontium-calcium movement from soil to man. *Science*, 126(3272): 485-492.
- Coplen, T.B., 1994. Reporting stable hydrogen, carbon, and oxygen isotopic abundances. *Pure and Applied Chemistry*, 66: 271-276.
- Coplen, T.B., Brand, W.A., Gehre, M., Groning, M., Meijer, H.A.J., Toman, B. and Verkouteren, R.M., 2006. New guidelines for $\delta^{13}\text{C}$ measurements. *Analytical Chemistry*, 78(7): 2439-2441.
- Dalerum, F., Bennett, N.C. and Clutton-Brock, T.H., 2007. Longitudinal differences in ^{15}N between mothers and offspring during and after weaning in a small cooperative mammal, the meerkat (*Suricata suricatta*). *Rapid Communications in Mass Spectrometry*, 21(12): 1889-1892.
- DeNiro, M.J., 1985. Post-mortem preservation and alteration of "in vivo" bone collagen ratios: implications for paleodietary analysis. *Nature*, 317: 806-809.
- Ducatez, S., Dalloyau, S., Richard, P., Guinet, C. and Cherel, Y., 2008. Stable isotopes document winter trophic ecology and maternal investment of adult female southern elephant seals (*Mirounga leonina*) breeding at the Kerguelen Islands. *Marine Biology*, 155(4): 413-420.
- Elliott, J.C., 2002. Calcium phosphate biominerals. In: M.J. Kohn, J. Rakovan and J.M. Hughes (Editors), *Phosphates: Geochemical, Geobiological, and Materials Importance*. Reviews in Mineralogy and Geochemistry. Mineralogical Society of America, Washington, D.C., pp. 427-453.
- Ferretti, M.P., 2003. Structure and evolution of mammoth molar enamel. *Acta Palaeontologica Polonica*, 48(3): 383-396.
- Fisher, D.C., 1996. Extinction of proboscideans in North America. In: J. Shoshani and P. Tassy (Editors), *The Proboscidea: Evolution and Palaeoecology of Elephants and Their Relatives*. Oxford University Press, Oxford, pp. 296-315.
- Fisher, D.C., 2009. Paleobiology and extinction of proboscideans in the Great Lakes region of North America. In: G. Haynes (Editor), *American megafaunal*

- extinctions at the end of the Pleistocene. *Vertebrate Paleobiology and Paleoanthropology Series*. Springer, pp. 55-75.
- Fisher, D.C. and Fox, D.L., 2007. Season of death of the Dent mammoths: Distinguishing single from multiple mortality events. In: R.H. Brunswig and B.L. Pitblado (Editors), *Frontiers in Colorado Paleoindian archaeology: From the Dent site to the Rocky Mountains*. University Press of Colorado, Boulder, pp. 123-153.
- Fizet, M., Mariotti, A., Bocherens, H., Langebadre, B., Vandermeersch, B., Borel, J.P. and Bellon, G., 1995. Effect of diet, physiology and climate on carbon and nitrogen stable isotopes of collagen in a Late Pleistocene anthropic palaeoecosystem: Marillac, Charente, France. *Journal of Archaeological Science*, 22(1): 67-79.
- Fogel, M.L., Tuross, N. and Owsley, D., 1989. Nitrogen isotope tracers of human lactation in modern and archaeological populations, Annual Report of the Director, Geophysical Laboratory, Carnegie Institute, New York.
- Fox-Dobbs, K., Leonard, J.A. and Koch, P.L., 2008. Pleistocene megafauna from eastern Beringia: Paleoecological and paleoenvironmental interpretations of stable carbon and nitrogen isotope and radiocarbon records. *Palaeogeography Palaeoclimatology Palaeoecology*, 261(1-2): 30-46.
- Fuller, B.T., Fuller, J.L., Harris, D.A. and Hedges, R.E.M., 2006. Detection of breastfeeding and weaning in modern human infants with carbon and nitrogen stable isotope ratios. *American Journal of Physical Anthropology*, 129(2): 279-293.
- Fuller, B.T., Richards, M.P. and Mays, S.A., 2003. Stable carbon and nitrogen isotope variations in tooth dentine serial sections from Wharram Percy. *Journal of Archaeological Science*, 30(12): 1673-1684.
- Germonpre, M., 1993. Osteometric data on Late Pleistocene mammals from the Flemish Valley, Belgium. *Documents de travail de l'Institute Royal des Sciences Naturelles de Belgique*, 72: 1-33.
- Gilbert, C., Sealy, J. and Sillen, A., 1994. An investigation of barium, calcium and strontium as palaeodietary indicators in the Southwestern Cape, South Africa. *Journal of Archaeological Science*, 21(2): 173-184.
- Guthrie, R.D., 1990. *Frozen fauna of the Mammoth Steppe: the story of Blue Babe*. University of Chicago Press, Chicago, 323 pp.
- Guthrie, R.D. and Stoker, S., 1990. Paleoecological significance of mummified remains of Pleistocene horses from the North Slope of the Brooks Range, Alaska. *Arctic*, 43(3): 267-274.
- Hajdas, I., Bonani, G., Furrer, H., Mader, A. and Schoch, W., 2007. Radiocarbon chronology of the mammoth site at Niederweningen, Switzerland: Results from dating bones, teeth, wood, and peat. *Quaternary International*, 164-65: 98-105.
- Handley, L.L. and Raven, J.A., 1992. The use of natural abundance of nitrogen isotopes in plant physiology and ecology *Plant Cell and Environment*, 15(9): 965-985.
- Harington, C.R., 1977. *Pleistocene mammals of the Yukon Territory*, The University of Alberta, Edmonton.
- Harington, C.R., 1996a. *American lion*, Government of Yukon, Department of Tourism and Culture, Whitehorse.
- Harington, C.R., 1996b. *American scimitar cat*, Government of Yukon, Department of Tourism and Culture, Whitehorse.

- Harington, C.R., 2002. Annotated bibliography of Quaternary vertebrates of northern North America, with radiocarbon dates. University of Toronto Press, Toronto.
- Haynes, G., 1991. Mammoths, mastodonts, and elephants: biology, behavior, and the fossil record. Cambridge University Press, Cambridge New York, 413 pp.
- Hillson, S., 2005. Teeth. Cambridge manuals in archaeology. Cambridge University Press, Cambridge, UK ; New York, 373 pp.
- Humphrey, L.T., Dean, M.C., Jeffries, T.E. and Penn, M., 2008a. Unlocking evidence of early diet from tooth enamel. Proceedings of the National Academy of Sciences of the United States of America, 105(19): 6834-6839.
- Humphrey, L.T., Dirks, W., Dean, M.C. and Jeffries, T.E., 2008b. Tracking dietary transitions in weanling baboons (*Papio hamadryas anubis*) using strontium/calcium ratios in enamel. Folia Primatologica, 79(4): 197-212.
- Jenkins, S.G., Partridge, S.T., Stephenson, T.R., Farley, S.D. and Robbins, C.T., 2001. Nitrogen and carbon isotope fractionation between mothers, neonates, and nursing offspring. Oecologia, 129(3): 336-341.
- Jenness, R., 1974. The composition of milk. In: B.L. Larson and V.R. Smith (Editors), Lactation: A Comprehensive Treatise. Academic Press, New York, pp. 3-107.
- Joubert, D., 2006. Hunting behaviour of lions (*Panthera leo*) on elephants (*Loxodonta africana*) in the Chobe National Park, Botswana. African Journal of Ecology, 44(2): 279-281.
- Katzenberg, M.A., Herring, D.A. and Saunders, S.R., 1996. Weaning and infant mortality: Evaluating the skeletal evidence. Yearbook of Physical Anthropology, 39: 177-199.
- Katzenberg, M.A., Saunders, S.R. and Fitzgerald, W.R., 1993. Age differences in stable carbon and nitrogen isotope ratios in a population of prehistoric maize horticulturists. American Journal of Physical Anthropology, 90(3): 267-281.
- Knobbe, N., Vogl, J., Pritzkow, W., Panne, U., Fry, H., Lochotzke, H.M. and Preiss-Weigert, A., 2006. C and N stable isotope variation in urine and milk of cattle depending on the diet. Analytical and Bioanalytical Chemistry, 386(1): 104-108.
- Knodel, J. and Kintner, H., 1977. Impact of breastfeeding patterns on biometric analysis of infant mortality. Demography, 14(4): 391-409.
- Koch, P.L., 1998. Isotopic reconstruction of past continental environments. Annual Review of Earth and Planetary Sciences, 26: 573-613.
- Koch, P.L. and Barnosky, A.D., 2006. Late Quaternary extinctions: State of the debate. Annual Review of Ecology Evolution and Systematics, 37: 215-250.
- Krachler, M., Rossipal, E. and Micetic-Turk, D., 1999. Trace element transfer from the mother to the newborn - investigations on triplets of colostrum, maternal and umbilical cord sera. European Journal of Clinical Nutrition, 53(6): 486-494.
- Laws, R.M., 1966. Age criteria for the African elephant, *Loxodonta a. africana*. East African Wildlife Journal, 4: 1-37.
- Laws, R.M., Parker, I.S.C. and Johnstone, R.C.B., 1975. Elephants and their habitats: the ecology of elephants in North Bunyoro, Uganda. Clarendon Press, Oxford [Eng.], xii, 376 p. pp.
- Lee, P.C. and Moss, C.J., 1986. Early maternal investment in male and female African elephant calves. Behavioral Ecology and Sociobiology, 18(5): 353-361.
- LeGeros, R.Z., 1991. Calcium Phosphates in Oral Biology and Medicine. Monographs in Oral Science, 15. Karger, New York.

- Longin, R., 1971. New method of collagen extraction for radiocarbon dating. *Nature*, 230: 241-242.
- Lough, S.A., Rivera, J. and Comar, C.L., 1963. Retention of strontium, calcium, and phosphorus in human infants. *Proceedings of the Society for Experimental Biology and Medicine*, 112(3): 631-636.
- Maglio, 1973. Origin and evolution of the Elephantidae. *Transactions of the American Philosophical Society, New Series*, 63(3): 1-149.
- Main, R.G., Dritz, S.S., Tokach, M.D., Goodband, R.D. and Nelssen, J.L., 2004. Increasing weaning age improves pig performance in a multisite production system. *Journal of Animal Science*, 82(5): 1499-1507.
- Mariotti, A., 1983. Atmospheric nitrogen is a reliable standard for natural ^{15}N abundance measurements. *Nature*, 303: 685-687.
- Maschenko, E., 2002. Individual development, biology and evolution of the woolly mammoth. *Cranium*, 19(1): 4-120.
- Masud, Z., Vallet, C. and Martin, G.J., 1999. Stable isotope characterization of milk components and whey ethanol. *Journal of Agricultural and Food Chemistry*, 47(11): 4693-4699.
- Metcalf, J.Z., Longstaffe, F.J. and White, C.D., 2009. Method-dependent variations in stable isotope results for structural carbonate in bone bioapatite. *Journal of Archaeological Science*, 36(1): 110-121.
- Metges, C., Kempe, K. and Schmidt, H.L., 1990. Dependence of the carbon-isotope contents of breath carbon dioxide, milk, serum and rumen fermentation products on the $\delta^{13}\text{C}$ value of food in dairy cows. *British Journal of Nutrition*, 63(2): 187-196.
- Miller, J.F., Millar, J.S. and Longstaffe, F.J., 2008. Carbon- and nitrogen-isotope tissue-diet discrimination and turnover rates in deer mice, *Peromyscus maniculatus*. *Canadian Journal of Zoology-Revue Canadienne De Zoologie*, 86(7): 685-691.
- Minagawa, M. and Wada, E., 1984. Stepwise enrichment of ^{15}N along food chains: Further evidence and the relation between $\delta^{15}\text{N}$ and animal age. *Geochimica et Cosmochimica Acta*, 48(5): 1135-1140.
- Morlan, R.E., 2003. Some primitive mammoth teeth from Old Crow Loc. 47, northern Yukon. In: J.E. Storer (Editor), 3rd International Mammoth Conference 2003: Program and Abstracts. Occasional Papers in Earth Sciences No. 5. Yukon Government, Whitehorse, pp. 112-113.
- Newsome, S.D., Koch, P.L., Etnier, M.A. and Auriolles-Gambao, D., 2006. Using carbon and nitrogen isotope values to investigate maternal strategies in northeast Pacific otariids. *Marine Mammal Science*, 22(3): 556-572.
- Owen-Smith, R.N., 1988. Megaherbivores: the influence of very large body size on ecology. *Cambridge studies in ecology*. Cambridge University Press, Cambridge ; New York, xiii, 369 p. pp.
- Polischuk, S.C., Hobson, K.A. and Ramsay, M.A., 2001. Use of stable-carbon and -nitrogen isotopes to assess weaning and fasting in female polar bears and their cubs. *Canadian Journal of Zoology-Revue Canadienne De Zoologie*, 79(3): 499-511.
- Power, R.J. and Compion, R.X.S., 2009. Lion predation on elephants in the Savuti, Chobe National Park, Botswana. *African Zoology*, 44(1): 36-44.

- Renou, J.P., Deponge, C., Gachon, P., Bonnefoy, J.C., Coulon, J.B., Garel, J.P., Verite, R. and Ritz, P., 2004. Characterization of animal products according to geographic origin and feeding diet using nuclear magnetic resonance and isotope ratio mass spectrometry: cow milk. *Food Chemistry*, 85(1): 63-66.
- Rossipal, E., Krachler, M., Li, F. and Micetic-Turk, D., 2000. Investigation of the transport of trace elements across barriers in humans: studies of placental and mammary transfer. *Acta Paediatrica*, 89(10): 1190-1195.
- Rountrey, A.N., Fisher, D.C., Vartanyan, S. and Fox, D.L., 2007. Carbon and nitrogen isotope analyses of a juvenile woolly mammoth tusk: Evidence of weaning. *Quaternary International*, 169: 166-173.
- Saragusty, J., Hermes, R., Goritz, F., Schmitt, D.L. and Hildebrandt, T.B., 2009. Skewed birth sex ratio and premature mortality in elephants. *Animal Reproduction Science*, 115(1-4): 247-254.
- Sare, D.T.J., Millar, J.S. and Longstaffe, F.J., 2005. Nitrogen- and carbon-isotope fractionation between mothers and offspring in red-backed voles (*Clethrionomys gapperi*). *Canadian Journal of Zoology-Revue Canadienne De Zoologie*, 83(5): 712-716.
- Schaller, G.B., 1972. *The Serengeti lion: A study of predator-prey relationships*. Wildlife Behavior and Ecology. The University of Chicago Press, Chicago, 480 pp.
- Schwarcz, H.P., 2000. Some biochemical aspects of carbon isotopic paleodiet studies. In: S.H. Ambrose and M.A. Katzenberg (Editors), *Biogeochemical Approaches to Paleodietary Analysis*. Kluwer Academic, New York, pp. 189-209.
- Shoshani, J., 1996. Skeletal and other basic anatomical features of elephants. In: J. Shoshani and P. Tassy (Editors), *The Proboscidea: Evolution and palaeoecology of elephants and their relatives*. Oxford University Press, Oxford, pp. 9-20.
- Sillen, A. and Smith, P., 1984. Weaning patterns are reflected in strontium-calcium ratios of juvenile skeletons. *Journal of Archaeological Science*, 11(3): 237-245.
- Sponheimer, M., de Ruiter, D., Lee-Thorp, J. and Spath, A., 2005. Sr/Ca and early hominin diets revisited: new data from modern and fossil tooth enamel. *Journal of Human Evolution*, 48(2): 147-156.
- Sponheimer, M. and Lee-Thorp, J.A., 2006. Enamel diagenesis at South African Australopith sites: Implications for paleoecological reconstruction with trace elements. *Geochimica et Cosmochimica Acta*, 70(7): 1644-1654.
- Stumpf, P. and Welsch, U., 2004. Secretory and defensive functions of the duct system of the lactating mammary gland of the African elephant (*Loxodonta africana*, Proboscidea). *Zoomorphology*, 123(3): 155-167.
- Sukumar, R., 2003. *The living elephant: evolutionary ecology, behavior, and conservation*. Oxford University Press, Oxford, 478 pp.
- Sukumar, R. and Ramesh, R., 1992. Stable carbon isotope ratios in Asian elephant collagen: Implications for dietary studies. *Oecologia*, 91(4): 536-539.
- Szpak, P., Grocke, D.R., Debruyne, R., MacPhee, R.D.E., Guthrie, R.D., Froese, D., Zazula, G.D., Patterson, W.P. and Poinar, H.N., 2010. Regional differences in bone collagen $\delta^{13}\text{C}$ and $\delta^{15}\text{N}$ of Pleistocene mammoths: Implications for paleoecology of the mammoth steppe. *Palaeogeography Palaeoclimatology Palaeoecology*, 286(1-2): 88-96.

- Tieszen, L.L., 1991. Natural variations in the carbon isotope values of plants: Implications for archaeology, ecology, and paleoecology. *Journal of Archaeological Science*, 18: 227-248.
- Tieszen, L.L. and Fagre, T., 1993. Effect of diet quality and composition on the isotopic composition of respiratory CO₂, bone collagen, bioapatite, and soft tissues. In: J.B. Lambert and G. Grupe (Editors), *Prehistoric Human Bone: Archaeology at the Molecular Level*. Springer-Verlag, Berlin, pp. 121-155.
- Trueman, C.N. and Tuross, N., 2002. Trace elements in recent and fossil bone apatite. *Phosphates: Geochemical, Geobiological, and Materials Importance*, 48: 489-521.
- Turner, A., 1997. *The big cats and their fossil relatives: An illustrated guide to their evolution and natural history*. Columbia University Press, New York, 234 pp.
- van Klinken, G.J., 1999. Bone collagen quality indicators for paleodietary and radiocarbon measurements. *Journal of Archaeological Science*, 26(687-695).
- Vaughan, T.A., Ryan, J.M. and Czaplewski, N.J. (Editors), 2000. *Mammalogy*, 4th Edition. Saunders College Publishing, New York.
- Williams, J.S., White, C.D. and Longstaffe, F.J., 2005. Trophic level and macronutrient shift effects associated with the weaning process in the Postclassic Maya. *American Journal of Physical Anthropology*, 128(4): 781-790.
- Wilson, G.F., Mackenzie, D.D.S., Brookes, I.M. and Lyon, G.L., 1988. Importance of body tissues as sources of nutrients for milk synthesis in the cow, using ¹³C as a marker. *British Journal of Nutrition*, 60(3): 605-617.
- Witt, G.B. and Ayliffe, L.K., 2001. Carbon isotope variability in the bone collagen of red kangaroos (*Macropus rufus*) is age dependent: Implications for palaeodietary studies. *Journal of Archaeological Science*, 28(3): 247-252.
- Wood, J.W., Milner, G.R., Harpending, H.C. and Weiss, K.M., 1992. The osteological paradox: Problems of inferring prehistoric health from skeletal samples. *Current Anthropology*, 33(4): 343-370.
- Wooller, M.J., Zazula, G.D., Edwards, M., Froese, D.G., Boone, R.D., Parker, C. and Bennett, B., 2007. Stable carbon isotope compositions of Eastern Beringian grasses and sedges: Investigating their potential as paleoenvironmental indicators. *Arctic, Antarctic and Alpine Research*, 39(2): 318-331.
- Wright, L.E. and Schwarcz, H.P., 1998. Stable carbon and oxygen isotopes in human tooth enamel: Identifying breastfeeding and weaning in prehistory. *American Journal of Physical Anthropology*, 106(1): 1-18.
- York, A.E., Thomason, J.R., Sinclair, E.H. and Hobson, K.A., 2008. Stable carbon and nitrogen isotope values in teeth of Steller sea lions: age of weaning and the impact of the 1975-1976 regime shift in the North Pacific Ocean. *Canadian Journal of Zoology-Revue Canadienne De Zoologie*, 86(1): 33-44.
- Zazula, G.D., Hare, P.G. and Storer, J.E., 2009. New radiocarbon-dated vertebrate fossils from Herschel Island: Implications for the palaeoenvironments and glacial chronology of the Beaufort Sea coastlines. *Arctic*, 62(3): 273-280.
- Zazula, G.D. and Wooller, M., 2008. Comment on "Environmental setting, (micro)morphologies and stable C-O isotope composition of cold climate carbonate precipitates - a review and evaluation of their potential as paleoclimatic proxies" by Denis Lacelle, *Quaternary Science Reviews* 26, 1670-1689. *Quaternary Science Reviews*, 27(15-16): 1659-1660.

Zherekhova, I.Y., 1977. Description and measurements of the teeth of the mammoths of Berelekh. In: O.A. Skarlato (Editor), Academy of Sciences of the USSR: Proceedings of the Zoological Institute, Leningrad, pp. 91-106.

Chapter 4

Mammoth tooth enamel growth rates inferred from stable isotope analysis and histology: Implications for sampling methodologies

4.1 Introduction

Stable isotope analysis of serially-sampled tooth enamel is widely used to reconstruct seasonal changes in diet and climate (recent studies include Bernard et al., 2009; Eberle et al., 2009; Feranec et al., 2009; Widga et al., 2010; Zazzo et al., 2010). However, in order to devise appropriate sampling strategies and to interpret variations in stable isotope compositions as seasonal or annual signals, an understanding of tooth growth rate is needed. For example, Passey et al. (2005) developed an “inverse model” for reconstructing the isotopic compositions of body fluids from incrementally sampled tooth isotope results. Their model requires knowledge of species- and tooth-specific growth parameters (i.e., length of tooth undergoing maturation at a given point in time, length of tooth undergoing matrix deposition a given point in time, proportion of final mineral content formed during matrix deposition), and assumes a constant growth rate. Growth rates can vary considerably among species, among individual teeth, and within individual teeth. For modern species, growth rates of individual teeth can be precisely determined using controlled feeding studies (e.g., Balasse, 2002; Zazzo et al., 2005, 2010). For fossil teeth, growth rates can be estimated based on incremental features (e.g., Fisher, 2009; Nargolwalla et al., 2005). However, isotopic studies of fossil species often assume growth rates based on the isotopic data themselves, and the apparent seasonal patterns they suggest. This approach can be problematic since seasonal changes in “input” signals (i.e., drinking water $\delta^{18}\text{O}$ values) do not always follow regular sinusoidal patterns, and one period in the isotope curve does not always correspond to one year of growth. Indeed, regular but not sinusoidal “input” signals can sometimes produce patterns in the isotopic data for tooth enamel that appear sinusoidal (Passey and Cerling, 2004).

Proboscidean teeth are well-suited to serial sampling and stable isotope analysis because of their large size and relatively long period of growth. The first study of this type was conducted on proboscidean tusk dentin (Koch et al., 1989), and many isotopic studies of proboscidean tusks have been conducted subsequently (e.g., Fisher and Fox,

2003, 2007; Fox and Fisher, 2004; Fox et al., 2007). However, enamel is typically the preferred tissue for stable isotope analysis of bioapatite, because of its greater resistance to diagenetic alteration (Zazzo et al., 2004).

To our knowledge, there are no published full reports on the duration and rate of formation of proboscidean molar tooth enamel, though detailed work is underway (Dirks et al., 2010). In this study, we investigate the growth rate of tooth enamel from a Columbian mammoth in two dimensions (along the tooth height/occlusal-basal plane and through the enamel thickness), using a combination of stable isotope and histological measurements. We implement a method for serially-sampling tooth enamel that was shown in modern teeth to minimize “dampening” caused by tooth growth geometry (Zazzo et al., 2005). To our knowledge, this is one of the first applications of this method to fossil teeth. This approach may prove useful in guiding sampling strategies for future isotopic studies of proboscidean tooth enamel.

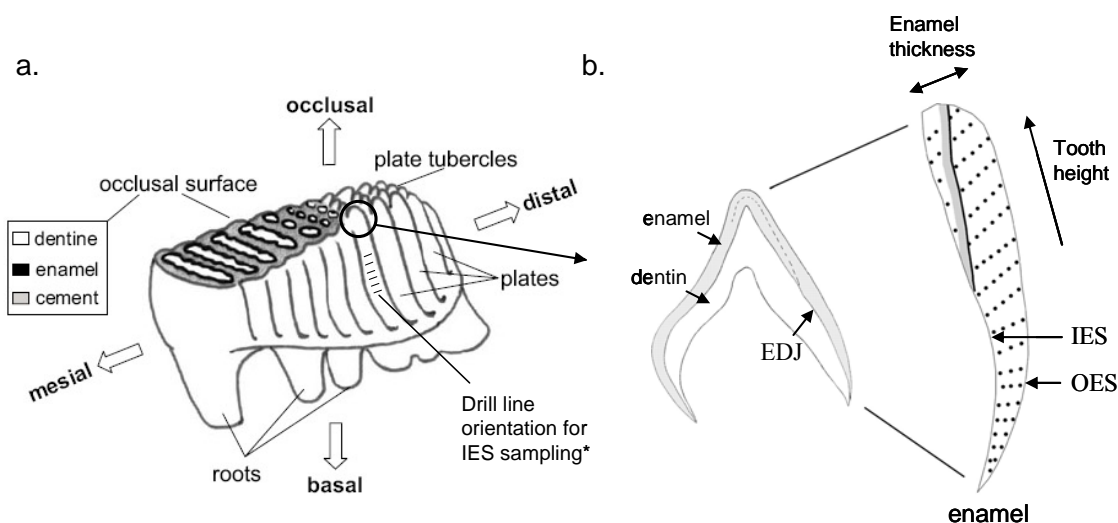


Figure 4.1 (a) Proboscidean tooth morphology (adapted from Ferretti 2003: Fig. 2). *Drill lines are depicted on the outer enamel surface (OES), as in “traditional” sampling techniques. However, in this study, lines in the same orientation were drilled on the inner enamel surface (IES). (b) Growth geometry of sectioned enamel (adapted from Humphrey et al. 2008: Fig. 2.). EDJ = enamel-dentin junction. Dashed line and solid lines nearly parallel to the EDJ or OES represent Striae of Retzius. Dotted lines represent enamel prisms. Spaces between dots represent cross-striations (not to scale).

4.2 Enamel Formation

Mammalian tooth enamel begins to form at the uppermost (occlusal) point of the enamel-dentin junction (EDJ) and growth progresses outwards through the enamel thickness (towards the outer enamel surface) and downwards along the tooth height (towards the cervix, in the occlusal-basal direction) (Figure 4.1) (Hillson, 2005). Growth rate in the occlusal-basal direction is referred to as the extension rate (Shellis, 1984). Here, we refer to growth perpendicular to the EDJ as “enamel thickness growth rate”.

Enamel growth occurs in two stages. During the secretory stage, ameloblast cells secrete an organic matrix onto which bioapatite (substituted carbonate hydroxyapatite) crystallites are seeded (Smith and Tafforeau, 2008). During this stage, incremental features that correspond to intrinsic biological rhythms are formed (e.g., cross-striations, which reflect daily rhythms, constant among species; Striae of Retzius, which represent a period of days to weeks, variable among species but constant within individuals) (Bromage et al., 2009; FitzGerald, 1998). Only about 20-30% of the final mineral content of the tooth (by weight) is formed during the secretory stage (Passey et al., 2005, and references therein). During the second or maturation stage, enamel crystals grow in volume, and the matrix proteins and enamel fluid are removed (Smith, 1998). This stage encompasses about two-thirds of the total formation time (Smith, 1998).

The typical sampling strategy for studies of seasonality using stable isotope compositions of teeth is to drill lines on the outer enamel surface, perpendicular to the height of the tooth, through most or all of the enamel thickness (Balasse, 2003). The drill line closest to the occlusal surface represents the earliest-formed enamel, and the line closest to the roots represents the latest-formed enamel. Both the geometry of sampling and the prolonged maturation stage result in “dampening” of the original input signal (i.e., the amplitude of seasonal changes in body water $\delta^{18}\text{O}$ values and blood bicarbonate $\delta^{13}\text{C}$ values) and decreased temporal resolution (Balasse, 2002; Passey and Cerling, 2002).

In artiodactyls, primates, rodents, and carnivores, the innermost enamel adjacent to the EDJ is strongly mineralized just after its formation (e.g., ~80-90% of the final mineral content in rhinoceros) (Allan, 1967; Suga, 1979, 1989; Tafforeau et al., 2007). Balasse (2003) was the first to recommend sampling of the innermost layer of enamel for isotopic analysis. In a controlled feeding study, Zazzo et al. (2005) confirmed that

sampling the innermost enamel of cow teeth resulted in the recovery of original variations in input δ -values (even when non-sinusoidal), and found that the degree of isotopic dampening was constant when teeth were sampled using this method, regardless of the structure of the environmental signal. In contrast, sampling using the “traditional” method resulted in variable degrees of signal dampening, and averaging of non-sinusoidal input signals such that they appeared sinusoidal. Although this study showed inner enamel sampling to be superior to conventional strategies (at least for bovines), to our knowledge the approach has not been further utilized, probably because of the technical difficulties in sampling the innermost enamel layer.

Formation of a rapidly mineralized inner enamel layer has not been demonstrated for proboscideans, but is probable given its existence across diverse taxa. The innermost enamel layer in proboscideans consists of 3D enamel, an enamel type unique to that order (Ferretti, 2003, 2008). However, other mammals with hypsodont (high crowned) molars (e.g., *Equus*, *Bos*, *Phacochoerus*) also have specialized enamel types near the EDJ, which are structurally different but functionally similar to 3D enamel (Ferretti, 2003). The 3D enamel layer makes up about 10-20% of the total enamel thickness in *Mammuthus* (Ferretti, 2003), which comprises about 150 to 700 μm in Columbian mammoths, given a total enamel thickness for M5 and M6 of 1.5 to 3.5 mm (Saunders, 1970). The highly-mineralized inner enamel layer in other taxa is very thin [only 20 μm thick in rhinoceros (Tafforeau et al., 2007) and 8 μm in primates (Suga, 1989)], so it may not encompass the entire 3D enamel layer of proboscideans. However, the entire inner two-thirds of the enamel thickness mineralizes more quickly than the outer one-third, at least in primates (Suga, 1989). In addition, Balter et al. (2008) have pointed out that hypsodont tooth enamel grows much faster in height (occlusal-basal direction) than it does in thickness. For all of these reasons, drilling the inner enamel surface (IES) should provide better temporal resolution and less dampening of the isotope signal than drilling the same depth from the outer enamel surface.

4.3 Methods

4.3.1 Sampling from intact specimen

The specimen chosen for study was a third adult molar [M6, after Laws (1966)] of Eloise, a Columbian mammoth from the San Pedro Valley of Arizona (sample AZ1; see Chapter 5). This is a highly significant specimen, since Eloise was the last known mammoth to die at Murray Springs prior to the onset of the Younger Dryas cold period, and was certainly either hunted or scavenged by Clovis people. Eloise was approximately 41-47 years old at the time of death (Haynes and Huckell, 2007), so this tooth should have been completely formed before death (Metcalf et al., 2010) (Chapter 3, Table 3.1).

The tooth was sampled near the cervix on the 10th lamella from the posterior end (plate X). A wedge-shaped section of enamel and dentin was removed from the tooth by making two cuts with a Dremel circular saw blade on the side of the tooth, parallel to the tooth height (i.e., from top to bottom of an enamel loop edge). The lowermost portion of this section was used for IES sampling (~40 mm in occlusal-basal “height”). A piece of enamel (~3mm in “height”) directly above the segment used for IES sampling was used for enamel thickness (ET) sampling. A piece of enamel (~20 mm in “height”) directly above the IES sample, adjacent to the ET-sample, was used for thin section preparation

4.3.2 Histology

4.3.2.1 “Thin” Section Preparation

The sample was embedded in Epofix epoxy under vacuum. A cut was made parallel to the height of the tooth (occlusal-basal axis) and perpendicular to the length of the tooth (mesial-distal axis) (see Figure 4.1) using an Isomet saw. The cut specimen was glued to a slide with hot Crystal Bond, and a section approximately 1 mm thick was cut using the Isomet saw. The section was thinned with 400 grit sandpaper on a polishing wheel, then polished on both sides with 3 μm alumina slurry and final finishing polishing cloths, and with 1 μm aluminum oxide slurry on a glass mirror. The polished section was attached to a new slide using UV-activated Loctite 363. The final thickness of the section was measured with digital calipers to about 450 μm . Attempts to thin the section further

were discontinued because of sample fragmentation. Figure 4.2 shows photomicrographs of the thin section used for the measurements described below.

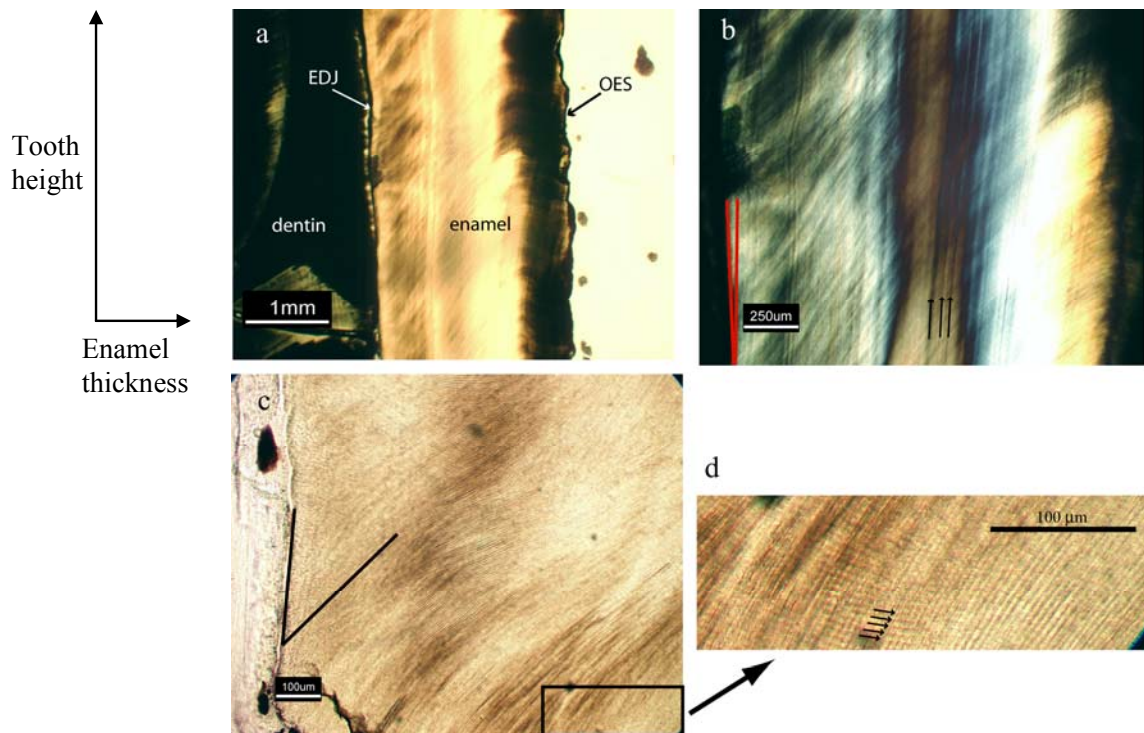


Figure 4.2 Thin section images for enamel from AZ1 (Eloise), taken in plane-polarized (a, c, d) and cross-polarized light (b). All photomicrographs are oriented with the enamel-dentin junction (EDJ) on the left and outer enamel surface (OES) on the right. (a) The entire enamel thickness. (b) Striae of Retzius (arrows) and angle between Striae of Retzius and EDJ (red lines). (c) Angle between enamel prisms and EDJ (black lines). Boxed area is enlarged in (d). (d) Cross-striations (arrows).

4.3.2.2 Extension Rate

Shellis (1984) calculated the enamel growth rate in the occlusal-basal direction (i.e., extension rate), using the following equation:

$$c = d[(\sin I/\tan D) - \cos I] \quad [\text{Equation 4.1}],$$

where c is the “height” of enamel formed per day in the occlusal-basal direction, D is the angle between the EDJ and the Striae of Retzius (in the occlusal direction), I is the angle between the EDJ and the enamel prisms (in the occlusal direction), and d is the

cross striation interval (distance between cross striations along an enamel prism). These features are all visible in thin section (Figure 4.2). The measurements reported here were made in Adobe Photoshop, using photomicrographs taken in regular, plane-polarized, or cross-polarized light, as described below. The extension rate estimate obtained using this method is given as a range of values, derived from the maximum and minimum measured d , I , and D values.

4.3.2.2.1 Cross-Striation Interval (d) Estimates of d were obtained in two ways: (1) by directly counting the number of cross-striations within a given length of enamel prism and dividing the length by the number of cross-striation intervals (Figure 4.2d) ($n = 8$ measurements in different portions of the section), and (2) by measuring the distance between successive Striae of Retzius along enamel prisms, and dividing by the cross-striation repeat interval (number of cross-striation intervals between Striae of Retzius; for *Mammuthus columbi*, the value is 14) (Figure 4.2b) ($n = 6$ measurements) (Bromage et al., 2009). Method 2 was used as a check on Method 1, since cross-striations can be difficult to identify definitively in thin section.

4.3.2.2.2 Striae of Retzius – EDJ Angle (D) Striae of Retzius in *Mammuthus* are nearly parallel to the EDJ (Ferretti 2003), making the angle difficult to measure accurately (Shellis, 1984). Estimates of D ($n = 6$) were obtained for AZ1 from photomicrographs taken using cross-polarized light (Figure 4.2b).

4.3.2.2.3 Enamel Prism – EDJ Angle (I) Enamel prisms in *Mammuthus* are not straight; rather, they depart from the EDJ at approximately 90° and curve towards the occlusal surface as they move towards the outer enamel surface (OES). Since the prisms are curved, measurement of I (the angle between the EDJ and prisms) can depend on which section of the prism is used. Furthermore, the prisms that comprise proboscidean 3D enamel display variable directions of growth in three dimensions, rather than a more consistent unidirectional pattern (Ferretti, 2003, 2008). We measured the angle of the most prominent bundles of prisms in the 3D enamel that were oriented in an occlusal-

OES direction from the EDJ (Figure 4.2c). Nine measurements from different portions of the section were obtained to encompass the reasonable range of prism angles.

4.3.2.3 Enamel Thickness Growth Rate

Enamel thickness growth rate was measured using histological methods combined with simple trigonometry. We defined a right triangle where the hypotenuse is the cross-striation interval (d) along an enamel prism and the other sides are the EDJ and the distance grown perpendicular to the EDJ in one day (x). Then, x can be calculated as follows:

$$x = d (\sin I) \quad \text{[Equation 4.2]}$$

This approach assumes that the angle between the EDJ and enamel prisms (I) is constant and that prisms show no curvature, which is not the case. To minimize any error resulting from this assumption, measurements of I were obtained from portions of prisms less than 600 μm from the EDJ, close to the distance covered by ET sampling for isotopic analysis. Numerous measurements were obtained to encompass the range in prism angles (Section 4.3.2.2.3). Moreover, the enamel prisms were almost straight in this portion of the section, and tended to curve nearer the OES, beyond the range of the ET sampling conducted in the present study. Thus, this method should give a reasonable estimate of growth rate through the enamel thickness for the portion of enamel sampled using the ET method. The enamel thickness growth rate calculated using this method is given as a range of values, obtained by using the maximum and minimum measured d and I values.

4.3.3 Stable Isotope Analysis

4.3.3.1 Preparation and Sampling (IES and ET)

Dentin was soft and chalk-like, and was removed easily with a dental pick and wire brush. For IES sampling, a large, intact section of enamel was cleaned with acetone and de-ionized water, and mounted on a microdrill plate with the IES facing up. Lines were drilled in the distal-mesial direction, perpendicular to the height of the tooth, on the IES, using a Merchantek MicroMill (see Figure 4.1). IES drill lines were exactly 100 μm wide (occlusal-basal direction), 1 mm apart (occlusal-basal direction), 125-250 μm deep

(enamel thickness direction), and about 8 mm long (mesial-distal direction) (see Chapter 5, Figure 5.2a). The length and depth of each line varied slightly in order to obtain sufficient powder for isotopic analysis. Shallow depths and narrow widths were chosen to minimize any possible time-averaging caused by sampling geometry and tooth maturation, as was described earlier. For enamel thickness (ET) sampling, a piece of enamel was mounted on a glass slide with the IES facing up, and that slide was mounted vertically on a microdrill plate, so that the IES was facing sideways, and the sample could be drilled parallel to the IES using the side of the drill bit, following the method described by Zazzo et al. (2005). Using this sampling strategy, sampling resolution is not constrained by the size of the drill bit, but only by the precision of the Micromill software's drill path co-ordinates and step size. All drilled increments comprised about 3 mm of tooth height (occlusal-basal direction) and about 5 mm in the mesial-distal direction. The first sample comprised the first 100 μm from the IES, and subsequent samples were obtained at increments of 10 to 50 μm from the previous sample. The ET sampling strategy covered a total distance of 360 μm from the IES, so the isotope results for this method also represent growth of the innermost (3D) enamel, but in a different direction to that represented by IES sampling. In other words, the IES sampling strategy follows growth in the occlusal-basal direction, representing growth in tooth height (i.e., extension rate) while the ET sampling strategy follows growth from the IES to OES, representing growth through the enamel thickness (Figure 4.1).

Drilled powder was collected and transferred to vials using dental tools. Initial tests showed no difference between conventionally pretreated versus untreated samples for $\delta^{13}\text{C}$ ($<0.1\text{‰}$, within analytical error) and only small offsets for $\delta^{18}\text{O}$ ($0.5 \pm 0.2\text{‰}$). [Samples were pretreated at room temperature using 2-3% NaOCl for 24 hours, followed by 0.1 M acetic acid for 4 hours, after Koch et al. (1997) and Garvie-Lok et al. (2004).] Because omitting the pretreatment step allows smaller samples to be utilized (resulting in less isotopic averaging of growth increments), the samples described here were not pretreated prior to analysis.

4.3.3.2. Analysis

Samples were reacted with ortho-phosphoric acid at 90°C for 25 minutes, using a MultiPrep automated sampling device configured so that the connection with the cold trap is closed for the duration of the reaction (i.e., a “sealed vessel” reaction condition) (Metcalf et al., 2009). The resulting CO₂ gas was cryogenically purified and analyzed using an Optima isotope ratio mass spectrometer in dual-inlet mode.

Stable isotope results are presented in standard delta (δ) notation, in units of per mil (‰), relative to VSMOW (oxygen) and VPDB (carbon) (Coplen, 1994; Coplen et al., 2006). The results were calibrated using NBS-19 and Suprapur ($\delta^{13}\text{C}$), and NBS-19 and NBS-18 ($\delta^{18}\text{O}$). The average reproducibility (1σ) for enamel samples was 0.10 for $\delta^{13}\text{C}$ and 0.15 for $\delta^{18}\text{O}$.

4.3.3.3. Extension Rate Estimate

For comparison with the extension rate estimated using histological measurements, extension rate was also estimated directly from the stable isotope data obtained by IES sampling. For this estimate, we used the carbon-isotope curve, which was smoother than the oxygen-isotope curve. However, since both have approximately the same period, using the latter gives the same result. Each $\delta^{13}\text{C}$ maximum and minimum were identified, and the distance between sequential maxima (or minima) was inferred to represent one year of growth. The ET growth rate was not estimated using stable isotope results because less than a full period of variation was present for the carbon and oxygen isotope curves obtained by ET sampling.

4.4 Results

4.4.1 Diagenesis

Several lines of evidence indicate that the enamel is well-preserved: its macroscopic appearance (yellowish to white, translucent to opaque), the visibility of incremental growth features in thin section (e.g., Striae of Retzius, cross-striations) (Figure 4.2), the minimal differences between pretreated and untreated $\delta^{13}\text{C}$ and $\delta^{18}\text{O}$ values (Section 4.3.3.1), and a lack of correlation between carbonate contents and $\delta^{13}\text{C}$ or

$\delta^{18}\text{O}$ values (which might occur if significant quantities of diagenetic carbonate were contributing to the gas produced during analysis) (Pearson's $r = -0.09$, $df = 36$; $r = 0.18$, $df = 36$, respectively). Fourier-Transform Infrared Spectroscopy (FTIR) analysis of untreated enamel from AZ1 showed no evidence of calcite contamination, and the sample had a Crystallinity Index of 3.0, which is close to those of modern suid, bovid, and camelid enamel (3.4 to 4.4) (Roche et al., 2010) and to those of other well-preserved proboscidean enamel specimens (Chapters 6, 7) (see Chapter 2 for FTIR methods). Furthermore, the sinusoidal variation in $\delta^{13}\text{C}$ and $\delta^{18}\text{O}$ values obtained from incrementally sampled enamel (described below) is typical of seasonal variation, and is unlikely to have been preserved if significant post-mortem isotopic alteration had occurred.

4.4.2 Inner Enamel Surface (IES)

4.4.2.1 Histology

The length of prism formed per day (d) measured using Method 1 ranged from 3.6 to 5.2 μm , and generally increased with distance from the EDJ (ca. 100 to 812 μm away). Measurements of d obtained using Method 2 (2.1 to 5.6 μm) encompass a larger range than those obtained using Method 1, but are generally consistent. Thus, Method 2 validates Method 1, which should be more accurate. The angle between Striae of Retzius and the EDJ (D) ranged from 5.2 to 7.1°. The angle between enamel prisms and the EDJ (I) ranged from 37 to 45°. Measurements of I from a photomicrograph at lower magnification (using portions of prisms further from the EDJ) ranged from 46 to 53°.

The enamel extension rate (c) was calculated for AZ1 using Equation 4.1 (Shellis, 1984) and the measurements above. The c values ranged from 15 to 40 $\mu\text{m}/\text{day}$, corresponding to yearly extension rates of 5.3 to 14.6 mm/year .

4.4.2.2 Stable Isotopes

The $\delta^{13}\text{C}$ and $\delta^{18}\text{O}$ values plotted against distance are approximately sinusoidal, with equal periods (Figure 4.3a). The $\delta^{13}\text{C}$ curve is much smoother than the $\delta^{18}\text{O}$ curve, making it easier to identify maxima and minima. The distance between sequential

maxima and minima (estimated extension rate) based on the carbon isotope results for IES sampling is 13-14 mm per year. The oxygen isotope curve also appears to have the same period, which results in an identical estimate for extension rate.

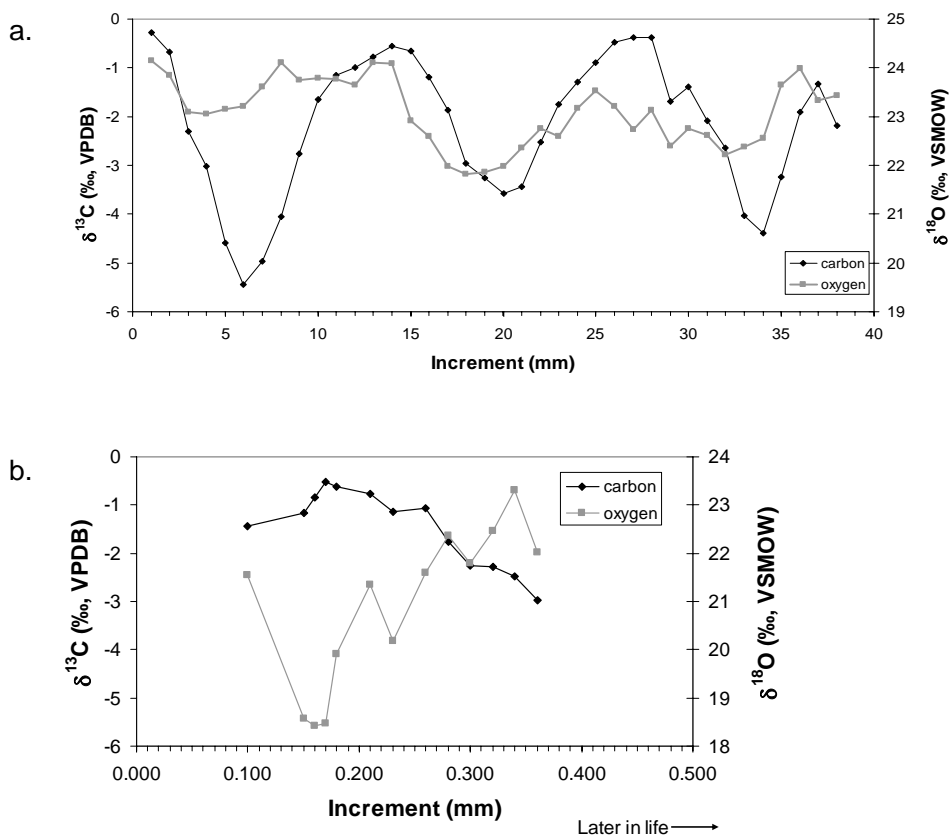


Figure 4.3 Carbon and oxygen isotope results for AZ1 obtained using IES (a) and ET (b) sampling strategies, as described in the text. Increment numbers increase in the basal (cervical) direction (a) or towards the outer enamel surface (b).

4.4.3 Enamel Thickness (ET)

4.4.3.1 Histology

Using the *d* and *I* values measured for AZ1 (above), the ET growth rate is calculated to be 2.2 to 4.2 $\mu\text{m}/\text{day}$, corresponding to a yearly rate of 0.8 to 1.5 mm/year .

4.4.3.2. Stable Isotopes

Assuming that annual variations in $\delta^{13}\text{C}$ and $\delta^{18}\text{O}$ values were approximately sinusoidal (as described for IES sampling), it is likely that less than half a full period of variation is represented by the ET stable isotope results (Figure 4.3b). The range of $\delta^{13}\text{C}$ values obtained using this method (2.4‰) is smaller than that obtained from IES sampling (5.2‰), but the range of $\delta^{18}\text{O}$ values is greater (4.9 versus 2.3‰, respectively).

4.5 Discussion

4.5.1 Extension Rate (IES Sampling)

The extension rate estimated using the IES stable isotope data (13-14 mm/year) lies within the range of estimates obtained from thin section measurements (5.3 to 14.6 mm/year). The relatively large range obtained from thin section measurements is a result of several factors, including (1) variations in extension rate along the height of the tooth (thin sections were obtained from a section several mm above that used for micromilling), (2) the high degree of error in measuring *D* when the angle is very low, as in *Mammuthus*, and (3) the necessity of measuring Striae of Retzius angles, cross-striation lengths, and enamel prism angles in different parts of the section, because of variations in visibility of these features. Smith et al. (2006) found the method of Shellis (1984) to underestimate true extension rates, which may explain why those estimates range to lower values than those made using the isotope data. In addition, the extension rate derived from thin section measurements does not distinguish between the different enamel layers, whereas the isotope results (IES sampling) correspond only to 3D enamel near the EDJ, which likely mineralizes faster than the rest of the enamel (see Section 4.2). All things considered, there is relatively good agreement between the histological and isotopic (IES

sampling) evidence for enamel extension rate. Furthermore, these results are consistent with the extension rates calculated for a Columbian mammoth M5/M6 by Dirks et al. (2010), using a different histological method. For the Columbian mammoth tooth utilized in the present study, the hypothesis that one period of variation in $\delta^{13}\text{C}$ and $\delta^{18}\text{O}$ versus distance (obtained using the sampling strategy described here) is equal to one year of growth is supported by the independent histological evidence. The extension rate of this sample was essentially constant over the distance sampled (37 mm), which represents about 3 years of growth. Additional studies are needed to determine the extent to which extension rates vary within and among proboscidean teeth.

The agreement between extension rates estimated from stable isotope data and incremental features is somewhat surprising, since the isotopic compositions reflect mineralization during both the secretory and maturation stages, whereas incremental features are formed only during the former stage. However, this agreement may in part be a result of sampling only the IES, which mineralizes faster than the rest of the enamel. It remains to be determined whether “traditional” sampling strategies, which involve drilling in the same orientation but through the entire enamel thickness, would produce a similar match. Attempts to reconstruct “input” values from measured stable isotope compositions in teeth should pay special attention to the details of the sampling strategy, since different parts of the tooth may have considerably different growth parameters (overall growth rate, maturation time, etc.).

4.5.2 Enamel Thickness Growth Rate (ET sampling)

The enamel thickness growth rate calculated using histological measurements (0.8 to 1.5 mm/year) is consistent with the ET stable isotope results (less than half a period is represented by 0.36 mm sampling distance). The growth rate through the enamel thickness is much slower than that along the height of the tooth (extension rate), so the ET sampling method described here could be used to investigate shorter-term (e.g., weekly) variations in $\delta^{13}\text{C}$ and $\delta^{18}\text{O}$ values, whereas the IES sampling method is more suited to investigating longer-term (i.e., monthly or yearly) variations. The different ranges of $\delta^{13}\text{C}$ and $\delta^{18}\text{O}$ values can be partially explained by the different growth rates represented by the IES and ET sampling methods. The smaller range of $\delta^{13}\text{C}$ values

obtained using ET sampling may indicate that the proportions of C₃ to C₄ vegetation in the mammoth's diet changed less in the short-term (from day-to-day or week-to-week) than in the long-term (i.e., seasonally). In contrast, the larger range of $\delta^{18}\text{O}$ values in the ET curve may reflect the large isotopic variations that can occur in different rainfall events or within different water sources (e.g., evaporated puddles, rivers, and springs), which are averaged over a longer time scale (i.e., in the IES curve).

4.6 Conclusions

An enamel extension rate of 13-14 mm/year, and an enamel thickness growth rate of 0.8 to 1.5 mm/year, were inferred from stable isotope analysis and thin section measurements of the innermost enamel of an adult Columbian mammoth tooth. Despite the dampening caused by the maturation stage of enamel mineralization, there is general agreement between growth rates estimated using histology and those inferred from the periodicity of stable isotope results. In part, this agreement may result from sampling enamel near the EDJ, which mineralizes much faster than enamel closer to the outer enamel surface.

We have shown that it is feasible to sample the inner enamel surface (IES) for stable isotope analysis, as recommended by previous authors (Balasse, 2003; Zazzo et al., 2005). The large, regular variations in $\delta^{13}\text{C}$ and $\delta^{18}\text{O}$ values obtained in this study suggest that IES sampling is an effective strategy for recovering seasonal changes in the isotopic compositions of diet and drinking water. Sampling sequential layers through the enamel thickness (ET sampling) may be useful for studying short-term variations in proboscidean diet and drinking water, but for studies of seasonal changes the IES sampling method is probably superior. Further research is required to determine the degree to which growth rates vary within and among proboscidean teeth, and to determine the degree of input-signal dampening associated with the IES method relative to that of traditional methods.

4.7 References

- Allan, J.H., 1967. Maturation of enamel. In: A.E.W. Miles (Editor), *Structural and Chemical Organization of Teeth*. Academic Press, New York, pp. 467-494.
- Balasse, M., 2002. Reconstructing dietary and environmental history from enamel isotopic analysis: Time resolution of intra-tooth sequential sampling. *International Journal of Osteoarchaeology*, 12(3): 155-165.
- Balasse, M., 2003. Potential biases in sampling design and interpretation of intra-tooth isotope analysis. *International Journal of Osteoarchaeology*, 13(1-2): 3-10.
- Balter, V., Telouk, P., Reynard, B., Braga, J., Thackeray, F. and Albarede, F., 2008. Analysis of coupled Sr/Ca and Sr-87/Sr-86 variations in enamel using laser-ablation tandem quadrupole-multicollector ICPMS. *Geochimica et Cosmochimica Acta*, 72(16): 3980-3990.
- Bernard, A., Daux, V., Lecuyer, C., Brugal, J.P., Genty, D., Wainer, K., Gardien, V., Fourel, F. and Jaubert, J., 2009. Pleistocene seasonal temperature variations recorded in the $\delta^{18}\text{O}$ of *Bison priscus* teeth. *Earth and Planetary Science Letters*, 283(1-4): 133-143.
- Bromage, T.G., Lacruz, R.S., Hogg, R., Goldman, H.M., McFarlin, S.C., Warshaw, J., Dirks, W., Perez-Ochoa, A., Smolyar, I., Enlow, D.H. and Boyde, A., 2009. Lamellar bone is an incremental tissue reconciling enamel rhythms, body size, and organismal life history. *Calcified Tissue International*, 84(5): 388-404.
- Coplen, T.B., 1994. Reporting stable hydrogen, carbon, and oxygen isotopic abundances. *Pure and Applied Chemistry*, 66: 271-276.
- Coplen, T.B., Brand, W.A., Gehre, M., Groning, M., Meijer, H.A.J., Toman, B. and Verkouteren, R.M., 2006. New guidelines for $\delta^{13}\text{C}$ measurements. *Analytical Chemistry*, 78(7): 2439-2441.
- Dirks, W., Bromage, T.G. and Agenbroad, L., 2010. The timing of molar lamellae formation in *Mammuthus columbi* and *Palaeoloxodon cypriotes* from dental histology., *The World of Mammoths: Vth International Conference on Mammoths and their Relatives*, Le Puy en Velay, France.
- Eberle, J., Fricke, H. and Humphrey, J., 2009. Lower-latitude mammals as year-round residents in Eocene Arctic forests. *Geology*, 37(6): 499-502.
- Feranec, R.S., Hadly, E.A. and Paytan, A., 2009. Stable isotopes reveal seasonal competition for resources between late Pleistocene bison (*Bison*) and horse (*Equus*) from Rancho La Brea, southern California. *Palaeogeography Palaeoclimatology Palaeoecology*, 271(1-2): 153-160.
- Ferretti, M.P., 2003. Structure and evolution of mammoth molar enamel. *Acta Palaeontologica Polonica*, 48(3): 383-396.
- Ferretti, M.P., 2008. Enamel structure of *Cuvieronius hyodon* (Proboscidea, Gomphotheriidae) with a discussion on enamel evolution in elephantoids. *Journal of Mammalian Evolution*, 15(1): 37-58.
- Fisher, D.C., 2009. Paleobiology and extinction of proboscideans in the Great Lakes region of North America. In: G. Haynes (Editor), *American megafaunal extinctions at the end of the Pleistocene*. *Vertebrate Paleobiology and Paleoanthropology Series*. Springer, pp. 55-75.

- Fisher, D.C. and Fox, D.L., 2003. Season of death and terminal growth histories of Hiscock mastodons. In: R.S. Laub (Editor), *The Hiscock Site: Late Pleistocene and Holocene Paleoecology and Archaeology of Western New York State: Proceedings of the Second Smith Symposium*, held at the Buffalo Museum of Science, October 14-15, 2001. Buffalo Society of Natural Sciences, Buffalo, pp. 83-101.
- Fisher, D.C. and Fox, D.L., 2007. Season of death of the Dent mammoths: Distinguishing single from multiple mortality events. In: R.H. Brunswig and B.L. Pitblado (Editors), *Frontiers in Colorado Paleoindian archaeology: From the Dent site to the Rocky Mountains*. University Press of Colorado, Boulder, pp. 123-153.
- FitzGerald, C.M., 1998. Do enamel microstructures have regular time dependency? Conclusions from the literature and a large-scale study. *Journal of Human Evolution*, 35(4-5): 371-386.
- Fox, D.L. and Fisher, D.C., 2004. Dietary reconstruction of Miocene Gomphotherium (Mammalia, Proboscidea) from the Great Plains region, USA, based on the carbon isotope composition of tusk and molar enamel. *Palaeogeography Palaeoclimatology Palaeoecology*, 206(3-4): 311-335.
- Fox, D.L., Fisher, D.C., Vartanyan, S., Tikhonov, A.N., Mol, D. and Buigues, B., 2007. Paleoclimatic implications of oxygen isotopic variation in late Pleistocene and Holocene tusks of *Mammuthus primigenius* from northern Eurasia. *Quaternary International*, 169: 154-165.
- Garvie-Lok, S.J., Varney, T.L. and Katzenberg, M.A., 2004. Preparation of bone carbonate for stable isotope analysis: the effects of treatment time and acid concentration. *Journal of Archaeological Science*, 31(6): 763-776.
- Haynes, C.V. and Huckell, B.B. (Editors), 2007. *Murray Springs: A Clovis site with multiple activity areas in the San Pedro Valley, Arizona*. Anthropological papers of the University of Arizona, No. 71. The University of Arizona Press, Tucson, 308 pp.
- Hillson, S., 2005. *Teeth*. Cambridge manuals in archaeology. Cambridge University Press, Cambridge, UK ; New York, 373 pp.
- Humphrey, L.T., Dean, M.C., Jeffries, T.E. and Penn, M., 2008. Unlocking evidence of early diet from tooth enamel. *Proceedings of the National Academy of Sciences of the United States of America*, 105(19): 6834-6839.
- Koch, P.L., Fisher, D.C. and Dettman, D., 1989. Oxygen isotope variation in the tusks of extinct proboscideans: a measure of season of death and seasonality. *Geology*, 17: 515-519.
- Koch, P.L., Tuross, N. and Fogel, M.L., 1997. The effects of sample treatment and diagenesis on the isotopic integrity of carbonate in biogenic hydroxylapatite. *Journal of Archaeological Science*, 24(5): 417-429.
- Laws, R.M., 1966. Age criteria for the African elephant, *Loxodonta a. africana*. *East African Wildlife Journal*, 4: 1-37.
- Metcalfe, J.Z., Longstaffe, F.J. and White, C.D., 2009. Method-dependent variations in stable isotope results for structural carbonate in bone bioapatite. *Journal of Archaeological Science*, 36(1): 110-121.
- Metcalfe, J.Z., Longstaffe, F.J. and Zazula, G.D., 2010. Nursing, weaning, and tooth development in woolly mammoths from Old Crow, Yukon, Canada: Implications

- for Pleistocene extinctions. *Palaeogeography Palaeoclimatology Palaeoecology*, 298: 257-270.
- Nargolwalla, M.C., Begun, D.R., Dean, M.C., Reid, D.J. and Kordos, L., 2005. Dental development and life history in *Anapithecus hernyaki*. *Journal of Human Evolution*, 49(1): 99-121.
- Passey, B.H. and Cerling, T.E., 2002. Tooth enamel mineralization in ungulates: Implications for recovering a primary isotopic time-series. *Geochimica et Cosmochimica Acta*, 66(18): 3225-3234.
- Passey, B.H. and Cerling, T.E., 2004. Response to the comment by M.J. Kohn on "Tooth enamel mineralization in ungulates: Implications for recovering a primary isotopic time-series," by B.H. Passey and T.E. Cerling (2002). *Geochimica et Cosmochimica Acta*, 68(2): 407-409.
- Passey, B.H., Cerling, T.E., Schuster, G.T., Robinson, T.F., Roeder, B.L. and Krueger, S.K., 2005. Inverse methods for estimating primary input signals from time-averaged isotope profiles. *Geochimica et Cosmochimica Acta*, 69(16): 4101-4116.
- Roche, D., Segalen, L., Balan, E. and Delattre, S., 2010. Preservation assessment of Miocene-Pliocene tooth enamel from Tugen Hills (Kenyan Rift Valley) through FTIR, chemical and stable-isotope analyses. *Journal of Archaeological Science*, 37(7): 1690-1699.
- Saunders, J.J., 1970. The distribution and taxonomy of *Mammuthus* in Arizona, The University of Arizona, Tucson.
- Shellis, R.P., 1984. Variations in growth of the enamel crown in human teeth and a possible relationship between growth and enamel structure *Archives of Oral Biology*, 29(9): 697-705.
- Smith, C.E., 1998. Cellular and chemical events during enamel maturation. *Critical Reviews in Oral Biology & Medicine*, 9(2): 128-161.
- Smith, T.M., Reid, D.J. and Sirianni, J.E., 2006. The accuracy of histological assessments of dental development and age at death. *Journal of Anatomy*, 208(1): 125-138.
- Smith, T.M. and Tafforeau, P., 2008. New visions of dental tissue research: Tooth development, chemistry, and structure. *Evolutionary Anthropology*, 17(5): 213-226.
- Suga, S., 1979. Comparative histology of progressive mineralization pattern of developing incisor enamel of rodents. *Journal of Dental Research*, 58: 1025-1026.
- Suga, S., 1989. Enamel hypomineralization viewed from the pattern of progressive mineralization of human and monkey developing enamel. *Advances in Dental Research*, 3(2): 188-198.
- Tafforeau, P., Bentaleb, I., Jaeger, J.J. and Martin, C., 2007. Nature of laminations and mineralization in rhinoceros enamel using histology and X-ray synchrotron microtomography: Potential implications for palaeoenvironmental isotopic studies. *Palaeogeography Palaeoclimatology Palaeoecology*, 246(2-4): 206-227.
- Widga, C., Walker, J.D. and Stockli, L.D., 2010. Middle Holocene bison diet and mobility in the eastern Great Plains (USA) based on $\delta^{13}\text{C}$, $\delta^{18}\text{O}$, and $^{87}\text{Sr}/^{86}\text{Sr}$ analyses of tooth enamel carbonate. *Quaternary Research*, 73(3): 449-463.
- Zazzo, A., Balasse, M., Passey, B.H., Moloney, A.P., Monahan, F.J. and Schmidt, O., 2010. The isotope record of short- and long-term dietary changes in sheep tooth enamel: Implications for quantitative reconstruction of paleodiets. *Geochimica et Cosmochimica Acta*, 74(12): 3571-3586.

- Zazzo, A., Balasse, M., Patterson, W.P. and Patterson, P., 2005. High-resolution $\delta^{13}\text{C}$ intratooth profiles in bovine enamel: Implications for mineralization pattern and isotopic attenuation. *Geochimica et Cosmochimica Acta*, 69(14): 3631-3642.
- Zazzo, A., Lecuyer, C., Sheppard, S.M.F., Grandjean, P. and Mariotti, A., 2004. Diagenesis and the reconstruction of paleoenvironments: A method to restore original $\delta^{18}\text{O}$ values of carbonate and phosphate from fossil tooth enamel. *Geochimica et Cosmochimica Acta*, 68(10): 2245-2258.

Chapter 5

Stable isotope records of climate, diet, and seasonality from “bulk” and inner enamel “incremental” sampling of mammoth tooth enamel, San Pedro Valley, Arizona ¹

Note on the text: Whenever possible, ages are reported as conventional radiocarbon years before AD 1950, in the form “17,000 ± 100 BP” (mean ± 1 SD). When citing literature that reported only calibrated (“cal”) dates, the dates are reported in the form “17,000 cal BP.”

5.1 Introduction

Mammoths were once widespread in North America, but became extinct shortly after the appearance of Clovis people, just prior to the onset of the Younger Dryas stadial (Haynes, 2002a). Models of extinction processes and Clovis foraging behaviour both rely on assumptions about mammoth behaviour during this critical time period (Haynes, 2002b), but little direct evidence exists. The San Pedro Valley (SPV) in southeastern Arizona contains 4 of the 14 uncontested Clovis-mammoth associations in all of North America (Murray Springs, Lehner, Naco, and Escapule) (Surovell and Waguespack, 2008), as well as two Clovis-mammoth sites (Leikem, Navarette) that lack clear association (Haynes, 2005, 2006). As such, this region is pivotal for understanding the relationship between mammoth hunting and extinction in North America.

During the Last Glacial Maximum (LGM) (~20-18,000 BP), the American southwest was relatively wet, with large pluvial lakes filling playa basins that are dry today (Thompson et al., 1993). Following the LGM, the region experienced increasing aridity (Holmgren et al., 2006), culminating in the “Clovis drought”. This drought coincided with the Clovis occupation of the SPV and local extinction of mammoths (10,900 BP, or ca. 13,250 to 12,660 cal BP), and preceded the cold, wet Younger Dryas (YD) period (Haynes, 1991a, 2008; Waters and Stafford, 2007). Plant macrofossil and pollen evidence suggest that from the last glacial-interglacial transition to the present,

¹ An earlier version of this paper was presented as a poster at the International Council for Archaeozoology 11th International Conference, Paris, France (August 2010).

precipitation in the region occurred primarily during winter and summer (Holmgren et al., 2007). However, little else is known about seasonality in the Late Pleistocene SPV, or how it affected mammoth ecology.

Here, we investigate mammoth paleoecology in the SPV using the carbon and oxygen isotope compositions of structural carbonate (sc) from tooth enamel bioapatite. We use “bulk” sampling (i.e., tooth segments that average several seasons of growth) to reconstruct general trends such as the overall proportion of C₄ plants in the diet and the mean isotopic compositions of drinking water, and “serial” or “incremental” sampling (i.e., numerous thin lines drilled from each specimen, which represent shorter periods of time) to reconstruct seasonal variations. We compare the climatic conditions, diets, and seasonal behaviour of Clovis-associated mammoths (those with direct, undisputed Clovis artifact associations), “Clovis-age” mammoths (those discovered in “Clovis-age” sediments, indicating that they are either contemporary to or slightly older than Clovis-associated mammoths), and pre-Clovis mammoths (specimens from clearly older sediments) in the SPV, to provide insight into both mammoth and Clovis human ecology and foraging behaviour. We use the isotope data to address several specific questions. Did the Naco mammoth escape from a mass kill at Lehner? Did Eloise, the last mammoth to die at Murray Springs (just prior to the onset of the Younger Dryas) experience abruptly different climatic conditions from other SPV mammoths? Do mammoth teeth record evidence of a Clovis drought? Did Clovis mammoths cluster around water sources in the SPV or did they venture further afield? Stable isotope data cannot answer all of these questions definitively, but can provide insights that aid in evaluating competing models of Clovis foraging behaviours and mammoth extinction.

5.1.1 Study Area and Samples

The San Pedro Valley (SPV) is located in the Basin and Range province of the American Southwest, in an area of transition between the modern Chihuahuan and Sonoran Deserts. The valley is oriented north-south, and is surrounded by mountain ranges: the Huachuca in the west, the Mule Mountains and Tombstone Hills in the east (Figure 5.1) (Wahi et al., 2008). All of the sampled sites are within about 60 km of one

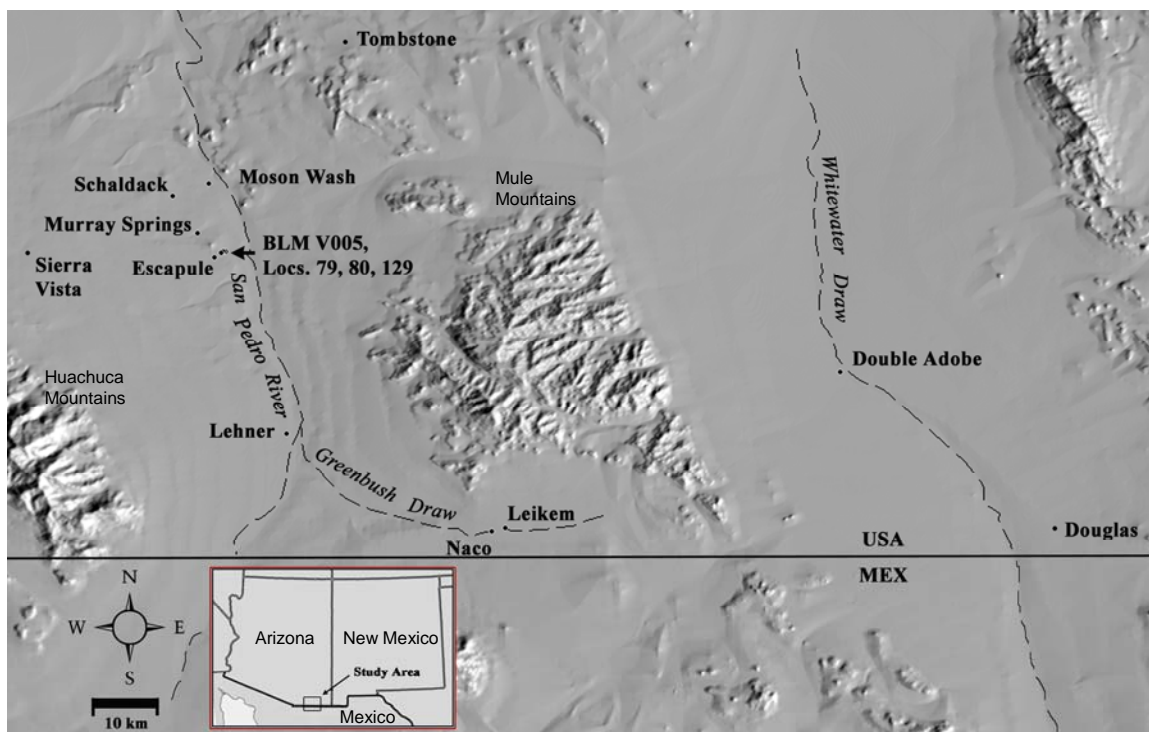


Figure 5.1 Map of the San Pedro Valley, showing the locations where mammoth specimens utilized in this study were found. Inset map shows the location of the study area within the State of Arizona.

another, and no barriers to free movement exist along this portion of the river valley. Terminal Pleistocene mammoth remains in the SPV are typically found in dry streambed sediments on erosional surfaces, directly underneath a “black mat” that formed during the Younger Dryas stadial, beginning at about 10,900 BP (Haynes, 2005, 2008). Clovis artifacts are found throughout North America between 11,050 and 10,800 BP (Waters and Stafford, 2007); at Murray Springs and Lehner, the Clovis occupation has been dated to $10,940 \pm 40$ BP and $10,980 \pm 50$ BP, respectively (average of several dates) (Haynes, 2005; Taylor et al., 1996). In the southwest, megafaunal remains have never been found within or above the “black mat”, which suggests that they went extinct immediately prior to the YD period. Moreover, mammoths were extinct throughout mainland North America by the early Holocene at the latest (Haynes, 2008). Thus, the mammoths killed or scavenged by Clovis hunters in the San Pedro Valley were among the latest known on the continent.

Table 5.1 Specimen information and context

LSIS #	Mus #	Field #	Site	Latitude °N	Longitude °E	Elevation m ASL	Context*	Clovis association	Era	Tooth	References
AZ1	3403a	MS-85	MS (Eloise)	31.571	110.178	1270	Area 3, Stratum Z ₁₋₂ , directly under black mat	Secure	Clovis	M6	Haynes and Huckell, 2007
AZ2	2409	MS-78	MS	31.571	110.178	1270	Area 2, Stratum β ₁ , directly under black mat	None	Clovis?	M6	Haynes and Huckell, 2007; Haynes 2005
AZ3	(fragments)	MS		31.571	110.178	1270	Area 1, Stratum D; may be same individual as AZ9	Possible	Clovis?	adult	Haynes and Huckell, 2007
AZ4	2430		Leikem	31.346	109.952	1380	Stratum β ₁ , directly under black mat	Likely	Clovis?	M6	Haynes, 2005; Saunders, 1983
AZ5	3297		Lehner	31.423	110.113	1280	Stratum β ₁ , directly under black mat	Secure	Clovis	M4	Haynes, 2005; Saunders, 1970
AZ6	2578c		Schalduck	31.598	110.197	1260	Directly under black mat	None	Clovis?	M5	Haynes, 2005
AZ7	17354		BLM V-005	31.556	110.163	1270	Stratum β ₁ , directly under black mat	None	Clovis?	adult	Haynes, 2005
AZ7X	-	-	BLM V-005	31.556	110.163	1270	Directly under black mat	None	Clovis?	adult	Haynes, 2005
AZ8	P-92b		Double Adobe	31.464	109.701	1220	Redeposited (?)	-	Pre-Clovis?	M6	
AZ9	2417	MS-58	MS	31.571	110.178	1270	Area 1, Stratum β ₁ ; tooth in mandible	Possible	Clovis?	M6	Haynes and Huckell, 2007
AZ10	P-88		Naco	31.349	109.958	1380	Stratum β ₁ , directly under black mat	Secure	Clovis	M6	Haynes, 2005; Saunders, 1970
AZ11	-	-	MS	31.571	110.178	1270	Area 8, Stratum D ₁ spring conduit sands, >29,000 BP	-	Pre-LGM	adult	Haynes and Huckell, 2007; Pigati et al., 2009
AZ12	-	-	HTD, Loc 80	31.557	110.159	1260	Stratum D, ~5 cm below black mat	None	Clovis?	adult	Jesse Ballenger, personal communication
AZ13	-	-	HTD, Loc 129	31.557	110.159	1260	Stratum D, directly under black mat	None	Clovis?	adult	Jesse Ballenger, personal communication
AZ14	-	-	Moson Wash	31.607	110.170	1230	Stratum D/Z contact, >29,000 BP	-	Pre-LGM	adult	Jesse Ballenger, personal communication
AZ15	-	-	HTD, Loc 79	31.557	110.157	1260	Stratum D, below black mat	None	Clovis?	adult	Jesse Ballenger, personal communication

LSIS # = identifier assigned for laboratory analysis, Mus # = museum number, Field # = identifier assigned during excavation

AZ7 and AZ7X may or may not be from the same individual

MS = Murray Springs

BLM = Bureau of Land Management

HTD = Horsethief Draw

*Strata names follow Haynes 2005: β₁ = Terminal Pleistocene channel sands, and Haynes & Huckell 2007: Z = Millville Formation, D₁ = Moson Ranch sand, D = Sobaipuri mudstone

“Clovis-associated” mammoths (i.e., specimens found in direct association with Clovis artifacts) were obtained from Murray Springs (i.e., the mammoth referred to as Eloise), Lehner, and Naco (Table 5.1). The Naco mammoth was certainly hunted (based on the presence of several fluted points in the chest area), whereas Eloise and the Lehner mammoth were either hunted or scavenged (Haury et al., 1953; Haury et al., 1959; Haynes and Huckell, 2007). Two other mammoths from Murray Springs (AZ3, AZ9) and one from Leikem may also have been hunted or scavenged, but the rest were not associated with Clovis activities (Table 5.1). The latter are referred to in this paper as “Clovis-age”, since they were recovered in sediments directly underlying the black mat. However, since the Clovis surface below the black mat is erosional, some of the “Clovis-age” mammoths may actually pre-date Clovis by hundreds of years or more. Mammoth teeth that are definitely from older time periods are relatively difficult to obtain, but two samples that lived prior to 29,000 BP (pre-LGM; based on stratigraphic context) were obtained from Murray Springs and Moson Wash (Table 5.1). A mammoth tooth from Double Adobe (Haury, 1960), suspected to be redeposited from older sediments (C. V. Haynes, personal communication), was also analyzed.

5.1.2 Oxygen Isotopes and Climate

The oxygen isotope compositions ($\delta^{18}\text{O}$ values) of phosphate and structural carbonate in mammalian bioapatite are in equilibrium with body water (Bryant et al., 1996; Iacumin et al., 1996; Longinelli, 1984). The $\delta^{18}\text{O}$ value of an animal’s body water is determined by its physiological balance of oxygen inputs (drinking water, liquid water in plants, metabolic oxygen derived from food, and atmospheric oxygen) and outputs (liquid – urine, fecal water, sweat; transcutaneous water vapour; and expired CO_2) (Bryant and Froelich, 1995; Kohn and Cerling, 2002). In large-bodied obligate drinkers, including elephants, there is a direct correlation between the $\delta^{18}\text{O}$ values of tooth enamel and meteoric water (Ayliffe et al., 1992; Levin et al., 2006). Indeed, the animals that best record the $\delta^{18}\text{O}$ values of surface drinking waters are those with the largest body sizes (Bryant and Froelich, 1995), which makes proboscideans ideal for reconstructing paleoenvironments. Meteoric water $\delta^{18}\text{O}$ values vary geographically as a result of latitude, altitude, distance from the coast, amount of precipitation, and surface air

temperature (Dansgaard, 1964). The $\delta^{18}\text{O}$ values of other water sources (e.g., lakes, rivers, groundwater) may be different from meteoric water as a result of evaporative enrichment or mixing with other water sources.

The modern climate in the San Pedro Valley is semiarid (353 mm precipitation per year), with two wet seasons (low-intensity long-lived winter storms, 81 mm per yr; high-intensity, short-lived summer monsoons, 244 mm per year) (Baillie et al., 2007). Plant macrofossil and pollen evidence suggests that this “biannual” pattern of rainfall has persisted since the last glacial-interglacial transition (<40,000 BP) (Holmgren et al., 2007).

In most mid- to high-latitude inland regions, the $\delta^{18}\text{O}$ values of precipitation in summer are higher than those in winter (Rozanski et al., 1993). This is true for modern Tucson and the San Pedro Valley, where average seasonal precipitation $\delta^{18}\text{O}$ values are 4‰ and 5‰ higher in summer than winter, respectively (Baillie et al., 2007; Wagner et al., 2010, supplementary information). Within the summer or winter seasons, $\delta^{18}\text{O}$ values and temperature are poorly correlated, but $\delta^{18}\text{O}$ values and amount of precipitation are negatively correlated (Wagner et al., 2010, supplementary information; Wright et al., 2001), a phenomenon known as the “amount effect”. When only July-August precipitation is considered, however, there is a positive correlation between $\delta^{18}\text{O}$ and temperature in addition to the negative correlation between $\delta^{18}\text{O}$ and precipitation amount (Wright et al., 2001). To complicate matters further, inter-annual variations in seasonal $\delta^{18}\text{O}$ values are affected by moisture source. Based on correlations between sea surface temperature and the isotopic composition of precipitation, Wright et al. (2001) argued that summer monsoon precipitation is primarily derived from subtropical Pacific/Gulf of Mexico moisture sources in warmer, wetter years (with higher $\delta^{18}\text{O}$ values), and from tropical moisture in cooler, drier (lower $\delta^{18}\text{O}$ value) years.

The modern amount-weighted mean $\delta^{18}\text{O}$ values of seasonal precipitation/runoff in the Upper San Pedro Basin (2000-2005) are -11.2‰ (winter) and -6.3‰ (summer) (Baillie et al., 2007; Wahi et al., 2008). The $\delta^{18}\text{O}$ values of groundwater from different parts of the SPV range from $-9.6 \pm 0.2\text{‰}$ to $-7.7 \pm 0.6\text{‰}$, and San Pedro River surface waters range from $-8.6 \pm 1.7\text{‰}$ to -6.2 ± 0.6 , with a mean of -7.4‰ (Baillie, 2005; Baillie et al., 2007).

5.1.3 Carbon Isotopes and Vegetation

The $\delta^{13}\text{C}$ values of animal tissues are derived from the $\delta^{13}\text{C}$ values of foods, plus tissue-dependent isotopic fractionations ($\alpha = 1.0145$ for large herbivore tooth enamel enrichment over diet, or about 14.4‰) (Cerling and Harris, 1999). Most terrestrial plants use photosynthesis to fix atmospheric CO_2 ($\delta^{13}\text{C} = -8\text{‰}$ in 1989) (Marino and McElroy, 1991), but the degree to which photosynthetic plants discriminate against ^{13}C depends on their photosynthetic pathway: C_3 (Calvin Cycle), C_4 (Hatch-Slack Cycle), or CAM (Crassulacean Acid Metabolism). Terrestrial C_3 plants (trees, most shrubs and herbs, and some grasses) and C_4 plants (grasses, sedges, and some herbs) have very different $\delta^{13}\text{C}$ values (ranges = -35 to -21‰ and -20 to -6‰ , respectively), while those of CAM plants (cacti and succulents) overlap those of C_3 and C_4 plants (O'Leary, 1988; Smith and Epstein, 1971).

Both C_3 and C_4 plants use Rubisco to catalyze fixation of CO_2 into organic molecules during photosynthesis (Sage, 2004). However, C_4 plants have structural and biochemical adaptations (including the use of PEP carboxylase and other enzymes) that allow them to concentrate CO_2 around Rubisco (Sage, 2004). This produces a less variable quantum yield (ratio of carbon gains to photons absorbed, a measure of photosynthetic efficiency), because it prevents C_4 plants from undergoing photorespiration (i.e., binding O_2 rather than CO_2 to Rubisco, resulting in no net energy gain) (Ehleringer, 1978; Ehleringer et al., 1997; Sage, 2004). For C_3 plants, photorespiration is increased (and hence, quantum yields are decreased) under various conditions, including (1) high temperatures, which directly stimulate photorespiration and decrease the solubility of CO_2 relative to O_2 (Brooks and Farquhar, 1985; Ehleringer and Pearcy, 1983; Jordan and Ogren, 1984; Sharkey, 1988), and (2) dry and saline conditions, which promote stomatal closure, thus reducing intercellular CO_2 concentrations (Guy et al., 1980; Sage, 2004). The combination of high temperature, high salinity, low humidity, and drought would have provided the optimal conditions for the evolution of C_4 photosynthesis (Ehleringer and Monson, 1993). However, C_4 photosynthesis is not an adaptation to these conditions *per se*, but rather a compensation for high rates of photorespiration and carbon deficiency (Sage, 2004). This distinction helps explain why

geographical distributions of C₄ plants do not always match expectations based on simple ideas about C₄ photosynthesis. Most importantly for this study, C₄ grass abundances (proportion of biomass) in the seasonally dry grasslands of North America are positively correlated with mean annual temperature (MAT), mean annual precipitation (MAP), and the proportion of annual rainfall that occurs during summer (Epstein et al., 1997; Paruelo and Lauenroth, 1996; Yang et al., 1998). Indeed, C₄ plants are most common in desert and sub-tropical regions with warm-season rains (Hattersley, 1983; Paruelo and Lauenroth, 1996). In regions with low MAP and summer rainfall, but high MAT, C₃ shrubs tend to dominate the biomass (Paruelo and Lauenroth, 1996). In regions with very low temperatures (i.e., July minimum less than 8°C), C₄ plants are very rare (Teeri and Stowe, 1976).

Pollen and plant macrofossils from the Peloncillo Mountains Wilderness Area of southeastern Arizona (<150 km from the SPV, elevation ~1300 - 1500 m) demonstrate that from 36,200 to 15,410 cal BP, a pinyon-juniper woodland and a rich understory of C₃ shrubs, C₄ annuals, and C₄ grasses occupied the hills surrounding large pluvial lakes (Holmgren et al., 2006). From 15,210 cal BP to 12,405 cal BP (just prior to the Younger Dryas period, during the Clovis era), xeric species increased in abundance, while *Pinus edulis* (a species that is not adapted to extremely warm or dry conditions) retreated upslope and temporarily disappeared. After the onset of the cooler, wetter Younger Dryas period, *P. edulis* returned to lower altitudes (Holmgren et al., 2006).

A wide variety of summer-flowering C₄ herbs and grasses persisted in the region from the Late Pleistocene (~50,000 cal BP) to the present (Holmgren et al., 2006; Holmgren et al., 2007). The lower levels of atmospheric CO₂ throughout the Pleistocene likely played a role in the persistence of C₄ plants, even during cooler intervals (Koch et al., 2004); however, fluctuations in pCO₂ alone did not control C₄ plant abundances during the Pleistocene (Higgins and MacFadden, 2009). Regardless of the cause, evidence from pollen, plant macrofossils, and the stable isotope compositions of soil carbonates and herbivore tooth enamel indicate that a C₄ grassland existed between central Texas and southern Arizona during the Pleistocene (Connin et al., 1998; Koch et al., 2004; Liu et al., 1996; Mehringer and Haynes, 1965; Monger et al., 1998). Holmgren et al. (2007) proposed that this grassland “greened up” in response to mid-to-late summer rains.

The transition from desert grassland to desert shrubland in the American southwest occurred around 5000 cal BP (Holmgren et al., 2007). Since cacti and succulents are associated with the modern desert shrub environment, it is reasonable to assume that CAM plants were scarce during the Pleistocene, and did not significantly contribute to mammoth diets. Mammoth dung contents from southern Utah support the contention that grasses and sedges were the primary components of mammoth diets in the southwest (Mead et al., 1986).

5.1.4 Seasonality and Elephant Behavior

Climate variations strongly influence African elephant migrational patterns and dietary choices. Elephants are obligate drinkers, and drink up to 225 L of water per day, though they can survive for several days without water (Sukumar, 1989). During dry seasons or droughts they often restrict their migrational ranges and cluster around water sources (Cerling et al., 2009; Haynes, 1991b). Despite their high-crowned teeth (adapted to grazing), modern elephants are mixed feeders, consuming different proportions of grass and browse depending on the region, vegetation types, water availability, soil nutrients, and season (Codron et al., 2006). Modern elephants tend to forage in the greenest areas of a landscape throughout the year (Loarie et al., 2009). During the wet season, elephants seek out areas that “green up” for only a few months, such as open woodlands, shrublands, and grasslands; during the dry season they prefer areas like closed woodlands, which are more consistently green year-round (Loarie et al., 2009). Typically, more browse is consumed during the dry season and more grass during the wet season (Codron et al., 2011; Sukumar, 1989). Stable isotope studies of modern elephants in northern Kenya, coupled with GPS monitoring of movements, revealed that during the dry season the animals remained within about 2 km of the riparian corridor and consumed a diet of <20% C₄ plants, but during the wet season they migrated farther and consumed more C₄ plants (Cerling et al., 2009). Elephants in South Africa also consume more C₄ plants during the wet season, when grasses are more abundant and their nutrient contents are high (Codron et al., 2011).

Mammoth teeth were even more specialized for grazing than those of modern elephants (Maglio, 1973), and stable isotope studies support the contention that grass was

their primary or preferred food (Koch et al., 1998). However, isotopic studies as well as other lines of evidence (e.g., gut contents and dung) indicate that a variety of other species and plant parts were sometimes consumed by mammoths, including bark, twigs, fruits, seeds, and herbs (Aptroot and van Geel, 2006; Koch et al., 2004; Koch et al., 1998; Mead et al., 1986; van Geel et al., 2008).

5.1.5 Clovis Drought

The “Clovis drought” figures strongly in interpretations of mammoth extinction and Clovis hunting in the American Southwest. During droughts, modern African elephants constrict their feeding ranges to areas with permanent water, and increase their reliance on woody vegetation, as a result of decreased grass availability (Cerling et al., 2009; Gaugris and van Rooyen, 2010). Gary Haynes (1991b) has proposed that mammoths weakened during the Clovis drought clustered around water sources in the SPV, making them easier targets for Clovis hunters and ultimately contributing to their extinction. Evidence from the Murray Springs site indicates that a water hole was dug through a dry creek bed, likely by a mammoth, just prior to the death of “Eloise” (Haynes, 1991a). The hole and skeleton were buried by the black mat before appreciable weathering or pedogenesis could occur, likely less than a year after the death of Eloise. This drought may have been the final stage of water table decline since the Last Glacial Maximum. Here, we investigate the timing and nature of the drought and its effects on mammoth behaviour. We expect that mammoth tooth enamel formed during a long-term drought would have several characteristics: (1) higher $\delta^{18}\text{O}$ values, because of less rainfall (amount effect) and more evaporation (note: this could be confounded by changes in temperature or water source), (2) “smooth” and low-amplitude seasonal changes in $\delta^{18}\text{O}$ values if mammoths were tethered to a single water source with minimal seasonal changes in isotopic composition (e.g., a groundwater spring), or irregular variations in $\delta^{18}\text{O}$ values if mammoths were migrating among different ephemeral water sources, (3) lower $\delta^{13}\text{C}$ values because of fewer C_4 grasses in the diet (even though C_4 photosynthesis is commonly viewed as a drought adaptation, the proportion of C_4 plants in North American grasslands decrease with decreasing mean annual and summer precipitation, as described in Section 5.1.3; we also assume that growth of C_4 grasses and summer annuals

would be severely inhibited during droughts, whereas C₃ shrubs and trees – with their deeper root systems and greater reliance on winter precipitation – would have been more likely to survive, especially in river valleys), and (4) lower amplitudes of variation in $\delta^{13}\text{C}$ values, because of fewer C₄ plants “greening up” in the summer.

5.2 Materials and Methods

5.2.1 Sampling

For each specimen, a wedge-shaped section of enamel and dentin was removed by making two cuts with a Dremel circular saw blade on the lingual or buccal aspect (depending on ease of sampling), parallel to the height of the tooth (i.e., from top to bottom of an enamel loop edge). Dentin was soft and chalk-like, and was removed easily with a dental pick and wire brush. For “bulk” sampling, pieces of enamel that spanned the entire enamel thickness and >1 cm of tooth height were removed and ground using a mortar and pestle. These samples should represent at least several seasons of growth (Chapter 4).

Four Clovis-age mammoths and two mammoths from older burial contexts (“pre-Last Glacial Maximum (LGM) mammoths”) were selected for inner enamel surface (IES) “incremental” microsampling, in order to reconstruct seasonal variations in the isotopic compositions of diet and drinking water (Figure 5.2). The IES sampling methodology was described in Chapter 4.

Two of the specimens chosen for incremental sampling (AZ10, Naco; AZ13, Horsethief Draw Loc. 129) were enamel cones that were still developing at the time of death, so their isotopic compositions reflect conditions a few years or less before death. The other specimens were obtained from fully-developed enamel plates from more basal portions of the tooth (Chapter 4, Figure 4.1), which formed years or even decades prior to death. When possible, samples were obtained near the cervix, so they reflected conditions closer to the time of death. However, because of the very long development time of mammoth adult molars (Chapter 3) (Metcalfé et al., 2010), it is not possible to determine exactly when each specimen formed.

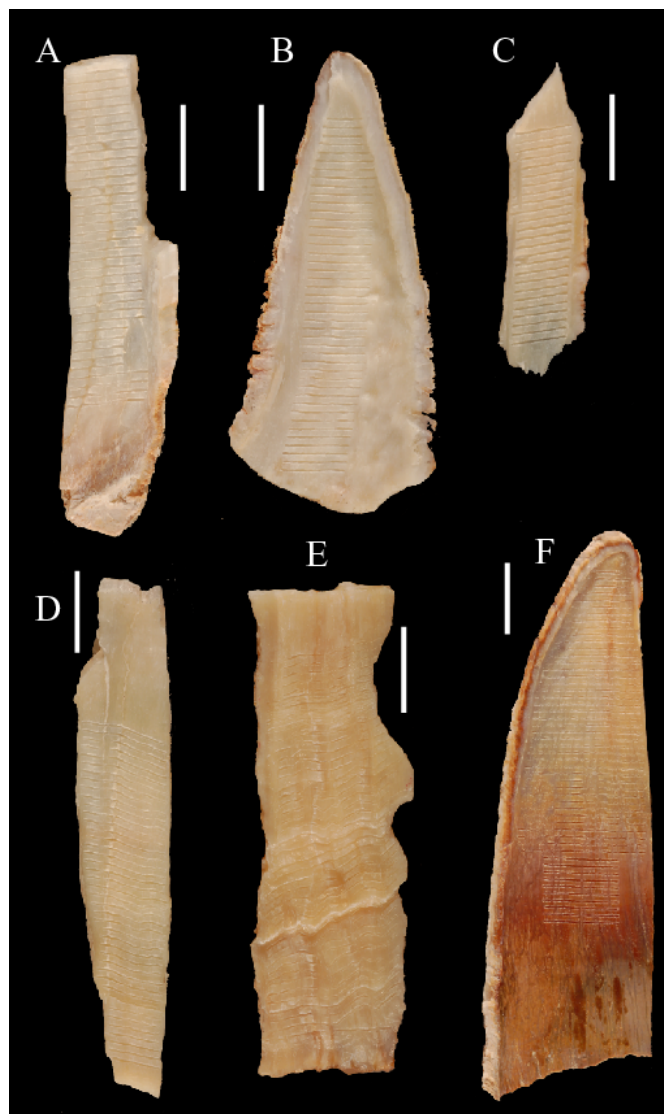


Figure 5.2 “Incrementally sampled” specimens. (A) AZ1 (Eloise), (B) AZ10 (Naco), (C) AZ5 (Lehner), (D) AZ11 (Murray Springs, Pre-LGM), (E) AZ14 (Moson Wash, Pre-LGM), (F) AZ13 (Horsethief Draw Loc. 129). Scale bars show 10 mm. The occlusal direction is towards the top of the image and the cervical direction is towards the bottom.

Table 5.2 Stable isotope results for "bulk" analyses, and their corresponding diet and drinking water compositions.

LSIS #	Site	Structural Carbonate			Diet			Water
		$\delta^{13}\text{C}$ (‰)	$\delta^{18}\text{O}$ (‰)	CO_3 Wt %	$\delta^{13}\text{C}$ (‰)	% C4 ¹	% C4 ²	$\delta^{18}\text{O}$ (‰)
Clovis-Associated								
AZ1 ^c	Murray Springs	-0.9	24.1	5.0	-15.2	71	56	-8.6
AZ5 ^a	Lehner	-1.7	27.2	2.9	-15.9	65	48	-5.3
AZ10 ^a	Naco	-1.0	25.9	4.0	-15.3	70	55	-6.7
Clovis-Age*								
AZ2 ^a	Murray Springs	-0.6	26.7	5.9	-14.9	73	59	-5.8
AZ3 ^b	Murray Springs	-1.2	25.9	5.2	-15.5	68	53	-6.6
AZ4 ^a	Leikem	-1.9	25.6	6.1	-16.2	64	46	-7.0
AZ6 ^a	Schaldaack	-2.1	26.5	3.7	-16.3	62	44	-6.0
AZ7 ^a	BLM V-005	-1.1	25.0	2.7	-15.4	69	54	-7.6
AZ7X ^d	BLM V-005	0.1	28.4	3.9	-14.2	78	67	-4.0
AZ9 ^a	Murray Springs	-1.2	24.9	6.1	-15.5	69	53	-7.7
AZ12 ^d	HTD, Loc 80	-0.3	26.0	6.0	-14.6	75	62	-6.6
AZ13 ^d	HTD, Loc 129	-0.8	25.4	5.4	-15.1	71	57	-7.2
AZ15 ^{a,d}	HTD, Loc 79	-0.7	25.7	5.9	-14.9	72	58	-6.9
^e	<i>Murray Springs</i>	-2.3	26.0		-16.6	61	41	-6.5
^e	<i>Murray Springs</i>	-1.7	27.2		-16.0	65	48	-5.3
^e	<i>Seff</i>	-0.9	27.1		-15.2	71	56	-5.4
	Mean**	-1.0	25.9	4.8	-15.3	70	55	-6.6
	SD**	0.6	1.1	1.2	0.6	4	6	1.1
Pre-Clovis*								
AZ8 ^a	Double Adobe	-2.5	23.7	4.2	-16.8	59	39	-9.0
AZ11 ^d	Murray Springs	-4.9	22.0	5.2	-19.1	43	14	-10.7
AZ14 ^d	Moson Wash	-5.6	24.0	5.6	-19.9	38	7	-8.6
	Mean	-4.4	23.2	5.0	-18.6	46	20	-9.4
	SD	1.6	1.0	0.7	1.6	11	17	1.1

*Possible, likely, and certain; see Table 1

** Includes Clovis-associated and Clovis-age samples analyzed in this study (values obtained by Connin et al. 1998 are excluded)

^a Results are mean of 2 analyses

^b Results are mean of 3 analyses

^c Results are means of 4 analyses

^d Samples were untreated

^e Data from Connin et al. 1998 (sites listed in italics); not included in mean or SD calculation

¹ %C₄ calculated using model 1, (lower $\delta^{13}\text{C}$ value for C₃ plant endmember - see text)

² %C₄ calculated using model 2, (higher $\delta^{13}\text{C}$ value for C₃ plant endmember, very conservative %C₄ estimate - see text)

5.2.2 Carbonate Pretreatment and Stable Isotope Analysis

Most bulk enamel samples were pretreated with 2-3% bleach (24 hours) and 0.1 M acetic acid (4 hours), to remove organics and secondary carbonates (Garvie-Lok et al., 2004; Koch et al., 1997). Pretreated samples were reacted with ortho-phosphoric acid at 90°C using a MultiPrep automated sampling device in standard operating mode (in which evolved CO₂ is immediately frozen into a cold finger), and analyzed using an Optima isotope ratio mass spectrometer in dual-inlet mode. Pretreated samples were analyzed 2-5 times. A few results were excluded because of problems with acid delivery; the remainder had good reproducibility: on average, 0.10 ‰ for δ¹³C and 0.15 ‰ for δ¹⁸O (1 SD).

The effects of pretreatment were investigated to determine whether further analyses could be conducted using untreated enamel, which would significantly reduce the sample size required. Unlike bone and dentin, enamel contains little organic matter and has large crystals, which offer little space for secondary carbonate formation or bicarbonate adsorption (Koch et al., 1997). Thus, enamel bioapatite tends to preserve its original biogenic isotopic composition better than bone or dentin. The δ¹³C values of pretreated and untreated aliquots of the same enamel samples (n=4) were all within analytical error (<0.1‰). The δ¹⁸O values of untreated samples were on average 0.5 ± 0.2‰ lower than those of treated samples (range = 0.2 to 0.8‰ lower). Since these differences are relatively small, untreated enamel was used in subsequent analyses (i.e., all microsamples and some bulk samples, as noted in Table 5.2).

5.2.2.1. Open vs Sealed Vessel Analyses

One pretreated sample (AZ8) produced δ¹⁸O values that were very low relative to those of the other San Pedro Valley mammoth enamel δ¹⁸O values, and had very poor reproducibility (up to 8‰ differences in δ¹⁸O values among analyses of the same aliquot of sample). Anomalously low δ¹⁸O values have been previously observed when bone samples are reacted with phosphoric acid and immediately frozen in a cold trap (“open” reaction condition); this occurrence can be prevented by closing the connection with the cold trap (“SV” (sealed vessel) reaction condition) for the duration of the reaction (Chapter 2) (Metcalf et al., 2009). When an untreated aliquot of AZ8 was reacted under SV conditions, its δ¹⁸O value was consistent with the other SPV specimens, and duplicate

analyses were reproducible (1 SD = 0.2‰ for carbon, 0.1‰ for oxygen). Three additional enamel samples were reacted under both “sealed vessel” and “open” reaction conditions, and their results differed by a maximum of 0.7‰ for both $\delta^{13}\text{C}$ and $\delta^{18}\text{O}$. Thus, although many samples produce similar values when analyzed under “open” vs. “sealed vessel” conditions, other samples require “sealed vessel” conditions to produce reliable results. We conclude that “sealed vessel” reaction conditions should be used when analyzing structural carbonate in bioapatite.

5.2.3 Diet $\delta^{13}\text{C}$ and %C₄ Calculations

The $\delta^{13}\text{C}_{\text{diet}}$ value is estimated using an enamel-diet fractionation factor, α , of 1.0145 (Cerling and Harris, 1999; Cerling et al., 1997), which corresponds to a $\Delta^{13}\text{C}_{\text{sc-diet}}$ of about 14.3‰:

$$\delta^{13}\text{C}_{\text{diet}} = [(\delta^{13}\text{C}_{\text{sc}} + 1000)/1.0145] - 1000 \quad [\text{Equation 5.1}]$$

The proportion of C₄ plants in the diet can be calculated using a mass-balance equation:

$$\delta^{13}\text{C}_{\text{diet}} = (x)(\delta^{13}\text{C}_{\text{C4 plants}}) + (1-x)(\delta^{13}\text{C}_{\text{C3 plants}}), \quad [\text{Equation 5.2}]$$

where x = %C₄ plants in the diet, $\delta^{13}\text{C}_{\text{C4 plants}}$ and $\delta^{13}\text{C}_{\text{C3 plants}}$ are end-member values.

This calculation requires defining the $\delta^{13}\text{C}$ values of C₃ and C₄ plant end-members, whereas in reality the $\delta^{13}\text{C}$ values of C₃ (and to a lesser extent, C₄) plants vary considerably, both within and among environments (Farquhar et al., 1989; Murphy and Bowman, 2009; Swap et al., 2004). To account for some of the uncertainty involved in these calculations, we use two different mixing models to estimate %C₄: model 1 uses the mean $\delta^{13}\text{C}$ values of modern C₃ and C₄ grasses plus 1.5‰ to account for the industrial effect (i.e., -25.2 and -11.0‰, respectively) (Cerling et al., 1997); model 2 uses a higher $\delta^{13}\text{C}$ value for C₃ plants (-20.5‰), near the upper limit of values for C₃ plants, which typically occurs only in very dry environments (van de Water et al., 2002). The latter method produces a highly conservative %C₄ estimate.

5.2.4 Drinking Water $\delta^{18}\text{O}$ Value Calculations

We estimate the $\delta^{18}\text{O}$ values of drinking water consumed by San Pedro Valley mammoths using a two-step calculation. First, the oxygen isotope composition of

structural carbonate is converted to its equivalent as phosphate, using an equation that is robust for many different species (Bryant et al., 1996; Iacumin et al., 1996):

$$\delta^{18}\text{O}_p = 0.98 \delta^{13}\text{C}_{sc} - 8.32 \quad [\text{Equation 5.3}]$$

Second, the oxygen isotope composition of phosphate is converted to that of drinking water, using the relationship determined for modern elephants (Ayliffe et al., 1992):

$$\delta^{18}\text{O}_w = (\delta^{18}\text{O}_p - 23.3)/0.94 \quad [\text{Equation 5.4}]$$

This approach assumes that the physiology of mammoths did not differ substantially from that of modern elephants, which is reasonable given their similar body sizes and close evolutionary relationship (Owen-Smith, 1988; Shoshani, 1998).

5.2.5 Incremental Samples: Data Transformations

The goal of incremental sampling is to reconstruct seasonal variations in animal diet and drinking water. Passey et al. (2005) presented an “inverse model” for reconstructing the isotopic compositions of body fluids from incrementally sampled tooth isotope results. This model requires knowledge of species- and tooth-specific growth parameters: l_m = length of maturation (the length of tooth enamel that is undergoing maturation at any point in time), l_a = length of apposition (the region that is undergoing initial matrix deposition at any point in time), and f_i = the proportion of the final mineral content formed during initial matrix deposition. None of these parameters have been determined for proboscidean teeth. In addition, previous determinations of these parameters for other species have utilized the entire enamel thickness, which differs markedly in mineralization rate from the innermost enamel layer (Suga, 1989; Tafforeau et al., 2007). As such, these measurements are inapplicable to the inner enamel surface sampling methodology employed in the present study. Equally importantly, the Passey et al. (2005) model assumes (1) a constant enamel growth rate, which is not valid for proboscidean teeth (perikymata visible on the outer enamel surface and isotope profiles presented in the present study both indicate that the growth rate decreases near the cervix, as also demonstrated by Tafforeau et al. (2007) for rhinoceros), and (2) a constant maturation rate and uniform maturation geometry, which are also not true for teeth in general (Suga, 1982, 1989; Tafforeau et al., 2007). Thus, until a more detailed

understanding of proboscidean enamel formation and maturation is developed, we have not attempted to reconstruct the “original” amplitudes of isotope variation from those obtained in the present study.

The periods of the isotope curves (distance between maxima or minima) obtained in this study are variable, both within and among individuals (see Section 5.3.3), which suggests that differences in growth rate must be considered to make meaningful comparisons. We tested sophisticated statistical methods for converting the distance axis of the isotope profiles to time (i.e., a phase demodulation approach) (De Ridder et al., 2004), but found that the best fit for curves among individuals was obtained using a simpler, anchor-point method. To transform distance to time using the anchor point method, we first identified each peak and valley of curves inferred to have a period of one year. [Chapter 4 presents evidence that one period for $\delta^{13}\text{C}$ and $\delta^{18}\text{O}$ versus distance is equal to one year of growth in Eloise (AZ1). Other Clovis-age samples had similar periods to Eloise, and thus were also assumed to represent one year of growth. The methods used for pre-LGM specimens AZ11 and AZ14 are described below.] Assuming a constant growth rate between each peak and valley (half-year interval), we divided 0.5 years by the distance, to obtain the growth rate in mm/year. For any remaining portions of the curves (i.e., before the first peak/valley or after the last), we assumed the growth rate was equal to that in the nearest portion of the curve. For all the Clovis-age mammoths, we used $\delta^{13}\text{C}$ curves for the distance-time transformation, since they were “smoother” and displayed more systematic variation than $\delta^{18}\text{O}$ curves. For AZ11, we used the $\delta^{18}\text{O}$ curve because it displayed more systematic variation and its period was similar to those of the Clovis mammoth samples (see Section 5.4.3.2). For AZ14, which lacked the regular periodicity present in the other specimens, we assumed a constant growth rate equal to that of AZ1 and AZ11 (mean = 14 mm/year), whose profiles were obtained from similar locations on the tooth (i.e., enamel near the cervix).

We emphasize that the amplitudes of isotopic variation in our incremental samples are attenuated relative to the variations in $\delta^{13}\text{C}$ of diet or $\delta^{18}\text{O}$ of drinking water. Thus, they represent a minimum degree of variation. However, our strategy of sampling only the innermost enamel surface should result in the recovery of original *patterns* of variation with minimal, constant dampening (Zazzo et al., 2005).

5.3 Results

5.3.1 Diagenesis

Evidence that the enamel obtained from Eloise is well-preserved was presented in Chapter 4. The other specimens analyzed here also had macroscopic appearances similar to modern enamel (yellowish to white, translucent to opaque), minimal differences in $\delta^{13}\text{C}$ and $\delta^{18}\text{O}$ values for pretreated and untreated aliquots (Section 5.2.2), carbonate contents (mean = $4.9 \pm 1.1\%$) (Table 5.2) similar to those of modern enamel (2.7 to 5.0) (Hillson, 1996), and a lack of correlation between carbonate contents and $\delta^{13}\text{C}$ or $\delta^{18}\text{O}$ values (which might occur if significant quantities of diagenetic carbonate contributed to the gas produced during analysis). Also, the sinusoidal variation in $\delta^{13}\text{C}$ and $\delta^{18}\text{O}$ values obtained from incrementally sampled enamel (described below) is typical of seasonal variation, and is unlikely to have been preserved if significant post-mortem isotopic alteration had occurred.

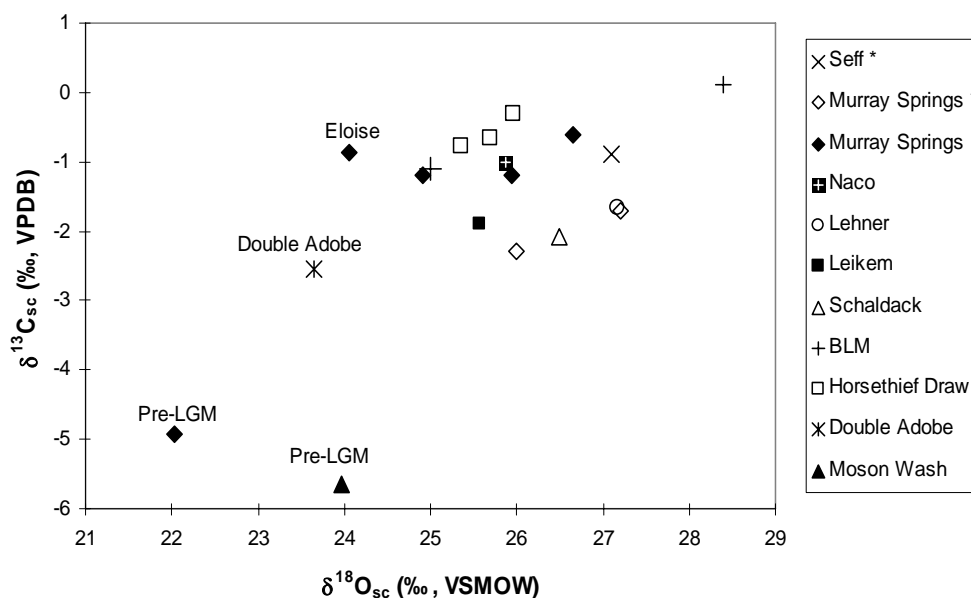


Figure 5.3 Carbon and oxygen isotope results obtained for “bulk” samples of SPV mammoth tooth enamel. *The data for Seff and some Murray Springs samples (open diamonds) are from Connin et al., (1998)

5.3.2 Bulk Carbonate

The $\delta^{13}\text{C}$ values of the San Pedro Valley mammoths range from -5.6 to 0.1‰, and the $\delta^{18}\text{O}$ values range from 22.0 to 28.4‰ (Figure 5.3, Table 5.2). Most of the mammoths analyzed in the present study ($n = 11$), as well as the San Pedro Valley mammoths analyzed by Connin et al. (1998) ($n = 3$), cluster within a range of 2.0‰ for $\delta^{13}\text{C}$ (mean = -1.2 ± 0.6 ‰) and 2.3‰ for $\delta^{18}\text{O}$ (mean = 26.1 ± 0.8 ‰) (Figure 5.3). There are no systematic differences in $\delta^{13}\text{C}$ or $\delta^{18}\text{O}$ values of mammoths with definite Clovis artifact associations and those of apparent Clovis age (Table 5.2). Eloise (AZ1, Murray Springs) has a slightly lower $\delta^{18}\text{O}$ value than the rest of the Clovis mammoths, but her $\delta^{13}\text{C}$ value does not differ. AZ7X (BLM) has somewhat higher $\delta^{13}\text{C}$ and $\delta^{18}\text{O}$ values than the others. The Double Adobe mammoth (suspected to be pre-Clovis age) has a clearly lower $\delta^{18}\text{O}$ value but only slightly lower $\delta^{13}\text{C}$ value. The pre-LGM mammoths (Moson Wash, Murray Springs) have clearly lower $\delta^{13}\text{C}$ and $\delta^{18}\text{O}$ values than the Clovis-age mammoths.

The Clovis-associated and Clovis-age mammoths analyzed here consumed diets high in C_4 plants, ranging from 62-78% C_4 (mean = $70 \pm 4\%$ C_4 , model 1) or 44-67% C_4 (mean = $55 \pm 6\%$, model 2) (Table 5.2). The pre-LGM mammoth (AZ11, AZ14) diets and the Double Adobe (AZ8) mammoth diet contained fewer C_4 plants (ranges = 7-43%, 39-59%, respectively) (Table 5.2). The mean $\delta^{18}\text{O}_{\text{water}}$ value for Clovis-age SPV mammoths is -6.6 ± 1.1 ‰, whereas those of the pre-Clovis mammoths are lower, ranging from -10.7 to -8.6‰ (Table 5.2).

5.3.3 Incremental Carbonate

The $\delta^{13}\text{C}$ and $\delta^{18}\text{O}$ values of Clovis-age mammoths plotted against distance are approximately sinusoidal (Table 5.3, Figure 5.4). For each Clovis-age individual except AZ13 (Horsethief Draw), the periods of the $\delta^{13}\text{C}$ and $\delta^{18}\text{O}$ curves are approximately equal (range = 13 to 23 mm) and there is approximate correspondence in the location of peaks and troughs (Table 5.4, Figure 5.4). For AZ13, the period of the $\delta^{18}\text{O}$ curve is about half that of the $\delta^{13}\text{C}$ curve (Table 5.4, Figure 5.4). For all the Clovis-age mammoths, the $\delta^{13}\text{C}$ curves are generally very “smooth” whereas the $\delta^{18}\text{O}$ curves are somewhat “jagged” (Figure 5.4). Intra-tooth variations (i.e., max - min δ -values for each specimen) range from 2.4 to 5.6‰ for carbon, and from 2.3 to 5.3‰ for oxygen (Table 5.5).

Table 5.3 Stable isotope results for "incremental" analyses, and their corresponding diet and drinking water compositions.

Position* (mm)	Structural Carbonate			Diet			Water
	$\delta^{13}\text{C}$ (‰)	$\delta^{18}\text{O}$ (‰)	CO_3 Wt %	$\delta^{13}\text{C}$ (‰)	% C4 ¹	% C4 ²	$\delta^{18}\text{O}$ (‰)
Murray Springs, "Eloise" (AZ1), Clovis-associated							
1	-0.3	24.1	5.7	-14.6	75	62	-8.5
2	-0.7	23.8	6.2	-15.0	72	58	-8.8
3	-2.3	23.1	7.4	-16.6	61	41	-9.6
4	-3.0	23.1	7.5	-17.3	56	34	-9.6
5	-4.6	23.2	7.7	-18.8	45	18	-9.5
6	-5.4	23.2	7.0	-19.7	39	9	-9.4
7	-5.0	23.6	7.4	-19.2	42	14	-9.0
8	-4.0	24.1	7.0	-18.3	49	23	-8.5
9	-2.8	23.7	7.3	-17.0	58	37	-8.9
10	-1.6	23.8	7.0	-15.9	65	48	-8.8
11	-1.1	23.8	7.1	-15.4	69	53	-8.9
12	-1.0	23.7	7.5	-15.3	70	55	-9.0
13	-0.8	24.1	6.4	-15.1	71	57	-8.5
14	-0.5	24.1	7.3	-14.8	73	60	-8.5
15	-0.7	22.9	7.1	-14.9	72	58	-9.7
16	-1.2	22.6	7.3	-15.5	69	53	-10.1
17	-1.9	22.0	7.2	-16.1	64	46	-10.7
18	-3.0	21.8	4.5	-17.2	56	35	-10.9
19	-3.3	21.9	5.2	-17.5	54	31	-10.9
20	-3.6	22.0	7.1	-17.8	52	28	-10.7
21	-3.4	22.4	6.3	-17.7	53	30	-10.3
22	-2.5	22.8	7.1	-16.8	59	39	-9.9
23	-1.7	22.6	7.0	-16.0	65	47	-10.1
24	-1.3	23.2	7.5	-15.6	68	52	-9.5
25	-0.9	23.5	4.3	-15.2	71	56	-9.1
26	-0.5	23.2	7.6	-14.8	73	60	-9.4
27	-0.4	22.7	7.1	-14.7	74	62	-9.9
28	-0.4	23.1	7.4	-14.7	74	61	-9.5
29	-1.7	22.4	6.8	-15.9	65	48	-10.3
30	-1.4	22.8	5.2	-15.7	67	51	-9.9
31	-2.1	22.6	4.7	-16.4	62	44	-10.0
32	-2.6	22.2	6.9	-16.9	58	38	-10.5
33	-4.0	22.4	6.9	-18.3	49	24	-10.3
34	-4.4	22.6	7.2	-18.6	46	20	-10.1
35	-3.2	23.6	6.3	-17.5	54	32	-9.0
36	-1.9	24.0	6.5	-16.2	64	46	-8.6
37	-1.3	23.3	6.8	-15.6	68	51	-9.3
38	-2.2	23.4	7.4	-16.4	62	43	-9.2
Lehner (AZ5), Clovis-associated							
1	-4.5	26.1	2.8	-18.7	46	19	-6.5
2	-4.2	26.2	6.0	-18.5	47	21	-6.3
3	-2.2	26.0	6.5	-16.4	62	43	-6.6
4	-1.2	25.7	1.4	-15.5	69	53	-6.9
5	-0.6	25.8	6.0	-14.9	72	59	-6.7

Table 5.3 cont.

Position* (mm)	Structural Carbonate			Diet			Water
	$\delta^{13}\text{C}$ (‰)	$\delta^{18}\text{O}$ (‰)	CO_3 Wt %	$\delta^{13}\text{C}$ (‰)	% C4 ¹	% C4 ²	$\delta^{18}\text{O}$ (‰)
6	-0.4	26.2	5.9	-14.7	74	61	-6.3
7	-0.3	26.0	6.4	-14.6	75	62	-6.5
8	0.1	26.6	6.2	-14.2	78	67	-5.9
9	0.2	27.5	6.0	-14.1	78	67	-5.0
10	0.2	28.2	6.1	-14.0	79	68	-4.3
11	0.4	28.1	3.2	-13.9	79	69	-4.3
12	0.3	28.1	4.7	-14.0	79	69	-4.3
13	-0.3	27.6	1.1	-14.6	75	62	-4.9
14	-0.6	27.0	3.8	-14.8	73	60	-5.5
15	-0.8	26.4	6.4	-15.1	71	57	-6.1
16	-1.0	25.9	2.2	-15.3	70	55	-6.6
17	-1.0	26.0	6.3	-15.3	70	55	-6.5
18	-1.5	25.2	6.3	-15.8	66	50	-7.3
19	-2.0	24.5	6.3	-16.2	63	45	-8.0
20	-2.1	24.2	6.4	-16.4	62	43	-8.4
21	-2.2	23.8	6.5	-16.5	62	43	-8.8
22	-1.5	24.1	6.7	-15.8	66	49	-8.5
23	-1.1	24.3	1.2	-15.4	69	54	-8.3
24	-0.3	24.4	5.9	-14.6	74	62	-8.2
25	-0.1	24.1	6.4	-14.4	76	65	-8.5
Naco (AZ10), Clovis-associated							
1	-0.5	25.4	6.9	-14.8	73	60	-7.1
2	-1.0	23.5	7.3	-15.2	70	55	-9.1
3	-1.2	23.9	7.2	-15.5	69	53	-8.7
4	-1.7	22.7	7.7	-16.0	65	48	-10.0
5	-2.4	22.6	6.7	-16.6	60	41	-10.1
6	-4.1	22.1	6.8	-18.4	48	23	-10.6
7	-4.7	22.2	7.2	-18.9	44	17	-10.5
8	-4.0	23.5	4.1	-18.3	49	24	-9.1
9	-3.8	22.9	5.9	-18.0	51	26	-9.8
10	-3.6	22.6	7.3	-17.8	52	28	-10.1
11	-2.4	23.5	7.2	-16.7	60	40	-9.1
12	-2.3	23.2	7.0	-16.5	61	42	-9.4
13	-1.9	23.8	7.4	-16.2	63	45	-8.8
14	-1.4	23.8	7.0	-15.7	67	50	-8.8
15	-1.2	23.9	7.4	-15.5	68	53	-8.7
16	-0.9	24.2	7.5	-15.2	70	56	-8.4
17	-0.7	25.0	7.2	-15.0	72	58	-7.6
18	-0.6	24.8	7.1	-14.9	73	59	-7.7
19	-0.7	24.7	7.2	-15.0	72	58	-7.9
20	-0.9	24.1	7.2	-15.2	71	56	-8.5
21	-0.8	24.5	7.2	-15.1	71	57	-8.1
22	-1.6	23.3	7.4	-15.9	66	49	-9.3
23	-2.1	23.1	7.0	-16.3	62	44	-9.5
24	-2.5	22.8	7.3	-16.8	59	39	-9.8
25	-3.3	23.2	7.0	-17.5	54	32	-9.5

Table 5.3 cont.

Position* (mm)	Structural Carbonate			Diet			Water
	$\delta^{13}\text{C}$ (‰)	$\delta^{18}\text{O}$ (‰)	CO_3 Wt %	$\delta^{13}\text{C}$ (‰)	% C4 ¹	% C4 ²	$\delta^{18}\text{O}$ (‰)
26	-4.2	22.6	7.3	-18.4	48	22	-10.1
27	-4.9	22.5	7.6	-19.1	43	14	-10.2
28	-5.5	22.6	7.2	-19.7	39	8	-10.1
29	-5.8	22.4	7.2	-20.0	36	5	-10.3
30	-5.9	23.2	7.4	-20.1	36	4	-9.4
31	-5.9	23.3	7.4	-20.1	36	5	-9.4
32	-4.5	23.6	7.4	-18.7	46	19	-9.1
33	-2.9	24.7	7.4	-17.2	56	35	-7.9
34	-1.3	25.9	7.3	-15.6	67	51	-6.6
35	-0.9	25.7	7.2	-15.2	70	56	-6.8
36	-0.7	26.0	7.4	-14.9	72	58	-6.6
37	-0.7	25.6	7.1	-15.0	72	58	-6.9
38	-0.6	25.8	7.0	-14.9	73	59	-6.7
39	-0.6	25.7	7.1	-14.8	73	59	-6.9
40	-0.3	27.0	6.7	-14.6	75	62	-5.5
41	-0.3	26.6	7.3	-14.6	74	62	-5.9
42	-0.3	25.6	7.2	-14.6	75	62	-7.0
43	-0.5	24.3	7.0	-14.8	74	60	-8.3
Horsethief Draw, Locality 129 (AZ13), Clovis-age							
1	-0.9	22.8	7.6	-15.2	71	56	-9.8
2	-1.5	22.6	6.8	-15.8	66	49	-10.1
3	-1.5	22.4	6.6	-15.8	66	50	-10.2
4	-2.1	21.5	7.5	-16.4	62	43	-11.3
5	-1.9	23.1	6.6	-16.1	64	46	-9.6
6	-2.6	22.2	7.1	-16.8	59	39	-10.5
7	-3.0	22.2	8.0	-17.2	56	35	-10.5
8	-3.8	22.2	8.0	-18.0	51	26	-10.5
9	-3.8	22.5	8.0	-18.1	50	26	-10.2
10	-3.5	21.7	7.0	-17.7	53	29	-11.0
11	-2.6	22.7	7.0	-16.9	59	38	-10.0
12	-1.9	23.9	9.1	-16.1	64	46	-8.7
13	-1.0	24.2	8.4	-15.3	70	55	-8.4
14	-0.3	25.0	7.1	-14.5	75	63	-7.6
15	0.0	25.0	6.3	-14.3	77	65	-7.6
16	0.0	24.5	6.8	-14.3	77	65	-8.0
17	0.1	24.5	8.3	-14.2	77	66	-8.0
18	-0.1	24.6	8.3	-14.4	76	65	-8.0
19	0.0	23.5	7.4	-14.3	77	65	-9.1
20	0.1	22.8	7.3	-14.2	77	66	-9.9
21	0.4	22.6	8.5	-13.9	80	70	-10.1
22	0.5	22.2	7.2	-13.8	80	70	-10.5
23	0.5	22.4	9.4	-13.8	81	71	-10.3
24	0.4	22.3	7.3	-13.9	80	69	-10.4
25	0.2	22.7	7.5	-14.1	78	67	-10.0
26	-0.1	22.9	7.4	-14.4	76	64	-9.8

Table 5.3 cont.

Position* (mm)	Structural Carbonate			Diet			Water
	$\delta^{13}\text{C}$ (‰)	$\delta^{18}\text{O}$ (‰)	CO_3 Wt %	$\delta^{13}\text{C}$ (‰)	% C4 ¹	% C4 ²	$\delta^{18}\text{O}$ (‰)
27	-0.8	23.3	7.4	-15.0	72	58	-9.3
28	-1.4	23.5	8.4	-15.7	67	51	-9.1
29	-1.7	24.3	7.0	-15.9	65	48	-8.4
30	-2.2	23.4	7.9	-16.5	61	42	-9.2
31	-2.5	23.1	7.3	-16.7	60	40	-9.6
32	-2.1	22.8	8.0	-16.4	62	43	-9.9
33	-1.7	23.1	7.3	-15.9	65	48	-9.5
34	-1.2	23.9	7.6	-15.5	68	52	-8.7
35	-0.6	24.4	7.3	-14.9	72	59	-8.1
36	-0.1	25.0	7.6	-14.3	76	65	-7.6
37	0.1	25.4	4.6	-14.2	78	67	-7.1
38	0.5	26.0	7.2	-13.8	80	70	-6.5
39	0.9	26.0	7.2	-13.4	83	74	-6.5
40	0.5	25.1	7.9	-13.8	80	70	-7.5
41	0.0	23.5	2.7	-14.3	77	65	-9.2
42	0.3	21.4	5.9	-14.0	79	68	-11.3
43	0.5	21.4	5.9	-13.8	80	71	-11.3
44	0.6	21.4	5.6	-13.7	81	71	-11.3
45	0.3	21.1	6.4	-14.0	79	69	-11.6
46	0.0	20.8	5.9	-14.3	77	65	-12.0
47	-0.4	20.9	6.7	-14.7	74	61	-11.8
48	-1.0	21.2	6.8	-15.3	70	55	-11.5
49	-1.8	21.9	5.3	-16.1	64	47	-10.8
50	-2.5	22.6	6.4	-16.7	60	40	-10.1
51	-2.3	22.9	6.5	-16.6	61	41	-9.8
Murray Springs (AZ11), pre-LGM, >29,000 BP							
1	-4.6	18.6	7.6	-18.8	45	18	-14.2
2	-4.7	18.5	7.5	-18.9	44	17	-14.4
3	-4.7	18.6	7.5	-19.0	44	16	-14.3
4	-4.8	18.9	7.7	-19.1	43	15	-14.0
5	-5.4	19.3	7.5	-19.6	40	10	-13.5
6	-5.7	20.0	6.7	-19.9	37	6	-12.8
7	-6.0	19.9	7.5	-20.2	35	3	-12.9
8	-5.9	20.2	3.9	-20.1	36	4	-12.5
9	-5.5	20.3	7.7	-19.7	38	8	-12.4
10	-4.8	20.7	7.1	-19.0	44	16	-12.1
11	-3.9	20.5	7.5	-18.1	50	25	-12.2
12	-3.5	20.1	7.4	-17.7	53	29	-12.6
13	-4.0	20.0	7.0	-18.2	49	24	-12.8
14	-5.0	19.7	7.0	-19.2	42	13	-13.1
15	-4.6	19.4	7.5	-18.8	45	18	-13.5
16	-3.0	19.1	7.9	-17.2	56	34	-13.8
17	-3.1	18.7	7.6	-17.3	56	34	-14.2
18	-4.4	18.0	7.4	-18.6	46	20	-14.9
19	-4.5	18.4		-18.8	45	18	-14.4
20	-3.9	18.5	7.4	-18.2	50	25	-14.3

Table 5.3 cont.

Position* (mm)	Structural Carbonate			Diet			Water
	$\delta^{13}\text{C}$ (‰)	$\delta^{18}\text{O}$ (‰)	CO_3 Wt %	$\delta^{13}\text{C}$ (‰)	% C4 ¹	% C4 ²	$\delta^{18}\text{O}$ (‰)
21	-3.8	19.3	7.4	-18.0	51	26	-13.5
22	-4.3	19.4	7.5	-18.5	47	21	-13.4
23	-4.3	20.5	7.1	-18.5	47	21	-12.3
24	-5.3	20.9	4.9	-19.5	40	10	-11.8
25	-5.6	21.2	8.5	-19.8	38	8	-11.6
26	-2.6	21.4	1.5	-16.9	59	38	-11.4
27	-3.4	21.2	7.8	-17.6	53	30	-11.6
28	-4.4	20.2	6.1	-18.7	46	19	-12.6
29	-3.6	19.5	7.8	-17.8	52	28	-13.3
30	-3.4	18.8	7.6	-17.7	53	30	-14.0
31	-4.7	18.7	6.1	-18.9	44	17	-14.1
32	-4.7	18.3	7.7	-19.0	44	16	-14.5
33	-4.5	19.0	6.8	-18.8	45	18	-13.8
34	-3.4	18.5	6.7	-17.6	53	30	-14.4
35	-3.0	19.2	7.3	-17.3	56	34	-13.6
36	-3.9	20.0	5.8	-18.1	50	25	-12.7
37	-4.9	20.3	7.1	-19.1	43	15	-12.4
38	-4.5	20.6	8.1	-18.7	46	19	-12.2
39	-4.9	20.0	7.8	-19.2	42	14	-12.8
40	-3.3	19.5	7.8	-17.5	54	31	-13.3
41	-3.1	17.8	8.0	-17.4	55	33	-15.1
Moson Wash (AZ14), pre-LGM, >29,000 BP							
1	-2.9	22.7	6.4	-17.2	56	35	-10.0
2	-1.7	22.2	6.9	-16.0	65	47	-10.5
3	-2.1	22.0	6.6	-16.3	63	44	-10.7
4	-3.0	21.7	6.8	-17.2	56	34	-11.0
5	-4.9	22.4	6.4	-19.1	43	14	-10.3
5.5	-6.1	21.9	2.8	-20.3	35	2	-10.8
6.5	-6.5	22.3	7.0	-20.7	32	-2	-10.4
7	-7.3	23.0	3.9	-21.5	26	-10	-9.7
7.5	-5.5	22.2	7.4	-19.7	39	9	-10.5
8.5	-4.6	22.0	8.7	-18.9	45	17	-10.7
9.7	-5.8	21.9	6.2	-20.0	37	5	-10.8
10	-6.3	22.0	6.6	-20.5	33	0	-10.7
11	-7.3	22.0	6.3	-21.5	26	-11	-10.7
12	-7.5	22.9	6.3	-21.6	25	-12	-9.8
13	-6.7	22.9	6.5	-20.9	30	-4	-9.8
14	-5.6	22.7	6.9	-19.8	38	7	-10.0
15	-4.5	22.4	6.7	-18.7	46	19	-10.3
16	-4.4	22.5	6.8	-18.6	47	20	-10.2
17	-5.2	22.0	6.4	-19.5	40	11	-10.7
18	-7.6	21.6	6.6	-21.8	24	-13	-11.2
19	-9.0	22.0	6.3	-23.1	14	-28	-10.7
20	-8.8	22.8	6.0	-22.9	16	-26	-9.9
21	-7.6	21.8	6.6	-21.8	24	-14	-10.9
22	-7.6	22.3	6.5	-21.8	24	-14	-10.4

Table 5.3 cont.

Position* (mm)	Structural Carbonate			Diet			Water
	$\delta^{13}\text{C}$ (‰)	$\delta^{18}\text{O}$ (‰)	CO_3 Wt %	$\delta^{13}\text{C}$ (‰)	% C4 ¹	% C4 ²	$\delta^{18}\text{O}$ (‰)
23	-7.3	22.4	6.2	-21.5	26	-11	-10.3
24	-6.8	22.3	6.9	-21.0	30	-5	-10.4
25	-5.7	21.8	6.3	-19.9	38	7	-10.9
26	-3.6	22.6	6.3	-17.8	52	28	-10.0
27	-2.3	22.9	6.3	-16.5	61	42	-9.8
28	-3.2	21.4	5.8	-17.5	54	32	-11.4
29	-8.3	23.0	6.7	-22.5	19	-21	-9.7
31	-6.6	22.1	6.3	-20.8	31	-3	-10.6
32	-2.7	21.9	6.5	-17.0	58	37	-10.8
33	-1.6	22.0	6.5	-15.9	66	48	-10.7
34	-2.4	23.0	6.6	-16.7	60	40	-9.7
35	-1.4	22.9	6.1	-15.7	67	51	-9.7
36	-1.9	23.1	6.7	-16.1	64	46	-9.5
37	-4.8	22.9	6.6	-19.0	44	16	-9.8
38	-6.1	22.7	7.5	-20.3	35	3	-10.0
39	-5.2	21.1	7.0	-19.4	41	12	-11.6
40	-5.3	22.3	6.2	-19.5	40	10	-10.4
41	-4.2	21.6	6.0	-18.4	48	22	-11.2
42	-2.1	22.2	6.4	-16.4	62	43	-10.4

* Position numbers start at an arbitrary point and increase as they get closer to the cervix

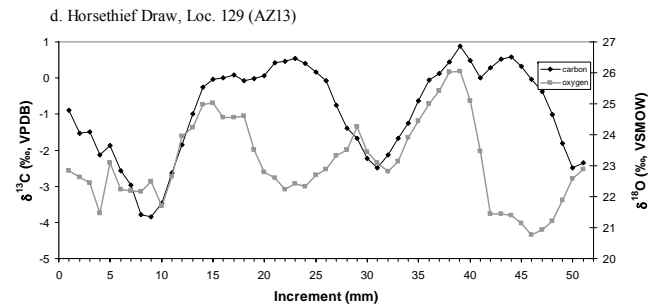
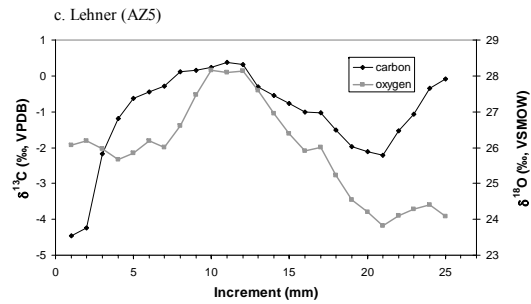
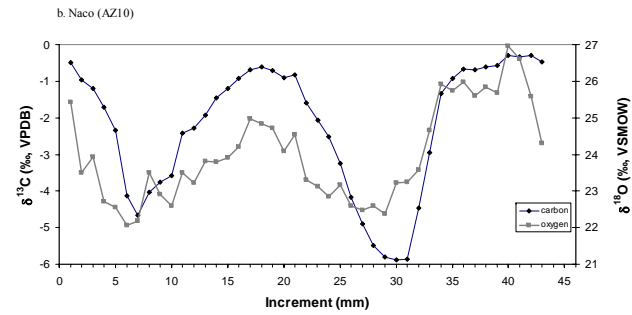
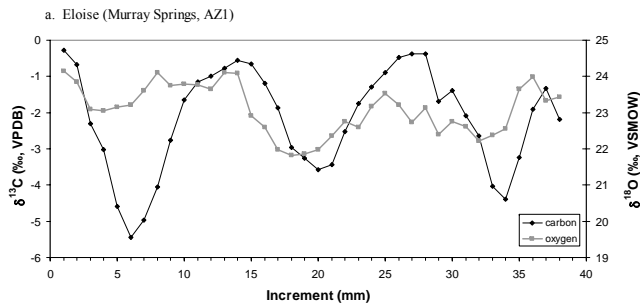
¹ %C₄ calculated using model 1, (lower $\delta^{13}\text{C}$ value for C₃ plant endmember - see text)

² %C₄ calculated using model 2, (higher $\delta^{13}\text{C}$ value for C₃ plant endmember, very conservative %C₄ estimate - see text)

Values in bold are the result of duplicate analyses

Negative values for %C₄ are possible because the calculation method uses discrete endpoints for plant $\delta^{13}\text{C}$ values, whereas in reality plants can have higher or lower values (see text).

Clovis-age samples



Pre-LGM samples

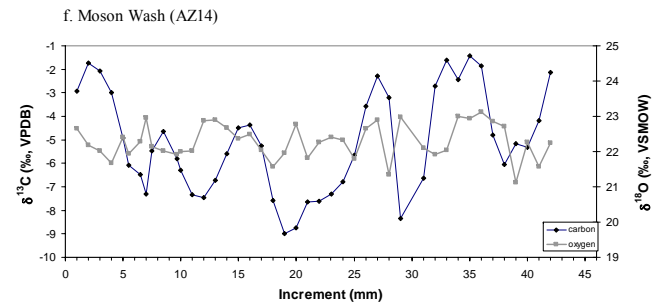
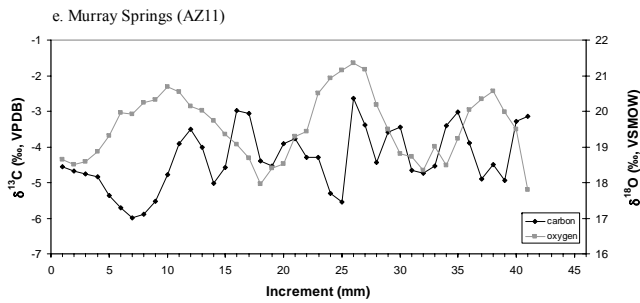


Figure 5.4 Carbon and oxygen isotope results for “incremental” sampling of Clovis-age and pre-LGM mammoths from the SPV.

The patterns for the pre-LGM mammoths are very different from those of the Clovis-age mammoths (Figure 5.4). AZ11 (Murray Springs) has a smooth, sinusoidal $\delta^{18}\text{O}$ curve (total range of values = 3.6‰) with regular periods (>9-16 mm) that decrease closer to the cervix, and a $\delta^{13}\text{C}$ curve (total range of values = 3.4‰) with much shorter periods (3-11 mm) and an irregular shape (Table 5.4, Figure 5.4). AZ14 (Moson Wash) has a low-amplitude $\delta^{18}\text{O}$ curve (total range of values = 2.0‰) with no regular periodicity, and a high-amplitude $\delta^{13}\text{C}$ curve (total range of values = 7.6‰) with irregular periodicity (Table 5.4, Figure 5.4).

Table 5.4 Periods of the isotope curves for serially-sampled mammoth enamel.

LSIS #	Site	$\delta^{18}\text{O}$		$\delta^{13}\text{C}$		Sampling	
		Period (mm)	No. **	Period (mm)	No. **	Location	Distance
Clovis-associated and Clovis-age							
AZ1 (Eloise)	Murray Springs	14 to 15	>2.5	13 to 14	>2.5	Cervical	37
AZ5	Lehner	~17	>1	20	>1	Mid-crown	24
AZ10	Naco	~23	>2	21 to 23	>2	Occlusal (d.c.)	42
AZ13	HTD Loc 129	~9 to 15	>4?	19 to 22*	>2	Occlusal (d.c.)	50
Pre-LGM (>29,000 BP)							
AZ11	Murray Springs	>9 to 16*	~3	3 to 11 [^]	>7?	Cervical	40
AZ14	Moson Wash	?	?	6 to 11 [^]	>4?	Cervical	42

** Number of periods recorded in isotope record

* Periods decrease with increasing distance from occlusal surface (i.e., closer to the cervix)

[^] Periods are very irregular

d.c. = developing enamel cone

5.4 Discussion

5.4.1 Comparison of “Bulk” and “Incremental” Stable Isotope Results

Isotopic compositions obtained for “bulk” analyses are means that average growth over several seasons, as are the mean δ -values of all incremental samples from a given specimen. Are these multi-season means directly comparable? There is a good correlation between bulk and incremental means for both $\delta^{13}\text{C}$ ($r = 0.92$, $df = 4$, $p < 0.01$) and $\delta^{18}\text{O}$ ($r = 0.97$, $df = 4$, $p < 0.01$). There is no systematic offset between incrementally sampled

mean $\delta^{13}\text{C}$ values and bulk $\delta^{13}\text{C}$ values (mean difference = -0.2‰ , range of offsets = -1.3 to 0.6‰), but the incrementally sampled mean $\delta^{18}\text{O}$ values are on average 1.8‰ lower than the bulk values (range of offsets = 2.5 to 1.0‰ lower). These differences cannot be attributed to the fact that incremental samples were not pretreated, because (1) three of the bulk specimens were pretreated and three were not, yet all showed offsets, (2) the offsets were larger than those observed as a result of pretreatment (see Section 5.2.2), and (3) the incremental-bulk difference was slightly smaller for pretreated than untreated bulk samples, even though pretreatment should have increased the offset by increasing the bulk $\delta^{18}\text{O}$ values (see Section 5.2.2).

There are several possible explanations for the lower mean $\delta^{18}\text{O}$ values obtained for incremental samples relative to “bulk” samples: dentin contamination of incrementally sampled enamel, a seasonal bias in either of the means, or differences in mineralization processes. The first possibility can be rejected because dentin $\delta^{18}\text{O}$ values (between 19.7 and 20.1‰ , measured for two different individuals) are higher than the incrementally-sampled mean $\delta^{18}\text{O}$ value for one of the specimens. A seasonal bias can also be rejected since one specimen displays no “seasonal” variations in oxygen isotope composition and yet still shows the typical offset. Also, the $\delta^{13}\text{C}$ curves tend to show greater seasonal variation than the $\delta^{18}\text{O}$ curves for most samples, yet there was no pretreatment offset for $\delta^{13}\text{C}$ values. A difference in mineralization processes is arguably the most likely explanation, since the innermost enamel (i.e., that used for incremental sampling) mineralizes faster than the rest of the enamel in various species (Allan, 1967; Tafforeau et al., 2007). More rapid mineralization could involve differences in the isotopic composition of fluids from which bioapatite forms, as a result of changes in the transport of bicarbonate ions to developing enamel by ameloblasts (Smith, 1998), or of depletion of bicarbonate in the fluid surrounding the enamel, which would result in the incorporation of more ^{16}O -containing bicarbonate into bioapatite. Alternatively, the rapid formation of inner enamel could be insufficient for bioapatite to reach isotopic equilibrium with enamel fluids. Regardless of the explanation, the consistent offset between “bulk” and mean “incremental” $\delta^{18}\text{O}$ values indicates that the values obtained using the different methods are not directly comparable. However, the strong correlations between the methods indicate that comparisons among specimens sampled the same way remain valid.

5.4.2 Bulk Carbonate

The mean $\delta^{18}\text{O}_{\text{water}}$ value calculated using Clovis-age SPV mammoths ($-6.6 \pm 1.1\text{‰}$) is very close to the modern amount-weighted mean $\delta^{18}\text{O}$ of San Pedro Valley precipitation during the summer (-6.2‰) (Wahi et al., 2008), and higher than modern SPV groundwater, river water, or monsoon floodwater (see Section 5.1.2). The similarity to modern summer precipitation $\delta^{18}\text{O}$ values does not necessarily indicate that the Terminal Pleistocene climate was as warm and dry as that of the modern San Pedro Valley, although numerous lines of evidence do indicate that it was warm and dry (Haynes, 2005; Holmgren et al., 2006; Pigati et al., 2009; Wagner et al., 2010). Higher $\delta^{18}\text{O}$ values can also result from (1) increased evaporation, (2) differences in moisture source and atmospheric circulation patterns (i.e., rain clouds that originated closer to the San Pedro Valley, evaporated from cooler surface water with lower specific humidity, and experienced less rainout prior to reaching the SPV), (3) greater input from summer than winter precipitation, and (4) greater input from lower- than higher-altitude precipitation. Any or all of these factors could have contributed to the relatively high $\delta^{18}\text{O}_{\text{water}}$ values.

The $\delta^{18}\text{O}_{\text{water}}$ values calculated using the pre-Clovis mammoths (Table 5.2) are within the range of modern winter precipitation $\delta^{18}\text{O}$ values from Tucson and the San Pedro Valley (Baillie et al., 2007; Wagner et al., 2010, supplementary information). These lower values could theoretically result from either behavioural differences (i.e., selection of different water sources, migration to different geographical regions) or climatic differences (i.e., temperature, rainfall amount, contributions of winter vs. summer precipitation, moisture source region, atmospheric circulation patterns). Since the two specimens with the lowest $\delta^{18}\text{O}$ values (Murray Springs, Moson Wash) were recovered from older contexts than the rest of the samples, a climatic explanation is likely at least partially responsible. The lower $\delta^{18}\text{O}$ values of the pre-LGM individuals suggest cooler and/or wetter climates. The pre-LGM mammoths also consumed substantially fewer C_4 plants, which tend to grow under warmer conditions. These interpretations are consistent with the multiple lines of evidence that show generally cooler and wetter conditions prevailed in the American Southwest during much of the Pleistocene (Thompson et al., 1993).

5.4.3 Incremental Carbonate

5.4.3.1 *Clovis Mammoths*

Considering that sinusoidal variations in the $\delta^{13}\text{C}$ and $\delta^{18}\text{O}$ values of tooth enamel are characteristic of seasonal changes in drinking water and diet, and that growth rate estimates from a thin section of Eloise are consistent with estimates based on the distance between isotopic maxima or minima in these curves (Chapter 4), and that periods for $\delta^{13}\text{C}$ curves among individuals are similar (Table 5.4) we assume that one period of variation represents one year of growth for Clovis mammoths. Since the $\delta^{18}\text{O}$ values of meteoric water (and river, lake, or groundwater with meteoric water inputs) are higher in summer and lower in winter (Baillie et al., 2007; Wahi et al., 2008), the peaks in the $\delta^{18}\text{O}$ and $\delta^{13}\text{C}$ curves in Clovis mammoths (which approximately coincide) almost certainly represent summer, and the troughs, winter.

The correspondence between peaks and troughs in the $\delta^{13}\text{C}$ and $\delta^{18}\text{O}$ curves of Clovis mammoths suggest that they were eating C_4 -dominated diets in summer, and mixed C_3 - C_4 diets in winter. Summer highs ranged from 62-83% C_4 plants, while winter lows were between 4 and 50% C_4 plants (Tables 5.3, 5.5). Since the same pattern of seasonal dietary change was observed in enamel from several individuals, and mammoth tooth enamel grows over a period of years to decades (Chapter 3) (Metcalf et al., 2010), we infer that Clovis mammoth seasonal dietary behaviour was quite consistent over time (Figure 5.5). The amplitudes of variation in $\delta^{18}\text{O}$ values for Clovis-age mammoths were similar to those of modern seasonal precipitation in the SPV (Figure 5.6). Bearing in mind that the former represent minimum amplitudes of drinking water variations (because of “dampening” that can occur as a result of enamel maturation and sampling geometry; see Chapter 4), this suggests that seasonal variations in Pleistocene SPV drinking water were at least as great as those of modern SPV precipitation.

The Horsethief Draw (AZ13) mammoth’s incrementally sampled $\delta^{18}\text{O}$ pattern differs from those of the other Clovis-age mammoths (Figure 5.4). We infer that for this

Table 5.5 Summary of stable isotope results for "incremental" analyses, and corresponding diet and drinking water compositions.

LSIS #	Site	n	$\delta^{13}\text{C}_{\text{sc}}$ (‰)				%C ₄				$\delta^{18}\text{O}_{\text{sc}}$ (‰)				$\delta^{18}\text{O}_{\text{water}}$ (‰)			
			Mean	Min	Max	Range	Mean ¹	Mean ²	Min ³	Max ³	Mean	Min	Max	Range	Mean	Min	Max	Range
Clovis-associated and Clovis-age																		
AZ1 (Eloise)	Murray Springs	38	-2.2 ± 1.4	-5.4	-0.3	5.2	62 ± 10	43 ± 15	9 - 39	62 - 75	23.1 ± 0.7	21.8	23.1	2.3	-9.6 ± 0.7	-11	-8.5	2.4
AZ5	Lehner	25	-1.1 ± 1.3	-4.5	0.4	4.8	69 ± 9	54 ± 13	19 - 46	69 - 79	25.9 ± 1.3	23.8	28.2	4.3	-6.6 ± 1.4	-8.8	-4.3	4.5
AZ10	Naco	43	-2.2 ± 1.8	-5.9	-0.3	5.6	61 ± 12	42 ± 18	4 - 36	62 - 75	24.0 ± 1.3	22.1	27.0	4.9	-8.6 ± 1.4	-11	-5.5	5.1
AZ13	HTD Loc 129	51	-0.9 ± 1.3	-3.8	0.9	4.7	70 ± 9	56 ± 13	26 - 50	74 - 83	23.1 ± 1.3	20.8	26.0	5.3	-9.6 ± 1.4	-12.0	-6.5	5.5
Pre-LGM (>29,000 BP)																		
AZ11	Murray Springs	41	-4.3 ± 0.9	-6.0	-2.6	3.4	47 ± 6	20 ± 9	3 - 35	38 - 59	19.6 ± 0.9	17.8	21.4	3.6	-13.2 ± 1.0	-15	-11	3.7
AZ14	Moson Wash	43	-5.1 ± 2.2	-9.0	-1.4	7.6	41 ± 15	12 ± 22	-28 - 14	51 - 67	22.3 ± 0.5	21.1	23.1	2.0	-10.4 ± 0.5	-12	-9.5	2.1

¹ %C₄ calculated using model 1, (lower $\delta^{13}\text{C}$ value for C₃ plant endmember - see text)

² %C₄ calculated using model 2, (higher $\delta^{13}\text{C}$ value for C₃ plant endmember, very conservative %C₄ estimate - see text)

³ Minimum (maximum) %C₄ range is calculated from the lowest (highest) $\delta^{13}\text{C}$ values, using model 2 (first number) and model 1 (second number)

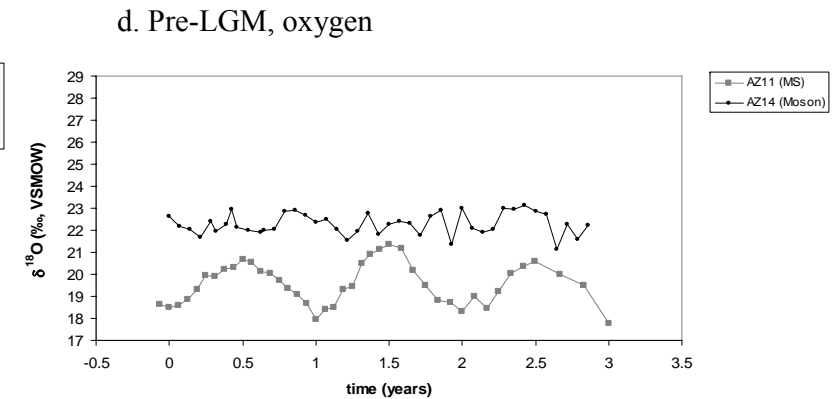
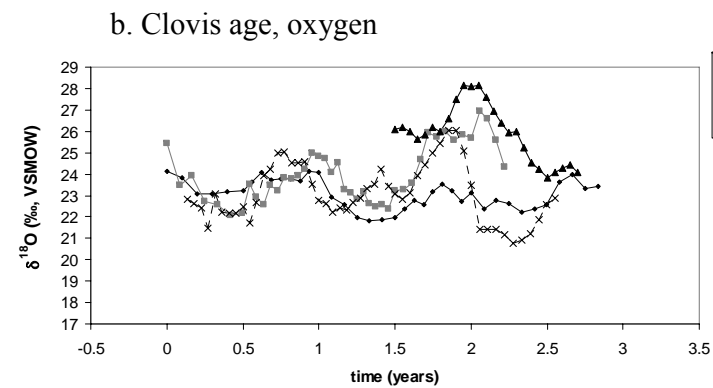
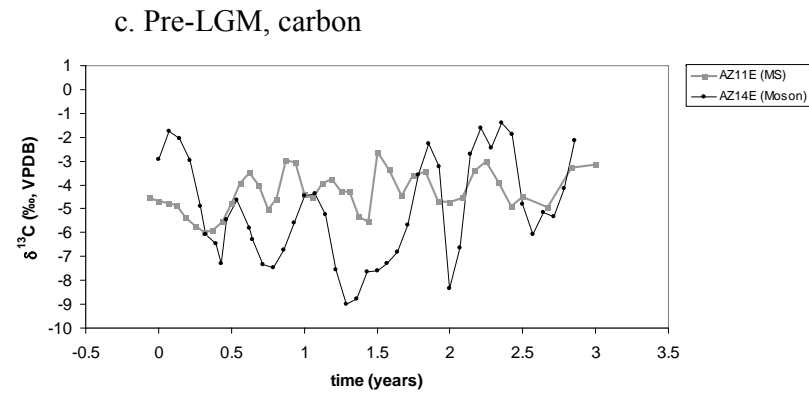
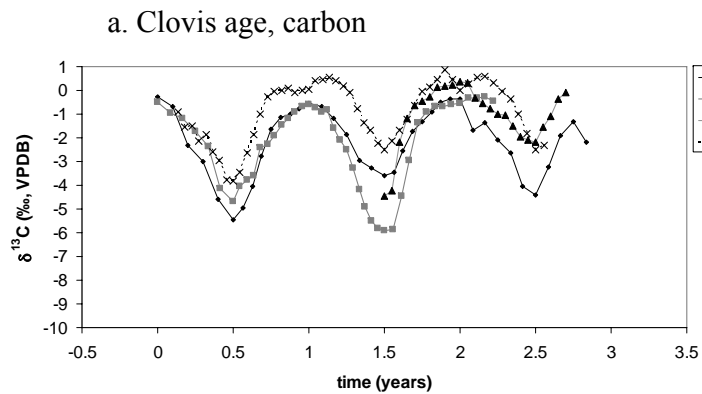


Figure 5.5 Comparison of carbon and oxygen isotope results for “incremental” sampling of Clovis-age (a, b) and pre-LGM (c, d) mammoths from the SPV. The “distance” axis has been transformed to time, as described in the text. The reference point for time is arbitrary, so although the data are stacked for comparison of seasonal trends, the true “calendar” years of formation for each sample likely differ.

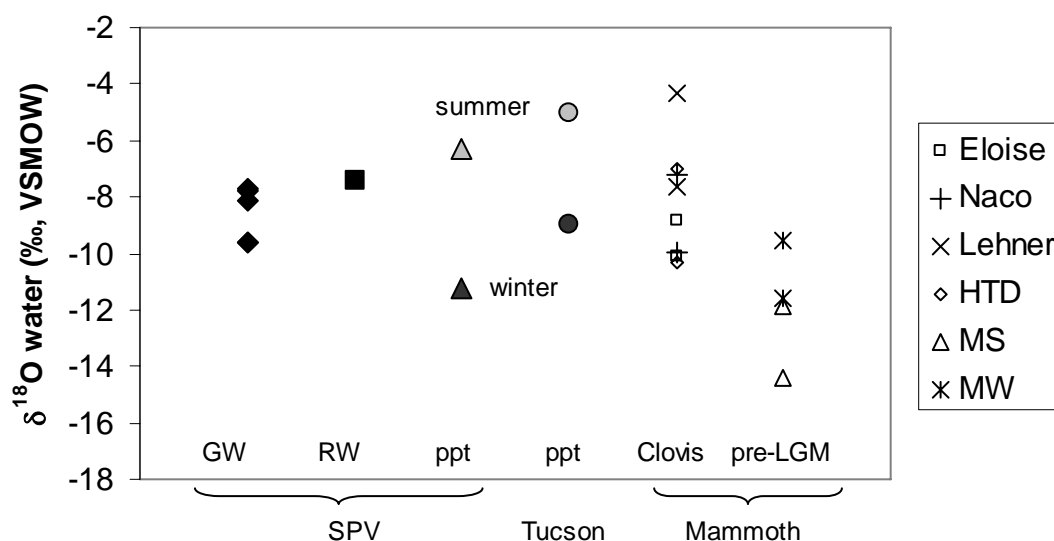


Figure 5.6 Comparison of seasonal extremes in the $\delta^{18}\text{O}$ values of mammoth drinking water to the $\delta^{18}\text{O}$ values of seasonal precipitation in the modern SPV and Tucson, and the $\delta^{18}\text{O}$ values of modern SPV perennial water sources. Winter means are dark grey symbols and summer means are light grey. Mammoth seasonal extremes are the averages of peak (for summer) or trough (for winter) drinking water $\delta^{18}\text{O}$ values (calculated from enamel $\delta^{18}\text{O}$ values, as described in text) from each specimen's time-series curve. Thus, all data points are averages over several years/seasons. SPV water data are from Baillie (2005), Baillie et al. (2007); Tucson water data is from Wagner et al. (2010, supplementary material). Sampling geometry, enamel maturation, and residence time in the body results in some dampening of the seasonal extremes relative to those of drinking water. GW = groundwater, RW = river water, ppt = precipitation, SPV = San Pedro Valley, pre-LGM = pre-Last Glacial Maximum, MS = Murray Springs, MW = Moson Wash.

individual, as for the other Clovis mammoths, one period in the $\delta^{13}\text{C}$ curve is equal to one year of growth. This inference is based on the similar period (19-22 mm) and shape of the HTD $\delta^{13}\text{C}$ curve to those of the Naco mammoth (period = 23 mm), both of which were obtained from developing enamel cones and thus should have had similar growth rates (Table 5.4). Unlike the other Clovis-age mammoths, the HTD mammoth has large and sustained decreases in $\delta^{18}\text{O}$ values during the latter half of the inferred summers (Figure 5.4). This indicates either very different drinking water sources during late summer, unusual metabolic effects, or significantly different meteorological conditions. The similarity of the $\delta^{13}\text{C}$ curves of the HTD and other Clovis-age mammoths suggests that their seasonal dietary patterns were not considerably different. We know of no metabolic

effect that would decrease $\delta^{18}\text{O}$ values by 3-5‰ during late summer but leave the rest of the seasonal pattern unaffected. However, an “amount effect” resulting from severe, sustained monsoon rains during the latter half of the summer could produce large decreases in summer precipitation $\delta^{18}\text{O}$ values. This pattern is seen in modern precipitation at Waco, Texas during early fall (September-October): temperatures remain high but the amount of precipitation more than doubles relative to the previous months, and the $\delta^{18}\text{O}$ values decrease by more than 5‰ (Higgins and MacFadden, 2004; IAEA/WMO, 2010). In November, less rainfall occurs and the $\delta^{18}\text{O}$ values of precipitation increase. Monsoon rainfall would also explain the slight increase in $\delta^{13}\text{C}$ values that coincides with the low $\delta^{18}\text{O}$ values, and the generally higher $\delta^{13}\text{C}$ values of this individual relative to the other Clovis-age mammoths (i.e., more “greening up” of seasonal C_4 plants).

5.4.3.2 *Pre-LGM Mammoths*

The patterns of the pre-LGM mammoth “incremental” results are very different from those of Clovis mammoths, and also from one another (Figures 5.4, 5.5). Given that the radiocarbon ages of these mammoths could differ by thousands of years, this is not unexpected.

AZ11 (Murray Springs) has smooth, sinusoidal variations in $\delta^{18}\text{O}$ values, and a period (>9-16 mm) similar to those of the Clovis-age mammoths (Figure 5.4, Table 5.4). However, all the $\delta^{18}\text{O}$ values of this mammoth, including the highest peaks in the time-series, are lower than those of the Clovis mammoths (Figure 5.5), suggesting lower temperatures and/or greater rainfall amounts throughout the entire year. Thus, this individual likely lived in the SPV during a glacial or stadial period. The relatively small range of $\delta^{18}\text{O}$ values, and smooth appearance of the curve, suggests less seasonal variability in meteoric water $\delta^{18}\text{O}$ values, which further suggest wetter conditions, smaller seasonal temperature or humidity variations, and/or reliance on a more stable water source. The $\delta^{13}\text{C}$ values are generally lower than those of the Clovis-age mammoths, indicating less C_4 plant consumption, but there is still good evidence for some C_4 plant consumption at various times of the year (enamel $\delta^{13}\text{C}$ values greater than -7‰) (Cerling et al., 1997), consistent with a generally cooler climate. The magnitude of variation in

$\delta^{13}\text{C}$ values for AZ11, while small, is greater than those typical of mammoths living in C_3 -only ecosystems (Chapters 6, 7), which further suggests mixed C_3 - C_4 plant consumption. However, unlike the single peak in C_4 plant consumption during summer observed in the Clovis-age mammoths, this individual had 2 to 3 peaks in C_4 -plant consumption per year, perhaps as a result of greater movement among microhabitats (grasslands, woodlands) throughout the year.

AZ14 (Moson Wash) has unique $\delta^{13}\text{C}$ and $\delta^{18}\text{O}$ patterns. The range of $\delta^{18}\text{O}$ values is very small (2.0‰), and there is no apparent seasonal signal (Figure 5.4, Table 5.4). This likely resulted from reliance on a primary water source (or sources) with relatively invariant $\delta^{18}\text{O}$ values (e.g., one of the large lakes that occupied playa basins in the southwest during much of the Pleistocene, or a groundwater spring). The $\delta^{18}\text{O}$ values of this individual are higher than those of the other pre-LGM mammoth, and overlap the lower values of the Clovis-age mammoths, suggesting that it lived during a relatively warm interglacial period. The range of $\delta^{13}\text{C}$ values for this individual (7.6‰) is much larger than that of any other SPV mammoth. The $\delta^{13}\text{C}$ values for this individual indicate that maximum C_4 plant consumption was intermediate between that of the Clovis mammoths and the other pre-LGM mammoth. Minimum $\delta^{13}\text{C}$ values were much lower than those of the Clovis mammoths or the other pre-LGM mammoth, indicating greater reliance on C_3 plants or aquatic vegetation. In fact, most of the $\delta^{13}\text{C}$ minima for this mammoth are below the cutoff for unambiguous C_4 plant consumption (Cerling et al., 1997), suggesting 100% C_3 plant consumption. Assuming that the growth rate of this tooth was not extremely different from the other mammoth teeth (13-20 mm per year for mid-crown to cervical samples) (Table 5.4), we infer that peaks in C_4 plant consumption occurred 2-3 times per year, as was the case for the other pre-LGM mammoth (Figure 5.5). We speculate that this mammoth spent much of its time near large pluvial lakes, where C_3 plants likely predominated, but periodically migrated to grassy areas further from the lake, which supported C_4 plants.

5.4.4 Migration

We cannot fully evaluate the extent of migration from carbon and oxygen isotope compositions alone. However, if mammoths were undertaking long-distance migrations

among various regions, we would expect to see upward or downward trends in $\delta^{18}\text{O}$ values superimposed on the seasonal variations, and/or a lack of sinusoidal variations. Since we do not see such trends in Clovis-age mammoths, they likely remained within a relatively small home range, such as the San Pedro basin.

5.4.5 Double Adobe

The substantially lower $\delta^{18}\text{O}$ value of the Double Adobe mammoth (obtained by “bulk” analysis) relative to Clovis-age mammoths is consistent with the hypothesis that the former lived in a cooler and/or wetter environment, and thus may pre-date the Clovis-age mammoths. Its slightly lower $\delta^{13}\text{C}$ value is also consistent with this inference.

5.4.6 The Naco Mammoth: Escape from Lehner?

The variability in “bulk” isotopic results for all Clovis-associated and Clovis-age mammoths (1 SD = 0.6‰ for $\delta^{13}\text{C}$) was similar to that found by Hoppe (2004) in a single herd that died at Waco, Texas (1 SD = 0.5‰), and lower than that of a time-averaged assemblage from Friesenhahn Cave (1.4‰). This is not to say that all Clovis-age SPV mammoths were necessarily part of a single herd, but rather that they lived within a relatively short window of time and had similar diets. Because of the low level of variability among all Clovis-age mammoths, the data are insufficient to evaluate the hypothesis that the Naco mammoth escaped from a mass-kill at the Lehner site. Future study of developing enamel cones from Lehner mammoths, which record the time just prior to death, could provide better insight into this question.

5.4.7 Eloise: The Last Mammoth at Murray Springs

From “bulk” isotopic analysis, Eloise had the lowest $\delta^{18}\text{O}$ value of all the Clovis-age mammoths (Table 5.2). From “incremental” analysis, her maximum and mean $\delta^{18}\text{O}$ values were lower (though the latter was equivalent to that of the HTD mammoth), and her range of $\delta^{18}\text{O}$ values was smaller than those of other Clovis-age mammoths, but her minimum $\delta^{18}\text{O}$ value was not the lowest (Table 5.5). Together, these data suggest that Eloise may have experienced somewhat cooler and/or wetter conditions, particularly during summer; that she was drinking from a water source with more attenuated seasonal

variations in $\delta^{18}\text{O}$ values; and/or that she migrated shorter distances than the other Clovis-age mammoths. Given that the range of $\delta^{13}\text{C}$ values for Eloise is similar to that obtained for the other Clovis-age mammoths, it is unlikely that her migrational range was substantially different. It is notable that Eloise died very shortly prior to the onset of the Younger Dryas period, which was cold and wet in the American southwest (Haynes and Huckell, 2007). Thus, her isotopic compositions could reflect the early onset of Younger Dryas conditions (prior to deposition of the black mat). However, it should be noted that the isotopic data for Eloise span a period of only about 3 years (Table 5.4, Figure 5.4), and were not necessarily the years immediately preceding her death. Since the differences between Eloise and other Clovis mammoth are relatively small, they could simply reflect typical inter-annual variations during the Terminal Pleistocene, prior to the Younger Dryas.

5.4.8 Clovis Drought

To evaluate the evidence for a Clovis drought, we compare the isotopic compositions of Clovis-associated mammoths with those of Clovis-age mammoths. None of our expectations for isotopic evidence of drought (see Section 5.1.5) are fulfilled. There are no differences in “bulk” isotopic compositions between the groups, which suggests that they experienced similar climatic conditions and consumed similar diets. All of the Clovis-associated and Clovis-age mammoths had diets high in C_4 plants (likely grasses), which suggest relatively high temperatures and significant amounts of precipitation, especially during summer (Epstein et al., 1997; Paruelo and Lauenroth, 1996; Yang et al., 1998), and thus do not indicate drought. In particular, the occurrence of high $\delta^{13}\text{C}$ values during inferred summer growth periods, observed in both Clovis-associated and Clovis-age mammoths, suggests consistently abundant summer rainfall. Clovis-associated mammoths have slightly lower ranges of incrementally-sampled $\delta^{18}\text{O}$ values than the single non-Clovis-associated mammoth analyzed, but the curves are more irregular (less “smooth”). The irregularity of the Clovis mammoth $\delta^{18}\text{O}$ curves may be attributable to changes in rainfall amount, as argued by Higgins and MacFadden (2004) for horse and bison specimens, or it could have resulted from different water sources or physiological conditions. In addition, the Clovis-associated mammoths have a higher

range of $\delta^{13}\text{C}$ values for incremental samples, whereas a lower range was expected from animals that experienced drought.

There is evidence for monsoon rainfall during the lifetime of the Clovis-age Horsethief Draw (AZ13) mammoth (see Section 5.4.3.1). This was the only “Clovis-age”, not Clovis-associated specimen selected for incremental sampling. If the HTD specimen pre-dates the Clovis occupation, and if the pattern of this individual was typical of late Alleröd pre-Clovis mammoths, it could indicate that monsoon rains were more severe prior to the Clovis presence in the SPV. In other words, the SPV may have been somewhat drier during the Clovis occupation than in the immediately preceding years. Incremental analyses of additional “Clovis-age” mammoths that were not associated with Clovis artifacts, and more precise dating control, are needed to determine whether the HTD mammoth pattern was typical. However, previous studies have also found evidence for relatively heavy summer rainfall in the Late Glacial (15,000 to 10,000 BP) Chihuahuan Desert region (Higgins and MacFadden, 2004).

In summary, there is no evidence for seriously debilitating drought in the San Pedro Valley during the period of time recorded in the Clovis-age mammoth teeth. However, it is possible that the mammoths died so soon after the onset of drought that it was not recorded in their teeth. If so, drought onset must have been no more than a few years prior to the death of the Clovis-age mammoths, since the enamel cone of the Naco mammoth formed only a few years prior to its death, yet its $\delta^{13}\text{C}$ and $\delta^{18}\text{O}$ patterns were similar to those of the other Clovis mammoths. This conclusion is consistent with the extremely sudden and brief nature of the drought inferred from stratigraphic and geomorphic evidence at Murray Springs (Haynes, 1991a).

5.4.9 Implications for Clovis Hunting and Extinction

The seasonal dietary behaviour of Clovis-age mammoths in the SPV was consistent and predictable: in summer, they sought out areas with abundant C_4 grasses. Stable carbon isotopes in soil carbonates and organic matter, and pollen evidence suggest that C_4 grasses were not present in the SPV riverine corridor during the Clovis occupation, ca. 13,000 cal BP (Ballenger, 2010). However, plant macrofossils and pollen from packrat middens provide clear evidence that C_4 plants were present on hillsides in

regions close to the SPV (Holmgren et al., 2006), and pollen from the Lehner site indicates that a “desert grassland” (heterogenous mixture of dense grassy areas and sparse grasses mixed with shrubs) existed on the SPV floodplain (Mehringer and Haynes, 1965). Thus, we propose that that mammoths ventured beyond the riverine corridor during the summer to obtain C₄ plants from the “bajada”, and foraged closer to the river during winter. This pattern is very similar to that of modern elephants in Kenya, who remain in the riparian corridor, consuming mainly C₃ plants, during the dry season, but migrate further from the river and consume more C₄ plants during the wet season (Cerling et al. 2009). Such predictable seasonal behaviours would have made SPV mammoths particularly easy for human hunters to track, even prior to the proposed Clovis drought (Haynes, 2002b). Furthermore, an extremely sudden Clovis drought would have been highly disruptive to these seasonal cycles. Based on the consistency in seasonal patterns among Clovis-age mammoths, they would probably have never experienced such a drastic change in climatic conditions, making it difficult to adapt.

5.5 Conclusions

Isotopic data obtained from mammoth skeletal remains provides insight into the climatic conditions experienced by mammoths and Clovis humans alike, just prior to mammoth extinction. Clovis-associated and Clovis-age mammoth experienced climates that were relatively consistent over time, and consumed similar diets. Clovis-age mammoths experienced warmer, and probably drier, conditions than pre-LGM mammoths. We found no evidence of severe drought from the isotopic compositions of mammoth teeth, but the different seasonal changes in $\delta^{18}\text{O}$ values between Clovis-associated mammoths and the single analyzed “Clovis-age” (not artifact-associated) mammoth suggest a possible reduction in summer monsoon intensity during the Clovis era. Nevertheless, summer rainfall during Clovis times was sufficient to support a seasonal C₄ grassland.

All SPV mammoths consumed some C₄ plants, but Clovis-age mammoths consumed more than pre-LGM mammoths throughout most of the year. Clovis-age mammoths consumed diets very high in C₄ plants during summer, and mixed C₃-C₄ diets in winter. This supports the contention that Late Pleistocene grasslands in the American

southwest “greened up” during summer (Holmgren et al. 2007), likely as a result of increased summer rains. Furthermore, Clovis-era mammoths appear to have sought out these greener areas in the landscape, as do modern elephants (Loarie et al. 2009). This may have increased their susceptibility to both human hunting and sudden climate change. Unlike Clovis-age mammoths, pre-LGM mammoths shifted the proportion of C₃ to C₄ plants in their diet several times per year, probably because in their cooler, wetter environments, a greater variety of green plants were available year-round, and grasslands did not undergo as significant seasonal growth as they did during Clovis times.

We employed inner enamel sampling to ensure minimal dampening of stable isotope records of seasonality (Zazzo et al., 2005), but further research on proboscidean enamel mineralization is required to determine the extent of dampening that remains. Of particular relevance to this study, differences in the mineralization of inner enamel relative to the rest of the enamel may produce lower $\delta^{18}\text{O}$ values relative to those of whole (“bulk”) enamel.

5.6 References

- Allan, J.H., 1967. Maturation of enamel. In: A.E.W. Miles (Editor), *Structural and Chemical Organization of Teeth*. Academic Press, New York, pp. 467-494.
- Aptroot, A. and van Geel, B., 2006. Fungi of the colon of the Yukagir Mammoth and from stratigraphically related permafrost samples. *Review of Palaeobotany and Palynology*, 141(1-2): 225-230.
- Ayliffe, L.K., Lister, A.M. and Chivas, A.R., 1992. The preservation of glacial-interglacial climatic signatures in the oxygen isotopes of elephant skeletal phosphate. *Palaeogeography Palaeoclimatology Palaeoecology*, 99(3-4): 179-191.
- Baillie, M.N., 2005. Quantifying baseflow inputs to the San Pedro River: A geochemical approach. M.Sc. Thesis, The University of Arizona, Tucson.
- Baillie, M.N., Hogan, J.F., Ekwurzel, B., Wahi, A.K. and Eastoe, C.J., 2007. Quantifying water sources to a semiarid riparian ecosystem, San Pedro River, Arizona. *Journal of Geophysical Research: Biogeosciences*, 112(G3): G03S02, doi: 10.1029/2006JG000263
- Ballenger, J.A.M., 2010. Palominas Arroyo: a 12.9 ka BP palaeoenvironmental record from the Upper San Pedro River, southeastern Arizona, U.S.A. Unpublished PhD Thesis, The University of Arizona, Tucson.
- Bryant, J.D. and Froelich, P.N., 1995. A model of oxygen-isotope fractionation in body-water of large mammals. *Geochimica et Cosmochimica Acta*, 59(21): 4523-4537.
- Bryant, J.D., Koch, P., Froelich, P.N., Showers, W.J. and Genna, B.J., 1996. Oxygen isotope partitioning between phosphate and carbonate in mammalian apatite. *Geochimica et Cosmochimica Acta*, 60(24): 5145-5148.
- Cerling, T.E. and Harris, J.M., 1999. Carbon isotope fractionation between diet and bioapatite in ungulate mammals and implications for ecological and paleoecological studies. *Oecologia*, 120(3): 347-363.
- Cerling, T.E., Harris, J.M., MacFadden, B.J., Leakey, M.G., Quade, J., Eisenmann, V. and Ehleringer, J.R., 1997. Global vegetation change through the Miocene/Pliocene boundary. *Nature*, 389(6647): 153-158.
- Cerling, T.E., Wittemyer, G., Ehleringer, J.R., Remien, C.H. and Douglas-Hamilton, I., 2009. History of Animals using Isotope Records (HAIR): A 6-year dietary history of one family of African elephants. *Proceedings of the National Academy of Sciences of the United States of America*, 106(20): 8093-8100.
- Codron, J., Codron, D., Lee-Thorp, J., Sponheimer, M., Kirkman, K., Duffy, K. and Sealy, J., 2011. Landscape-scale feeding patterns of African elephant inferred from carbon isotope analysis of feces. *Oecologia*, 165(1): 89-99.
- Codron, J., Lee-Thorp, J.A., Sponheimer, M., Codron, D., Grant, R.C. and de Ruiter, D.J., 2006. Elephant (*Loxodonta africana*) diets in Kruger National Park, South Africa: spatial and landscape differences. *Journal of Mammalogy*, 87(1): 27-34.
- Connin, S.L., Betancourt, J. and Quade, J., 1998. Late Pleistocene C₄ plant dominance and summer rainfall in the southwestern United States from isotopic study of herbivore teeth. *Quaternary Research*, 50(2): 179-193.
- Dansgaard, W., 1964. Stable isotopes in precipitation. *Tellus*, 16: 436-468.

- De Ridder, F., Pintelon, R., Schoukens, J., Gillikin, D.P., André, L., Baeyens, W., de Brauwere, A. and Dehairs, F., 2004. Decoding nonlinear growth rates in biogenic environmental archives. *Geochemistry, Geophysics, Geosystems*, 5(12): 1-16.
- Ehleringer, J.R., 1978. Implications of quantum yield differences on distributions of C₃ and C₄ grasses. *Oecologia*, 31(3): 255-267.
- Ehleringer, J.R., Cerling, T.E. and Helliker, B.R., 1997. C₄ photosynthesis, atmospheric CO₂, and climate. *Oecologia*, 112(3): 285-299.
- Ehleringer, J.R. and Monson, R.K., 1993. Evolutionary and ecological aspects of photosynthetic pathway variation *Annual Review of Ecology and Systematics*, 24: 411-439.
- Epstein, H.E., Lauenroth, W.K., Burke, I.C. and Coffin, D.P., 1997. Productivity patterns of C₃ and C₄ functional types in the US Great Plains. *Ecology*, 78(3): 722-731.
- Farquhar, G.D., Ehleringer, J.R. and Hubick, K.T., 1989. Carbon isotope discrimination and photosynthesis. *Annual Review of Plant Physiology and Plant Molecular Biology*, 40: 503-537.
- Gaugris, J.Y. and van Rooyen, M.W., 2010. Effects of water dependence on the utilization pattern of woody vegetation by elephants in the Tembe Elephant Park, Maputaland, South Africa. *African Journal of Ecology*, 48(1): 126-134.
- Guy, R.D., Reid, D.M. and Krouse, H.R., 1980. Shifts in carbon isotope ratios of two C₃ halophytes under natural and artificial conditions. *Oecologia*, 44(2): 241-247.
- Haury, E.W., 1960. Association of fossil fauna and artifacts of the sulphur spring stage, Cochise culture. *American Antiquity*, 25: 609-610.
- Haynes, C.V., 1991a. Geoarchaeological and paleohydrological evidence for a Clovis-age drought in North America and its bearing on extinction. *Quaternary Research*, 35: 438-450.
- Haynes, C.V., 2005. Clovis, pre-Clovis, climate change, and extinction. In: R. Bonnicksen, B.T. Lepper, D. Stanford and M.R. Waters (Editors), *Paleoamerican Origins: Beyond Clovis*. Center for the Study of the First Americans, College Station, Texas, pp. 113-132.
- Haynes, C.V., 2006. The Rancholabrean Termination: Sudden extinction in the San Pedro Valley, Arizona, 11,000 BP. In: J.E. Morrow and C. Gnecco (Editors), *Paleoindian Archaeology: A Hemispheric Perspective*. University Press of Florida, Gainesville, pp. 139-163.
- Haynes, C.V., 2008. Younger Dryas "black mats" and the Rancholabrean termination in North America. *Proceedings of the National Academy of Sciences of the United States of America*, 105(18): 6520-6525.
- Haynes, C.V. and Huckell, B.B. (Editors), 2007. *Murray Springs: A Clovis site with multiple activity areas in the San Pedro Valley, Arizona*. Anthropological papers of the University of Arizona, No. 71. The University of Arizona Press, Tucson, 308 pp.
- Haynes, G., 1991b. *Mammoths, mastodons, and elephants: biology, behavior, and the fossil record*. Cambridge University Press, Cambridge New York, 413 pp.
- Haynes, G., 2002a. The catastrophic extinction of North American mammoths and mastodons. *World Archaeology*, 33(3): 391-416.
- Haynes, G., 2002b. *The early settlement of North America: the Clovis era*. Cambridge University Press, Cambridge, 345 pp.

- Higgins, P. and MacFadden, B.J., 2004. "Amount Effect" recorded in oxygen isotopes of Late Glacial horse (*Equus*) and bison (*Bison*) teeth from the Sonoran and Chihuahuan deserts, southwestern United States. *Palaeogeography Palaeoclimatology Palaeoecology*, 206(3-4): 337-353.
- Higgins, P. and MacFadden, B.J., 2009. Seasonal and geographic climate variabilities during the Last Glacial Maximum in North America: Applying isotopic analysis and macrophysical climate models. *Palaeogeography, Palaeoclimatology, Palaeoecology*, 283(1-2): 15-27.
- Hillson, S., 1996. *Dental Anthropology*. Cambridge University Press, Cambridge, 373 pp.
- Holmgren, C.A., Betancourt, J.L. and Rylander, K.A., 2006. A 36,000-yr vegetation history from the Peloncillo Mountains, southeastern Arizona, USA. *Palaeogeography Palaeoclimatology Palaeoecology*, 240(3-4): 405-422.
- Holmgren, C.A., Norris, J. and Betancourt, J.L., 2007. Inferences about winter temperatures and summer rains from the late Quaternary record of C₄ perennial grasses and C₃ desert shrubs in the northern Chihuahuan Desert. *Journal of Quaternary Science*, 22(2): 141-161.
- Hoppe, K.A., 2004. Late Pleistocene mammoth herd structure, migration patterns, and Clovis hunting strategies inferred from isotopic analyses of multiple death assemblages. *Paleobiology*, 30(1): 129-145.
- Iacumin, P., Bocherens, H., Mariotti, A. and Longinelli, A., 1996. Oxygen isotope analyses of co-existing carbonate and phosphate in biogenic apatite: a way to monitor diagenetic alteration of bone phosphate? *Earth and Planetary Science Letters*, 142: 1-6.
- IAEA/WMO, 2010. Global Network of Isotopes in Precipitation. The GNIP Database. Accessible at: <http://www.iaea.org/water>.
- Koch, P.L., Diffenbaugh, N.S. and Hoppe, K.A., 2004. The effects of late Quaternary climate and pCO₂ change on C₄ plant abundance in the south-central United States. *Palaeogeography Palaeoclimatology Palaeoecology*, 207(3-4): 331-357.
- Koch, P.L., Hoppe, K.A. and Webb, S.D., 1998. The isotopic ecology of late Pleistocene mammals in North America - Part 1. Florida. *Chemical Geology*, 152(1-2): 119-138.
- Koch, P.L., Tuross, N. and Fogel, M.L., 1997. The effects of sample treatment and diagenesis on the isotopic integrity of carbonate in biogenic hydroxylapatite. *Journal of Archaeological Science*, 24(5): 417-429.
- Loarie, S.R., van Aarde, R.J. and Pimm, S.L., 2009. Elephant seasonal vegetation preferences across dry and wet savannas. *Biological Conservation*, 142(12): 3099-3107.
- Maglio, 1973. Origin and evolution of the Elephantidae. *Transactions of the American Philosophical Society, New Series*, 63(3): 1-149.
- Marino, B.D. and McElroy, M.B., 1991. Isotopic composition of atmospheric CO₂ inferred from carbon in C₄ plant cellulose. *Nature*, 349: 127-131.
- Mead, J.I., Agenbroad, L.D., Davis, O.K. and Martin, P.S., 1986. Dung of *Mammuthus* in the arid southwest, North America. *Quaternary Research*, 25(1): 121-127.
- Mehring, P.J. and Haynes, C.V., 1965. The pollen evidence for the environment of early man and extinct mammals at the Lehner Mammoth Site, southeastern Arizona. *American Antiquity*, 31(1): 17-23.

- Metcalfe, J.Z., Longstaffe, F.J. and White, C.D., 2009. Method-dependent variations in stable isotope results for structural carbonate in bone bioapatite. *Journal of Archaeological Science*, 36(1): 110-121.
- Metcalfe, J.Z., Longstaffe, F.J. and Zazula, G.D., 2010. Nursing, weaning, and tooth development in woolly mammoths from Old Crow, Yukon, Canada: Implications for Pleistocene extinctions. *Palaeogeography Palaeoclimatology Palaeoecology*, 298: 257-270.
- Murphy, B.P. and Bowman, D., 2009. The carbon and nitrogen isotope composition of Australian grasses in relation to climate. *Functional Ecology*, 23(6): 1040-1049.
- O'Leary, M., 1988. Carbon isotopes in photosynthesis. *Bioscience*, 38: 328-336.
- Owen-Smith, R.N., 1988. Megaherbivores: the influence of very large body size on ecology. *Cambridge studies in ecology*. Cambridge University Press, Cambridge, 369 pp.
- Paruelo, J.M. and Lauenroth, W.K., 1996. Relative abundance of plant functional types in grasslands and shrublands of North America. *Ecological Applications*, 6(4): 1212-1224.
- Passey, B.H., Cerling, T.E., Schuster, G.T., Robinson, T.F., Roeder, B.L. and Krueger, S.K., 2005. Inverse methods for estimating primary input signals from time-averaged isotope profiles. *Geochimica et Cosmochimica Acta*, 69(16): 4101-4116.
- Pigati, J.S., Bright, J.E., Shanahan, T.M. and Mahan, S.A., 2009. Late Pleistocene paleohydrology near the boundary of the Sonoran and Chihuahuan Deserts, southeastern Arizona, USA. *Quaternary Science Reviews*, 28(3-4): 286-300.
- Rozanski, K., Araguas-Araguas, L. and Gonfiantini, R., 1993. Isotopic patterns in modern global precipitation. In: P.K. Swart, J. McKenzie, K.C. Lohmann and S. Savin (Editors), *Climate Change in Continental Isotope Records*. AGU Geophysical Monograph. American Geophysical Union, Washington, DC, pp. 1-36.
- Sage, R.F., 2004. The evolution of C₄ photosynthesis. *New Phytologist*, 161(2): 341-370.
- Saunders, J.J., 1970. The distribution and taxonomy of *Mammuthus* in Arizona, The University of Arizona, Tucson.
- Saunders, J.J., 1983. Late Pleistocene vertebrates of the San Pedro Valley, Arizona, Manuscript on file, Arizona State Museum Archives. University of Arizona, Tucson, pp. 79.
- Shoshani, J., 1998. Understanding proboscidean evolution: a formidable task. *Trends in Ecology and Evolution*, 13(12): 480-487.
- Smith, B.N. and Epstein, S., 1971. Two categories of ¹³C/¹²C ratios for higher plants. *Plant Physiology*, 47: 380-384.
- Smith, C.E., 1998. Cellular and chemical events during enamel maturation. *Critical Reviews in Oral Biology & Medicine*, 9(2): 128-161.
- Suga, S., 1982. Progressive mineralization pattern of developing enamel during the maturation stage. *Journal of Dental Research*: 1532-1542.
- Suga, S., 1989. Enamel hypomineralization viewed from the pattern of progressive mineralization of human and monkey developing enamel. *Advances in Dental Research*, 3(2): 188-198.
- Sukumar, R., 1989. The Asian elephant: ecology and management. *Cambridge studies in applied ecology and resource management*. Cambridge University Press, Cambridge, 251 pp.

- Surovell, T.A. and Waguespack, N.M., 2008. How many elephant kills are 14? Clovis mammoth and mastodon kills in context. *Quaternary International*, 191: 82-97.
- Swap, R.J., Aranibar, J.N., Dowty, P.R., Gilhooly, W.P. and Macko, S.A., 2004. Natural abundance of ^{13}C and ^{15}N in C_3 and C_4 vegetation of southern Africa: patterns and implications. *Global Change Biology*, 10(3): 350-358.
- Tafforeau, P., Bentaleb, I., Jaeger, J.J. and Martin, C., 2007. Nature of laminations and mineralization in rhinoceros enamel using histology and X-ray synchrotron microtomography: Potential implications for palaeoenvironmental isotopic studies. *Palaeogeography Palaeoclimatology Palaeoecology*, 246(2-4): 206-227.
- Taylor, R.E., Haynes, C.V. and Stuiver, M., 1996. Clovis and Folsom age estimates: Stratigraphic context and radiocarbon calibration. *Antiquity*, 70(269): 515-525.
- Teeri, J.A. and Stowe, L.G., 1976. Climatic patterns and distribution of C_4 grasses in North America. *Oecologia*, 23(1): 1-12.
- Thompson, R.S., Whitlock, C., Bartlein, P.J., Harrison, S.P. and Spaulding, W.G., 1993. Climatic changes in the Western United States since 18,000 yr B.P. In: H.E. Wright (Editor), *Global climates since the Last Glacial Maximum*. University of Minnesota Press, Minneapolis, pp. 468-513.
- van de Water, P.K., Leavitt, S.W. and Betancourt, J.L., 2002. Leaf $\delta^{13}\text{C}$ variability with elevation, slope aspect, and precipitation in the southwest United States. *Oecologia*, 132(3): 332-343.
- van Geel, B., Aptroot, A., Baittinger, C., Birks, H.H., Bull, I.D., Cross, H.B., Evershed, R.P., Gravendeel, B., Kompanje, E.J.O., Kuperus, P., Mol, D., Nierop, K.G.J., Pals, J.P., Tikhonov, A.N., van Reenen, G. and van Tienderen, P.H., 2008. The ecological implications of a Yakutian mammoth's last meal. *Quaternary Research*, 69(3): 361-376.
- Wagner, J.D.M., Cole, J.E., Beck, J.W., Patchett, P.J., Henderson, G.M. and Barnett, H.R., 2010. Moisture variability in the southwestern United States linked to abrupt glacial climate change. *Nature Geoscience*, 3(2): 110-113.
- Wahi, A.K., Hogan, J.F., Ekwurzel, B., Baillie, M.N. and Eastoe, C.J., 2008. Geochemical quantification of semiarid mountain recharge. *Ground Water*, 46(3): 414-425.
- Waters, M.R. and Stafford, T.W., 2007. Redefining the age of Clovis: Implications for the peopling of the Americas. *Science*, 315(5815): 1122-1126.
- Wright, W.E., Long, A., Comrie, A.C., Leavitt, S.W., Cavazos, T. and Eastoe, C., 2001. Monsoonal moisture sources revealed using temperature, precipitation, and precipitation stable isotope timeseries. *Geophysical Research Letters*, 28(5): 787-790.
- Yang, L.M., Wylie, B.K., Tieszen, L.L. and Reed, B.C., 1998. An analysis of relationships among climate forcing and time-integrated NDVI of grasslands over the US northern and central Great Plains. *Remote Sensing of Environment*, 65(1): 25-37.
- Zazzo, A., Balasse, M., Patterson, W.P. and Patterson, P., 2005. High-resolution $\delta^{13}\text{C}$ intratooth profiles in bovine enamel: Implications for mineralization pattern and isotopic attenuation. *Geochimica et Cosmochimica Acta*, 69(14): 3631-3642.

Chapter 6

Isotopic paleoecology of mammoths and mastodons in the Great Lakes region (southern Ontario and western New York)

6.1 Introduction

Mammoths and mastodons were once widespread in North America, but became extinct throughout most of the continent at the end of the Pleistocene (ca. 11,000-10,000 BP) (Agenbroad, 2005; Waters and Stafford, 2007). The cause of Late Pleistocene megafaunal extinctions has been the subject of much controversy (Barnosky et al., 2004; Koch and Barnosky, 2006), and proboscideans have figured strongly in the debate (e.g., Haynes, 2002). However, relatively little direct evidence exists for patterns of mammoth and mastodon behaviour (e.g., diet, migration) in North America, and little is known about differences within and among regions.

Mammoth and mastodon skeletal remains have sometimes been used as paleoclimatic indicators. The presence of woolly mammoths has been interpreted to indicate steppe-tundra environments (e.g., Harington and Ashworth, 1986; Nielsen et al., 1988), and that of mastodons, open spruce forest environments (Zazula et al., 2006). These inferences make sense in terms of dental and other morphological adaptations of mammoths to grazing and mastodons to browsing (Harington and Ashworth, 1986; Haynes, 1991), and are supported by studies of tooth enamel isotopic compositions (Koch et al., 1998; MacFadden and Cerling, 1996), enamel microwear (Green et al., 2005), dung and gut contents (Newsom and Mihlbachler, 2006; Ukraintseva et al., 1996), and associated pollen and plant macrofossil assemblages (Dreimanis, 1967, 1968; Guthrie, 2001; Harington et al., 1993). However, the universal validity of these assumptions has been challenged. Saunders et al. (2010) present evidence that at least one woolly mammoth from Illinois inhabited a wet, forested environment. They suggest that woolly mammoths moved into Illinois immediately after deglaciation, but persisted in the region after the tundra shifted northwards. Cummings and Albert (2007) demonstrate that Columbian mammoths in Colorado utilized several environmental zones, based on the presence of grasses, conifers and possibly oak phytoliths in their tooth calculus. Gobetz and Bozarth (2001) showed that mastodon tooth calculus contained abundant grass

phytoliths, even though mastodons are believed to have been primarily browsers. Studies of mammoth and mastodon dung and digesta support the contention that both taxa were capable of significant dietary flexibility (e.g., Lepper et al., 1991; Mead et al., 1986; Newsom and Mithlacher, 2006; van Geel et al., 2008), as are their modern elephant relatives (Owen-Smith, 1988; Sukumar, 1989, 2003). The degree to which mammoth and mastodon environmental niches overlapped is important, since competition for resources would have increased their susceptibility to regional extinction during Late Pleistocene environmental changes (Saunders et al., 2010).

Here, we investigate environmental niche partitioning of mammoths and mastodons in the Great Lakes region (southern Ontario and western New York state) using the carbon-, nitrogen-, and oxygen-isotope compositions of bones and teeth. The Great Lakes region contains an abundance of mammoth and mastodon remains dating to the period between the retreat of glacial ice (ca. 15,500 BP for most of southwestern Ontario) and the beginning of the Holocene (ca. 10,000 BP) (Lewis et al., 1994). Thus, these proboscideans were among the last on the North American continent, and can provide important insights into the Late Pleistocene extinctions. As described in greater detail in Chapters 3-5 and elsewhere (e.g., Koch, 1998), stable isotope compositions of skeletal remains can contain information about an animal's diet, physiological status, and environment. In this chapter, we explore similarities and differences in the isotopic compositions of mammoths and mastodons from the Great Lakes region, in relation to their diet, drinking water, metabolism, and seasonal behaviour. In addition, we present new radiocarbon dates for Ontario mastodons, and explore the use of stable isotope compositions to identify non-local individuals in museum collections.

6.2 Methods

Mammoth and mastodon skeletal remains from Ontario and New York were obtained from university and museum collections (Table 6.1, Figure 6.1). Adult teeth and bones were selected for analysis. Sampling, collagen extraction, bioapatite carbonate pretreatment, microdrilling, and analytical instrumentation have been described elsewhere (Chapters 3-5). Stable isotope results are presented in standard delta (δ) notation, in units of per mil (‰), relative to VSMOW (oxygen) and VPDB (carbon), and AIR (nitrogen)

(Coplen, 1994; Coplen et al., 2006; Mariotti, 1983). Precision and accuracy for δ -values, %C, %N, and C/N ratios are as described in Chapters 3-5. Diet $\delta^{13}\text{C}$ values are calculated assuming an enrichment of 5‰ between collagen and diet (Ambrose and Norr, 1993; Koch, 1998), and an enamel-diet fractionation factor (α) of 1.0145 (Cerling and Harris, 1999) (see also Chapter 5). Drinking water $\delta^{18}\text{O}$ values are calculated as described in Chapter 5 (Ayliffe et al., 1992; Bryant et al., 1996; Iacumin et al., 1996). Radiocarbon dates were obtained for three specimens at the University of Arizona Accelerator Mass Spectrometry Laboratory, after collagen extraction, combustion, and graphitization (see Chapter 3). All dates described in this paper are reported as conventional radiocarbon years before AD 1950, in the form “17,000 \pm 100 BP” (mean \pm 1 SD). For one specimen (ON5), a “thin” section was prepared, incremental growth features were measured, and the crown extension rate was estimated as described in Chapter 4. To directly compare the serially-sampled isotopic results for different mastodon individuals (which have different growth rates), the distance axis was converted to time using a simple anchor-point method, as described in Chapter 5.

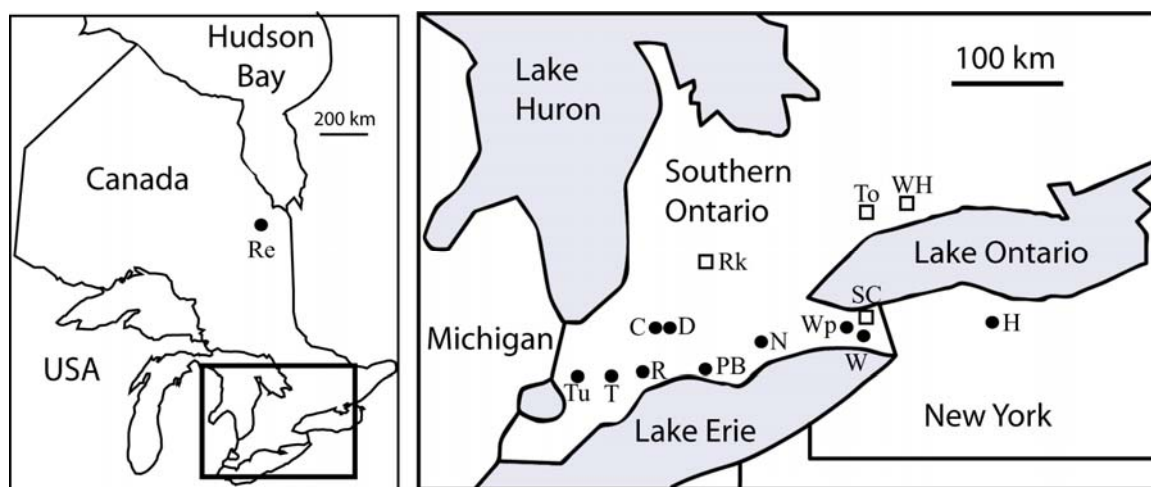


Figure 6.1 The discovery locations of mastodon (closed circle) and mammoth (open square) specimens analyzed in the present study. Inset box shows area enlarged in second map. Re = Renison, Tu = Tupperville, T = Thamesville, R = Rodney, C = Caradoc, D = Delaware, PB = Port Burwell, N = Norfolk, Wp = Wellandport, W = Welland, SC = Saint Catharine's, H = Hiscock, Rk = Rostock, To = Toronto, WH = West Hill.

Table 6.1 Sample information, including radiocarbon dates.

LSIS #	Source	Museum or Field #	Taxon	Site	Tissue used for Collagen	Tooth	Radiocarbon Date or pollen zone	Radiocarbon Lab #	Reference/Comments
ON2	UWO		<i>Mammut americanum</i>	Delaware	tusk				
ON3	UWO		<i>Mammut americanum</i>	Norfolk	dentin (crown)	M5/M6	11,820 ± 120	AA84989	This study (dentin)
ON4	UWO		<i>Mammut americanum</i>	Port Burwell	dentin (crown)	M4/M5			
ON5	UWO		<i>Mammut americanum</i>	unknown	dentin (crown)	M6			
ON6	UWO		<i>Mammuthus primigenius</i>	unknown	dentin (crown)	M6			
ON7	UWO		<i>Mammut americanum</i>	Caradoc	bone & dentin (crown)	M6	11,120 ± 110	AA84980	This study (bone)
ON8	MOA		<i>Mammuthus</i>	unknown	dentin (crown)				
ON9	MOA		<i>Mammut americanum</i>	Delaware?	bone & dentin (crown)	M6	12,360 ± 120	AA84998	This study (dentin)
ON10	UWO		<i>Mammut americanum</i>	Thamesville	bone (2 ribs)		11,380 ± 170 *	GSC-611	Lowdon and Blake, 1968
ON10X	ROM	52,589	<i>Mammut americanum</i>	Thamesville	dentin (root)	M5?	11,380 ± 170 *	GSC-611	Lowdon and Blake, 1968
ON12	ROM	29,753	<i>Mammuthus primigenius</i>	Rostock	tusk		10,790 ± 150		McAndrews and Jackson, 1988, Pilny et al., 1987
ON13	ROM	4184	<i>Mammut americanum</i>	Wellandport	bone (frags)	M5?	zone 1 (spruce)		McAndrews and Jackson, 1988
ON14	ROM	1792c	<i>Mammut americanum</i>	Rodney	dentin (root)	LLM6	11,400 ± 450, 12,000 ± 500		McAndrews and Jackson, 1988
ON15	ROM	03232	<i>Mammut americanum</i>	Tupperville	bone	ULM5			
ON16	ROM	41948	<i>Mammut americanum</i>	Renison ^	dentin (root)	M6	13,610 ± 170		ROM database
ON17	ROM	01195	<i>Mammuthus</i>	Toronto	dentin (root)				
ON18	ROM	1973	<i>Mammuthus</i>	West Hill	dentin (root)	URM6	post-12,800, pre-11,100 ***		post-glacial, Iroquois beach
ON19	ROM	3118	<i>Mammuthus</i>	St. Catherine's	cementum	ULM5/M6			
ON20	ROM	65?	<i>Mammut americanum</i>	Welland?	tusk		zone 1 (spruce)		McAndrews and Jackson, 1988
NY1	BMS	J2NE-85	<i>Mammut americanum</i>	Hiscock	bone (rib)		10,810 to 10,350 **		Laub, 2003:37
NY2	BMS	I2SE(S1/2)-61	<i>Mammut americanum</i>	Hiscock	bone (rib)		10,810 to 10,350 **		Laub, 2003:37
NY3	BMS	TailingI	<i>Mammut americanum</i>	Hiscock	dentin (crown)	URM5	10,810 to 10,350 **		Laub, 2003:37
NY4	BMS	TailingI	<i>Mammut americanum</i>	Hiscock	dentin (crown)	ULM6	10,810 to 10,350 **		Laub, 2003:37
NY6	BMS	G7SW-156	<i>Mammut americanum</i>	Hiscock	bone (R scapula)		10,810 to 10,350 **		Laub, 2003:37
NY7	BMS	I3NW-107	<i>Mammut americanum</i>	Hiscock	bone (R scapula)		10,810 to 10,350 **		Laub, 2003:37
NY8	BMS	F5NW-27	<i>Mammut americanum</i>	Hiscock	bone (R scapula)		10,810 to 10,350 **		Laub, 2003:37
NY9	BMS	I4SE-46	<i>Mammut americanum</i>	Hiscock	bone (R scapula)		10,810 to 10,350 **		Laub, 2003:37
NY10	BMS	I2NE-173	<i>Mammut americanum</i>	Hiscock	bone (R scapula)		10,810 to 10,350 **		Laub, 2003:37
NY11	BMS	G6SW-118	<i>Mammut americanum</i>	Hiscock	bone (L scapula)		10,810 to 10,350 **		Laub, 2003:37
NY12	BMS	G6SW-125	<i>Mammut americanum</i>	Hiscock	bone (L scapula)		10,810 to 10,350 **		Laub, 2003:37

LSIS #: Sample ID used for Laboratory for Stable Isotope Science analyses, and referred to in this study

Source: UWO = The University of Western Ontario, MOA = Museum of Ontario Archaeology, ROM = Royal Ontario Museum, BMS = Buffalo Museum of Science

Tooth LL = lower left, UL = upper left, UR = upper right

Radiocarbon dates in **bold** were obtained as part of the present study.

* Not completely certain that the radiocarbon date was for this individual

** Range for radiocarbon dated Hiscock mastodon bones found in the same stratigraphic layer as specimens listed here (Laub 2003:37 and personal communication, March 2009).

^ Site in far northern Ontario (Figure 6.1)

*** dates for Lake Iroquois based on Lewis et al. (1994)

Table 6.2 The isotopic compositions of collagen (various tissues) and structural carbonate in bioapatite (enamel) for Great Lakes mammoths and mastodons. Diet and drinking water isotopic compositions were calculated as described in the text and Chapter 5.

Taxon	LSIS #	Tissue	Collagen					Structural carbonate				Diet $\delta^{13}\text{C}$, from:		Water			
			C (%)	$\delta^{13}\text{C}$ (‰)	N (%)	$\delta^{15}\text{N}$ (‰)	C/N (Atomic)	Col Yield (%)	Tissue	$\delta^{13}\text{C}$ (‰)	$\delta^{18}\text{O}$ (‰)	CO_3 (%)	$\Delta^{13}\text{C}_{\text{sc-col}}$ (‰)	Col (‰)	SC (‰)	$\delta^{18}\text{O}$ (‰)	
<i>Mammut</i>																	
	ON3	Dentin (crown)	43.7	-20.7	16.3	4.6	3.1	13.3	Enamel	-10.9	23.3	3.5	9.8	-25.7	-25.1	-9.3	
	ON4	Dentin (crown)	44.1	-19.5	16.5	3.1	3.1	13.8	Enamel	-11.3	22.1	8.1	8.2	-24.5	-25.4	-10.6	
	ON7	Dentin (crown)	46.2	-19.9	17.4	3.6	3.1	17.7	Enamel	-11.2	20.6	3.9	8.7	-24.9	-25.3	-12.2	
	ON9	Dentin (crown)	41.9	-20.1	15.7	2.2	3.1	14.7	Enamel	-10.1	23.1	4.1	10.0	-25.1	-24.2	-9.5	
	NY3	Dentin (crown)	36.1	-21.0	13.5	3.5	3.1	9.8	Enamel	-11.8	22.1	3.9	9.2	-26.0	-25.9	-10.6	
	NY4	Dentin (crown)	37.3	-20.6	13.8	2.4	3.1	7.0	*	Enamel	-11.3	22.7	4.3	9.3	-25.6	-25.4	-10.0
	ON10X	Dentin (root)	46.6	-19.8	17.5	3.0	3.1	15.7	Enamel ^	-11.0	21.9	3.1	8.8	-24.8	-25.2	-10.8	
	ON14	Dentin (root)	45.1	-20.2	16.4	3.1	3.2	11	Enamel ^	-10.5	22.2	3.3	9.6	-25.2	-24.7	-10.5	
	ON13	see below							Enamel ^	-10.3	21.3	3.4	9.7		-24.5	-11.4	
	ON15	see below							Enamel ^	-10.7	20.5	3.2	10.0		-24.8	-12.2	
	ON2	Dentin (tusk)	20.7	-20.8	7.2	1.5	3.4	0.4						-25.8			
	ON10X	Dentin (tusk)	43.9	-20.5	16.3	2.6	3.1	3.5						-25.5			
	ON20	Dentin (tusk)	44.9	-20.7	16.3	2.2	3.2	3.8						-25.7			
	ON16**	Dentin (root)	46.2	-20.4	17.0	5.1	3.2	15.8	Enamel ^	-11.3	17.5	2.9	9.1	-25.4	-25.4	-15.4	
	ON5**	Dentin (crown)	37.0	-20.4	13.5	1.9	3.2	7.2	*	Enamel	-10.5	21.6	3.5	9.9	-25.4	-24.7	-11.1
		Mean (tooth)	41.0	-20.3	15.2	2.9	3.2	10.1		-10.9	22.0	4.1	9.3	-25.3	-25.1	-10.7	
		SD (tooth)	7.1	0.4	2.8	1.0	0.1	5.5		0.5	0.9	1.5	0.6	0.5	0.5	1.0	
		n	11														
	ON7	Bone	43.3	-20.1	16.2	2.6	3.1	13.2						-25.1			
	ON9	Bone	19.5	-20.9	6.7	2.0	3.4	1.5						-25.9			
	ON10-1	Bone	45.1	-20.0	16.9	2.0	3.1	16.1						-25.0			
	ON10-2	Bone	44.6	-20.0	16.4	2.0	3.2	10.9						-25.0			
	ON13	Bone	46.4	-20.0	17.3	1.8	3.1	7.8	*					-25.0			
	ON15	Bone	45.2	-20.6	15.9	2.0	3.3	4.6						-25.6			
	NY1	Bone	44.0	-21.2	16.6	2.3	3.1	14.6						-26.2			
	NY2	Bone	42.3	-21.1	16.1	2.5	3.1	7.2						-26.1			
	NY6	Bone	41.2	-21.3	15.4	2.5	3.1	8.7	*					-26.3			
	NY7	Bone	42.6	-21.0	16.0	2.7	3.1	6.6	*					-26.0			
	NY8	Bone	41.5	-21.5	15.7	2.3	3.1	15.3	*					-26.5			
	NY9	Bone	42.5	-21.4	16.0	2.3	3.1	13.2	*					-26.4			
	NY10	Bone	43.7	-21.4	16.5	2.4	3.1	9.9	*					-26.4			
	NY11	Bone	43.5	-21.6	16.3	2.5	3.1	10.3	*					-26.6			
	NY12	Bone	42.5	-20.8	16.0	2.7	3.1	14.1	*					-25.8			
		Mean (bone)	41.9	-20.9	15.6	2.3	3.1	10.3						-25.9			
		SD (bone)	6.4	0.6	2.5	0.3	0.1	4.2						0.6			
		n	15														
		Mean (all tissues)	41.5	-20.6	15.4	2.6	3.1	10.2		-10.9	22.0	4.1	9.3	-25.6	-25.1	-10.7	
		SD (all tissues)	6.7	0.6	2.7	0.6	0.1	4.8		0.5	0.9	1.5	0.6	0.6	0.5	1.0	
		n	26														

Table 6.2 cont.

Taxon	LSIS #	Tissue	Collagen					Structural carbonate				Diet $\delta^{13}\text{C}$, from:		Water		
			C (%)	$\delta^{13}\text{C}$ (‰)	N (%)	$\delta^{15}\text{N}$ (‰)	C/N (Atomic)	Col Yield (%)	Tissue	$\delta^{13}\text{C}$ (‰)	$\delta^{18}\text{O}$ (‰)	CO_3 (%)	$\Delta^{13}\text{C}_{\text{sc-col}}$ (‰)	Col (‰)	SC (‰)	$\delta^{18}\text{O}$ (‰)
<i>Mammuthus</i>																
	ON17	Dentin (root)	46.6	-20.5	17.2	8.0	3.2	17.8	Enamel ^	-10.9	19.3	4.2	9.6	-25.5	-25.0	-13.5
	ON18	Dentin (root)	45.8	-21.2	16.9	8.5	3.2	9.3	Enamel ^	-11.3	19.4	4.3	9.9	-26.2	-25.5	-13.4
	ON19	Cementum	45.4	-20.7	16.6	7.3	3.2	5.2	Enamel ^	-11.0	19.6	4.8	9.7	-25.7	-25.1	-13.2
	ON12**	Dentin (tusk)	46.6	-19.8	17.0	7.5	3.2	21.2	Enamel ^	-7.7	22.6	4.6	12.0	-24.8	-21.9	-10.0
	ON6**	<i>Cementum</i>	41.8	-20.7	15.2	7.0	3.2	8.6						-25.7		
	ON6**	<i>Dentin (crown)</i>	41.5	-20.2	15.3	7.5	3.2	4.0	<i>Enamel</i>	-11.0	11.8	5.1	9.2	-25.2	-25.2	-21.3
	ON8**	<i>Dentin (crown)</i>	40.9	-24.4	15.0	6.3	3.2	13.1	<i>Enamel</i>	-14.4	25.8	3.9	10.0	-29.4	-28.5	-6.8
	Mean (all tissues)		45.9	-20.8	16.9	7.9	3.2			-11.1	19.4	4.4	9.7	-25.8	-25.2	-13.4
	SD (all tissues)		0.6	0.4	0.3	0.6	0.0			0.2	0.2	0.3	0.1	0.4	0.2	0.2
	n		3													
<i>All specimens</i>																
	Mean		42.0	-20.7	15.6	3.6	3.2	10.5		-11.0	21.0	4.1	9.6	-25.7	-25.1	-11.8
	SD		6.1	0.8	2.4	2.1	0.1	5.0		1.2	2.9	1.2	0.8	0.8	1.2	3.1
	Max		46.6	-19.5	17.5	8.5	3.4	21.2		-7.7	25.8	8.1	12.0	-24.5	-21.9	-6.8
	Min		19.5	-24.4	6.7	1.5	3.1	0.4		-14.4	11.8	2.9	8.2	-29.4	-28.5	-21.3
	n		35													

LSIS #: Sample ID used for Laboratory for Stable Isotope Science analyses, and referred to in this study

Col = collagen, SC = structural carbonate

Values in italics are from specimens of unknown provenance

Values in bold are the results of duplicate analyses

* Yield is an underestimate because of variation in extraction protocol (e.g., aliquot taken for other analysis prior to gelatinization)

** Not included in summary statistics for the taxon, but is included in "all specimens" statistics

^ Enamel was not pretreated prior to structural carbonate analysis

6.3 Results and Discussion

6.3.1 Radiocarbon Dating

Table 6.1 lists the new radiocarbon dates for three Ontario mastodons (ON3, ON7, ON9). All three are post-glacial and within the principal period of mastodon occupation of Ontario (i.e., after 12,500 BP) (McAndrews and Jackson, 1988). ON9 dates to a period of glacial retreat ($12,360 \pm 120$ BP), during which Early Lake Algonquin and Lake Iroquois formed in the Huron and Ontario basins, respectively (Lewis et al., 1994). ON3 dates to the end of the same interstadial or to the beginning of the following stadial ($11,820 \pm 120$ BP). ON7 dates to another period of ice retreat ($11,120 \pm 110$ BP), during which regional climatic cooling occurred (based on pollen records) because of the presence of large glacial lakes and increased flow of glacial meltwater (Lewis et al., 1994).

6.3.2 Structural Carbonate Analysis Pretreatment Effects

Pretreatment is generally used for bone and dentin specimens to remove organic contaminants and diagenetic carbonates that could interfere with isotope measurements; however, enamel is much more resistant to diagenetic alteration (Koch et al., 1997). In this study, some enamel samples were pretreated prior to structural carbonate isotopic analysis (see Chapter 5 for methods), and others were not (Table 6.2). There were no significant differences between treated and untreated mastodon samples (different individuals) for $\delta^{13}\text{C}$ and $\delta^{18}\text{O}$ values, or CO_3 contents (independent-samples t-tests; New York and Renison specimens excluded so that all samples were from the same geographic area). Furthermore, pretreatment experiments on mammoth and mastodon enamel from other regions revealed minimal differences between treated and untreated aliquots of the same samples (see Chapters 5, 7). We conclude that for this study, results from treated and untreated enamel specimens are directly comparable.

6.3.3 Diagenesis

Well-preserved collagen has an extraction yield $>1\%$, C/N ratio between 2.9 and 3.6, carbon content of 30 to 43%, and nitrogen content of 11 to 16% (Ambrose, 1990;

DeNiro, 1985; van Klinken, 1999). Great Lakes mammoth and mastodon collagen is very well-preserved according to these measures (collagen yield = $10.5 \pm 5.0\%$ (mean \pm 1 SD), C/N = 3.2 ± 0.1 , %C = $42.0 \pm 6.1\%$, %N = $15.6 \pm 2.4\%$) (Table 6.2). Two specimens have some values that fall outside the “accepted” ranges (Table 6.2), but their inclusion does not affect the following discussion.

Multiple lines of evidence suggest that the Great Lakes enamel specimens are well-preserved. Their carbonate contents ($4.1 \pm 1.2\%$, Table 6.2) are close to those of mature enamel (2.7 to 5.0%) (Hillson, 1996). There is no correlation between carbonate contents and $\delta^{13}\text{C}_{\text{sc}}$ or $\delta^{18}\text{O}_{\text{sc}}$ values (which might occur if significant quantities of diagenetic carbonate contributed to the gas produced during analysis). Powder X-ray diffraction patterns of selected enamel specimens (ON3, ON4) are typical of carbonated hydroxyapatite, with no evidence of secondary mineral contamination. Fourier-Transform Infrared Spectroscopy (FTIR) analysis of one untreated specimen (ON3) showed no evidence of calcite contamination, and the sample had a Crystallinity Index of 3.1, which is close to those of modern suid, bovid, and camelid enamel (3.4 to 4.4) (nomenclature after Laws, 1966) (see Chapter 2 for FTIR methods). Thin section examination of one enamel specimen (ON 5) revealed clearly visible incremental growth features (e.g., Striae of Retzius, cross-striations). Finally, the presence of sinusoidal variations in the δ -values of serially-sampled tooth enamel is typical of seasonal variations, and is unlikely to have been preserved had significant post-mortem isotopic alteration occurred.

6.3.4 Tissue Comparisons

Mastodon molar tooth dentin (root and crown) had significantly higher $\delta^{15}\text{N}$ values than bone or tusk dentin ($F(2,23)=9.6$, $p=0.001$). Mammoth molar tooth dentin also had higher $\delta^{15}\text{N}$ values than tusk dentin or cementum, but sample size was insufficient for statistical comparison (Table 6.2, Figure 6.2). Theoretically, a nursing signal could have made some contribution to the dentin, since tooth formation may be initiated early in life, whereas continuously-growing or remodelling tusk, bone, and cementum can continue to form until the time of death (see Chapter 3 for more detailed discussion). The teeth used in the present study are M5s and M6s, except for one possible M4. According to the tooth formation time estimates made by Metcalfe et al. (2010)

(Chapter 3), mammoth M5s develop between age 13-28 African Elephant Years (AEY), whereas M6s develop between age 26-43 AEY, so nursing cannot be responsible for their elevated $\delta^{15}\text{N}$ values. Tooth formation in mastodons occurs considerably earlier than for mammoths, at least for later-developing teeth. Saunders (1977) estimates that M5s form during “youth” (i.e., 3-10 AEY), and lower M6s form in youth to young adulthood (3-18 AEY); however, no detailed studies of mastodon tooth formation times have been published. Since nursing past 3 years of age is a relatively common occurrence in modern elephants (Lee and Moss, 1986; Owen-Smith, 1988; Sukumar, 2003) and woolly mammoths (Metcalf et al., 2010; Rountrey et al., 2007), milk consumption may have contributed to elevated $\delta^{15}\text{N}$ values in mastodon tooth dentin, especially for M5s. However, different growth rates, routing of amino acids, or age-related changes in metabolism or diet could also potentially impact $\delta^{15}\text{N}$ values. A recent study found that growth rate did not affect bone $\delta^{15}\text{N}$ values (Waters-Rist and Katzenberg, 2010), but evaluation of the latter possibilities must await further research.

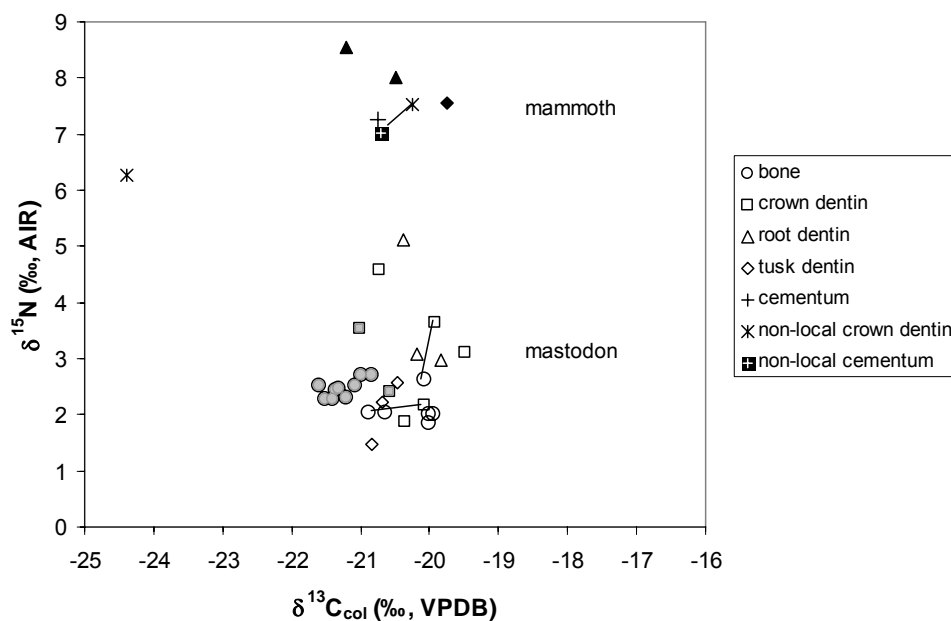


Figure 6.2 Carbon and nitrogen isotope results obtained for collagen from various mammoth and mastodon tissues. Black-filled symbols and non-local individuals are mammoths. Open and grey-filled symbols are mastodons, the former from Ontario and the latter from the Hiscock site (New York). Lines connect tissues from the same individuals.

Table 6.3 Relationships between metabolic, vegetational, and climatic factors and the $\delta^{13}\text{C}$ values of animals living in C_3 -only environments.

Category	Factor	Effect on $\delta^{13}\text{C}$	References
Metabolic	Starvation (fasting)	Variable*	1, 2, 3
	Slowed growth (fasting)	Increase	4
	Pregnancy & Lactation	Variable	3, 5
Vegetational	Canopy cover	Decrease	6
	Plant species	Variable, $<2\text{‰}$	7
	Plant parts: root, bark, wood, fruit	Increase	7, 8, 9
	Plant parts: leaves	Decrease	7, 8, 9
	Plant macronutrients: protein, lipid	Decrease	8, 10
	Plant macronutrients: carbohydrate	Increase	10
	Plant type	Tree $<$ grass $<$ shrub $<$ forb	11
	Plant type: lichen	Increase	12
Environmental	Wet environment/season	Decrease or no change	11, 13, 14, 15
	Soil nutrient increase	Increase	11
	Temperature increase	Increase	11
	High altitude	Increase	11

*Likely depends whether fat stores are metabolized (probable decrease in $\delta^{13}\text{C}$) or muscle is catabolized (probable increase in $\delta^{13}\text{C}$)

References

- 1 McCue and Pollock, 2008
- 2 Polischuk et al., 2001
- 3 Fuller et al., 2004
- 4 Warinner and Tuross, 2010
- 5 Fuller et al., 2006
- 6 van der Merwe and Medina, 1991
- 7 Codron et al., 2005
- 8 Hobbie and Werner, 2004
- 9 Ometto et al., 2006
- 10 Tieszen and Boutton, 1989
- 11 Tieszen, 1991
- 12 Bocherens, 2003
- 13 Stewart et al., 1995
- 14 Murphy and Bowman, 2009
- 15 Yoneyama et al., 2010

There are no differences between mastodon tusk dentin $\delta^{13}\text{C}_{\text{col}}$ values and those of molar tooth dentin or bone. However, the $\delta^{13}\text{C}_{\text{col}}$ values of mastodon bones are slightly lower than those of mastodon molar tooth dentin ($t = 2.6$, $df = 21$, $p = 0.02$). Most bones are from the Hiscock site, whereas most teeth are from Ontario (Figure 6.2). The small difference in $\delta^{13}\text{C}$ values between these regions could be attributed to a variety of different metabolic, vegetational, or climatic factors (Table 6.3), different timing of formation, or tissue-dependent isotopic fractionations.

6.3.5 Non-Local Individuals and Outliers

A mastodon tooth discovered in far northern Ontario (ON16, Renison; Figure 6.1) has a $\delta^{18}\text{O}$ value 4.5‰ lower than the mastodon mean, and 3‰ lower than the next lowest mastodon value (Table 6.2). This specimen was radiocarbon dated to $13,610 \pm 170$ BP, a time when the Laurentide ice sheet should have completely covered northern Ontario. The specimen was likely transported to this location, either by modern humans, glaciers, or northward post-glacial drainage. The specimen's low $\delta^{18}\text{O}$ value suggests that the animal lived at a significantly higher latitude or more continental location, and/or experienced a much cooler climate than the Great Lakes mastodons (Rozanski et al., 1993). Furthermore, its relatively high $\delta^{15}\text{N}$ value suggests that it lived in a drier environment than the other Ontario mastodons in this study (Schwarcz et al., 1999).

One mammoth (ON12, Rostock) was a high outlier for $\delta^{13}\text{C}_{\text{col}}$, $\delta^{13}\text{C}_{\text{sc}}$, and $\delta^{18}\text{O}_{\text{sc}}$ values. This specimen was radiocarbon dated to $10,790 \pm 150$ BP and was associated with the end of spruce pollen zone 1b (McAndrews and Jackson, 1988). The date and pollen zone place the specimen within the Younger Dryas period, relatively late for Ontario mammoths (Lewis and Anderson, 1992; Yu, 2000). In contrast to the other mammoths in this study, which were discovered close to the shorelines of proglacial lakes, this specimen was found further inland, in a more upland location. Its distinctive stable isotope compositions may reflect a different microhabitat. Specifically, less glacial meltwater (which has low $\delta^{18}\text{O}$ values) may have been available in this area, since it was further from the glacial lakes. The specimen's exceptionally high $\Delta^{13}\text{C}_{\text{sc-col}}$ value (12.0‰) further emphasizes its difference from both other mammoths and mastodons.

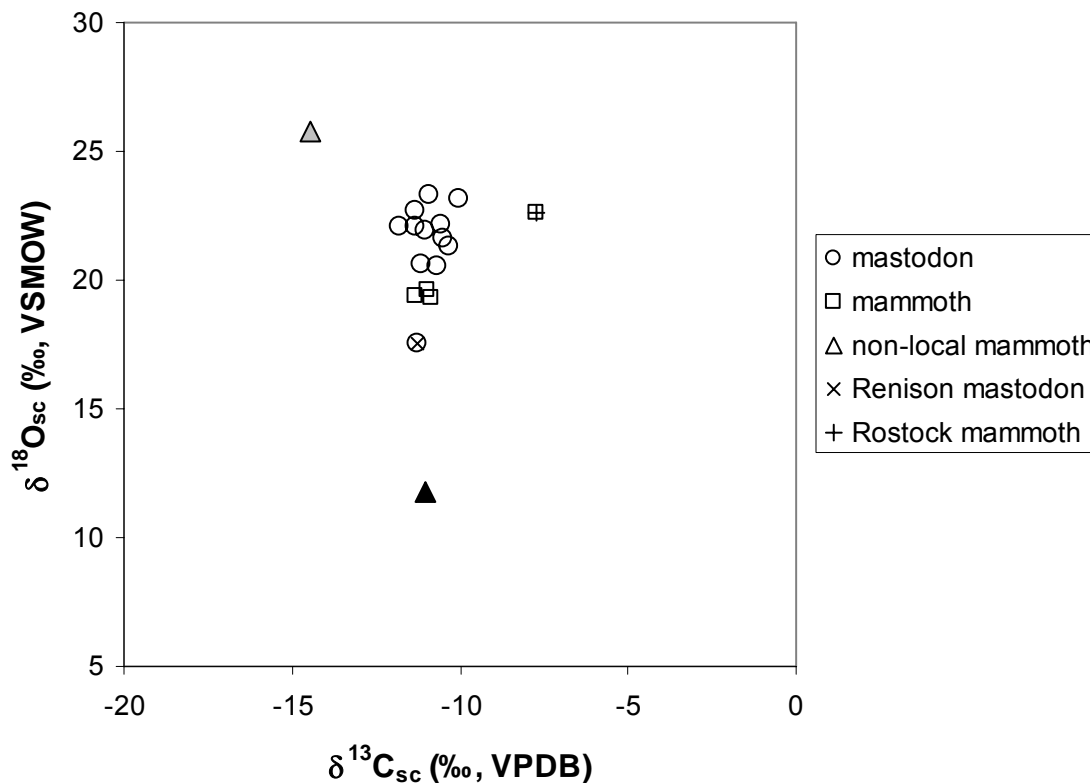


Figure 6.3 Carbon and oxygen isotope results obtained for structural carbonate in enamel bioapatite from mammoths and mastodons. Grey-filled triangle is ON8, black-filled triangle is ON6.

Three specimens (one mastodon, two mammoths) had no contextual information, but were thought to be from Ontario since they were part of small, mostly local collections (Table 6.1). Their stable isotope compositions provide evidence for their locations of origin. The mastodon (ON5) is within the range of southern Ontario mastodons for all isotopic measures (Table 6.2). Therefore, it likely is from southern Ontario. In contrast, one of the mammoths (ON6) is an extremely low outlier for $\delta^{18}\text{O}$ (11.8‰ versus a mean of 19.4‰ for Ontario mammoths), which suggests that it either lived during a much colder time period or is not from Ontario (Table 6.2, Figure 6.3). Its isotopic compositions are completely consistent with an origin in the Yukon (particularly Klondike), which is the most abundant source of mammoth remains in Canada (Chapter

7). We speculate that this specimen was discovered or purchased in Yukon and brought to The University of Western Ontario (UWO) as a comparative specimen several decades ago, after which records of its provenance were lost. The other mammoth (ON8) was an extremely high outlier for $\delta^{18}\text{O}$ (25.8‰), which suggests that it lived in a warmer or lower-latitude region (Table 6.2, Figure 6.3). Its $\delta^{13}\text{C}_{\text{sc}}$ (-14.4‰) and $\delta^{13}\text{C}_{\text{col}}$ (-24.4‰) values are lower than those of Ontario mammoths, though still consistent with a C_3 -dominated environment, and its $\delta^{15}\text{N}$ value (6.3‰) is also relatively low (Table 6.2, Figures 6.2, 6.3). These results further suggest that the specimen is not from Ontario. Since its isotopic compositions do not match those known for proboscideans from the southern Great Lakes region (Michigan, New York), American southwest, Texas, Florida, or Virginia (France et al., 2007; Koch, 1989; Koch et al., 2004; Koch et al., 1998) its location of origin remains unknown.

6.3.6 Isotopic Partitioning between Mammoths and Mastodons

The following discussion of isotopic differences between mammoths and mastodons excludes samples with unknown provenance (ON5, ON6, ON8), the Renison mastodon (ON16), and the Rostock mammoth (ON12) (see above).

6.3.6.1 Oxygen

The $\delta^{18}\text{O}_{\text{sc}}$ values of mammoths are significantly lower than those of mastodons ($t = 4.5$, $df = 11$, $p = 0.001$) (Table 6.2, Figure 6.3). The drinking water $\delta^{18}\text{O}$ values calculated using enamel $\delta^{18}\text{O}$ values ($\delta^{18}\text{O}_{\text{dw}} = -10.7 \pm 1.0\text{‰}$ for mastodons and $-13.4 \pm 0.2\text{‰}$ for mammoths) (Table 6.2) are lower than those of modern precipitation in the region (mean annual $\delta^{18}\text{O}$ values of -9.3 to -6.8‰) (Longstaffe & Ayalon, in preparation), or of modern Lake Ontario, Erie, or Huron surface water (-6.6, -6.7, -7.5‰, respectively) (Macdonald and Longstaffe, 2007), as expected for water from a colder climate and/or with some low- ^{18}O glacial meltwater input.

Why are the $\delta^{18}\text{O}$ values of mammoths and mastodons different? One possible explanation for the higher $\delta^{18}\text{O}$ values in mastodons is that they reflect some ^{18}O -enriched milk consumption. As discussed in Section 6.3.4, mastodon M5s and M6s begin to form at an early age (about 3 AEY), much earlier than mammoth M5s and M6s (13 and 26

AEY, respectively) (Metcalf et al., 2010; Saunders, 1977). Since modern elephants and mammoths can nurse well into youth (Lee and Moss, 1986; Metcalf et al., 2010; Owen-Smith, 1988; Rountrey et al., 2007; Sukumar, 2003), the possibility that milk contributed to enamel $\delta^{18}\text{O}$ values in mastodon enamel cannot be completely discounted. However, all of the mastodon teeth had higher $\delta^{18}\text{O}$ values than mammoth teeth, even though the former do continue to form into early adulthood (18 AEY) (Saunders, 1977).

Furthermore, there is no difference between mammoth and mastodon $\delta^{18}\text{O}$ values in Western Canada (Chapter 7), and there is no evidence from mastodon teeth of the lower $\delta^{13}\text{C}$ values expected for nursing individuals (Metcalf et al., 2010). Overall, the data suggest that nursing is not a sufficient explanation for higher $\delta^{18}\text{O}$ values in mastodons than mammoths.

A more likely explanation for the different $\delta^{18}\text{O}$ values of mammoths and mastodons is habitat differentiation. McAndrews and Jackson (1988) found no evidence that mammoths and mastodons occupied Ontario during distinct time periods or inhabited distinct vegetational zones (based on pollen analysis), but noted that their habitats were geographically distinct. Mammoth remains tend to be found in well-drained upland areas and on the western shores of Lake Iroquois (McAndrews and Jackson, 1988), which formed in the Ontario basin after 12,800 BP, as glacial ice retreated (Lewis et al., 1994). Mastodon remains have been found predominantly in the wetland areas of the Lake Warren plains (McAndrews and Jackson, 1988), which were contemporaneous with Lake Iroquois. This region of the Erie basin, formerly covered by Lake Warren, became exposed because the level of Early Lake Erie was exceptionally low (Lewis et al., 1994). The lower $\delta^{18}\text{O}$ values of mammoths are consistent with the proximity of this taxa to drinking water from a glacial lake directly formed by the melting Laurentide Ice Sheet. Glacial meltwater has very low $\delta^{18}\text{O}$ values (mean $\approx -31\text{‰}$, range ≈ -35 to -27‰) (Dansgaard et al., 1993; Dansgaard and Tauber, 1969; Sima et al., 2006). Estimated $\delta^{18}\text{O}$ values of bottom water in glacial Lake Main Algonquin (Huron basin) from about 12,000 to 10,500 BP range from -20‰ near the margins of the Laurentide Ice Sheet to about -13 to -10‰ in its southernmost regions (Hyodo, 2010; Rea et al., 1994). Contemporaneous bottom waters in the Erie basin are about 2‰ more positive than those in the southern Huron basin (i.e., about -11 to -8‰), and those in Georgian Bay are about 2‰ more

negative (i.e., about -15 to -12‰) (Rea et al., 1994). The $\delta^{18}\text{O}$ value of ancient lake bottom water calculated from ostracodes in glacial-period sediments of the Ontario and Simcoe basins is as low as -18‰ (Bumstead et al., 2009; Hladyniuk and Longstaffe, 2009, 2010). Surface waters in each basin would likely be slightly more positive than the aforementioned values, because of evaporative enrichment and precipitation inputs. In contrast to the glacial lakeshore environments apparently inhabited by mammoths, the wetland areas inhabited by mastodons were likely dominated by groundwater and/or precipitation inputs. Groundwater $\delta^{18}\text{O}$ values could be influenced by glacial input, depending on the local hydrology and flooding history, but precipitation would have had higher $\delta^{18}\text{O}$ values, leading to higher overall $\delta^{18}\text{O}$ values for potential mastodon water sources. That said, consumption by mammoths of plants growing in well-drained areas could have attenuated the contribution of low- ^{18}O lake water, minimizing the difference in $\delta^{18}\text{O}$ values between mammoths and mastodons. Water entering the diet through leaf consumption, in particular, would be considerably enriched in ^{18}O relative to lake water, especially under drier climatic conditions (Dongmann et al., 1974; Flanagan and Ehleringer, 1991; Gonfiantini et al., 1965).

6.3.6.2 Carbon

Great Lakes proboscideans consumed entirely C_3 -plant diets (mean $\delta^{13}\text{C}_{\text{diet}} = -25.7$ or -25.1‰ calculated from collagen or structural carbonate, respectively) (Table 6.2). There are no significant differences in $\delta^{13}\text{C}$ values (collagen or structural carbonate) between mastodons and mammoths (Table 6.2, Figures 6.2, 6.3). Previous studies have also shown similar $\delta^{13}\text{C}$ values in mammoths and mastodons living in C_3 -dominated environments (France et al., 2007; Saunders et al., 2010). Although it is possible that mammoths and mastodons were both generalists, their different tooth morphologies, previous data on dietary preferences from studies of isotopic compositions and gut/fecal contents (e.g., Haynes, 1991; Koch et al., 1998; Lepper et al., 1991; van Geel et al., 2008), and their different $\delta^{18}\text{O}$ and $\delta^{15}\text{N}$ values (Sections 6.3.6.1 and 6.3.6.3), suggest that their diets were not identical. Given that proboscideans have extremely large food requirements and that modern proboscideans forage opportunistically, there was likely some overlap in plant species consumed by mammoths and mastodons. However, their

similar $\delta^{13}\text{C}$ values, rather than indicating identical diets, are more likely a result of consuming a wide variety of taxa within their preferred category (i.e., grasses vs. trees/shrubs), thus averaging species-differences in $\delta^{13}\text{C}$ values.

The difference between $\delta^{13}\text{C}_{\text{sc}}$ and $\delta^{13}\text{C}_{\text{col}}$ values ($\Delta^{13}\text{C}_{\text{sc-col}}$) is sometimes used as an additional dietary proxy, typically to reconstruct trophic level (e.g., Metcalfe et al., 2009). However, Clementz et al. (2009) demonstrated that it can be also useful for understanding diet quality (protein/lipid/carbohydrate content) and for taxonomic screening. Mammoths and mastodons in this study had $\Delta^{13}\text{C}_{\text{sc-col}}$ values (means = 9.7 and 9.3, respectively) that were not significantly different (Table 6.2). Although this could further indicate a lack of dietary differences, Clementz et al. (2009) note that herbivore $\Delta^{13}\text{C}_{\text{sc-col}}$ values are remarkably consistent across a range of geographical locations and time periods. Thus, $\Delta^{13}\text{C}_{\text{sc-col}}$ values are not particularly useful for understanding differences in proboscidean diets.

6.3.6.3 Nitrogen

Great Lakes mammoths have significantly higher $\delta^{15}\text{N}$ values than mastodons ($7.9 \pm 0.6\text{‰}$, $2.6 \pm 0.6\text{‰}$, respectively) ($t = 13.7$, $df = 27$, $p < 0.001$) (Table 6.2, Figure 6.2). Numerous studies have noted that mammoths tend to have high $\delta^{15}\text{N}$ values relative to co-existing herbivores (Bocherens, 2003; Bocherens et al., 1996; Iacumin et al., 2000; Koch, 1991). Some studies have also shown that mastodons tend to have low $\delta^{15}\text{N}$ values relative to co-existing herbivores (Coltrain et al., 2004; France et al., 2007; Koch, 1991).

The difference in collagen nitrogen isotope compositions between mammoths and mastodons could be a result of different microhabitats, different plant choices, or metabolic differences (Table 6.4). Bocherens et al. (2003; 1996) discuss possible explanations for the high $\delta^{15}\text{N}$ values of mammoths, including nitrogen recycling and consumption of relatively older plant parts or plants from “disturbed environments”. Recently, coprophagy has also been considered as an explanation for high $\delta^{15}\text{N}$ values in mammoths (Clementz et al., 2009; van Geel et al., 2010). Although a definitive cause cannot yet be determined, the higher $\delta^{15}\text{N}$ values of mammoths are also consistent with drier environments and/or more grass consumption.

Table 6.4 Relationships between metabolic, vegetational, and environmental factors and the $\delta^{15}\text{N}$ values of animals living in C_3 environments

Category	Factor	Effect on $\delta^{15}\text{N}$	References
Metabolic			
	Starvation (fasting)	Increase ^	1, 2, 3, 4
	Slowed growth (fasting)	Increase	4, 5, 6
	Pregnancy & Lactation	Decrease	7, 8
Vegetational			
	Protein content	Increase	9
	Plant parts	twigs<needles ***	10
	Root depth	Increase (because of soil age; see below)	11
	Plant type	tree<shrub<grass****	12, 13
	Symbiotic N-fixation	Approaches atmospheric	14
	Symbiosis with fungi	ericoid-<ecto-< endo-<non-mycorrhiza*	14, 15
Environmental			
	Aridity increase	Increase	11, 15, 16, 17, 18, 19
	Soil nitrogen content increase	Increase	13, 15
	Soil nitrogen source	Variable	14
	Soil acidity increase	Decrease	13
	Temperature increase	Increase**	11, 15
	High altitude	Decrease	11
	Older soils	Increase	11
	Manure increase	Increase	11, 14, 20, 21
	Soil parent material	Variable	11
	Soil salinity increase	Increase	16
	Annual burning	Increase	22
	Land use intensity	Increase	23

^ Polishcuk et al. (2001) found that some polar bears had decreases, while others had increases

* in tundra and forest environments, but not tropical or alpine

** only where MAT ≥ -0.5 °C (Craine et al. 2009)

*** in *Picea abies* (Norway spruce)

**** *Picea*, *Vaccinium*, *Calamagrostis*

References

- 1 Fuller et al., 2005
- 2 Mekota et al., 2006
- 3 Polishcuk et al., 2001
- 4 Warinner and Tuross, 2010
- 5 Hobson et al., 1993
- 6 McCue and Pollock, 2008
- 7 Fuller et al., 2004
- 8 Fuller et al., 2006
- 9 Sponheimer et al., 2003
- 10 Gebauer and Schulze, 1991
- 11 Amundson et al., 2003
- 12 Schulze et al., 1994
- 13 Bocherens, 2003
- 14 Makarov, 2009
- 15 Craine et al. 2009
- 16 Heaton, 1987
- 17 Schwarcz et al., 1999
- 18 Murphy and Bowman, 2009
- 19 Wang et al., 2010
- 20 Bogaard et al., 2007
- 21 Comisso and Nelson, 2010
- 22 Schmidt and Stewart, 2003
- 23 Aranibar et al. 2008

The relatively low $\delta^{15}\text{N}$ values of mastodons in Michigan, Ohio, Indiana, western New York, and California have been interpreted as evidence for consumption of nitrogen-fixing plant taxa (e.g., alder or lichens) (Coltrain et al., 2004; Koch, 1991). The strong association of Ontario mastodons with open spruce forests (Dreimanis, 1967, 1968) may also be a key factor in their very low $\delta^{15}\text{N}$ values. The forest floor surrounding spruce trees is known to have extremely high nitrogen contents relative to that surrounding other tree species (beech, oak, maple, lime, and ash) (Vesterdal et al., 2008). Since high nitrogen contents in soils are related to lower $\delta^{15}\text{N}$ values in plants rooted in those soils (Amundson et al., 2003), plants rooted in the forest floor surrounding spruce trees would be expected to have lower $\delta^{15}\text{N}$ values than those in growing open environments or near other tree species. Furthermore, at least in modern Alaska, spruce needles are known to have significantly lower $\delta^{15}\text{N}$ values than the shrubs and grass leaves growing underneath them (mean $\delta^{15}\text{N} = -7.7$ (spruce), -4.3 (shrub), and 0.9‰ (grass)), likely because each plant utilizes different soil nitrogen sources (Schulze et al., 1994). Although many species avoid browsing on spruce because of its high-molecular weight terpenes and resins, mastodons may have dealt with the problem by ingesting silts and clays, which could act as laxatives and detoxifiers (McAndrews, 2003). Thus, whether mastodons consumed plants growing near spruce trees, or even spruce trees themselves, they would likely have had lower $\delta^{15}\text{N}$ values than mammoths consuming plants from more open, well-drained coastal areas.

6.3.7 Comparison of “Bulk” and “Serially-Sampled” Isotopic Results

For the Great Lakes mastodons, positive correlations existed between bulk and mean serially-sampled $\delta^{13}\text{C}$ ($r = 0.9$, $df = 2$, $p = 0.1$) and between bulk and mean serially-sampled $\delta^{18}\text{O}$ values ($r = 0.8$, $df = 2$, $p < 0.1$). Serially-sampled mean $\delta^{18}\text{O}$ values were on average 1.3‰ lower than bulk enamel $\delta^{18}\text{O}$ values (range of offsets = 2.1 to 0.9‰). There was little or no offset between the $\delta^{13}\text{C}$ values (mean = 0.4‰ higher in incremental than bulk, range of offsets = 0.1 to 0.7‰) (Tables 6.2, 6.8). Lower mean $\delta^{18}\text{O}$ values in incremental samples were also observed in Columbian mammoths from Arizona (Chapter 5), and may be a result of the shorter maturation time of inner enamel relative to the rest of the enamel thickness (see Chapter 5 for a more detailed discussion).

Table 6.5 Stable isotope compositions from serial sampling, and associated diet and drinking water compositions.

Position* (mm)	Structural Carbonate			Diet	Water
	$\delta^{13}\text{C}$ (‰)	$\delta^{18}\text{O}$ (‰)	CO_3 Wt %	$\delta^{13}\text{C}$ (‰)	$\delta^{18}\text{O}$ (‰)
ON9 (Delaware), 12,360 ± 120 BP					
1	-10.4	24.9	6.0	-24.5	-7.7
2	-10.0	24.2	5.5	-24.2	-8.4
3	-9.8	22.9	5.9	-23.9	-9.8
4	-9.4	22.5	5.7	-23.6	-10.2
5	-9.3	21.2	5.0	-23.5	-11.6
6	-9.5	20.7	6.4	-23.6	-12.1
8	-9.6	20.2	2.8	-23.7	-12.6
9	-9.4	20.0	6.0	-23.6	-12.8
10	-9.2	20.0	5.7	-23.4	-12.8
11	-9.1	21.1	6.0	-23.3	-11.6
12	-9.3	24.1	5.2	-23.5	-8.6
13	-9.7	25.1	2.0	-23.9	-7.5
14	-9.9	23.6	5.7	-24.1	-9.1
15	-9.6	23.6	4.6	-23.7	-9.0
16	-9.1	22.2	5.2	-23.2	-10.5
17	-9.3	21.6	6.3	-23.5	-11.1
18	-9.6	21.3	4.0	-23.8	-11.4
19	-9.4	21.0	3.6	-23.6	-11.7
20	-9.2	21.2	5.3	-23.3	-11.5
21	-9.0	23.9	4.2	-23.2	-8.8
22	-9.6	26.3	5.4	-23.7	-6.2
23	-9.5	27.6	4.0	-23.6	-4.8
24	-9.0	23.8	5.4	-23.2	-8.8
25	-9.1	20.8		-23.2	-12.0
26	-9.4	20.4	5.9	-23.6	-12.4
27	-9.9	20.3	5.8	-24.0	-12.5
28	-9.2	21.1	5.6	-23.3	-11.6
29	-9.3	25.1	5.3	-23.4	-7.4
30	-9.9	25.2	5.9	-24.1	-7.4
31	-9.3	22.6	5.3	-23.5	-10.1
32	-9.4	20.7	5.5	-23.6	-12.1
33	-10.1	19.7	6.2	-24.2	-13.1
34	-9.8	19.3	5.5	-23.9	-13.5
35	-9.3	21.4	5.4	-23.4	-11.3
36	-10.3	24.2	5.7	-24.5	-8.4
37	-9.2	22.6	5.1	-23.3	-10.1
38	-10.2	20.6	4.2	-24.4	-12.1
39	-9.6	19.5	5.9	-23.8	-13.3
ON14 (Rodney), 11,400 ± 450, 12,000 ± 500 BP					
1	-10.3	20.5	5.5	-24.5	-12.2
2	-10.5	23.1	5.8	-24.7	-9.6
3	-11.0	24.4	6.1	-25.1	-8.2
4	-11.2	22.8	6.2	-25.4	-9.9
5	-11.3	21.6	5.4	-25.5	-11.1

Table 6.5 cont.

Position* (mm)	Structural Carbonate			Diet	Water
	$\delta^{13}\text{C}$ (‰)	$\delta^{18}\text{O}$ (‰)	CO_3 Wt %	$\delta^{13}\text{C}$ (‰)	$\delta^{18}\text{O}$ (‰)
6	-11.1	20.5	5.0	-25.2	-12.3
7	-11.0	18.6	5.2	-25.2	-14.2
8	-10.9	19.1	5.0	-25.0	-13.7
9	-10.9	17.7	5.1	-25.0	-15.1
10	-10.8	17.8	5.2	-24.9	-15.1
11	-10.8	18.1	6.0	-24.9	-14.7
12	-10.9	19.8	5.6	-25.0	-13.0
13	-10.7	22.3	4.6	-24.9	-10.4
14	-10.7	22.8	5.4	-24.9	-9.9
15	-10.6	20.7	4.4	-24.8	-12.0
16	-10.4	18.7	4.3	-24.6	-14.1
17	-10.6	19.1		-24.8	-13.8
18	-10.4	19.7	4.7	-24.5	-13.1
19	-10.2	20.6	4.8	-24.4	-12.2
20	-10.4	23.2	4.8	-24.6	-9.5
21	-10.8	22.9	5.0	-25.0	-9.8
22	-10.1	20.8	5.8	-24.2	-12.0
23	-10.0	18.6	7.1	-24.1	-14.3
24	-10.0	17.8	5.6	-24.1	-15.1
25	-10.1	21.2	5.9	-24.3	-11.6
26	-10.7	23.5	5.6	-24.8	-9.1
27	-10.3	21.9	5.5	-24.5	-10.8
28	-10.2	19.3	5.6	-24.3	-13.5
29	-10.1	18.7	5.3	-24.2	-14.2
30	-10.0	19.4	5.0	-24.2	-13.4
31	-10.2	22.8	5.4	-24.4	-9.8
32	-10.3	24.2	5.3	-24.4	-8.4
33	-9.9	21.7	6.1	-24.0	-11.0
34	-9.7	18.9	5.5	-23.9	-13.9
35	-9.7	22.0	6.0	-23.8	-10.7
36	-10.6	23.6	5.0	-24.8	-9.0
ON7 (Caradoc), 11,120 ± 110 BP					
1	-10.8	20.5	5.5	-24.9	-12.2
2	-10.9	20.7	5.5	-25.0	-12.0
3	-11.0	20.3	5.3	-25.1	-12.5
4	-11.0	20.0	5.3	-25.2	-12.8
5	-10.9	19.5	4.9	-25.0	-13.3
6	-10.5	18.4	2.6	-24.7	-14.5
7	-10.5	18.7	5.5	-24.7	-14.2
8	-10.5	18.6	5.4	-24.6	-14.2
9	-10.5	18.4	5.5	-24.7	-14.4
10	-10.5	19.1	5.5	-24.6	-13.8
11	-10.4	20.1	5.9	-24.6	-12.6
12	-10.5	20.2	5.5	-24.6	-12.6
13	-10.5	21.4	4.6	-24.7	-11.3
14	-10.7	22.0	5.8	-24.9	-10.7

Table 6.5 cont.

Position* (mm)	Structural Carbonate			Diet	Water
	$\delta^{13}\text{C}$ (‰)	$\delta^{18}\text{O}$ (‰)	CO_3 Wt %	$\delta^{13}\text{C}$ (‰)	$\delta^{18}\text{O}$ (‰)
15	-10.9	21.7	4.9	-25.0	-11.0
16	-10.9	21.7	6.2	-25.0	-11.0
17	-10.1	19.1	5.0	-24.3	-13.7
18	-10.1	18.8	5.3	-24.3	-14.0
19	-10.1	18.5	4.9	-24.3	-14.3
20	-10.2	18.3	6.0	-24.3	-14.5
21	-10.3	18.3	4.2	-24.4	-14.5
22	-10.2	18.6	5.6	-24.3	-14.3
23	-10.3	18.7	5.6	-24.4	-14.1
24	-10.2	19.3	5.4	-24.3	-13.5
25	-10.4	21.5	5.0	-24.6	-11.3
26	-10.5	22.5	5.9	-24.6	-10.2
27	-10.9	21.5	5.8	-25.0	-11.2
28	-10.1	20.0	5.4	-24.3	-12.8
29	-10.2	18.0	5.2	-24.3	-14.9
30	-10.3	17.3	5.5	-24.4	-15.6
31	-10.2	17.7	4.9	-24.3	-15.2
33	-11.2	22.1	5.2	-25.3	-10.6
NY4 (Hiscock), 10,810 to 10,350 BP (not directly dated)					
2	-10.6	20.5	6.5	-24.7	-12.3
3	-10.7	20.6	6.0	-24.8	-12.2
4	-10.3	20.8	5.0	-24.5	-12.0
5	-10.2	21.1	7.9	-24.3	-11.6
6	-10.3	20.6	6.8	-24.5	-12.2
7	-10.8	20.8	5.5	-25.0	-12.0
8	-11.3	20.4	5.2	-25.5	-12.4
9	-11.4	18.8	6.1	-25.6	-14.0
10	-11.3	19.5	5.4	-25.4	-13.3
11	-11.4	19.2	5.3	-25.6	-13.7
13	-10.7	20.9	4.3	-24.8	-11.9
14	-11.5	22.4	3.0	-25.7	-10.3
15	-11.5	21.7	5.8	-25.6	-11.0
16	-11.2	20.4	4.9	-25.3	-12.4
17	-11.4	20.4	3.6	-25.6	-12.3

Values in **bold** are the results of duplicate analyses.

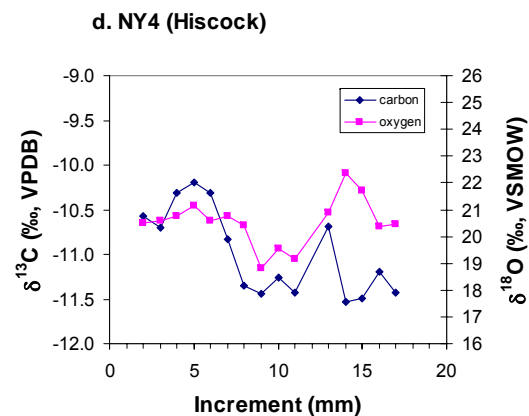
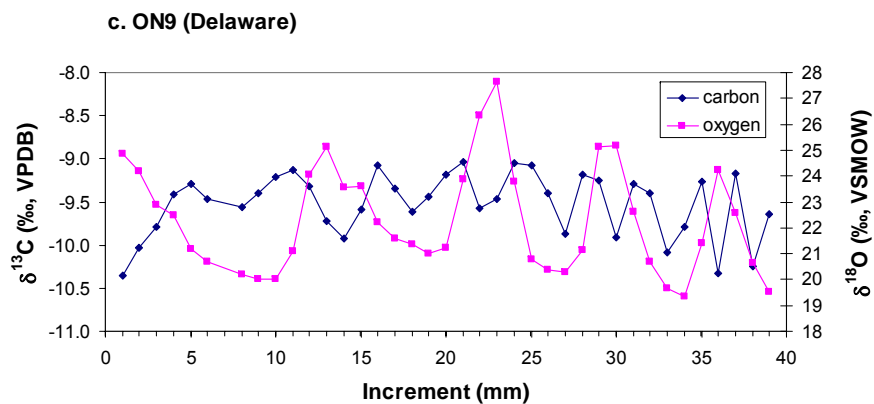
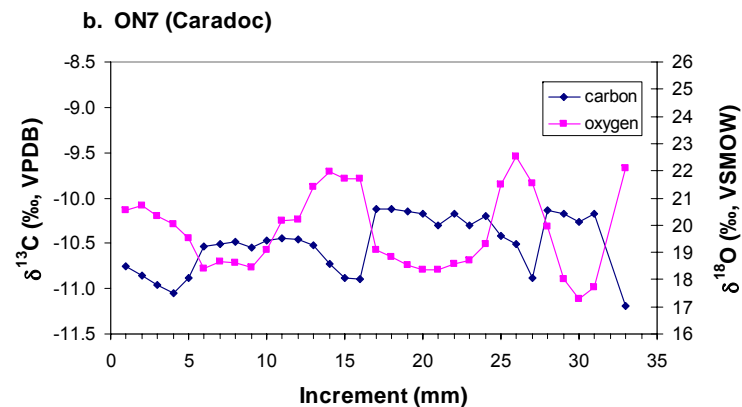
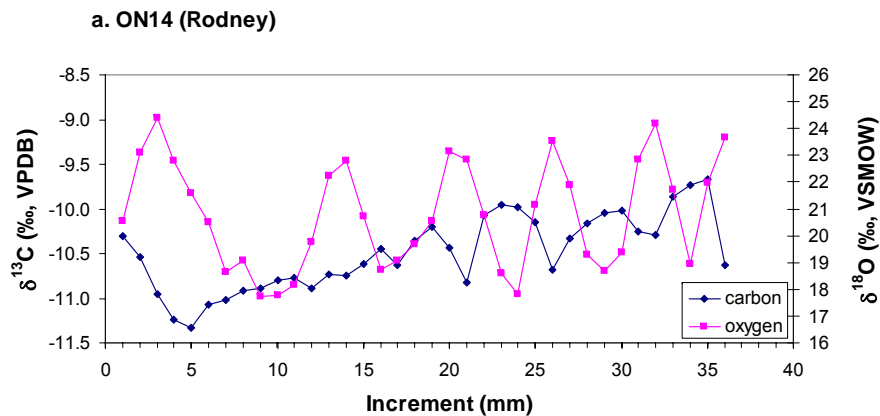


Figure 6.4 Carbon and oxygen isotope results for serial sampling of inner enamel from Great Lakes mastodons. Higher increment numbers are closer to the cervix.

Table 6.6 Periods of the isotope curves for serially-sampled mastodon enamel.

	$\delta^{18}\text{O}$		$\delta^{13}\text{C}$	
	Period (mm)	No. **	Period (mm)	No. **
ON9	11 to 6*	>4	6 to 2*	>9
ON7	12 to 6*	~3	12 to 5*	~3
ON14	11 to 4*	~5	? to 4	>4
NY4	$\geq 7?$?	$\geq 7?$?

* Periods decrease closer to the cervix

** Number of periods recorded in isotope record

Table 6.7 Histological measurements from photomicrographs (Figure 6.5) of mastodon enamel from ON5, after Shellis (1984).

	Enamel Region	
	Occlusal	Cervical
d (μm)	4.0 - 4.8	1.9 - 3.1
I ($^\circ$)	68.7 - 71.6	70.3 - 73.4
D ($^\circ$)	10.5 - 13.7	10.0 - 15.3
c ($\mu\text{m}/\text{day}$)	13.7 - 23.1	5.9 - 16.1
c (mm/yr)	5.0 - 8.4	2.2 - 5.9

d = distance between cross-striations, measured 100-600 μm from the enamel-dentin junction (EDJ)

I = angle between enamel prisms and the EDJ, in the occlusal direction

D = angle between Striae of Retzius and the EDJ, in the occlusal direction

c = extension rate (occlusal basal direction). $c = d[(\sin I/\tan D) - \cos I]$

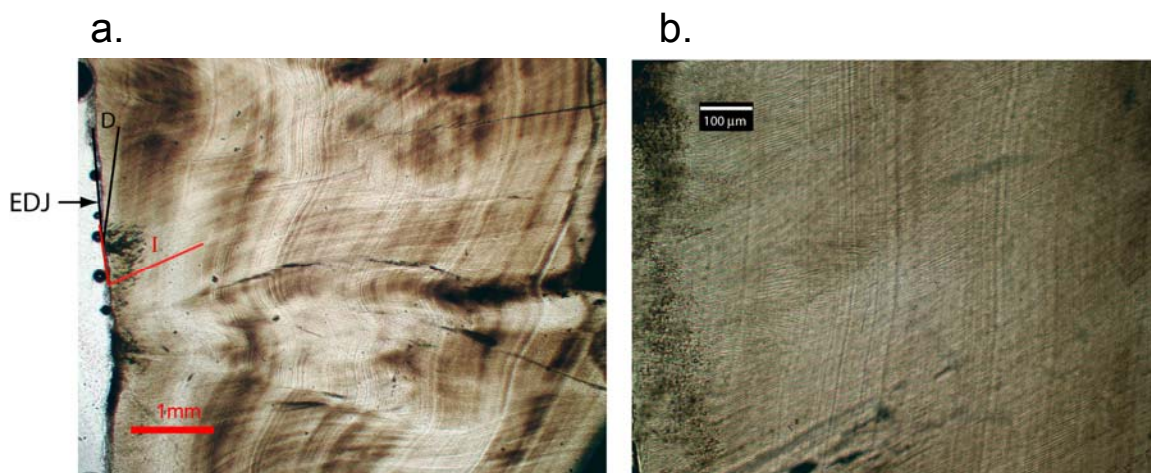


Figure 6.5 Thin section images for enamel from ON5, taken in plane-polarized light. (a) Low magnification photomicrograph showing the angle between the EDJ and Striae of Retzius (D) and between the EDJ and enamel prisms (I). (b) Higher magnification photomicrograph used to measure cross-striation intervals.

6.3.8 Serially-Sampled Enamel: Regular Periodicity

Three out of four mastodons have serially-sampled enamel $\delta^{13}\text{C}$ and/or $\delta^{18}\text{O}$ values that exhibit regular periodicity (Table 6.5, Figure 6.4a-c). The fourth may have such periodicity as well, but the isotopic record obtained is too short to know for certain (Table 6.5, Figure 6.4d). Table 6.6 lists the periods of the curves, based on the distance between peaks or valleys (i.e., maxima, minima, or centre of high or low plateaus) in each curve. Periods for $\delta^{18}\text{O}$ are quite consistent among individuals (11-12 mm/year in the enamel closest to the occlusal surface and 4-6 mm/year in the enamel nearest the cervix). In high latitude locations, the $\delta^{18}\text{O}$ values of precipitation typically follow a sinusoidal pattern over time, with a period of one year (Rozanski et al., 1993). We hypothesize that one period in the $\delta^{18}\text{O}$ curve for mastodon teeth represents one year of growth.

Crown extension rate estimates (i.e., rates of growth in the occlusal-basal direction, or tooth height; see Figure 4.1) for one mastodon tooth (ON5; see photomicrographs in Figure 6.5) were about 5-8 mm/year for enamel closer to the occlusal surface and 2-3 mm/year for enamel near the cervix (Table 6.7). These histological estimates are several mm lower than the estimates from isotopic measurements (11-12 mm and 4-6 mm, respectively). However, the histological estimates may represent enamel that is closer to the cervix than the isotopic estimates. Furthermore, histological extension rate estimates are known to underestimate the true extension rate (Smith et al., 2006). The periods inferred from both $\delta^{18}\text{O}$ values and histological estimates decrease with decreasing distance from the cervix. This is consistent with the known decrease in the growth rate of enamel approaching the cervix (Hillson, 2005; Smith et al., 2006), and further manifested by the more closely-spaced perikymata (ridges whose spacing represents equal intervals of time) observable on the outer enamel surface of many of the mastodon specimens used in the present study. Overall, the growth rate estimates are generally consistent with the hypothesis that one period for $\delta^{18}\text{O}$ represents a year of growth.

The growth rates of these mastodon teeth are lower than those of Columbian mammoth teeth (Chapters 4, 5). In other words, mammoth teeth compensate for their

larger size by growing faster, so their longer development time results entirely from an increase in tooth height and length. Similarly, Dirks (2010) found that the lamellae of Columbian mammoths develop about twice as fast as those of pygmy elephants, though the total formation time for the former is longer because they are about three times as large. Future studies using serially-sampled enamel should take these differences into account. That is, smaller spaces are needed between incremental samples for mastodons than mammoths in order to obtain a similar temporal resolution.

6.3.9 Serially-Sampled Enamel: Isotopic Composition of Diet and Drinking Water

The calculated $\delta^{13}\text{C}_{\text{diet}}$ values for Great Lakes specimens reflect 100% C_3 plant consumption throughout the year for all individuals (range = -25.7 to -23.2‰) (Table 6.8). The calculated $\delta^{18}\text{O}_{\text{water}}$ values range from -15.6 to -4.8‰ (Table 6.8). For comparison, the $\delta^{18}\text{O}$ values of modern seasonal precipitation on the shores of Lake Erie (multi-year mean of winter versus summer months) range from about -11 to -5‰ (Point Pelee and Rock Point; F. Longstaffe, personal communication). Monthly arithmetic mean $\delta^{18}\text{O}$ values of precipitation at Simcoe range from -17.3‰ in winter to -5.3‰ in summer (IAEA/WMO, 2010). There is considerable overlap between these ranges, suggesting that Great Lakes mastodon drinking water was primarily derived from precipitation with oxygen isotope compositions not unlike those in the region today. We note that this does not preclude some contribution from glacial meltwater (Section 6.3.6.1).

6.3.10 Serially-Sampled Enamel: Seasonal Patterns

Here, we assume that one period in the $\delta^{18}\text{O}$ curve represents one year of growth (see Section 6.3.7). A fundamental problem for interpreting the seasonal variations in serially-sampled enamel is determining which seasons are represented by the different portions of the isotope curves. In most mid- to high-latitude locations, the $\delta^{18}\text{O}$ values of precipitation follow a sinusoidal pattern over time, with highs during summers and lows during winters (Rozanski et al., 1993). The $\delta^{18}\text{O}$ values of lakes and rivers depend on the balance of the isotopic composition of their inputs (groundwater, stream flow, overland flow, direct precipitation) and outputs (evaporation, outflow) (Henderson and Shuman, 2009). Lakes and rivers that receive most of their input from precipitation (either directly

or through runoff) tend also to have higher $\delta^{18}\text{O}$ values in summer (as a result of temperature-effects on precipitation $\delta^{18}\text{O}$ and increased evaporation), though they typically have lower amplitudes of variation. However, in lakes or rivers with significant input from low- ^{18}O glacial meltwater, the opposite pattern may occur. That is, lower $\delta^{18}\text{O}$ values may occur during summer as a result of increased ice melting. In the modern Great Lakes, seasonal variations are particularly small because of the very large reservoir size; for example, western Lake Erie has monthly seasonal variations in $\delta^{18}\text{O}$ of less than 2‰, whereas monthly precipitation varies by about 8‰ (Huddart et al., 1999).

Koch et al. (1989) found that slow-growth zones in the tusk dentin of three mastodons and one mammoth from southern Michigan and western New York corresponded to minima in their serially-sampled $\delta^{18}\text{O}$ curves. This suggests that low $\delta^{18}\text{O}$ values were associated with winter growth, and further implies that variable quantities of glacial meltwater did not significantly contribute to seasonal $\delta^{18}\text{O}$ variations. This is not to say that drinking water sources lacked glacial meltwater input altogether, but rather that the proportion of meltwater in drinking water did not vary appreciably on a seasonal basis. In the following discussion, we assume that highs in the $\delta^{18}\text{O}$ curves represent warm-season growth, and lows, cold-season growth. We note that the proposed explanations for seasonal dietary changes would be reversed if seasonal variations in meltwater controlled the $\delta^{18}\text{O}$ cycles.

The relationship between the $\delta^{13}\text{C}$ and $\delta^{18}\text{O}$ curves within the four serially-sampled mastodon specimens exhibits three distinct patterns. Pattern 1 was observed in two individuals from Rodney and Caradoc (ON14, ON7). In these individuals, high $\delta^{13}\text{C}$ values were associated with low $\delta^{18}\text{O}$ values, and vice versa (i.e., an apparent negative relationship) (Figure 6.4 a, b). Pattern 2, observed in one individual from Delaware (ON9), was more complex: the period of the $\delta^{18}\text{O}$ curve was twice that of the $\delta^{13}\text{C}$ curve, and $\delta^{18}\text{O}$ valleys and peaks were both associated with $\delta^{13}\text{C}$ valleys (Figure 6.4c). In other words, both high and low $\delta^{18}\text{O}$ values (inferred warm- and cold-season) were associated with low $\delta^{13}\text{C}$ values. Pattern 3 was evident in the single individual from the Hiscock site (NY4). The $\delta^{13}\text{C}$ and $\delta^{18}\text{O}$ curves of this individual were similarly shaped, with high and low values for both curves occurring at approximately the same locations (i.e., an apparent positive relationship) (Figure 6.4d).

Table 6.3 lists the many factors that affect the $\delta^{13}\text{C}$ values of C_3 plants. Accordingly, possible explanations for Pattern 1 (ON14 and ON7; negative relationship between $\delta^{13}\text{C}$ and $\delta^{18}\text{O}$) include (1) starvation/fasting in winter, (2) increased bark and wood consumption in winter versus leaf and shrub consumption in summer, (3) drier climatic conditions in winter and wetter in summer, (4) lower-protein diets in winter and higher-protein diets in summer, and/or (5) changes in plant species consumed in winter versus summer (see Table 6.3). In addition to the similar relationship between $\delta^{13}\text{C}$ and $\delta^{18}\text{O}$ curves for ON7 and ON14, the δ -values for these two individuals are very similar (Table 6.8, Figure 6.6). Both lines of evidence suggest that these two mastodons experienced similar climatic conditions and engaged in similar seasonal behaviour. This inference is consistent with the radiocarbon dates of these two specimens, which are closer to one another than to ON9 (older) or NY4 (likely younger) (Table 6.1). The radiocarbon dates for the Pattern 1 individuals ($11,120 \pm 110$ BP, $11,400 \pm 450$ BP, $12,000 \pm 500$ BP) indicate that they likely lived between 12,500 and 11,100 BP (using 1 SD from the mean as the upper and lower limit on date range), which was a period of overall climate warming (glacial retreat) (Lewis et al., 1994). A brief glacial advance around 11,700 BP was apparently restricted to the Huron and Michigan basins, with little effect on Erie and Ontario (McAndrews and Jackson, 1988; Yu, 2000). This time interval is characterized by pollen profiles dominated by spruce (Lewis et al., 1994), and represents the principal period of mastodon occupation of the region.

For Pattern 2 (ON9), low- ^{13}C “summers” could have resulted from any of the factors described above for Pattern 1 (i.e., increased leaf consumption, wetter conditions, higher-protein diets, or different plant species). The low- ^{13}C “winters” observed for Pattern 2 might indicate (1) greater fat metabolism (as opposed to starvation/fasting effects, which suggests that this individual may have been fatter or healthier than the others), (2) wetter winters (and drier summers/falls), (3) colder winter temperatures, and/or (4) consumption of different plant parts or species. The radiocarbon date for ON9 ($12,360 \pm 120$ BP) suggests that this individual dates to a slightly earlier time period than the Pattern 1 specimens, around the time that Early Lake Algonquin formed from melting ice in the Huron basin (Lewis et al., 1994). At this time, Early Lake Algonquin flowed

into Early Lake Erie and from there into Lake Iroquois, whereas by 11,900 BP the Fenelon Falls (Kirkfield) outlet had opened between Glacial Lake Algonquin and Glacial Lake Iroquois, and flow between Algonquin and Erie had ceased (Lewis et al., 1994). Thus, we would expect ON9 to have had greater access to low- ^{18}O glacial meltwater than ON14 or ON7. Contrary to this expectation, the $\delta^{18}\text{O}$ and $\delta^{13}\text{C}$ values of ON9 tend to be higher than those of ON14 or ON7 all year long (Table 6.8, Figure 6.6). This strengthens the supposition that glacial meltwater did not make a significant contribution to mastodon drinking water. Further, it could indicate that ON9 experienced a somewhat warmer and/or drier environment than ON7 or ON14. The larger amplitude of variation for ON9 could potentially reflect greater reliance on precipitation than lake water, or alternatively, larger variations in lake water or precipitation $\delta^{18}\text{O}$ values on a seasonal basis. Both Pattern 1 and Pattern 2 individuals have amplitudes for $\delta^{18}\text{O}$ (5.5 to 8.6‰) close to those of modern monthly precipitation on the shores of Lake Erie (~8‰) (Huddart et al., 1999).

Pattern 3 (a generally positive relationship between $\delta^{13}\text{C}$ and $\delta^{18}\text{O}$) was obtained for the Hiscock mastodon (NY4). Four serially-sampled mastodon tusks from the same site had a similar relationship between $\delta^{13}\text{C}$ and $\delta^{18}\text{O}$ (Fisher and Fox, 2003), so the pattern may be characteristic of Hiscock mastodons. The relationship between $\delta^{13}\text{C}$ and $\delta^{18}\text{O}$ values for these specimens is different from those of the Ontario mastodons, which suggests a fundamental difference in seasonal vegetation dynamics, metabolic responses, or behaviour. Relative to the Ontario specimens, NY4 has attenuated and less regular $\delta^{18}\text{O}$ variations (Table 6.8, Figure 6.6a). The short record available for NY4 may be partially responsible, but patterns obtained for other Hiscock mastodon specimens also showed less regular periodicity and lower amplitudes than were observed in Ontario mastodons (Fisher and Fox, 2003). In addition, winter growth periods did not always match up with low $\delta^{18}\text{O}$ values in the Hiscock mastodon tusks (Fisher and Fox, 2003). These data suggest that Hiscock mastodons may have relied more heavily on groundwater or lake water, which would have had less pronounced seasonal variations in $\delta^{18}\text{O}$ than precipitation. Hiscock mastodons may also have utilized water sources with different isotopic compositions in a seasonally unpredictable way. Although NY4 was not directly dated, radiocarbon dates previously obtained for Hiscock mastodon bones are younger

Table 6.8 Summary of isotopic results for incrementally sampled Great Lakes mastodons.

LSIS #	Site	n	$\delta^{13}\text{C}_{\text{sc}}$ (‰)				$\delta^{13}\text{C}_{\text{diet}}$ (‰)				$\delta^{18}\text{O}_{\text{sc}}$ (‰)				$\delta^{18}\text{O}_{\text{water}}$ (‰)			
			Mean \pm SD	Min	Max	Range	Mean \pm SD	Min	Max	Range	Mean \pm SD	Min	Max	Range	Mean \pm SD	Min	Max	Range
ON9	Delaware	38	-9.5 \pm 0.4	-10.4	-9.0	1.3	-23.7 \pm 0.4	-24.5	-23.2	1.3	22.3 \pm 2.1	19.3	27.6	8.3	-10.4 \pm 2.2	-13.5	-4.8	8.6
ON7	Caradoc	32	-10.5 \pm 0.3	-11.2	-10.1	1.1	-24.6 \pm 0.3	-25.3	-24.3	1.1	19.7 \pm 1.5	17.3	22.5	5.2	-13.1 \pm 1.5	-15.6	-10.2	5.5
ON14	Rodney	36	-10.5 \pm 0.4	-11.3	-9.7	1.7	-24.6 \pm 0.4	-25.5	-23.8	1.6	20.8 \pm 2.0	17.7	24.4	6.7	-12.0 \pm 2.1	-15.1	-8.2	7.0
NY4	Hiscock	15	-11.0 \pm 0.5	-11.5	-10.2	1.3	-25.1 \pm 0.5	-25.7	-24.3	1.3	20.5 \pm 0.9	18.8	22.4	3.6	-12.2 \pm 0.9	-14.0	-10.3	3.7

LSIS #: Sample ID used for Laboratory for Stable Isotope Science analyses, and referred to in this study

than those of the above specimens, ranging from $10,810 \pm 50$ BP (Laub, 2003) to $10,350 \pm 60$ BP (Laub, personal communication). These dates correspond to a period of regional climatic cooling during the Younger Dryas period (10,920 to 10,000 BP) (Lewis et al., 1994; Yu, 2000). The $\delta^{18}\text{O}$ values of NY4 were within the range of those of Ontario mammoths. Regional cooling during the Younger Dryas period might have decreased the quantity of glacial meltwater inputs to water sources (because of less melting), but also decreased the mean $\delta^{18}\text{O}$ composition of precipitation. This could lead to $\delta^{18}\text{O}$ values of drinking water similar to those in previous time periods, despite profound changes in climatic conditions. The $\delta^{13}\text{C}$ values of NY4 tended to be lower than those of Ontario mastodons (Figure 6.6b), consistent with a cooler or wetter environment (though other explanations are also possible, as described in Table 6.3).

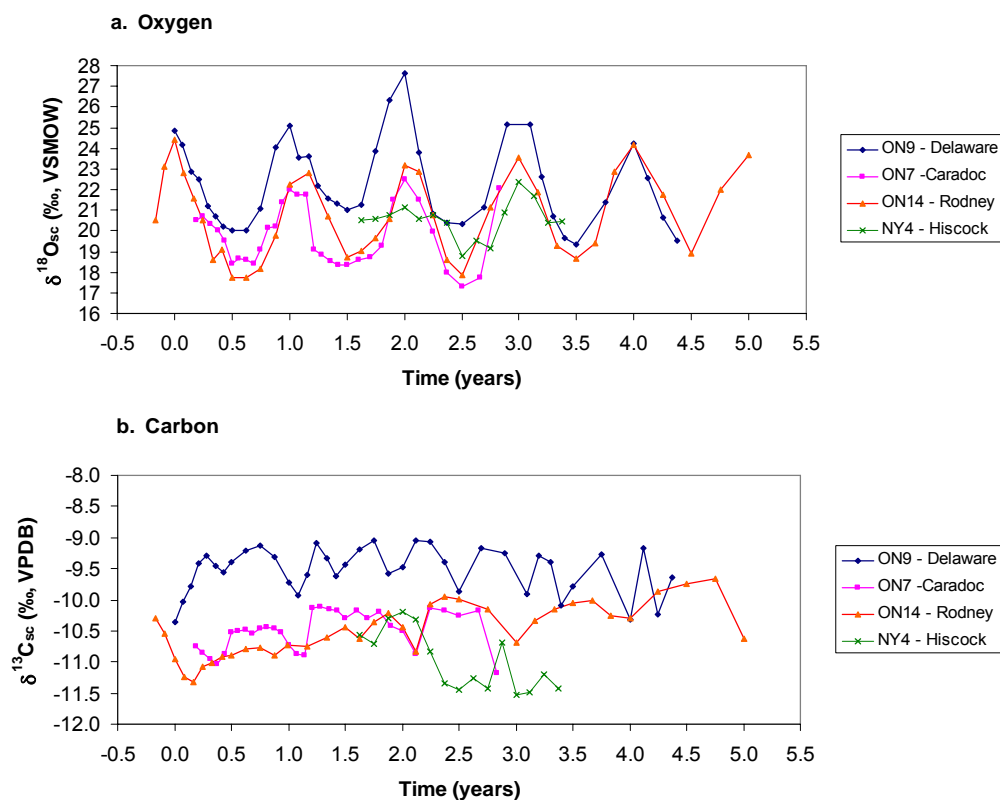


Figure 6.6 Comparison of carbon and oxygen isotope results for serial sampling of inner enamel from Great Lakes mastodons. The “distance” axis has been transformed to time, as described in the text. The reference point for time is arbitrary, so although the data are stacked for comparison of seasonal trends, the true “calendar” years of formation for each sample differed.

6.3.11 Hypotheses: Seasonal Variations in Mammoth Diet and Drinking Water

Great Lakes mammoth specimens suitable for serial-sampling were not available for this study. However, the hypothesis that water sources utilized by southern Ontario mammoths received more input from glacial meltwater, whereas those utilized by mastodons received more input from precipitation, could be evaluated through serial-sampling of enamel to reconstruct seasonal changes in drinking water $\delta^{18}\text{O}$ values. If mammoths relied primarily on drinking water from glacial lakes (i.e., Lake Iroquois) with significant amounts of low- ^{18}O meltwater input, we would expect mammoths to have (1) smaller-amplitude $\delta^{18}\text{O}$ curves than mastodons, because seasonal changes in the $\delta^{18}\text{O}$ values of lakes and rivers tend to be smaller than those of precipitation, (2) $\delta^{18}\text{O}$ values that are higher in winter and lower in summer, the opposite of the typical seasonal pattern for precipitation, and (3) particularly low $\delta^{18}\text{O}$ minima as a result of the extremely low $\delta^{18}\text{O}$ values of glacial meltwater. The serially-sampled mastodon enamel isotope results presented in this study can serve as a baseline for future comparisons with mammoths from southern Ontario.

6.4 Conclusions

Proboscideans in the Great Lakes region (southern Ontario, western New York) consumed 100% C_3 -plant diets, and drank waters with lower $\delta^{18}\text{O}$ values than modern precipitation or Great Lakes waters, consistent with a colder climate and proximity to lakes with glacial meltwater input. We suggest that the similar $\delta^{13}\text{C}$ values obtained for mammoths and mastodons are a result of the large dietary requirements of proboscideans combined with the relatively small variations of plant $\delta^{13}\text{C}$ values in C_3 ecosystems. The spatial separation of mammoth and mastodon sites (McAndrews and Jackson, 1988) and differences in $\delta^{18}\text{O}$ and $\delta^{15}\text{N}$ values suggest that the taxa occupied distinct environmental niches, even though they both consumed a wide variety of plant taxa. Thus, intense competition for resources between mammoths and mastodons was likely not a major factor in their extinction in the Great Lakes region.

Lower $\delta^{18}\text{O}$ values in mammoths are consistent with their apparent habitat preference for the shoreline of glacial Lake Iroquois, in contrast to the wetter Lake Warren plains preferred by mastodons. The reason for very high $\delta^{15}\text{N}$ values in

mammoths remains to be fully understood. We propose a new explanation for low $\delta^{15}\text{N}$ values in mastodons, related to the effects of spruce trees on plant $\delta^{15}\text{N}$ values. Further research on the nitrogen-isotope systematics of modern spruce environments, and on mastodon $\delta^{15}\text{N}$ values in areas that lack spruce, are needed to test this hypothesis. Mastodons from one area that likely lacked spruce (California) had low $\delta^{15}\text{N}$ values relative to co-existing herbivores (Coltrain et al., 2004), so the effects of spruce on soil $\delta^{15}\text{N}$ values may not be a sufficient explanation. However, if low $\delta^{15}\text{N}$ values in Great Lakes mastodons are related to spruce forest environments, it may be possible to test the hypothesis of Dreimanis (1967; 1968) that the loss of preferred spruce habitats was a major factor in mastodon extinction within the Great Lakes region. That is, any mastodons that lived during times of diminished spruce habitats are expected to have relatively high $\delta^{15}\text{N}$ values.

Serially-sampled mastodon teeth exhibited regular periodicity in their $\delta^{13}\text{C}$ and $\delta^{18}\text{O}$ values, which record seasonal variations in diet and drinking water. We suggest that mastodon drinking water was primarily derived from precipitation, with little seasonal variability in the proportion of glacial meltwater input. We hypothesize that mammoth drinking water contained more glacial meltwater input, and make predictions for the $\delta^{18}\text{O}$ patterns of serially-sampled mammoth enamel that should be tested in future studies.

Mastodon diets changed seasonally, but different patterns characterized different individuals. Further isotopic studies of seasonal behaviours of modern herbivores living in C_3 environments are needed to clarify the factors responsible for the seasonal $\delta^{13}\text{C}$ variations in Great Lakes mastodons. The difference between the patterns obtained for Ontario mastodons versus the Hiscock mastodon, and the similarity of the latter to those of Hiscock mastodon tusks examined previously (Fisher and Fox, 2003), suggests that patterns characteristic of a specific location or time period may be identifiable. A greater number of contemporaneous specimens are needed to determine if there are characteristic patterns for different time periods in Ontario. Recent research has shown that climate and vegetation changed very rapidly during the Pleistocene (Hofreiter and Stewart, 2009). If the causes of within-tooth $\delta^{13}\text{C}$ variations can be ascertained, these methods have the potential for providing multi-year “snapshots” of animal behaviour at precise time intervals leading up to the time of extinction.

Stable isotope compositions in this study were useful for classifying mammoth and mastodon specimens of unknown provenance as local or non-local. For one non-local individual, a probable location of origin was determined. This study also has implications for future sampling of proboscidean teeth. First, it is possible that the latest-developing mastodon teeth may preserve an isotopic record of weaning; more detailed study of formation times is needed to test this hypothesis. Second, although mastodon teeth have lower crowns than mammoth teeth, the former also grow more slowly. This difference in growth rate should be taken into account when designing sampling methodologies.

6.5 References

- Agenbroad, L.D., 2005. North American proboscideans: Mammoths - the state of knowledge, 2003. *Quaternary International*, 126-28: 73-92.
- Ambrose, S.H., 1990. Preparation and characterization of bone and tooth collagen for isotopic analysis. *Journal of Archaeological Science*, 17(4): 431-451.
- Ambrose, S.H. and Norr, L., 1993. Experimental evidence for the relationship of the carbon isotope ratios of whole diet and dietary protein to those of bone collagen and carbonate. In: J.B. Lambert and G. Grupe (Editors), *Prehistoric Human Bone: Archaeology at the Molecular Level*. Springer-Verlag, Berlin, pp. 1-37.
- Amundson, R., Austin, A.T., Schuur, E.A.G., Yoo, K., Matzek, V., Kendall, C., Uebersax, A., Brenner, D. and Baisden, W.T., 2003. Global patterns of the isotopic composition of soil and plant nitrogen. *Global Biogeochemical Cycles*, 17(1): 1031, doi:10.1029/2002GB001903.
- Aranibar, J.N., Anderson, I.C., Epstein, H.E., Feral, C.J.W., Swap, R.J., Ramontsho, J. and Macko, S.A., 2008. Nitrogen isotope composition of soils, C-3 and C-4 plants along land use gradients in southern Africa. *Journal of Arid Environments*, 72(4): 326-337.
- Ayliffe, L.K., Lister, A.M. and Chivas, A.R., 1992. The preservation of glacial-interglacial climatic signatures in the oxygen isotopes of elephant skeletal phosphate. *Palaeogeography Palaeoclimatology Palaeoecology*, 99(3-4): 179-191.
- Barnosky, A.D., Koch, P.L., Feranec, R.S., Wing, S.L. and Shabel, A.B., 2004. Assessing the causes of Late Pleistocene extinctions on the continents. *Science*, 306(5693): 70-75.
- Bocherens, H., 2003. Isotopic biogeochemistry and the paleoecology of the mammoth steppe fauna. *Deinsea*, 9: 57-71.
- Bocherens, H., Pacaud, G., Lazarev, P.A. and Mariotti, A., 1996. Stable isotope abundances (^{13}C , ^{15}N) in collagen and soft tissues from Pleistocene mammals from Yakutia: Implications for the palaeobiology of the Mammoth Steppe. *Palaeogeography Palaeoclimatology Palaeoecology*, 126(1-2): 31-44.
- Bogaard, A., Heaton, T.H.E., Poulton, P. and Merbach, I., 2007. The impact of manuring on nitrogen isotope ratios in cereals: archaeological implications for reconstruction of diet and crop management practices. *Journal of Archaeological Science*, 34(3): 335-343.
- Bryant, J.D., Koch, P., Froelich, P.N., Showers, W.J. and Genna, B.J., 1996. Oxygen isotope partitioning between phosphate and carbonate in mammalian apatite. *Geochimica et Cosmochimica Acta*, 60(24): 5145-5148.
- Bumstead, N.L., Longstaffe, F.J. and Macdonald, R.A., 2009. The paleolimnology of Lake Simcoe: oxygen-isotope compositions of ostracodes 11th International Paleolimnology Symposium, Guadalajara, Mexico.
- Cerling, T.E. and Harris, J.M., 1999. Carbon isotope fractionation between diet and bioapatite in ungulate mammals and implications for ecological and paleoecological studies. *Oecologia*, 120(3): 347-363.
- Clementz, M.T., Fox-Dobbs, K., Wheatley, P.V., Koch, P.L. and Doak, D.F., 2009. Revisiting old bones: coupled carbon isotope analysis of bioapatite and collagen as an ecological and palaeoecological tool. *Geological Journal*, 44(5): 605-620.

- Codron, J., Codron, D., Lee-Thorp, J.A., Sponheimer, M., Bond, W.J., de Ruiter, D. and Grant, R., 2005. Taxonomic, anatomical, and spatio-temporal variations in the stable carbon and nitrogen isotopic compositions of plants from an African savanna. *Journal of Archaeological Science*, 32(12): 1757-1772.
- Coltrain, J.B., Harris, J.M., Cerling, T.E., Ehleringer, J.R., Dearing, M.D., Ward, J. and Allen, J., 2004. Rancho La Brea stable isotope biogeochemistry and its implications for the palaeoecology of late Pleistocene, coastal southern California. *Palaeogeography Palaeoclimatology Palaeoecology*, 205(3-4): 199-219.
- Commisso, R.G. and Nelson, D.E., 2010. Stable nitrogen isotopic examination of Norse sites in the Western settlement of Greenland. *Journal of Archaeological Science*, 37(6): 1233-1240.
- Coplen, T.B., 1994. Reporting stable hydrogen, carbon, and oxygen isotopic abundances. *Pure and Applied Chemistry*, 66: 271-276.
- Coplen, T.B., Brand, W.A., Gehre, M., Groning, M., Meijer, H.A.J., Toman, B. and Verkouteren, R.M., 2006. New guidelines for $\delta^{13}\text{C}$ measurements. *Analytical Chemistry*, 78(7): 2439-2441.
- Craine, J.M., Elmore, A.J., Aidar, M.P.M., Bustamante, M., Dawson, T.E., Hobbie, E.A., Kahmen, A., Mack, M.C., McLauchlan, K.K., Michelsen, A., Nardoto, G.B., Pardo, L.H., Penuelas, J., Reich, P.B., Schuur, E.A.G., Stock, W.D., Templer, P.H., Virginia, R.A., Welker, J.M. and Wright, I.J., 2009. Global patterns of foliar nitrogen isotopes and their relationships with climate, mycorrhizal fungi, foliar nutrient concentrations, and nitrogen availability. *New Phytologist*, 183(4): 980-992.
- Cummings, L.S. and Albert, R.M., 2007. Phytolith and starch analysis of Dent site mammoth teeth calculus: new evidence for Late Pleistocene mammoth diets and environments. In: R.H. Brunswig and B.L. Pitblado (Editors), *Frontiers in Colorado Paleoindian Archaeology: From the Dent Site to the Rocky Mountains*. University Press of Colorado, Boulder, pp. 185-192.
- Dansgaard, W., Johnsen, S.J., Clausen, H.B., Dahljensen, D., Gundestrup, N.S., Hammer, C.U., Hvidberg, C.S., Steffensen, J.P., Sveinbjornsdottir, A.E., Jouzel, J. and Bond, G., 1993. Evidence for general instability of past climate from a 250-kyr ice-core record *Nature*, 364(6434): 218-220.
- Dansgaard, W. and Tauber, H., 1969. Glacier oxygen-18 content and Pleistocene ocean temperatures. *Science*, 166(3904): 499-502.
- DeNiro, M.J., 1985. Post-mortem preservation and alteration of "in vivo" bone collagen ratios: implications for paleodietary analysis. *Nature*, 317: 806-809.
- Dirks, W., Bromage, T.G. and Agenbroad, L., 2010. The timing of molar lamellae formation in *Mammuthus columbi* and *Palaeoloxodon cypriotes* from dental histology., *The World of Mammoths: Vth International Conference on Mammoths and their Relatives*, Le Puy en Velay, France.
- Dongmann, G., Nurnberg, H.W., Forstel, H. and Wagener, K., 1974. Enrichment of H_2^{18}O in leaves of transpiring plants. *Radiation and Environmental Biophysics*, 11(1): 41-52.
- Dreimanis, A., 1967. Mastodons, their geologic age and extinctions in Ontario, Canada. *Canadian Journal of Earth Sciences*, 4: 663-675.
- Dreimanis, A., 1968. Extinction of mastodons in eastern North America: testing a new climatic-environmental hypothesis. *The Ohio Journal of Science*, 68(6): 337-352.

- Fisher, D.C. and Fox, D.L., 2003. Season of death and terminal growth histories of Hiscock mastodons. In: R.S. Laub (Editor), *The Hiscock Site: Late Pleistocene and Holocene Paleoecology and Archaeology of Western New York State: Proceedings of the Second Smith Symposium, held at the Buffalo Museum of Science, October 14-15, 2001*. Buffalo Society of Natural Sciences, Buffalo, pp. 83-101.
- Flanagan, L.B. and Ehleringer, J.R., 1991. Stable Isotope Composition of Stem and Leaf Water: Applications to the Study of Plant Water-Use. *Functional Ecology*, 5(2): 270-277.
- France, C.A.M., Zelanko, P.M., Kaufman, A.J. and Holtz, T.R., 2007. Carbon and nitrogen isotopic analysis of Pleistocene mammals from the Saltville Quarry (Virginia, USA): Implications for trophic relationships. *Palaeogeography Palaeoclimatology Palaeoecology*, 249(3-4): 271-282.
- Fuller, B.T., Fuller, J.L., Harris, D.A. and Hedges, R.E.M., 2006. Detection of breastfeeding and weaning in modern human infants with carbon and nitrogen stable isotope ratios. *American Journal of Physical Anthropology*, 129(2): 279-293.
- Fuller, B.T., Fuller, J.L., Sage, N.E., Harris, D.A., O'Connell, T.C. and Hedges, R.E.M., 2004. Nitrogen balance and $\delta^{15}\text{N}$: why you're not what you eat during pregnancy. *Rapid Communications in Mass Spectrometry*, 18(23): 2889-2896.
- Fuller, B.T., Fuller, J.L., Sage, N.E., Harris, D.A., O'Connell, T.C. and Hedges, R.E.M., 2005. Nitrogen balance and $\delta^{15}\text{N}$: why you're not what you eat during nutritional stress. *Rapid Communications in Mass Spectrometry*, 19(18): 2497-2506.
- Gebauer, G. and Schulze, E.D., 1991. Carbon and nitrogen isotope ratios in different compartments of a healthy and a declining *Picea-Abies* forest in the Fichtelgebirge, NE Bavaria *Oecologia*, 87(2): 198-207.
- Gobetz, K.E. and Bozarth, S.R., 2001. Implications for late Pleistocene mastodon diet from opal phytoliths in tooth calculus. *Quaternary Research*, 55(2): 115-122.
- Gonfiantini, R., Gratzu, S. and Tongiorgi, E., 1965. Oxygen isotopic composition of water in leaves, *Proceedings of the symposium on the use of isotopes and radiation in soil-plant nutrition studies, 28 June-2 July, 1965, Ankara, Turkey*. International Atomic Energy Agency, Vienna, pp. 405-410.
- Green, J.L., Semprebon, G.M. and Solounias, N., 2005. Reconstructing the palaeodiet of Florida *Mammuthus americanus* via low-magnification stereomicroscopy. *Palaeogeography Palaeoclimatology Palaeoecology*, 223(1-2): 34-48.
- Guthrie, R.D., 2001. Origin and causes of the mammoth steppe: a story of cloud cover, woolly mammal tooth pits, buckles, and inside-out Beringia. *Quaternary Science Reviews*, 20(1-3): 549-574.
- Harington, C.R. and Ashworth, A.C., 1986. A mammoth (*Mammuthus primigenius*) tooth from Late Wisconsin deposits near Embden, North-Dakota, and comments on the distribution of woolly mammoths south of the Wisconsin ice sheets. *Canadian Journal of Earth Sciences*, 23(7): 909-918.
- Harington, C.R., Grant, D.R. and Mott, R.J., 1993. The Hillsborough, New Brunswick, mastodon and comments on other Pleistocene mastodon fossils from Nova Scotia. *Canadian Journal of Earth Sciences*, 30: 1242-1253.

- Haynes, G., 1991. *Mammoths, mastodons, and elephants: biology, behavior, and the fossil record*. Cambridge University Press, Cambridge New York, 413 pp.
- Haynes, G., 2002. The catastrophic extinction of North American mammoths and mastodons. *World Archaeology*, 33(3): 391-416.
- Heaton, T.H.E., 1987. The $^{15}\text{N}/^{14}\text{N}$ ratios of plants in South Africa and Namibia: Relationship to climate and coastal saline environments. *Oecologia*, 74(2): 236-246.
- Henderson, A.K. and Shuman, B.N., 2009. Hydrogen and oxygen isotopic compositions of lake water in the western United States. *Geological Society of America Bulletin*, 121(7-8): 1179-1189.
- Hillson, S., 1996. *Dental Anthropology*. Cambridge University Press, Cambridge, 373 pp.
- Hillson, S., 2005. *Teeth*. Cambridge manuals in archaeology. Cambridge University Press, Cambridge, UK ; New York, 373 pp.
- Hladyniuk, R. and Longstaffe, F.J., 2009. Paleolimnology of Lake Ontario: An assessment of meltwater influx using the oxygen-isotope composition of ostracodes, 11th International Paleolimnology Symposium Guadalajara, Mexico.
- Hladyniuk, R. and Longstaffe, F.J., 2010. Paleolimnology of Lake Ontario: an assessment of glacial meltwater influx, AGU Fall Meeting, San Francisco, USA.
- Hobbie, E.A. and Werner, R.A., 2004. Intramolecular, compound-specific, and bulk carbon isotope patterns in C-3 and C-4 plants: a review and synthesis. *New Phytologist*, 161(2): 371-385.
- Hobson, K.A., Alisauskas, R.T. and Clark, R.G., 1993. Stable-isotope enrichment in avian tissues due to fasting and nutritional stress: Implications for isotopic analyses of diet *Condor*, 95(2): 388-394.
- Hofreiter, M. and Stewart, J., 2009. Ecological change, range fluctuations and population dynamics during the Pleistocene. *Current Biology*, 19(14): R584-R594.
- Huddart, P.A., Longstaffe, F.J. and Crowe, A.S., 1999. δD and $\delta^{18}\text{O}$ evidence for inputs to groundwater at a wetland coastal boundary in the southern Great Lakes region of Canada. *Journal of Hydrology*, 214(1-4): 18-31.
- Hyodo, A., 2010. *The Holocene paleolimnology of Lake Superior*, The University of Western Ontario, London, 353 pp.
- Iacumin, P., Bocherens, H., Mariotti, A. and Longinelli, A., 1996. Oxygen isotope analyses of co-existing carbonate and phosphate in biogenic apatite: a way to monitor diagenetic alteration of bone phosphate? *Earth and Planetary Science Letters*, 142: 1-6.
- Iacumin, P., Nikolaev, V. and Ramigni, M., 2000. C and N stable isotope measurements on Eurasian fossil mammals, 40 000 to 10 000 years BP: Herbivore physiologies and palaeoenvironmental reconstruction. *Palaeogeography Palaeoclimatology Palaeoecology*, 163(1-2): 33-47.
- IAEA/WMO, 2010. *Global Network of Isotopes in Precipitation*. The GNIP Database. Accessible at: <http://www.iaea.org/water>.
- Koch, P., 1989. *Paleobiology of Late Pleistocene mastodons and mammoths from southern Michigan and western New York*, The University of Michigan, 280 pp.
- Koch, P.L., 1991. The isotopic ecology of Pleisocene proboscideans. *Journal of Vertebrate Paleontology*, 11(Suppl. 3): 40A.
- Koch, P.L., 1998. Isotopic reconstruction of past continental environments. *Annual Review of Earth and Planetary Sciences*, 26: 573-613.

- Koch, P.L. and Barnosky, A.D., 2006. Late Quaternary extinctions: State of the debate. *Annual Review of Ecology Evolution and Systematics*, 37: 215-250.
- Koch, P.L., Diffenbaugh, N.S. and Hoppe, K.A., 2004. The effects of late Quaternary climate and pCO₂ change on C₄ plant abundance in the south-central United States. *Palaeogeography Palaeoclimatology Palaeoecology*, 207(3-4): 331-357.
- Koch, P.L., Fisher, D.C. and Dettman, D., 1989. Oxygen isotope variation in the tusks of extinct proboscideans: a measure of season of death and seasonality. *Geology*, 17: 515-519.
- Koch, P.L., Hoppe, K.A. and Webb, S.D., 1998. The isotopic ecology of late Pleistocene mammals in North America - Part 1. Florida. *Chemical Geology*, 152(1-2): 119-138.
- Koch, P.L., Tuross, N. and Fogel, M.L., 1997. The effects of sample treatment and diagenesis on the isotopic integrity of carbonate in biogenic hydroxylapatite. *Journal of Archaeological Science*, 24(5): 417-429.
- Laub, R.S., 2003. The Hiscock site: structure, stratigraphy and chronology. In: R.S. Laub (Editor), *The Hiscock Site: Late Pleistocene and Early Holocene Paleoecology and Archaeology of Western New York State: Proceedings of the Second Smith Symposium, held at the Buffalo Museum of Science, October 14-15, 2001*. *Bulletin of the Buffalo Society of Natural Sciences*, vol. 37, Buffalo, NY, pp. 18-38.
- Laws, R.M., 1966. Age criteria for the African elephant, *Loxodonta a. africana*. *East African Wildlife Journal*, 4: 1-37.
- Lee, P.C. and Moss, C.J., 1986. Early maternal investment in male and female African elephant calves. *Behavioral Ecology and Sociobiology*, 18(5): 353-361.
- Lepper, B.T., Frolking, T.A., Fisher, D.C., Goldstein, G., Sanger, J.E., Wymer, D.A., Ogden, J.G. and Hooge, P.E., 1991. Intestinal contents of a Late Pleistocene mastodont from midcontinental North America. *Quaternary Research*, 36(1): 120-125.
- Lewis, C.F.M. and Anderson, T.W., 1992. Stable isotope (O and C) and pollen trends in eastern Lake Erie, evidence for a locally-induced climatic reversal of Younger Dryas age in the Great Lakes basin. *Climate Dynamics*, 6(3-4): 241-250.
- Lewis, C.F.M., Moore, T.C., Rea, D.K., Dettman, D.L., Smith, A.M. and Mayer, L.A., 1994. Lakes of the Huron Basin: Their record of runoff from the Laurentide Ice Sheet. *Quaternary Science Reviews*, 13(9-10): 891-922.
- Lowdon, J.A. and Blake, W., 1968. Geological Survey of Canada Radiocarbon Dates VII. *Radiocarbon*, 10(2): 207-245.
- Macdonald, R.A. and Longstaffe, F.J., 2007. The oxygen and hydrogen isotope compositions of the Great Lakes, International Association for Great Lakes Research (IAGLR) 50th Annual Conference, Pennsylvania State University, University Park, Pennsylvania, pp. 117-118.
- MacFadden, B.J. and Cerling, T.E., 1996. Mammalian herbivore communities, ancient feeding ecology, and carbon isotopes: A 10 million-year sequence from the Neogene of Florida. *Journal of Vertebrate Paleontology*, 16(1): 103-115.
- Makarov, M.I., 2009. The nitrogen isotopic composition in soils and plants: Its use in environmental studies (A Review). *Eurasian Soil Science*, 42(12): 1335-1347.
- Mariotti, A., 1983. Atmospheric nitrogen is a reliable standard for natural ¹⁵N abundance measurements. *Nature*, 303: 685-687.

- McAndrews, J.H., 2003. Postglacial ecology of the Hiscock site. In: R.S. Laub (Editor), *The Hiscock Site: Late Pleistocene and Early Holocene Paleoecology and Archaeology of Western New York State: Proceedings of the Second Smith Symposium*, held at the Buffalo Museum of Science, October 14-15, 2001. Buffalo Society of Natural Sciences, Buffalo, pp. 190-198.
- McAndrews, J.H. and Jackson, L.J., 1988. Age and environment of Late Pleistocene mastodont and mammoth in southern Ontario. In: R.S. Laub, N.G. Miller and D.W. Steadman (Editors), *Late Pleistocene and Early Holocene Paleoecology and Archeology of the Eastern Great Lakes Region: Proceedings of the Smith Symposium*. Bulletin of the Buffalo Society of Natural Sciences. Buffalo Society of Natural Sciences, Buffalo, pp. 161-172.
- McCue, M.D. and Pollock, E.D., 2008. Stable isotopes may provide evidence for starvation in reptiles. *Rapid Communications in Mass Spectrometry*, 22(15): 2307-2314.
- Mead, J.I., Agenbroad, L.D., Davis, O.K. and Martin, P.S., 1986. Dung of *Mammuthus* in the arid southwest, North America. *Quaternary Research*, 25(1): 121-127.
- Mekota, A.M., Grupe, G., Ufer, S. and Cuntz, U., 2006. Serial analysis of stable nitrogen and carbon isotopes in hair: monitoring starvation and recovery phases of patients suffering from anorexia nervosa. *Rapid Communications in Mass Spectrometry*, 20(10): 1604-1610.
- Metcalfe, J.Z., Longstaffe, F.J. and Zazula, G.D., 2010. Nursing, weaning, and tooth development in woolly mammoths from Old Crow, Yukon, Canada: Implications for Pleistocene extinctions. *Palaeogeography Palaeoclimatology Palaeoecology*, 298: 257-270.
- Metcalfe, J.Z., White, C.D., Longstaffe, F.J., Wrobel, G., Cook, D.C. and Pyburn, K.A., 2009. Isotopic evidence for diet at Chau Hiix, Belize: Testing regional models of hierarchy and heterarchy. *Latin American Antiquity*, 20(1): 15-36.
- Murphy, B.P. and Bowman, D., 2009. The carbon and nitrogen isotope composition of Australian grasses in relation to climate. *Functional Ecology*, 23(6): 1040-1049.
- Newsom, L.A. and Mihlbachler, M.C., 2006. Mastodons (*Mammuthus americanus*) diet foraging patterns based on analysis of dung deposits. In: S.D. Webb (Editor), *First Floridians and Last Mastodons: The Page-Ladson site in the Aucilla River*. Springer, pp. 263-331.
- Nielsen, E., Churcher, C.S. and Lammers, G.E., 1988. A woolly mammoth (*Proboscidea, Mammuthus primigenius*) molar from the Hudson Bay Lowland of Manitoba. *Canadian Journal of Earth Sciences*, 25: 933-938.
- Ometto, J.P.H.B., Ehleringer, J.R., Domingues, T.F., Berry, J.A., Ishida, F.Y., Mazzi, E., Higuchi, N., Flanagan, L.B., Nardoto, G.B. and Martinelli, L.A., 2006. The stable carbon and nitrogen isotopic composition of vegetation in tropical forests of the Amazon Basin, Brazil. *Biogeochemistry*, 79(1-2): 251-274.
- Owen-Smith, R.N., 1988. *Megaherbivores: the influence of very large body size on ecology*. Cambridge studies in ecology. Cambridge University Press, Cambridge, 369 pp.
- Pilny, J.J., Morgan, A.V. and Morgan, A., 1987. Paleoclimatic implications of a Late Wisconsinan insect assemblage from Rostock, southwestern Ontario. *Canadian Journal of Earth Sciences*, 24: 617-630.

- Polischuk, S.C., Hobson, K.A. and Ramsay, M.A., 2001. Use of stable-carbon and -nitrogen isotopes to assess weaning and fasting in female polar bears and their cubs. *Canadian Journal of Zoology-Revue Canadienne De Zoologie*, 79(3): 499-511.
- Rea, D.K., Moore, T.C., Anderson, T.W., Lewis, C.F.M., Dobson, D.M., Dettman, D.L., Smith, A.J. and Mayer, L.A., 1994. Great Lakes paleohydrology: complex interplay of glacial meltwater, lake levels, and sill depths. *Geology*, 22(12): 1059-1062.
- Rountrey, A.N., Fisher, D.C., Vartanyan, S. and Fox, D.L., 2007. Carbon and nitrogen isotope analyses of a juvenile woolly mammoth tusk: Evidence of weaning. *Quaternary International*, 169: 166-173.
- Rozanski, K., Araguas-Araguas, L. and Gonfiantini, R., 1993. Isotopic patterns in modern global precipitation. In: P.K. Swart, J. McKenzie, K.C. Lohmann and S. Savin (Editors), *Climate Change in Continental Isotope Records*. AGU Geophysical Monograph. American Geophysical Union, Washington, DC, pp. 1-36.
- Saunders, J.J., 1977. Late Pleistocene vertebrates of the Western Ozark Highland, Missouri.
- Saunders, J.J., Grimm, E.C., Widga, C.C., Campbell, G.D., Curry, B.B., Grimley, D.A., Hanson, P.R., McCullum, J.P., Oliver, J.S. and Treworgy, J.D., 2010. Paradigms and proboscideans in the southern Great Lakes region, USA. *Quaternary International*, 217(1-2): 175-187.
- Schmidt, S. and Stewart, G.R., 2003. $\delta^{15}\text{N}$ values of tropical savanna and monsoon forest species reflect root specialisations and soil nitrogen status. *Oecologia*, 134(4): 569-577.
- Schulze, E.D., Chapin, F.S. and Gebauer, G., 1994. Nitrogen nutrition and isotope differences among life forms at the northern treeline of Alaska. *Oecologia*, 100(4): 406-412.
- Schwarcz, H.P., Dupras, T.L. and Fairgrieve, S.I., 1999. ^{15}N enrichment in the Sahara: In search of a global relationship. *Journal of Archaeological Science*, 26(6): 629-636.
- Sima, A., Paul, A., Schulz, M. and Oerlemans, J., 2006. Modeling the oxygen-isotopic composition of the North American Ice Sheet and its effect on the isotopic composition of the ocean during the last glacial cycle. *Geophysical Research Letters*, 33(15): 5.
- Smith, T.M., Reid, D.J. and Sirianni, J.E., 2006. The accuracy of histological assessments of dental development and age at death. *Journal of Anatomy*, 208(1): 125-138.
- Sponheimer, M., Robinson, T., Ayliffe, L., Roeder, B., Hammer, J., Passey, B., West, A., Cerling, T., Dearing, D. and Ehleringer, J., 2003. Nitrogen isotopes in mammalian herbivores: Hair $\delta\text{N-15}$ values from a controlled feeding study. *International Journal of Osteoarchaeology*, 13(1-2): 80-87.
- Stewart, G.R., Turnbull, M.H., Schmidt, S. and Erskine, P.D., 1995. ^{13}C natural abundance in plant communities along a rainfall gradient: A biological integrator of water availability. *Australian Journal of Plant Physiology*, 22(1): 51-55.
- Sukumar, R., 1989. *The Asian elephant: ecology and management*. Cambridge studies in applied ecology and resource management. Cambridge University Press, Cambridge, 251 pp.
- Sukumar, R., 2003. *The living elephant: evolutionary ecology, behavior, and conservation*. Oxford University Press, Oxford, 478 pp.

- Tieszen, L.L., 1991. Natural variations in the carbon isotope values of plants: Implications for archaeology, ecology, and paleoecology. *Journal of Archaeological Science*, 18: 227-248.
- Tieszen, L.L. and Boutton, T.W., 1989. Stable carbon isotopes in terrestrial ecosystem research. *Ecological Studies*, 68: 167-195.
- Ukrainitseva, V.V., Agenbroad, L.D. and Mead, J.I., 1996. Palaeoenvironmental research biotic records: A palaeoenvironmental reconstruction of the "Mammoth Epoch" of Siberia. In: F.H. West (Editor), *American beginnings: The prehistory and palaeoecology of Beringia*. University of Chicago Press, Chicago, pp. 129-136.
- Van Der Merwe, N.J. and Medina, E., 1991. The canopy effect, carbon isotope ratios and foodwebs in Amazonia. *Journal of Archaeological Science*, 18(3): 249-260.
- van Geel, B., Aptroot, A., Baittinger, C., Birks, H.H., Bull, I.D., Cross, H.B., Evershed, R.P., Gravendeel, B., Kompanje, E.J.O., Kuperus, P., Mol, D., Nierop, K.G.J., Pals, J.P., Tikhonov, A.N., van Reenen, G. and van Tienderen, P.H., 2008. The ecological implications of a Yakutian mammoth's last meal. *Quaternary Research*, 69(3): 361-376.
- van Geel, B., Guthrie, R.D., Altmann, J.G., Broekens, P., Bull, I.D., Gill, F.L., Jansen, B., Nieman, A.M. and Gravendeel, B., 2010. Mycological evidence of coprophagy from the feces of an Alaskan Late Glacial mammoth. *Quaternary Science Reviews*, In Press, Corrected Proof.
- van Klinken, G.J., 1999. Bone collagen quality indicators for paleodietary and radiocarbon measurements. *Journal of Archaeological Science*, 26(687-695).
- Vesterdal, L., Schmidt, I.K., Callesen, I., Nilsson, L.O. and Gundersen, P., 2008. Carbon and nitrogen in forest floor and mineral soil under six common European tree species. *Forest Ecology and Management*, 255(1): 35-48.
- Wang, L.X., D'Odorico, P., Ries, L. and Macko, S.A., 2010. Patterns and implications of plant-soil $\delta^{13}\text{C}$ and $\delta^{15}\text{N}$ values in African savanna ecosystems. *Quaternary Research*, 73(1): 77-83.
- Warinner, C. and Tuross, N., 2010. Brief communication: Tissue isotopic enrichment associated with growth depression in a pig: Implications for archaeology and ecology. *American Journal of Physical Anthropology*, 141(3): 486-493.
- Waters-Rist, A.L. and Katzenberg, M.A., 2010. The effect of growth on stable nitrogen isotope ratios in subadult bone collagen. *International Journal of Osteoarchaeology*, 20(2): 172-191.
- Waters, M.R. and Stafford, T.W., 2007. Redefining the age of Clovis: Implications for the peopling of the Americas. *Science*, 315(5815): 1122-1126.
- Yoneyama, T., Okada, H. and Ando, S., 2010. Seasonal variations in natural ^{13}C abundances in C_3 and C_4 plants collected in Thailand and the Philippines. *Soil Science and Plant Nutrition*, 56(3): 422-426.
- Yu, Z.C., 2000. Ecosystem response to lateglacial and early holocene climate oscillations in the Great Lakes region of North America. *Quaternary Science Reviews*, 19(17-18): 1723-1747.
- Zazula, G.D., Telka, A.M., Harington, C.R., Schweger, C.E. and Mathewes, R.W., 2006. New spruce (*Picea* spp.) macrofossils from Yukon Territory: Implications for Late Pleistocene refugia in Eastern Beringia. *Arctic*, 59(4): 391-400.

Chapter 7

Paleoclimate and paleoenvironment of Pleistocene Western Canada (Yukon, Alberta, British Columbia) inferred from mammoth and mastodon skeletal remains

7.1 Introduction

Skeletal remains of mammoths and mastodons have been found throughout western Canada, including Beringia (the unglaciated area between Siberia and northwest North America), central Alberta, and coastal British Columbia. However, mammoths and mastodons were extinct throughout mainland North America by the end of the Pleistocene (ca. 11,000-10,000 BP) (Agenbroad, 2005; Waters and Stafford, 2007). Explanations for Late Pleistocene megafaunal extinctions have been vigorously debated for decades. Most researchers argue that climate change and/or human hunting were the decisive factors, but there is still no general consensus (Barnosky et al., 2004; Haynes, 2009; Koch and Barnosky, 2006). Megafaunal extinctions were not globally synchronous (Kuzmin, 2010), so local chronologies of climate change, vegetational shifts, and human dispersals must be considered when evaluating explanatory models. In Alaska and Yukon, many species (including mastodon) seem to have become extinct prior to the Last Glacial Maximum (LGM; ca. 18,000 BP), others (including mammoths) became extinct just prior to the Holocene (sometime after 11,500 BP), and still others (e.g., bison) survived the Pleistocene-Holocene transition (Guthrie, 2006). Using patterns of radiocarbon dates and pollen profiles, Guthrie (2006) rejected “paleo-disease” (Lyons et al., 2004; MacPhee and Marx, 1997; MacPhee et al., 2002; Rothschild and Laub, 2006), “keystone species” (Zimov et al., 1995), and “Blitzkrieg overkill” (Martin, 1984) extinction hypotheses for Alaska-Yukon. He shows that radical ecological restructuring (including extinction of some species and expansion of others) took place in the context of dramatic climatic and vegetational changes. In order to understand megafaunal responses to climate and vegetational shifts, it is important to understand differences in megafaunal diets and habitats both within and among regions.

In general, it is believed that mammoths were primarily grazers that occupied open steppe-tundra environments, whereas mastodons were primarily browsers that preferred wetter, more forested environments. However, recent research has shown that

these assumptions are not universally valid (Cummings and Albert, 2007; Gobetz and Bozarth, 2001; Saunders et al., 2010; van Geel et al., 2008). In this paper, we examine regional differences in the isotopic compositions of proboscidean (mammoth and mastodon) skeletal remains from Yukon, Alberta, and British Columbia, which can provide insights into dietary and climatic variations over time and space. We explore the isotopic records of proboscidean diet and drinking water using “bulk” analyses, which integrate a period of several years, and “incremental” analyses, which allow the reconstruction of seasonal variations. We examine evidence for environmental niche partitioning between mammoths and mastodons, as done previously for specimens from the Great Lakes region (Chapter 6). Finally, we present new radiocarbon dates for Western Canada proboscideans, and explore tissue-dependent differences in proboscidean isotopic compositions. Ultimately, we aim to improve our understanding of the Late Pleistocene environments of western Canada and proboscidean paleobiology.

7.1.1 Late Pleistocene Environments in Yukon, Alberta, and British Columbia

The unglaciated portions of Yukon comprise the easternmost portion of Beringia as it is currently defined (Hoffecker and Elias, 2003). During the Pleistocene, much of the Holarctic, including Beringia, was covered by a vast “mammoth steppe”. This environment was characterized by a relatively uniform large mammal community (including woolly mammoth, *Mammuthus primigenius*; horse, *Equus* sp.; and bison, *Bison* sp.) and much more arid conditions than exist in the north today (Guthrie, 2001). Despite these generalities, considerable climatic and ecological variations existed on temporal (e.g., stadial versus interstadial), regional (e.g., east versus west) and local scales (e.g., valley bottoms versus upland plains) (Anderson and Lozhkin, 2001; Elias et al., 1997; Guthrie, 1990; Szpak et al., 2010; Zazula et al., 2006a, 2007). Central Beringia (the region containing the Bering Land Bridge) has been hypothesized to be more mesic, acting as a “buckle” to prevent some xeric-adapted species from crossing from Asia to the Americas (i.e., woolly rhinoceros, *Coelodonta antiquitatus*) or from the Americas into Asia (i.e., camel, *Camelops*) (Guthrie, 2001). Eastern Beringia (Alaska and Yukon) was generally colder and drier than central Beringia. Vegetation was dominated by sage (*Artemisia*), grass (Poaceae) and forbs, comprising a productive, open-grassland

ecosystem (Zazula et al., 2003). However, this xeric steppe was interspersed with higher-elevation herb-tundra, midslope steppe-tundra, mesic graminoid meadows, and riparian grassy meadows (Zazula et al., 2006a, 2006b). Trees were relatively rare even during interstadials (Anderson and Lozhkin, 2001; Bigelow et al., 2003), but present in at least some local habitats, such as valley bottoms (Zazula et al., 2006c).

Studies of glacial features and faunal distributions demonstrate that central Alberta was unglaciated throughout most of the Pleistocene, with complete coalescence of the Cordilleran and Laurentide Ice Sheets occurring only during the LGM, between about 22,000 and 12,000 BP (Burns, 1996, 2010; Burns and Young, 1994; Catto et al., 1996; Young et al., 1994). Prior to the LGM, Alberta large mammal communities in the unglaciated interior of Alberta were dominated by mammoth, bison and horse (Burns, 2010), which suggests at least superficially similar environmental conditions to eastern Beringia (i.e., cool, dry, open grasslands). Alberta was a key part of the “biogeographical corridor” linking Eastern Beringia and the areas south of the continental ice sheets (MacDonald and McLeod, 1996), facilitating interchange between fauna from the two regions (Burns, 2010; Matheus et al., 2004; Shapiro et al., 2004). Pollen evidence suggests that after the last glaciation (ca. 12,000 to 10,000 BP), central Alberta was relatively cool and dry, with vegetation dominated by herbs, grasses, and deciduous shrubs, and very few trees (MacDonald and McLeod, 1996; Mandryk, 1996). At the same time, spruce woodlands and steppe parklands were present in the eastern- and western-central portions of the province (MacDonald and McLeod, 1996; Mandryk, 1996). By 10,000 BP, spruce had expanded to form a continuous and closed forest throughout most of the region, effectively closing the biogeographical corridor to most large-bodied grazers (Beaudoin and Oetelaar, 2003; Beaudoin et al., 1996; MacDonald and McLeod, 1996). Similar transitions from open grasslands to spruce woodlands may have occurred during previous glacial-interglacial transitions (MacDonald and McLeod, 1996). However, there is little direct evidence for climatic and vegetational dynamics in Alberta prior to the LGM.

Mammoth, horse, and bison also lived on the central and southern mainland of British Columbia prior to the LGM (Keddie, 1979). These taxa also inhabited Vancouver Island, which they may have reached either during interglacial periods (by crossing the

large floodplains that filled the Strait of Georgia) or during glacial periods, when sea levels were considerably lower (Fedje and Josenhans, 2000; Harington, 1975; Josenhans et al., 1997). Pollen evidence suggests that around 43,000 BP, the climate on Vancouver Island was warmer and/or drier than at present, with a gradual shift to cooler and wetter conditions until 25,000 BP (Keddie, 1979). From 25,000 to 19,000 BP, major climatic cooling and glacial advance over the Coast Mountains occurred (Keddie, 1979). A giant short-faced bear (*Arctodus simus*) ulna, radiocarbon dated to $22,750 \pm 140$ BP, was found on Vancouver Island in a context similar to that of the specimens discussed in the present study (Steffen and Harington, 2010). Steffen and Harington (2010) argue that the animal occupied an open, periglacial coastal plain characterized by parkland, cold steppe grassland, or heath-adapted species. Glacial ice reached its maximum extent in coastal British Columbia around 16,000 BP (Menounos et al., 2009), which likely resulted in local extirpations of previously abundant taxa (Steffen and Harington, 2010). Ice-free terrains were again present on the B.C. coast by $13,790 \pm 150$ BP (Fedje and Josenhans, 2000; Hetherington et al., 2003). After deglaciation, pioneering vegetation was likely herb tundra (Lacourse, 2005; Lacourse et al., 2005). Between 12,200 and 11,700 BP, an open woodland environment dominated by pine (*Pinus contorta*) existed on northern Vancouver Island (Lacourse, 2005), and the continental shelf was dry, connecting modern islands to the mainland (Hetherington et al., 2004). Between 12,000 and 11,000 BP, herb- and shrub- dominated landscapes associated with the bones of mastodon, caribou, and bison existed on the mainland south and east of Vancouver Island (Petersen et al., 1983; Wilson et al., 2009), and vegetation on the Island was a mixed conifer woodland dominated by spruce (*Picea*) and hemlock (*Tsuga*) (Lacourse, 2005).

For each of these regions, pre-LGM environmental records can be difficult to obtain. Traditional environmental proxies such as pollen and plant macrofossils have the advantage of providing continuous records of environmental change, but the disadvantage of considerable time-averaging (often on the order of hundreds to thousands of years). Stable isotope analyses of faunal remains cannot provide continuous records, but can provide “snapshots” of seasonal variations that occurred within shorter windows of time than are usually possible using other proxies (i.e., monthly or yearly variations). In this paper, we focus on the complementary evidence that isotopic compositions of mammoth

and mastodon skeletal materials can bring to understanding Pleistocene environmental conditions in Yukon, Alberta, and British Columbia prior to the LGM.

7.2 Materials and Methods

Mammoth and mastodon skeletal remains (bone, enamel, and dentin from molar crowns, roots, and tusks) were obtained from museum collections, representing a number of geographical locations within western Canada (Table 7.1, Figure 7.1). Alberta specimens were obtained from gravel deposits, mostly in the Edmonton and Villeneuve areas (Burns and Young, 1994; Young et al., 1994). One specimen was found further south in Cochrane, near Calgary (Churcher, 1968; Stalker, 1968), and another north-west of Edmonton, near Bezanson. Yukon specimens were also found in secondary depositional contexts, having been transported from their original locations. Old Crow specimens were mostly recovered from the surface of modern alluvial point bars along the Old Crow River, having been removed and transported from primary Pleistocene fossil-bearing sediment exposures (Chapter 3) (Metcalf et al., 2010). Klondike specimens were recovered from perennially frozen silt and gravel deposits uncovered during placer mining activity in the Klondike goldfields region. Herschel Island specimens were recovered from beach deposits concentrated at Simpson Point, near Pauline Cove (Zazula et al., 2009). Most of the British Columbia specimens were found in Quadra sand deposits at Cordova Bay, near Victoria (Keddie, 1979). One additional specimen was found in northern British Columbia, but more detailed contextual information was unavailable.

Adult teeth and bones were selected for analysis. Sampling, collagen extraction, bioapatite carbonate pretreatment, microdrilling, and analytical instrumentation were conducted as described in Chapters 3-5. Stable isotope results are presented in standard delta (δ) notation, in units of per mil (‰), relative to VSMOW (oxygen), VPDB (carbon), and AIR (nitrogen) (Coplen, 1994; Coplen et al., 2006; Mariotti, 1983). Precision and accuracy for δ -values, %C, %N, and C/N ratios are as described in Chapters 3-5. Diet $\delta^{13}\text{C}$ values are calculated assuming an enrichment of 5‰ between collagen and diet (Ambrose and Norr, 1993; Koch, 1998), and an enamel-diet fractionation factor (α) of



Figure 7.1 Locations of origin for specimens discussed in this study. VI = Vancouver Island, C = Cochrane, E/V = Edmonton/Villeneuve, B = Bezanson, K = Klondike, OC = Old Crow, H = Herschel Island. Adapted from <http://jan.ucc.nau.edu>

Table 7.1 Sample information.

Specimen										Radiocarbon		
LSIS #	Source	Museum #	Taxon	Area	Site	Tissues used	Bone	Tooth	Date	Lab #	Ref	
British Columbia												
BC5	RBCM	EH1994.003.0040	Proboscidea	Vanc. Island	Cordova Bay	B	humerus		17,000 ± 240	GSC-2829	1	
BC3-1	RBCM	EH1994.003.0039	Proboscidea	Vanc. Island	Cordova Bay	T		tusk			1	
BC1	RBCM	EH2009.008.0001	Proboscidea	Vanc. Island	Island View Beach	T		tusk				
BC2	RBCM	EH1994.003.0041	Proboscidea	Vanc. Island	Cordova Bay	T^		tusk			1	
BC4	UWO		Proboscidea	Northern BC		T		tusk				
Alberta												
AB1	RAM	P97.11.1B	<i>Mammuthus</i>	Edmonton	Riverview Pit	B, D, C, E		mandibular symphysis	LLM6	43,300 ± 3000		2
AB2	RAM	P94.1.698	<i>Mammuthus</i>	Edmonton	Consolidated Concrete Pit 48	D, C, E			URM5	>37,700	AA84996	2, 3
AB4	RAM	P94.16.1B	<i>Mammut</i>	Edmonton	Apex Galloway Pit	B, D, E, P		mandible (ascending ramus)	LRM5			3
AB5	RAM	P90.7.1	<i>Mammuthus</i>	Villeneuve	Alberta Conceret Products Ltd.	D, C, E			ULM6			4
AB11	RAM	P00.2.1	<i>Mammuthus</i>	Bezanson	Smoky River	D, C, E			LRM4/M5	40,000 ± 3500	AA84979	
AB6	RAM	P94.4.3	<i>Mammuthus</i>	Villeneuve	Consolidated Concrete Pit 46	D, C^, E			LLM6			3
AB10	RAM	P97.7.1	<i>Mammut</i>	Villeneuve	Consolidated Concrete Pit 46	D, P, E			LLM6	>41,100	AA84997	3
AB3	RAM	P94.1.427	Proboscidea	Edmonton	Consolidated Concrete Pit 48	B		left innominate				2, 3
AB7	RAM	P91.11.9	Proboscidea	Villeneuve	Consolidated Concrete Pit 46	B		cortical				3
AB8	RAM	P94.4.1	Proboscidea	Villeneuve	Consolidated Concrete Pit 46	B		right scapula				3
AB12	RAM	P96.12.1	Proboscidea	Cochrane	Burnco Pit	B		humerus (deltoid tuberosity)		10,760 ± 160; 11,370 ± 170		5
AB9	RAM	P94.4.2	<i>Mammuthus</i>	Villeneuve	Consolidated Concrete Pit 46	C^			URM6			3
Yukon												
YT30	YG	302.26	<i>Mammuthus</i>	Klondike	Skookum Gulch	B, E		mandible	M5/M6	>39,200	AA84983	
YT31	YG	2.4	<i>Mammuthus</i>	Klondike	Hester Creek	B, E		mandible	M6?	27380 ± 730	AA85000	
YT27	YG	29.248	<i>Mammuthus</i>	Klondike	Hunker Creek	B		mandible		43500 ± 1900	UCIAMS41493	6
YT29	YG	358.1	<i>Mammuthus</i>	Klondike		B, E		mandible	M6			
YT49	YG	5.46	<i>Mammuthus</i>	Klondike	Hunker Creek	B		rib		22430 ± 140	UCIAMS41487	6
YT28a,b	YG	6.51, 6.49	<i>Mammuthus</i>	Klondike	Gold Run Creek	B, E		mandible	LLM6,LRM6	17950 ± 120	Beta 70099	
YT47	YG	2.7	<i>Mammuthus</i>	Klondike	Hester Creek	B		fibula		27540 ± 270	UCIAMS 41488	6
YT48	YG	133.21	<i>Mammuthus</i>	Klondike	Whitman Gulch	B		right tibia		34180 ± 590	UCIAMS41489	6
YT26	YG	2.14	<i>Mammuthus</i>	Klondike	Hester Creek	C, E			adult	35500 ± 2000	AA84986	
YT25	YG	2.16	<i>Mammuthus</i>	Klondike	Hester Creek	C, E			adult			
YT32	YG	84.1	<i>Mammuthus</i>	Klondike	Hunker Creek	C, E			adult			
YT24	YG	78.1	<i>Mammuthus</i>	Klondike	Last Chance Creek	RD, E			M6	>48,800	UCIAMS41491	6
YT35	YG	26.1	<i>Mammut</i>	Klondike	Gold Run Creek	RD, E			M6	>50,300; >51,700	UCIAMS 78705, 78704	7
YT36	YG	50.1	<i>Mammut</i>	Klondike	Thistle Creek	RD, E			M5?	>41,100	AA84994	
YT37	YG	139.5	<i>Mammut</i>	Klondike	Unknown?	B, E		mandible	M6	>41,100	AA84985	
YT33	YG	159.83	<i>Mammut</i>	Klondike	Quartz Creek	B		fibula				
YT34	YG	43.2	<i>Mammut</i>	Klondike	Upper Gold Run	RD, E			M6	>49,200	UCIAMS75320	8*
(Keck)	CMN	33897	<i>Mammut</i>	Klondike	Sixtymile Loc. 5	RD/D			?	>51700	UCIAMS78694	8
(Keck)	CMN	11697	<i>Mammut</i>	Klondike	Dawson Loc. 19	RD/D			?	>51700	UCIAMS78698	8
(Keck)	CMN	42551	<i>Mammut</i>	Klondike	Sixtymile Loc. 3	RD/D			?	>51700	UCIAMS78699	8
(Keck)	CMN	8707	<i>Mammut</i>	Klondike	Dawson	RD/D			?	>51700	UCIAMS78700	8
(Keck)	CMN	333	<i>Mammut</i>	Klondike	McQuesten Creek	RD/D			?	40,600 ± 1000	UCIAMS78701	8

Table 7.1 cont.

Specimen										Radiocarbon		Ref
LSIS #	Source	Museum #	Taxon	Area	Site	Tissues used	Bone	Tooth	Date	Lab #		
(Keck)	CMN	42552	<i>Mammut</i>	Klondike	Sixtymile, Loc. 3	RD/D		?	>41,100	UCIAMS78703	8	
YT50	YG	219.3	<i>Mammuthus</i>	Stewart River	Ash Bend	B	long bone fragments					
YT51	YG	317.51	<i>Mammuthus</i>	Old Crow	CRH 11	T		tusk	MIS5, ~140,000			
YT5	YG	60.2	<i>Mammuthus</i>	Old Crow	OCR, Bluffs-R bank	RD, E		LRM5/M6			9	
YT1	YG	291.1	<i>Mammuthus</i>	Old Crow	Old Crow River	RD, E		LRM6	>41,100	AA84987	9	
YT2	YG	122.2	<i>Mammuthus</i>	Old Crow	CRH 94	RD, E		ULM6	>41,100	AA84992	9	
YT3	YG	173.5	<i>Mammuthus</i>	Old Crow	Ch'jee's Bluff	D, E		U M6			9	
YT4	YG	285.1	<i>Mammuthus</i>	Old Crow	OCR, REM 78-1	B, E		LRM6	>39,100	AA85002	9	
YT6	YG	57.1	<i>Mammuthus</i>	Old Crow	OCR, Bluffs-R bank	C, E		LRM6			9	
YT7	YG	325.22	<i>Mammuthus</i>	Old Crow	HH-68-10	B, E		ULM6	>40,100	AA84984	9	
YT9	YG	284.4	<i>Mammuthus</i>	Old Crow	CRH 11	C, E		ULM6			9	
YT10	YG	252.2	<i>Mammuthus</i>	Old Crow	CRH 20	RD, E		LLM6	>40,000	AA85001	9	
YT11	YG	173.1	<i>Mammuthus</i>	Old Crow	Ch'jee's Bluff	RD, C, E		U M6			9	
YT8	YG	357.1	<i>Mammut</i>	Old Crow	Old Crow River	D, E		M5/M6	>41,100	AA84995		
(Keck)	CMN	15352	<i>Mammut</i>	Old Crow	Loc. 14N	RD/D		?	45700 ± 2500	UCIAMS78695	8	
(Keck)	CMN	31898	<i>Mammut</i>	Old Crow	Loc. 74	RD/D		?	50300±3500	UCIAMS78696	8	
(Keck)	CMN	33066	<i>Mammut</i>	Old Crow	Loc. 46	RD/D		?	>49900	UCIAMS78697	8	
YT46	YG	271.93	<i>Mammuthus</i>	Herschel	Simpson Point	B	thoracic vertebra					
YT40	YG	68.4	<i>Mammuthus</i>	Herschel	Simpson Point	C, E		fragment	>35,900	AA84988		
YT39	YG	68.2	<i>Mammuthus</i>	Herschel	Simpson Point	D, E		fragment				
YT42	YG	12.9	Proboscidea	Herschel	Simpson Point	T		tusk	34100 ± 1,700	AA84999		
YT45	YG	68.1	Proboscidea	Herschel	Simpson Point	T		tusk	>39,400	AA84982		
YT41	YG	154.2	Proboscidea	Herschel	South Shore	T		tusk				
YT43	YG	206.29	Proboscidea	Herschel	Simpson Point	T		tusk				
YT44	YG	33.7	Proboscidea	Herschel	Simpson Point	T		tusk				
YT38	YG	33.3	<i>Mammut</i>	Herschel	Simpson Point	B	cuboid		>45 130	Beta 189291	10	

LSIS #: Sample ID used for Laboratory for Stable Isotope Science analyses, and referred to in this study

Source of skeletal materials: RBCM = Royal British Columbia Museum, RAM = Royal Alberta Museum, YG = Yukon Government, CMN = Canadian Museum of Nature.

Tissue: RD = root dentin, D = crown dentin, T = tusk dentin, B = bone, C = cementum, E = enamel

Keck/CMN samples were analyzed in a different study (Zazula et al., in prep) but are included for comparison

Radiocarbon dates in bold were obtained as part of the present study

^ insufficient collagen preservation; no data

* A previous date of 18460 ± 350 (TO-7745) for this specimen (Storer, 2002; Zazula et al., 2006) is now considered erroneous

References

- Keddie, 1979
- Burns and Young, 1994
- Young et al., 1994
- Burns et al., 2003
- Churcher, 1968; Stalker 1968, RAM fossil database
- Debruyne et al., 2008
- Dated to **39200 ± 3200 (AA84981)** as part of this study, but later redated as shown (Zazula et al., in prep)
- Zazula et al., in prep
- Metcalfe et al., 2010; Chapter 3, this thesis
- Zazula et al., 2009

1.0145 (Cerling and Harris, 1999). Drinking water $\delta^{18}\text{O}$ values are calculated as described in Chapter 5 (Ayliffe et al., 1992; Bryant et al., 1996; Iacumin et al., 1996). For one mammoth specimen (AB6), a “thin” section was prepared, incremental growth features were measured, and the crown extension rate was estimated as described in Chapter 4.

Radiocarbon dates were obtained for 18 specimens at the University of Arizona Accelerator Mass Spectrometry Laboratory, after collagen extraction, combustion, and graphitization (see Chapter 3). All dates described in this paper are reported as conventional radiocarbon years before AD 1950, in the form “17,000 \pm 100 BP” (mean age measurement \pm 1 SD). Radiocarbon dates are reported as “limits” (e.g., >41,000 BP) when the fraction of modern carbon is less than twice the value of the measurement error. The age limit is then calculated according to the following equations:

$$\text{Limit value } L = 2 (\text{error}) + (\text{fraction modern}) \quad [\text{Equation 7.1}]$$

$$\text{Age limit} = -8033 (\ln L) \quad [\text{Equation 7.2}]$$

Thus, the age limits reported are sample-dependent (Richard Cruz, personal communication).

7.3 Results and Discussion

7.3.1 Radiocarbon Dating

Table 7.1 lists new radiocarbon dates obtained for 3 Alberta and 15 Yukon proboscideans, along with dates obtained in previous studies. With the exception of the Cochrane specimen, the dates obtained for all Alberta specimens are beyond the limits of the radiocarbon dating technique (see Section 7.2). These results agree with previous studies that indicate that mammoths were widespread in the unglaciated regions of Alberta during the last interstadial, prior to the LGM (Burns, 1996). The new dates for Yukon proboscideans fall within the range of dates obtained by previous studies (Table 7.1). All of the dated Old Crow specimens have ages >39,100 BP. In contrast, the Klondike specimens include dates from >51,700 BP to 17,950 \pm 120 BP. Herschel Island specimens date from >45,130 BP to 34,100 \pm 1,700 BP. Only one of the British Columbia specimens was dated (in a previous study), and its date (17,000 \pm 240 BP) is close to the Last Glacial Maximum. The Quadra Sand formation in which most of the British

Columbia specimens were found has been dated to between approximately 30,000 (at more northern locations) and 15,000 BP (at more southern locations) (Armstrong and Clague, 1977; Clague et al., 2005).

7.3.2 Pretreatment Effects on Structural Carbonate Analysis

Enamel bioapatite tends to preserve its original, biogenic isotopic compositions better than bone or dentin (Koch et al., 1997). Pretreatment experiments were conducted on four individuals (AB1, AB4, YT4, YT37) to evaluate this possibility for the samples examined in this study (data not shown). Dentin, cementum, and bone had $\delta^{13}\text{C}_{\text{sc}}$ and $\delta^{18}\text{O}_{\text{sc}}$ values that differed by up to several per mil from those of enamel from the same individual. Pretreatments using either NaOCl and 0.1 M acetic acid, or H_2O_2 and acetic acid-sodium acetate buffer (after Koch et al., 1997), intended to remove contaminants, only rarely brought the dentin, cementum and bone isotopic compositions closer to those of enamel. For example, $\delta^{13}\text{C}$ values of untreated dentin were about 1‰ higher than those of enamel, whereas those of pretreated dentin were 1‰ or more *lower* than those of enamel. We conclude that stable isotope results for structural carbonate from dentin, cementum, and bone are unreliable for these specimens, and therefore have used only enamel for structural carbonate analysis.

Pretreatment experiments for enamel were conducted using 2-3% NaOCl (24 hours) and 0.1 M acetic acid (4 hours) (Garvie-Lok et al., 2004; Koch et al., 1997). The $\delta^{13}\text{C}$ values of untreated aliquots of enamel were on average $0.1 \pm 0.1\text{‰}$ higher (range = 0.0 to 0.2‰ higher) than those of pretreated enamel ($n = 4$ individual). The $\delta^{18}\text{O}$ values of untreated enamel averaged $0.3 \pm 0.1\text{‰}$ higher (range = 0.2 to 0.4‰ higher) than those of pretreated enamel. Because these differences are within typical analytical error, and because significantly smaller lines can be drilled for incremental isotopic analysis if pretreatment is not conducted (i.e., less sample is required), untreated enamel was used for incremental analyses. All “bulk” enamel samples discussed in the present study were pretreated using the method described above.

7.3.3 Diagenesis

Well-preserved collagen has an extraction yield >1%, C/N ratio between 2.9 and 3.6, carbon content of 30 to 43%, and nitrogen content of 11 to 16% (Ambrose, 1990; DeNiro, 1985; van Klinken, 1999). The Western Canada mammoth and mastodon collagen is very well-preserved according to these measures (collagen yield = $13.9 \pm 5.1\%$ (mean ± 1 SD), C/N = 3.2 ± 0.1 , %C = $41.5 \pm 4.2\%$, %N = $15.3 \pm 1.6\%$) (Table 7.2). A few samples (i.e., dentin from AB5, AB11, and AB6) have carbon and nitrogen contents that are slightly lower than the accepted range, likely because of variations in the collagen extraction procedure used for these individuals (i.e., “incremental” analyses of collagen were attempted by demineralising larger chunks and then sectioning them). For these samples, X-ray diffraction (XRD) analyses showed that inorganic salts (brushite and halite) were present in the final extraction product. Since their C/N ratios were normal, and since brushite and halite contain no carbon or nitrogen, the $\delta^{13}\text{C}_{\text{col}}$ and $\delta^{15}\text{N}$ results obtained for these specimens are included in the discussion below.

Multiple lines of evidence suggest that enamel bioapatite samples used for structural carbonate analysis are well-preserved. Their carbonate contents ($4.9 \pm 0.8\%$, Table 7.2) are similar to those of mature enamel (2.7 to 5.0%) (Hillson, 1996). There are no correlations between carbonate contents and $\delta^{13}\text{C}_{\text{sc}}$ or $\delta^{18}\text{O}_{\text{sc}}$ values (which might occur if significant quantities of diagenetic carbonate contributed to the gas produced during analysis). XRD patterns of selected pretreated enamel specimens (AB2, AB4, AB5) are typical of carbonated hydroxyapatite, with no evidence of secondary mineral contamination (see Chapter 2 for XRD methods). Fourier-transform infrared spectroscopy (FTIR) analysis of one untreated specimen (AB4) showed no evidence of calcite contamination, and the sample had a Crystallinity Index of 3.2, which is close to those of modern suid, bovid, and camelid enamel (3.4 to 4.4) (Roche et al., 2010) (see Chapter 2 for FTIR methods). Thin section analysis of one enamel specimen (AB6) revealed clearly visible incremental growth features (e.g., Striae of Retzius, cross-striations). Finally, sinusoidal variations were present in the δ -values of serially-sampled tooth enamel. Such patterns are typical of seasonal variations, and are unlikely to have been preserved if significant post-mortem isotopic alteration had occurred.

Table 7.2 The isotopic compositions of collagen (various tissues) and structural carbonate in bioapatite (enamel) for Western Canada mammoths and mastodons. Diet and drinking water isotopic compositions have been calculated as described in the text.

Region	Taxon	LSIS #	Collagen							Structural carbonate					Diet $\delta^{13}\text{C}$, from:		Water	
			Tissue	C (%)	$\delta^{13}\text{C}$ (‰)	N (%)	$\delta^{15}\text{N}$ (‰)	C/N (Atomic)	Yield (%)	Lab*	Tissue	$\delta^{13}\text{C}$ (‰)	$\delta^{18}\text{O}$ (‰)	CO_3 (%)	$\Delta^{13}\text{C}_{\text{sc-col}}$ (‰)	Col (‰)	SC (‰)	$\delta^{18}\text{O}$ (‰)
British Columbia																		
<i>Proboscidea</i>																		
		BC5B	B	41.3	-21.3	15.2	5.9	3.2	11.0	LSIS								-26.3
		BC3T1	T	42.4	-20.7	15.8	6.9	3.1	6.3	LSIS								-25.7
		BC1T	T	38.4	-19.9	14.2	7.0	3.2	4.3	LSIS								-24.9
		BC4T	T	47.0	-21.3	17.4	6.9	3.1	22.9	LSIS								-26.3
		Mean		42.3	-20.8	15.7	6.7	3.1	11.1									-25.8
		SD		3.6	0.7	1.3	0.5	0.0	8.3									0.7
Alberta																		
<i>Proboscidea</i>																		
		AB3	B	32.8	-21.0	12.1	1.4	3.2	4.3	LSIS								-26.0
		AB7	B	42.0	-20.5	15.8	10.9	3.1	11.0	LSIS								-25.5
		AB8	B	39.9	-19.7	14.8	4.4	3.1	7.5	LSIS								-24.7
		AB12	B	41.5	-20.4	16.3	9.0	3.0	10.9	LSIS								-25.4
		Mean		39.0	-20.4	14.8	6.4	3.1	8.5									-25.4
		SD		4.3	0.5	1.8	4.3	0.1	3.2									0.5
		<i>Mammuthus</i>																
		AB1	B	44.4	-20.8	16.7	7.3	3.1	16.0	LSIS	E	-10.7	14.2	4.0	10.1	-25.8	-24.8	-18.9
		AB1	C	39.7	-20.6	14.9	8.0	3.1	>11.0	LSIS								-25.6
		AB1	D	38.6	-20.5	15.1	8.1	3.0	>5.9	LSIS								-25.5
		AB2	C	42.1	-21.1	15.6	9.9	3.1	14.4	AMS	E	-11.4	15.0	6.8	9.8	-26.1	-25.5	-18.0
		AB2	D	30.1	-21.1	10.9	9.5	3.2	>15.5	LSIS								-26.1
		AB5	C	41.9	-21.4	15.3	10.4	3.2	8.6	LSIS	E	-11.5	13.6	4.9	9.9	-26.4	-25.6	-19.5
		AB5	D	29.2	-21.6	10.6	10.2	3.2	3.6	LSIS								-26.6
		AB11	C	43.8	-20.3	16.3	5.9	3.1	16.1	AMS	E	-10.5	13.1	5.9	9.8	-25.3	-24.6	-20.0
		AB11	D	25.9	-21.0	9.7	5.1	3.1	>4.3	LSIS								-26.0
		AB6	D	28.0	-20.1	10.2	5.1	3.2	>14.7	LSIS	E	-10.7	15.2	5.6	9.4	-25.1	-24.8	-17.8
		Mean		36.4	-20.9	13.5	8.0	3.1	11.7			-10.9	14.2	5.4	9.8	-25.9	-25.1	-18.8
		SD		7.2	0.5	2.8	2.1	0.1	5.5			0.5	0.9	1.1	0.2	0.5	0.5	0.9

Table 7.2 cont.

Region	Taxon	LSIS #	Collagen							Structural carbonate				Diet $\delta^{13}\text{C}$, from:		Water		
			Tissue	C (%)	$\delta^{13}\text{C}$ (‰)	N (%)	$\delta^{15}\text{N}$ (‰)	C/N (Atomic)	Yield (%)	Lab*	Tissue	$\delta^{13}\text{C}$ (‰)	$\delta^{18}\text{O}$ (‰)	CO_3 (%)	$\Delta^{13}\text{C}_{\text{sc-col}}$ (‰)	Col (‰)	SC (‰)	$\delta^{18}\text{O}$ (‰)
Alberta (cont.)																		
<i>Mammut</i>																		
	AB4		B	43.5	-20.9	16.3	4.1	3.1	13.6	LSIS	E	-11.6	14.9	3.6	9.3	-25.9	-25.7	-18.1
	AB4		D	37.1	-20.7	13.8	4.8	3.1	>11.9	LSIS						-25.7		
	AB10		D	41.1	-19.5	15.4	5.0	3.1	12.4	AMS	E	-10.3	13.5	4.0	9.2	-24.5	-24.4	-19.5
	Mean			40.6	-20.3	15.2	4.6	3.1	13.0			-10.9	14.2	3.8	9.3	-25.3	-25.0	-18.8
	SD			3.2	0.8	1.3	0.4	0.0	0.9			0.9	1.0	0.3	0.1	0.8	0.9	1.0
Yukon - Klondike																		
<i>Mammuthus</i>																		
	YT30		B	41.5	-20.3	15.6	5.8	3.1	18.0	AMS	E	-12.1	10.5	5.1	8.3	-25.3	-26.2	-22.7
	YT31		B	37.8	-20.5	14.1	7.0	3.1	13.0	AMS						-25.5		
	YT27		B	44.4	-21.1	16.3	7.0	3.2	13.5	LSIS						-26.1		
	YT29		B	42.0	-20.6	15.2	7.2	3.2	12.7	LSIS	E	-11.4	12.0	5.1	9.2	-25.6	-25.5	-21.1
	YT49		B	45.0	-21.3	16.3	8.7	3.2	20.6	LSIS						-26.3		
	YT28a		B	47.5	-20.7	18.0	10.5	3.1	19.1	LSIS	E	-11.3	9.9	5.6	9.4	-25.7	-25.4	-23.3
	YT28b										E	-11.7	9.9	5.7			-25.8	-23.3
	YT47		B	46.8	-20.6	17.6	6.5	3.1	16.8	LSIS						-25.6		
	YT48		B	46.6	-20.7	17.3	6.8	3.1	21.0	LSIS						-25.7		
	YT26		C	43.3	-20.5	16.0	7.4	3.2	15.3	AMS	E	-12.5	12.3	5.3	8.0	-25.5	-26.6	-20.8
	YT25		C	42.0	-21.2	15.5	8.0	3.2	7.3	LSIS	E	-11.8	11.4	2.8	9.3	-26.2	-26.0	-21.7
	YT32		C	45.9	-20.7	16.9	7.7	3.2	12.4	LSIS	E	-11.1	11.7	5.0	9.6	-25.7	-25.3	-21.4
	YT24		RD	45.7	-20.8	16.9	8.2	3.2	20.2	LSIS	E	-11.7	10.1	5.4	9.1	-25.8	-25.8	-23.1
	Mean			44.1	-20.7	16.3	7.6	3.2	15.8			-11.7	11.0	5.0	9.0	-25.7	-25.8	-22.2
	SD			2.8	0.3	1.1	1.2	0.0	4.2			0.4	1.0	0.9	0.6	0.3	0.4	1.0
<i>Mammut</i>																		
	YT35		RD	42.4	-20.6	16.0	4.4	3.1	19.9	AMS	E	-11.3	10.4	4.0	9.3	-25.6	-25.4	-22.8
	YT36		RD	41.7	-21.2	15.6	4.3	3.1	12.6	AMS	E	-11.3	10.9	4.4	9.8	-26.2	-25.5	-22.2
	YT37		B	42.0	-20.6	15.0	3.5	3.3	14.5	AMS	E	-10.6	11.4	3.7	10.0	-25.6	-24.7	-21.8
	YT33		B	43.2	-20.9	15.8	6.9	3.2	18.5	LSIS						-25.9		
	YT34		RD	45.7	-20.0	16.9	4.5	3.2	18.4	LSIS	E	-11.4	10.8	4.9	8.6	-25.0	-25.5	-22.4

Table 7.2 cont.

Region	Taxon	LSIS #	Tissue	Collagen						Structural carbonate					Diet $\delta^{13}\text{C}$, from:		Water		
				C (%)	$\delta^{13}\text{C}$ (‰)	N (%)	$\delta^{15}\text{N}$ (‰)	C/N (Atomic)	Yield (%)	Lab*	Tissue	$\delta^{13}\text{C}$ (‰)	$\delta^{18}\text{O}$ (‰)	CO_3 (%)	$\Delta^{13}\text{C}_{\text{sc-col}}$ (%)	Col (‰)	SC (‰)	$\delta^{18}\text{O}$ (‰)	
Yukon - Klondike (cont.)																			
			K-33897	RD?	42.7	-19.9	15.7	4.9	3.2	>7.6	Keck							-24.9	
			K-11697	RD?	42.2	-20.5	15.4	4.6	3.2	>8.5	Keck							-25.5	
			K-42551	RD?	42.2	-20.1	15.1	3.0	3.3	>4.0	Keck							-25.1	
			K-8707	RD?	42.9	-20.8	15.6	4.3	3.2	>8.4	Keck							-25.8	
			K-333	RD?	43.7	-20.9	14.9	4.0	3.4	>4.5	Keck							-25.9	
			K-42552	RD?	39.1	-19.9	14.0	3.0	3.3	>0.6	Keck							-24.9	
			Mean		42.5	-20.5	15.5	4.3	3.2	16.8		-11.1	10.9	4.2	9.4	-25.5	-25.3	-22.3	
			SD		1.6	0.4	0.7	1.1	0.1	3.1		0.4	0.4	0.5	0.6	0.4	0.4	0.4	
Yukon- Old Crow																			
<i>Mammuthus</i>																			
			YT51	T	37.9	-20.7	13.9	11.3	3.2	18.6	LSIS							-25.7	
			YT5	RD	42.9	-21.5	15.5	9.8	3.2	11.2	LSIS	E	-8.4	10.5	5.1	13.1	-26.5	-22.5	-22.7
			YT1	RD	41.6	-21.4	15.6	8.7	3.1	14.4	AMS	E	-11.3	11.4	n.d.	10.1	-26.4	-25.4	-21.8
			YT2	RD	39.2	-20.9	14.6	8.4	3.1	11.0	AMS	E	-8.3	9.9	5.3	12.6	-25.9	-22.5	-23.3
			YT3	D	44.0	-21.8	16.4	9.7	3.1	>6.7	LSIS	E	-10.1	10.0	5.5	11.7	-26.8	-24.3	-23.2
			YT4	B	41.1	-21.4	15.2	9.5	3.1	13.1	AMS	E	-9.7	11.5	5.1	11.7	-26.4	-23.9	-21.6
			YT6	C	42.5	-21.7	15.2	7.7	3.3	10.1	LSIS	E	-9.7	9.8	4.6	12.0	-26.7	-23.9	-23.4
			YT7	B	42.3	-21.4	15.8	7.6	3.1	15.7	AMS	E	-9.1	10.2	5.3	12.4	-26.4	-23.2	-23.0
			YT9	C	41.4	-21.5	15.0	8.2	3.2	7.1	LSIS	E	-9.9	11.9	5.0	11.6	-26.5	-24.0	-21.2
			YT10	RD	38.9	-21.5	14.4	9.8	3.2	11.4	AMS	E	-10.9	10.7	5.3	10.6	-26.5	-25.0	-22.5
			YT11	C	44.1	-21.5	15.9	8.3	3.2	18.2	LSIS	E	-10.6	10.5	5.1	10.9	-26.5	-24.7	-22.6
			YT11	RD	47.2	-21.5	17.6	9.5	3.1	14.3	LSIS							-26.5	
			Mean		41.9	-21.4	15.4	9.0	3.2	13.2		-9.8	10.6	5.1	11.7	-26.4	-23.9	-22.5	
			SD		2.5	0.3	1.0	1.1	0.1	3.5		1.0	0.7	0.3	0.9	0.3	1.0	0.8	
<i>Mammut</i>																			
			YT8	D	42.3	-20.6	16.0	3.5	3.1	17.8	AMS	E	-11.1	11.6	4.4	9.5	-25.6	-25.3	-21.5
			K-15352	RD?	43.4	-19.6	14.8	4.1	3.4	>1.3	Keck							-24.6	
			K-31898	RD?	42.6	-19.9	15.2	2.4	3.3	>2.1	Keck							-24.9	
			K-33066	RD?	43.3	-20.1	15.3	2.5	3.3	>3.9	Keck							-25.1	
			Mean		42.9	-20.1	15.3	3.1	3.3									-25.1	
			SD		0.5	0.4	0.5	0.8	0.1									0.4	

Table 7.2 cont.

Region	Taxon	LSIS #	Tissue	Collagen						Structural carbonate					Diet $\delta^{13}\text{C}$, from:		Water		
				C (%)	$\delta^{13}\text{C}$ (‰)	N (%)	$\delta^{15}\text{N}$ (‰)	C/N (Atomic)	Yield (%)	Lab*	Tissue	$\delta^{13}\text{C}$ (‰)	$\delta^{18}\text{O}$ (‰)	CO_3 (%)	$\Delta^{13}\text{C}_{\text{sc-col}}$ (‰)	Col (‰)	SC (‰)	$\delta^{18}\text{O}$ (‰)	
Yukon- Herschel Island																			
<i>Proboscidea</i>																			
		YT42	T	42.7	-20.3	15.7	8.2	3.2	23.3	AMS								-25.3	
		YT45	T	43.6	-21.6	16.2	15.2	3.1	21.5	AMS									-26.6
		YT41	T	45.0	-22.1	16.7	10.7	3.1	17.8	LSIS									-27.1
		YT43	T	42.5	-21.9	15.5	8.0	3.2	15.1	LSIS									-26.9
		YT44	T	44.9	-20.7	16.4	8.8	3.2	18.5	LSIS									-25.7
		Mean		43.7	-21.3	16.1	10.2	3.2	19.2										-26.3
		SD		1.2	0.8	0.5	3.0	0.0	3.2										0.8
<i>Mammuthus</i>																			
		YT46	B	41.7	-21.6	15.5	5.5	3.1	14.8	LSIS									-26.6
		YT40	C	42.4	-21.5	15.9	6.8	3.1	14.1	AMS	E	-13.7	13.3	5.5	7.9	-26.5	-27.8		-19.8
		YT39	D	44.4	-21.7	16.2	9.7	3.2	9.0	LSIS	E	-13.8	12.2	5.0	8.0	-26.7	-27.9		-21.0
		Mean		42.8	-21.6	15.9	7.4	3.1	12.6			-13.7	12.7	5.2	7.9	-26.6	-27.8		-20.4
		SD		1.4	0.1	0.3	2.2	0.0	3.2			0.1	0.8	0.4	0.1	0.1	0.1		0.8
<i>Mammut</i>																			
		YT38	B	41.8	-21.8	15.1	5.8	3.2	13.9	LSIS									-26.8
Yukon - Stewart River																			
<i>Mammuthus</i>																			
		YT50	B	35.9	-20.8	12.9	7.2	3.3	1.2	LSIS									-25.8
All specimens																			
		Mean		41.5	-20.9	15.3	7.0	3.2	13.9			-11.0	11.7	4.9	10.0	-25.9	-25.1		-21.4
		SD		4.2	0.6	1.6	2.6	0.1	5.1			1.2	1.6	0.8	1.4	0.6	1.2		1.7

LSIS #: Sample ID used for Laboratory for Stable Isotope Science analyses, and referred to in this study

Values in **bold** are the means of duplicate analyses.

Tissue: RD = root dentin, D = crown dentin, T = tusk dentin, B = bone, C = cementum, E = enamel

* Laboratory in which collagen extraction was performed: LSIS (The University of Western Ontario), AMS (The University of Arizona), Keck (The University of California, Irvine); see text for variations in collagen extraction methodology at LSIS and AMS.

Keck (CMN) samples (sample names K-xxxx) were ultrafiltered, which results in lower collagen yields.

One sample (YT35RD) was extracted & analyzed both at LSIS & Keck: $\delta^{13}\text{C}_{\text{col}}$ and $\delta^{15}\text{N}_{\text{col}}$ values differed by a maximum of 0.3 and 0.4‰, respectively.

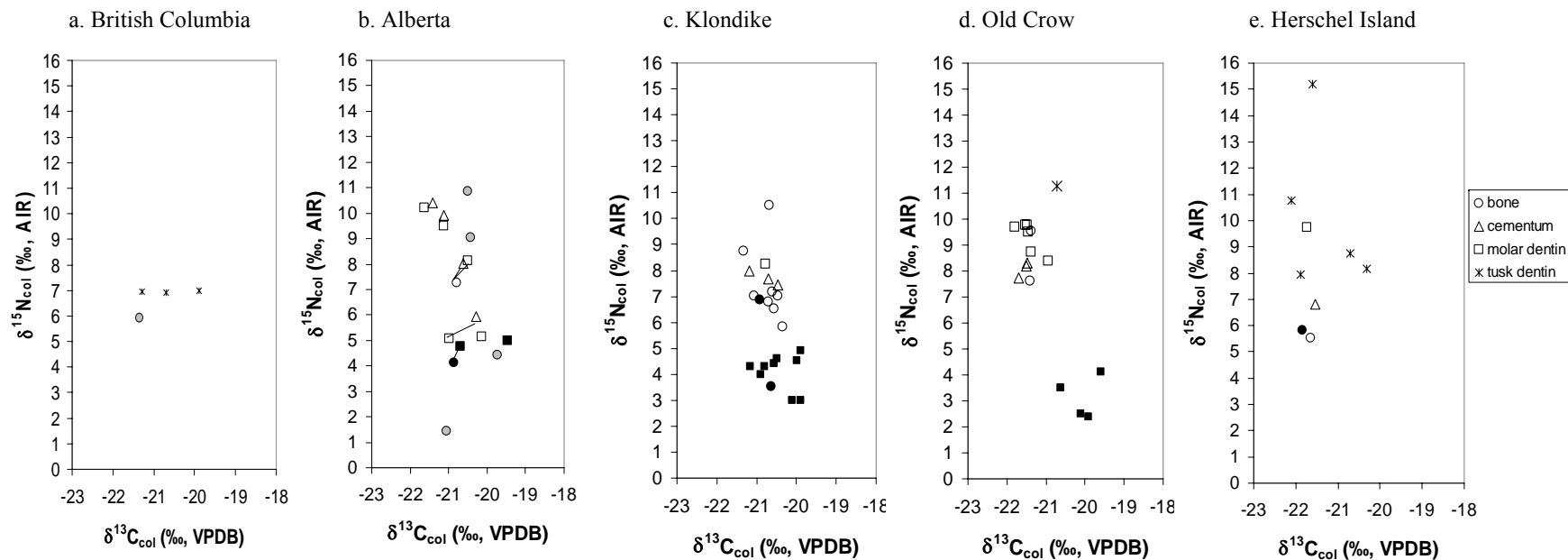


Figure 7.2 Carbon and nitrogen isotope results obtained for collagen from mammoths (open symbols) and mastodons (closed black symbols) from (a) British Columbia, (b) Alberta, (c) Klondike, (d) Old Crow, and (e) Herschel Island. Circles, squares, and triangles represent results obtained from bone, molar tooth dentin, and cementum, respectively. Asterisks represent results obtained from tusk dentin, which were identified only as Proboscidea. Grey filled circles represent bones from specimens identified only as Proboscidea. Lines connect tissues from the same individual.

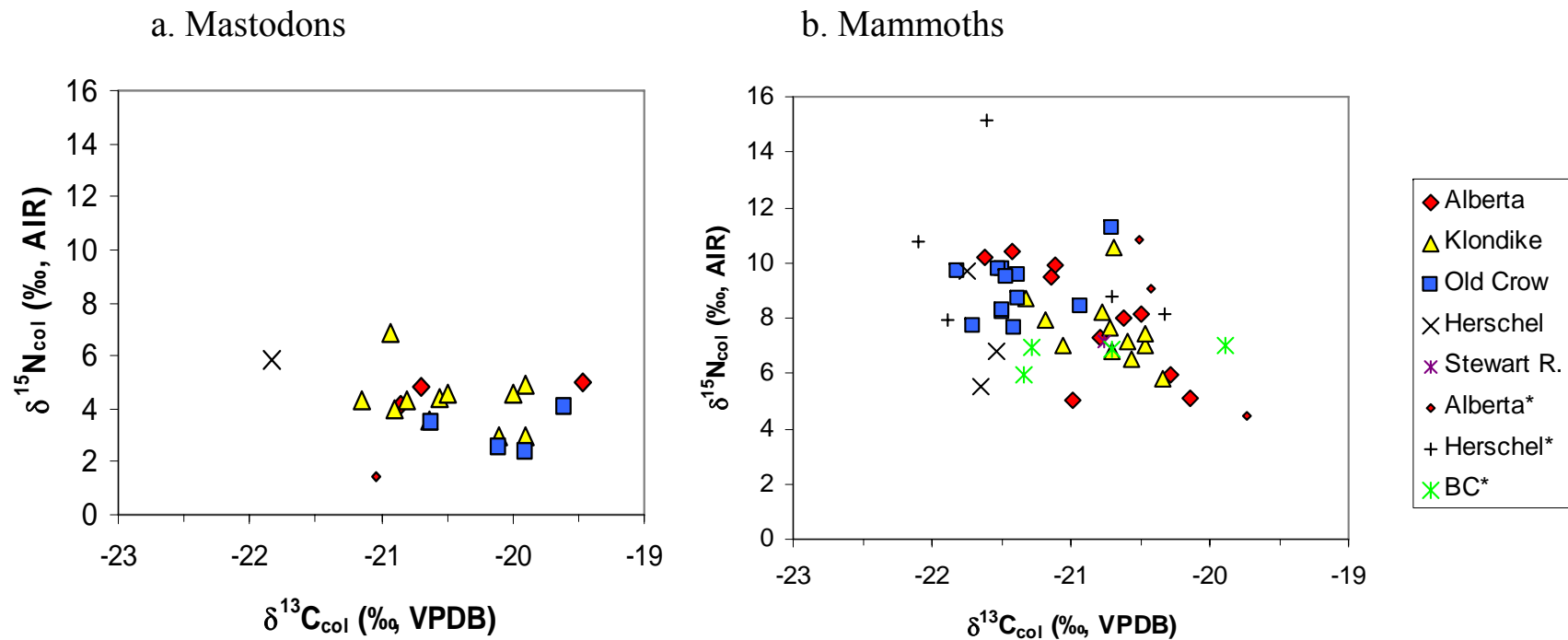


Figure 7.3 Carbon and nitrogen isotope compositions of collagen for (a) mastodons and (b) mammoths from Western Canada. Some specimens from Alberta, Herschel Island, and BC (marked with * in the legend) were identified only as Proboscidea. Since mammoth remains are more abundant than mastodon in these regions, these specimens are plotted alongside mammoths, except for one individual with a very low $\delta^{15}\text{N}$ value (plotted with mastodons).

7.3.4 Tissue Comparisons (Collagen)

Stable isotope results obtained for collagen extracted from different tissues were compared for four mammoths (AB1, AB2, AB5, AB11) and one mastodon (AB4) (Table 7.2). Bone had slightly lower $\delta^{13}\text{C}_{\text{col}}$ and $\delta^{15}\text{N}$ values than dentin or cementum (0.2 and 0.7‰ lower, respectively; $n = 2$ pairs). In combination with the results obtained for Great Lakes proboscideans (Chapter 6), this suggests the possibility of a small but consistent isotopic difference between bone and dental tissues, which may be the result of either tissue-specific isotopic fractionations or age-related changes in metabolism or diet. Since the teeth studied develop during adulthood (except the mastodon M5, which develops during youth; see Chapter 6), nursing is not a viable explanation for these offsets. For three of the mammoths, the isotopic results for dentin and cementum were very similar, but for the AB11 mammoth, dentin had a $\delta^{13}\text{C}_{\text{col}}$ value 0.7‰ lower, and a $\delta^{15}\text{N}$ value 0.9‰ lower, than cementum. Notably, the AB11 specimen may be an M4, which forms earlier in life than the other teeth examined here (M5s and M6s) (Table 7.1). Thus, the small offset for this individual is likely the result of different formation times for each tissue, and reflects slightly different dietary isotopic compositions and/or metabolic states at the time of formation.

7.3.5 Isotopic Partitioning between Mammoths and Mastodons: Paleoecological Implications

Western Canada mammoths had significantly higher $\delta^{15}\text{N}$ values than mastodons (Independent samples $t = 10.0$, $df = 14$, $p < 0.001$ for Old Crow; $t = 6.8$, $df = 21$, $p < 0.001$ for Klondike; $t = 2.7$, $df = 11$, $p < 0.05$ for Alberta) (Table 7.2, Figures 7.2, 7.3). A similar offset was also observed for Great Lakes proboscideans (Chapter 6) and is consistent with the generally high $\delta^{15}\text{N}$ values of mammoths, and low $\delta^{15}\text{N}$ values of mastodons, in other regions (Bocherens, 2003; Bocherens et al., 1996; Coltrain et al., 2004a; France et al., 2007; Iacumin et al., 2000; Koch, 1991). In the Old Crow region, the difference in $\delta^{15}\text{N}$ values for mammoths and mastodons is large (mean difference = 5.9‰) whereas in the other regions reported here it is smaller (mean difference = 3.4‰ for Alberta, 3.3‰ for Klondike). A large difference in $\delta^{15}\text{N}$ values (5.3‰) between mammoths and mastodons, similar to that observed for Old Crow specimens, was also observed in the Great Lakes

region (Chapter 6). In both Old Crow and the Great Lakes areas, there was no overlap in mammoth and mastodon $\delta^{15}\text{N}$ values, whereas in Alberta and Herschel Island a few mammoths and mastodons had similar $\delta^{15}\text{N}$ values. One Klondike mastodon has a $\delta^{15}\text{N}$ value that groups with the mammoth values, but it is possible that this fragmented fibula specimen was misidentified.

Tissue offsets are too small to account for the difference between mammoths and mastodons (Section 7.3.4). As discussed in Chapter 6, numerous other explanations for the difference are possible. The high $\delta^{15}\text{N}$ values of mammoths have primarily been attributed to nitrogen recycling, consumption of older plant parts, or coprophagy (Bocherens, 2003; Bocherens et al., 1996; Clementz et al., 2009; van Geel et al., 2010), but nutritional stress has also been considered (Koch, 1991; Kuitens, 2010) (see Section 7.3.6). The low $\delta^{15}\text{N}$ values of mastodons have been primarily attributed to association with nitrogen-fixing taxa such as *Alnus* (Coltrain et al., 2004a; Koch, 1991), or to association with spruce forest environments (Chapter 6). Other factors may also contribute (Chapter 6, Table 6.4).

Mammoths from Old Crow have significantly lower $\delta^{13}\text{C}_{\text{col}}$ values than mastodons (mean difference = 1.3‰) (Independent Samples $t = -1.4$, $df = 11$, $p < 0.001$) (Figures 7.2, 7.3). Mammoths from Alberta have slightly (though not significantly) lower $\delta^{13}\text{C}_{\text{col}}$ values than mastodons (mean difference = 0.6‰). Klondike and Herschel Island mammoths and mastodons have virtually identical $\delta^{13}\text{C}_{\text{col}}$ values (mean difference = 0.2‰) (Figures 7.2, 7.3). In eastern Beringia (Alaska and Yukon), modern plants grown in wet habitats tend to have lower $\delta^{13}\text{C}$ values than those grown in dry habitats (Wooller et al., 2007). However, mammoths are believed to have occupied drier habitats than mastodons, not vice versa. Szpak et al. (2010) interpreted lower $\delta^{13}\text{C}_{\text{col}}$ values in western than eastern Beringian mammoths as a function of lower temperatures or greater fat metabolism. Alternatively, consumption of lichens by mastodons could be responsible for both lower $\delta^{15}\text{N}$ and higher $\delta^{13}\text{C}$ values (Coltrain et al., 2004a; Coltrain et al., 2004b; Iacumin et al., 2000). The differences in $\delta^{13}\text{C}_{\text{col}}$ could also be attributed to a number of other factors (see Chapter 6, Table 6.3).

The only regions with sufficient structural carbonate isotopic data to make meaningful comparisons between mammoths and mastodons are Alberta and Klondike

(Table 7.2, Figure 7.4). There is no difference in $\delta^{13}\text{C}_{\text{sc}}$ values between the two taxa in Alberta. Mammoths from Klondike have slightly lower $\delta^{13}\text{C}_{\text{sc}}$ values than mastodons (mean difference = 0.6‰), although the difference is not statistically significant ($t = -2.1$, $df = 10$, $p = 0.06$). There are no correlations between $\delta^{13}\text{C}_{\text{col}}$ and $\delta^{13}\text{C}_{\text{sc}}$ values for Klondike mammoths, Old Crow mammoths, Yukon mastodons, or mammoths and mastodons from all regions combined. There is a positive correlation for Alberta mammoths (Pearson $r = 0.89$, $df = 3$, $p < 0.05$). Further research is required to determine why such a correlation might exist for Alberta mammoths but not for other groups.

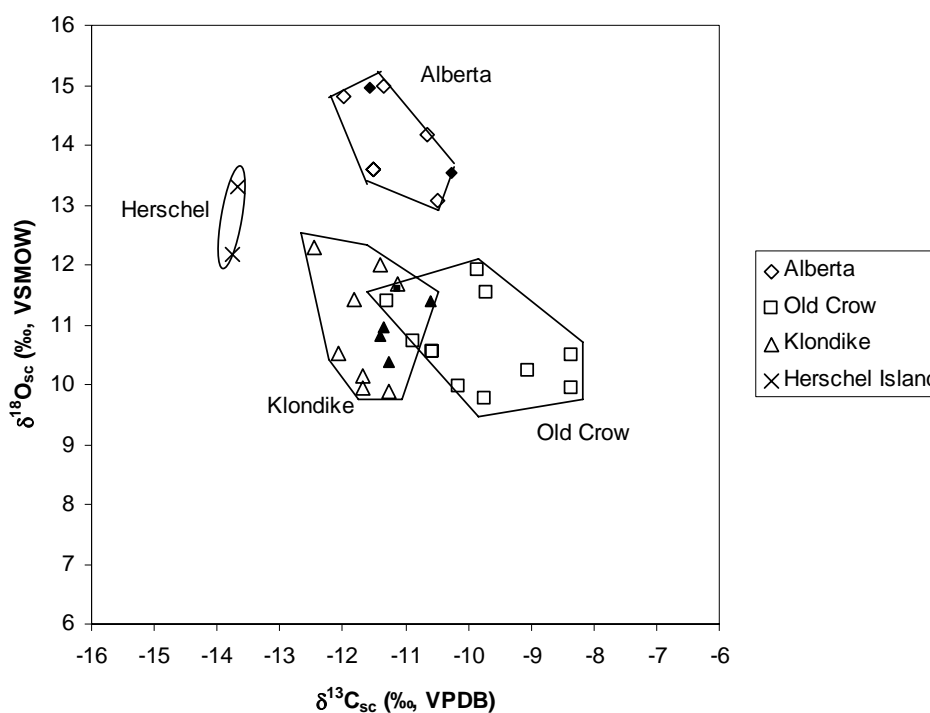


Figure 7.4 Carbon and oxygen isotope results obtained for structural carbonate in enamel bioapatite from mammoths (open symbols) and mastodons (closed symbols). Herschel Island specimens are mammoth. Borders enclose specimens from the different regions.

There is no significant difference in $\delta^{18}\text{O}_{\text{sc}}$ values between mammoths and mastodons in either Alberta or Klondike, which are the only regions with sufficient data for comparison (Table 7.2, Figure 7.4). This result is different from that for southern Ontario, where mammoths have lower $\delta^{18}\text{O}$ values than mastodons (Chapter 6). We

assume that any differences in $\delta^{18}\text{O}$ values between mammoths and mastodons are primarily related to differences in the isotopic composition of their drinking water and dietary (plant) water, and in the proportion of water obtained by drinking versus plant consumption. This is reasonable given the similar body size and evolutionary relationship of the two taxa, which suggest a lack of difference in physiological variables (e.g., vapour loss from skin, sweating vs. panting, and the ratio of water turnover to energy expenditure) that can cause differences in $\delta^{18}\text{O}$ among species (Kohn, 1996; Kohn et al., 1996). The similar $\delta^{18}\text{O}_{\text{sc}}$ values of mammoths and mastodons in Western Canada (Alberta, Klondike) suggest that the two taxa consumed waters with similar $\delta^{18}\text{O}$ values. In other words, they did not utilize isotopically distinct water sources. This does not preclude preferential consumption of plants in different microhabitats (e.g., mammoths in upland plains, mastodons in riparian valleys), but suggests that either the isotopic compositions of waters was relatively homogeneous, or that mammoths and mastodons obtained water ultimately derived from the same source(s).

The similar $\delta^{18}\text{O}$ values of mammoths and mastodons is somewhat surprising, since it is believed that mastodons were adapted to warmer climates and only survived in Beringia during warmer and wetter interglacial-interstadial periods (Guthrie, 2001; Zazula et al., in prep). Based on temperature alone, water $\delta^{18}\text{O}$ values calculated for proboscideans that lived during warmer intervals should be higher than those from those during colder intervals (Arppe and Karhu, 2006, 2010; Genoni et al., 1998; Tutken et al., 2007; Ukkonen et al., 2007). Possible explanations for the lack of a difference between mammoths and mastodons include (1) increased melting of low- ^{18}O ice during warmer intervals (e.g., permafrost melting during interglacials) (Reyes et al., 2010a), which, when mixed with higher- ^{18}O interglacial precipitation, could bring drinking water $\delta^{18}\text{O}$ values closer to the $\delta^{18}\text{O}$ values of glacial-period precipitation, or (2) reliance on groundwater rather than precipitation, which could in theory have the same $\delta^{18}\text{O}$ values during glacial and interglacial periods (if derived from the same source, such as glacial meltwater, permafrost, or old aquifers). Alternatively, it is possible that these mammoths and mastodons did not actually live during distinct time periods. Carbon isotope compositions could potentially provide further insight into this question. For at least the last 400,000 years, the concentration of atmospheric CO_2 decreased during cold periods and increased

during warm periods (Cowling, 1999; Cowling and Sykes, 1999). The increase in atmospheric CO₂ since the Last Glacial Maximum is associated with a decrease in the $\delta^{13}\text{C}_{\text{col}}$ values of several mammalian fauna (Hedges et al., 2004; Richards and Hedges, 2003; Stevens and Hedges, 2004). If this relationship also existed during previous glacial-interglacial cycles, we would expect mastodons living during warmer periods to have lower $\delta^{13}\text{C}$ values than mammoths living during colder periods. Instead, we found either the opposite, or no difference between the taxa for both $\delta^{13}\text{C}_{\text{col}}$ and $\delta^{13}\text{C}_{\text{sc}}$.

There is a statistically significant correlation between $\delta^{15}\text{N}$ and $\delta^{18}\text{O}$ values for Yukon (mostly Old Crow) mastodons (Pearson's $r = -0.896$, $df = 3$, $p < 0.05$), which might reflect variations between somewhat colder/drier and warmer/wetter conditions, assuming that $\delta^{18}\text{O}$ values are primarily related to temperature and $\delta^{15}\text{N}$ values to aridity. However, there are no such correlations between $\delta^{15}\text{N}$ and $\delta^{18}\text{O}$ values for mammoths in any of the regions, or for mammoths or mastodons when specimens from different regions were combined. This general lack of correlation likely reflects the large number of factors that can affect $\delta^{15}\text{N}$ and $\delta^{18}\text{O}$ values (see Chapter 6).

In sum, mammoths in Western Canada tend to have higher $\delta^{15}\text{N}$ values, similar (though sometimes lower) $\delta^{13}\text{C}_{\text{col}}$ and $\delta^{13}\text{C}_{\text{sc}}$ values, and similar $\delta^{18}\text{O}$ values relative to mastodons. The most parsimonious explanation for the isotopic differences between mammoths and mastodons is that they occupied distinct environmental niches (i.e., they consumed plants from different microhabitats), but likely obtained water from the same sources. The vast "mammoth steppe" comprised an "ecological mosaic" of vegetation types related to local environmental conditions (Guthrie, 1982; Velichko and Zelikson, 2005; Zazula et al., 2003, 2006a, 2006b). The similar $\delta^{13}\text{C}$ values of mammoths and mastodons likely reflect the wide variety of plant foods consumed by both taxa, which would average species- and environmental-differences in plant $\delta^{13}\text{C}$ values. The slightly lower $\delta^{13}\text{C}$ values of mammoths could reflect overall lower soil nutrient contents, but other explanations are also possible (see Chapter 6, Table 6.3). The higher mammoth $\delta^{15}\text{N}$ values could be caused by a combination of drier microenvironments, preference for grasses grown in low-nutrient soils, and greater coprophagy, whereas the lower mastodon $\delta^{15}\text{N}$ values could result from a preference for trees, shrubs, and woody plants growing in

nutrient-rich riparian environments, particularly those supporting spruce trees, and less coprophagy (see Table 6.4).

Velichko and Zelikson (2005) argue that mammoths in eastern Europe grazed in dry, upland forest-steppe environments but preferred river valleys during winter, as the latter provided protection against winds, greater access to vegetation because of thinner snow cover, and stable sources of water. In contrast, mastodons may have remained in river valleys and floodplain meadows throughout the year. Notably, the latter environments supported spruce trees, both in Eastern Europe and Yukon (Velichko and Zelikson, 2005; Zazula et al., 2006c). Spruce trees, and the plants growing underneath them, tend to have low $\delta^{15}\text{N}$ values, which could lead to the low $\delta^{15}\text{N}$ values of mastodons (see Chapter 6, Section 6.3.6.3). If mammoths preferred more open environments, they may have had greater opportunities to engage in coprophagy, since their dung would be deposited on drier soils. Furthermore, if mammoths followed regular migration routes, as do many groups of modern elephants (Haynes, 1991), the plants growing along these routes may have been “fertilized” by mammoth dung. Both direct consumption of dung and consumption of plants fertilized by dung could have increased the $\delta^{15}\text{N}$ values of mammoths. In contrast, mastodon dung would not have enriched their dietary plant $\delta^{15}\text{N}$ values to any great extent if the dung was rapidly diluted or removed by water in their riparian or wetland environments.

7.3.6 Nutritional Stress and $\delta^{15}\text{N}$ values

Dietary restriction (starvation, fasting) and slowed growth rates can cause increases in animal tissue $\delta^{15}\text{N}$ values (Fuller et al., 2005; Hobson et al., 1993; McCue and Pollock, 2008; Mekota et al., 2006; Warinner and Tuross, 2010). Some researchers have suggested that the unusually high $\delta^{15}\text{N}$ values of mammoths were a result of nutritional stress (Koch, 1991; Kuitens, 2010). However, it seems unlikely that severe nutritional stress could have caused the high $\delta^{15}\text{N}$ values that appear to characterize all woolly mammoth populations studied to date, from western Europe to eastern North America (Bocherens et al., 1996, 1997; Fox-Dobbs et al., 2008; Iacumin et al., 2000; Koch, 1991). Severe nutritional stress would likely impede reproductive success. However studies suggest that mammoths in Beringia did not experience measurable

population decline prior to their extinction (Barnes et al., 2007; Debruyne et al., 2008; Guthrie, 2006), though there is some indication for decline from mammoth tracks in southern Alberta (McNeil et al., 2005). Additionally, the magnitude of ^{15}N enrichment in mammalian tissues as a result of nutritional stress is typically around 1-2‰ (Fuller et al., 2005; McCue and Pollock, 2008; Mekota et al., 2006; Warinner and Tuross, 2010), whereas mammoth $\delta^{15}\text{N}$ values tend to average at least 3‰ higher than those of other herbivores.

The AB5 mammoth provides a special case that can be used to investigate the influence of nutritional stress on $\delta^{15}\text{N}$ values. This specimen is a morphologically normal upper left M6 which had a malformed, supernumerary M7 united to it by hypercementosis (Burns et al., 2003). According to Burns et al. (2003:83):

“The Villeneuve mammoth [AB5] was clearly in great pain due to a conspicuous bulging of the buccal alveolus, and it may be argued that it was the ultimate cause of death.... Normal chewing action was eventually rendered impossible. The secondary occlusal facet on the buccal edge of the molar suggests that the mammoth made an effort to avoid the painful passing of the muscle across the bulge... and the animal likely died of malnutrition shortly after cutting the new facet, at age 46 to 48 years, unable to process sufficient graze to survive.”

Collagen extracted from the cementum and dentin of AB5 had $\delta^{15}\text{N}$ values of 10.4 and 10.2‰, respectively. These values are more than 2‰ higher than the mean $\delta^{15}\text{N}$ for Alberta mammoths (and 0.5 or 0.3‰ higher, respectively, than the next highest mammoth tooth $\delta^{15}\text{N}$ value). It is quite possible that nutritional stress was responsible for the very high $\delta^{15}\text{N}$ values of the AB5 mammoth. Further study of this specimen could produce interesting information about the relationship between nutritional stress and mammoth stable isotope compositions.

7.3.7 Regional Comparisons

Because mammoths and mastodons have very different $\delta^{15}\text{N}$ values (Section 7.3.5), comparisons of collagen isotopic compositions among regions should consider the two taxa separately. For both mammoths and mastodons, there is significant overlap in the $\delta^{15}\text{N}$ and $\delta^{13}\text{C}_{\text{col}}$ values among different regions (Figure 7.3). Nevertheless, Old Crow

mammoths have significantly higher $\delta^{15}\text{N}$ values and lower $\delta^{13}\text{C}_{\text{col}}$ values than Klondike mammoths (Kruskall-Wallis and Dunn's tests, $p < 0.01$ for $\delta^{13}\text{C}_{\text{col}}$, $p < 0.05$ for $\delta^{15}\text{N}$). Old Crow mammoths also have significantly lower $\delta^{13}\text{C}_{\text{col}}$ values than Alberta mammoths (Kruskall-Wallis and Dunn's tests, $p < 0.05$) (Figure 7.3b, Table 7.2). Herschel Island specimens have the most variable $\delta^{15}\text{N}$ values, but these include several tusk samples that are identified only as Proboscidea. BC proboscideans have $\delta^{15}\text{N}$ values that group with the lower- $\delta^{15}\text{N}$ mammoths from other regions (Figure 7.3), consistent with a less arid environment. However, the BC specimens also fit within the high end of the mastodon range for $\delta^{15}\text{N}$ values. There are no statistically significant differences in mastodon $\delta^{13}\text{C}_{\text{col}}$ or $\delta^{15}\text{N}$ values among regions (Figure 7.3a, Table 7.2).

As described in Section 7.3.5, there are no differences between mammoth and mastodon structural carbonate isotopic compositions within regions, so they can be considered together. A plot of $\delta^{18}\text{O}_{\text{sc}}$ versus $\delta^{13}\text{C}_{\text{sc}}$ values shows good separation among regions (Figure 7.4). Klondike and Old Crow specimens have significantly lower $\delta^{18}\text{O}$ values than Alberta specimens ($F(3,28) = 33.5$, $p < 0.001$), as expected based on the typical decrease in meteoric water $\delta^{18}\text{O}$ values with latitude. The $\delta^{18}\text{O}$ values of samples from Herschel Island are higher than expected from latitude alone, but consistent with the island's coastal location.

Table 7.3 and Figure 7.5 compare the mean drinking water $\delta^{18}\text{O}$ values for each region calculated from proboscidean tooth enamel with the modern weighted mean annual $\delta^{18}\text{O}$ values of precipitation from 'nearby' locations. Data for Edmonton, Mayo, and Barrow were obtained from IAEA stations (IAEA/WMO, 2010). Data for Old Crow was estimated from Turner et al. (2010), using the $\delta^{18}\text{O}$ values of rain and snowpack that fell along the Global Meteoric Water Line (their Figure 4a), weighted by the 1951-2007 averages they reported for seasonal rainfall. The result is within the range of surface water $\delta^{18}\text{O}$ values reported for similar latitudes in Alaska (Sloat et al., 2010) and to the mean annual $\delta^{18}\text{O}$ value for a similar latitude location in the Northwest Territories (Inuvik, -24.2‰) (IAEA/WMO, 2010). Considering that not all of the pairs include modern and fossil data from the same location, and that the Old Crow value is estimated as described above, the modern and ancient water $\delta^{18}\text{O}$ values are reasonably well correlated, though the relationship is not statistically significant (Pearson's $r = 0.91$, $df =$

2, $p < 0.10$). Differences in the $\delta^{18}\text{O}$ values of meteoric water on a continental scale result from large-scale processes (e.g., temperature gradients and movement of moisture masses across the continent). These results indicate that such processes were fundamentally similar (on a continental scale) during the Pleistocene and today. However, the isotopic composition of Pleistocene water differed from that of modern water at each location because of changes in local conditions (e.g., local temperature, seasonal amounts of precipitation, etc.). For every location except Old Crow (which has the least accurate estimation for modern $\delta^{18}\text{O}$; see above), the Pleistocene water $\delta^{18}\text{O}$ values are lower than those of modern meteoric water (Table 7.3). Lower local water and precipitation $\delta^{18}\text{O}$ values during the LGM have previously been inferred for mid- to high-latitude locations in North America from both general circulation models (GCMs) and mammalian tooth enamel $\delta^{18}\text{O}$ values (Kohn and McKay, 2010).

There is no difference between the $\delta^{13}\text{C}_{\text{sc}}$ values of the Alberta and Klondike specimens. Some of the Old Crow $\delta^{13}\text{C}_{\text{sc}}$ values overlap those from Alberta and Klondike, but overall the former are significantly higher than the latter ($F(3,28) = 19.7$, $p < 0.001$). Old Crow mammoths appear to have experienced unique climatic conditions that led to relatively high $\delta^{13}\text{C}_{\text{sc}}$ values but low $\delta^{13}\text{C}_{\text{col}}$ values (Section 7.3.5). One possible explanation is that Old Crow soils had relatively high nutrient contents, which could lead to higher $\delta^{13}\text{C}$ values in plants (and hence, in proboscidean structural carbonate, which is formed from all dietary carbon sources) (Tieszen, 1991). If the supposed high-nutrient soils also produced plants with higher protein contents, mammoth collagen $\delta^{13}\text{C}$ values (which reflect the protein component of the diet) might be lower (since plant proteins are depleted of ^{13}C) (Tieszen, 1991) (see Chapter 6, Table 6.3). Herschel Island proboscideans had significantly lower $\delta^{13}\text{C}_{\text{sc}}$ values than specimens from any of the other regions. There are many potential reasons for this differences, including (1) more fat metabolism, (2) more grass or leaf consumption, and less woody plant or lichen consumption, (3) increased protein or lipid contents in plants, (4) a wetter environment, (5) lower soil nutrient content, and (6) lower temperature (see Chapter 6, Table 6.3). We note that the differences among regions may be related not only to geographic differences, but also potentially to temporal differences (see Table 7.1).

Table 7.3 Comparison of the "mean annual" and "seasonal extreme" isotopic compositions of drinking water (dw; calculated from proboscidean enamel) with the weighted mean annual and seasonal extreme isotopic compositions of modern meteoric water (mw) at locations of similar latitude.

Pleistocene						Modern						
Location	Latitude	Longitude	$\delta^{18}\text{O}_{\text{dw}}$			Location	Latitude	Longitude	$\delta^{18}\text{O}_{\text{mw}}$			yrs [^]
			Mean	SD	Seasonal*				Mean	SD	Seasonal*	
Alberta	53°34'12"	113°31'12"	-18.8	0.9	-23.9 to -15.3 (8.6)	Edmonton, AB	53°34'12"	113°31'12"	-17.1	0.9	-28.0 to -12.6 (15.4)	4
Klondike	64°3'	139°24'	-22.2	0.8	-25.9 to -19.4 (6.5)	Mayo, YT	63°22'12"	135°31'12"	-20.7	1.0	-26.9 to -15.6 (11.3)	3
Old Crow	67°30' to 68°08'	139°33' to 140°32'	-22.4	0.8	-26.2 to -20.1 (6.1)	Old Crow, YT	67°30' to 68°08'	139°33' to 140°32'	-23.9	-	-31.3 to -18.0 (13.3)	1
Herschel	69°35'	139°5'	-20.4	0.8	no data	Barrow, AK	71°18'0"	156°46'48"	-19.6	2.3	-24.9 to -12.9 (12.0)	2

Pleistocene water $\delta^{18}\text{O}$ values were calculated from bulk enamel $\delta^{18}\text{O}_{\text{sc}}$ values (for mean and SD) or incremental enamel values (for seasonal).

Modern mean $\delta^{18}\text{O}$ values for Edmonton, Mayo, and Barrow are weighted mean annual values obtained from the IAEA/WISER database (Edmonton, Mayo, Barrow) or as described in the text (Old Crow).

Latitude and longitude for Alberta specimens is that of Edmonton, and for Klondike is that of Dawson City.

* Minimum and maximum $\delta^{18}\text{O}$ values obtained from incremental analysis of tooth enamel (Pleistocene), monthly arithmetic mean $\delta^{18}\text{O}$ values (modern Edmonton, Mayo, Barrow), or as described in text (Old Crow).

Ranges are given in parentheses.

[^] Number of years of monthly data recorded.

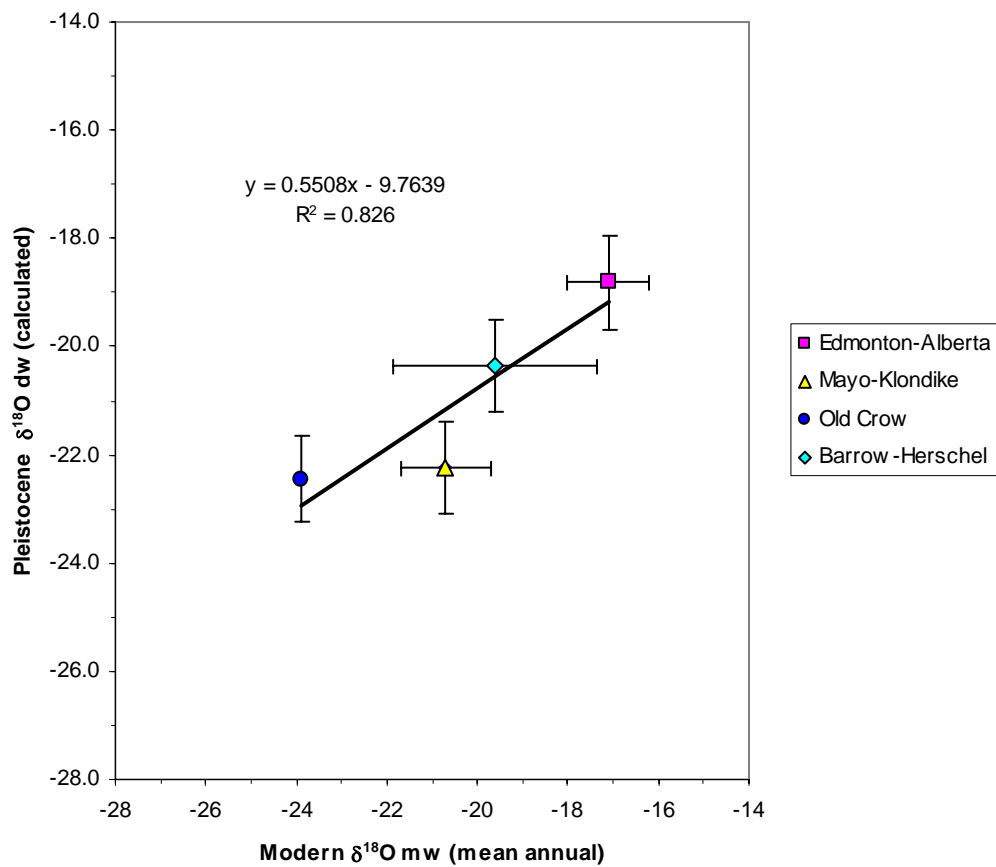


Figure 7.5 Comparison of the mean oxygen isotope compositions of Pleistocene drinking water and modern meteoric water at “nearby” locations (see text). Error bars represent one standard deviation. The equation for the best-fit regression line is shown.

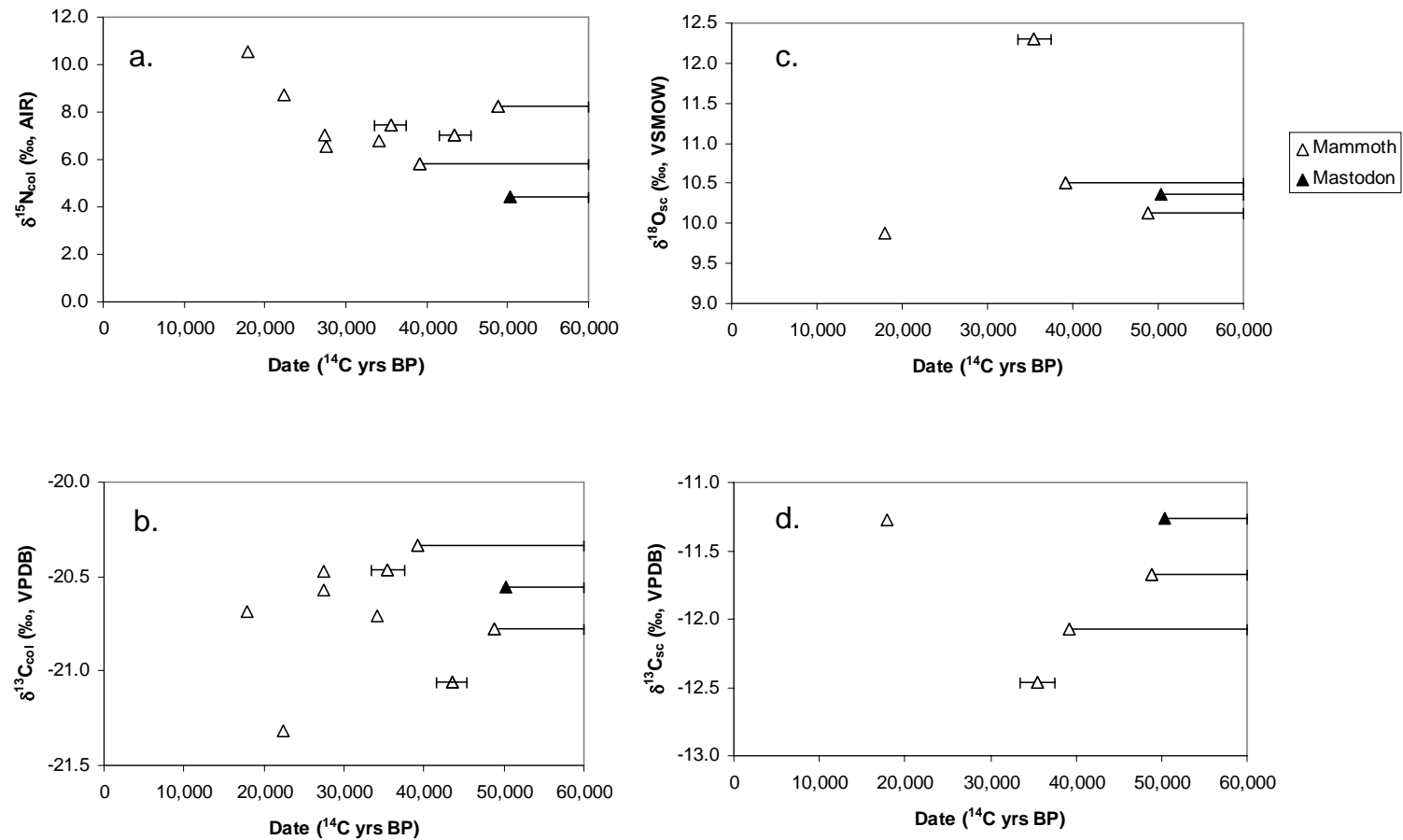


Figure 7.6 Temporal trends in isotopic compositions of Klondike proboscideans. (a) Nitrogen isotope composition of collagen, (b) carbon isotope composition of collagen, (c) oxygen isotope composition of structural carbonate in enamel bioapatite, (d) carbon isotope composition of structural carbonate in enamel bioapatite. Error bars represent one standard deviation (finite dates) or stretch to beyond the limits of the graph for “infinite” dates. For points with no error bars, one standard deviation was less than the size of the data point.

7.3.8 Temporal Trends

The only location for which analysis of temporal trends in stable isotope values is possible is Klondike (Figure 7.6). Nitrogen isotope compositions are highest in the most recent specimens, which date to the Last Glacial Maximum (about 22,000 – 17,000 BP) (Clark et al., 2009; Kennedy et al., 2010). One previous study also found an increase in the $\delta^{15}\text{N}$ values of eastern (but not western) Beringian mammoths during the LGM, consistent with colder and drier conditions during that time period (Szpak et al., 2010). Although there are no consistent changes in $\delta^{13}\text{C}_{\text{col}}$ values over time, one of the two LGM specimens has the lowest $\delta^{13}\text{C}_{\text{col}}$ value in the sample set. This is potentially related to the generally lower $\delta^{13}\text{C}_{\text{col}}$ values previously observed for LGM-age eastern Beringian samples, which possibly resulted from increased metabolism of stored fats (Szpak et al., 2010).

Few samples have both radiocarbon dates and structural carbonate isotopic data, but the single LGM-age sample has the lowest $\delta^{18}\text{O}$ value of any Klondike specimen, consistent with the lower $\delta^{18}\text{O}$ compositions of meteoric water in colder climates (Figure 7.6, Table 7.2). The same specimen has a $\delta^{13}\text{C}_{\text{sc}}$ value that is among the highest in the sample set. The $\delta^{13}\text{C}$ values of C_3 plants generally increase with aridity (Murphy and Bowman, 2009; Stewart et al., 1995; Swap et al., 2004), so higher $\delta^{13}\text{C}_{\text{sc}}$ values might be expected during the cold and dry LGM. However, if LGM-age mammoths were increasingly reliant on metabolism of seasonal fat stores (as suggested by Szpak et al., 2010), we would expect $\delta^{13}\text{C}_{\text{sc}}$ to be lower during that period. These opposing effects highlight the myriad of factors that can affect the carbon isotope compositions of mammalian tissues (see Chapter 6, Table 6.3).

7.3.9 Comparison of “Bulk” and “Incremental” Isotope Results

For Western Canada proboscideans, there is a strong correlation between bulk and mean incremental $\delta^{18}\text{O}$ values ($r = 0.97$, $df = 6$, $p < 0.001$) and between bulk and mean incremental $\delta^{13}\text{C}$ values (Pearson's $r = 0.92$, $df = 6$, $p < 0.01$). Serially-sampled mean $\delta^{18}\text{O}$ values were on average 0.9‰ lower than bulk enamel $\delta^{18}\text{O}$ values (range of offsets = 0.2‰ higher to 1.7‰ lower). Lower mean $\delta^{18}\text{O}$ values in incremental samples were also observed in Columbian mammoths from Arizona (Chapter 5) and mastodons from the

Great Lakes (Chapter 6) (mean difference = 1.8 and 1.3‰, respectively). The difference in maturation time for inner enamel versus the entire enamel thickness is likely the most important reason for this offset, as discussed in more detail in Chapter 5. Serially-sampled mean $\delta^{13}\text{C}$ values were the same or higher than bulk enamel $\delta^{13}\text{C}$ values for Western Canada specimens (mean difference = 0.5‰, range = 0.0 to 1.1‰). A similar offset in $\delta^{13}\text{C}$ values was observed for Great Lakes mastodons (mean difference = 0.4‰, range = 0.1 to 0.7‰) (Chapter 6). Arizona mammoths had more variable offsets (mean = -0.2‰, range = -1.3 to 0.6‰) (Chapter 5).

7.3.10 Serially-Sampled Enamel: Regular Periodicity

The serially-sampled enamel $\delta^{18}\text{O}_{\text{sc}}$ values exhibit regular periodicity in most samples, and a few samples also have $\delta^{13}\text{C}_{\text{sc}}$ values with regular periodicity (Table 7.4, Figures 7.7, 7.8). Table 7.5 lists the periods of the $\delta^{18}\text{O}$ curve for each specimen, based on the distance between peaks or valleys. For mammoths, periods ranged from 14 to 6 mm, and for mastodons, 18 to 3 mm. As observed previously for Great Lakes and Arizona specimens (Chapters 5, 6), periods for mastodons decrease with decreasing distance from the cervix, whereas periods for mammoths are more constant within each tooth. Since the $\delta^{18}\text{O}$ values of precipitation in high-latitude locations typically follows a sinusoidal pattern with a period of one year (Rozanski et al., 1993), we hypothesize that one period in the $\delta^{18}\text{O}$ curve represents one year of growth. Histological measurements of a mammoth specimen (AB6; likely *M. primigenius*) were used to test this assumption, as described in Chapters 4 and 6. On average, the cross-striation interval (d) was 5.1 ± 0.6 $\mu\text{m}/\text{day}$ (n = 9 measurements), the enamel prism-EDJ angle (I) was $48.6 \pm 4.9^\circ$ (n = 4), and the Striae of Retzius-EDJ angle (D) was $4.8 \pm 0.6^\circ$ (n = 5). These values correspond to an enamel extension rate of 15.4 mm/year, after Shellis (1984). Using the highest and lowest values measured for each variable, the extension rate estimate ranges from 9.6 to 23.1 mm/year. The period of the $\delta^{18}\text{O}$ curve for this specimen is 14 mm, which compares well to the average extension rate estimate of 15.4 mm/year. The estimates for this Alberta mammoth are also in good agreement with extension rate estimates for Columbian mammoths from Arizona (Chapters 4-5).

Table 7.4 Stable isotope compositions from "incremental" sampling, and their conversions to diet and drinking water compositions.

Position (mm)	Structural Carbonate			Diet	Water
	$\delta^{13}\text{C}$ (‰)	$\delta^{18}\text{O}$ (‰)	CO_3 Wt %	$\delta^{13}\text{C}$ (‰)	$\delta^{18}\text{O}$ (‰)
AB4E (Edmonton area mastodon)					
1	-11.2	14.9	5.3	-25.3	-18.1
2	-11.1	14.9	5.7	-25.2	-18.1
3	-10.9	13.8	6.3	-25.1	-19.3
4	-11.1	13.9	5.5	-25.3	-19.2
5	-11.2	13.9	4.7	-25.3	-19.1
6	-11.1	13.0	5.1	-25.3	-20.1
7	-11.1	12.5	5.1	-25.3	-20.6
8	-11.4	11.7	5.6	-25.5	-21.5
9	-11.0	12.4	5.4	-25.2	-20.7
10	-10.8	12.6	4.9	-25.0	-20.5
11	-10.8	13.1	4.9	-24.9	-20.0
12	-10.8	12.8	5.5	-24.9	-20.3
13	-10.8	12.7	5.5	-24.9	-20.4
14	-10.8	13.9	5.0	-24.9	-19.1
15	-10.7	14.6	5.7	-24.8	-18.4
16	-10.6	14.3	5.7	-24.8	-18.7
17	-10.4	15.6	4.5	-24.6	-17.4
18	-10.4	16.8	4.5	-24.5	-16.1
19	-9.7	17.6	4.9	-23.8	-15.3
20	-10.8	17.2	4.7	-24.9	-15.7
21	-10.9	15.9	5.6	-25.1	-17.0
22	-10.8	13.4	5.3	-24.9	-19.7
23	-10.6	13.1	5.6	-24.7	-20.0
24	-10.1	14.0	4.4	-24.3	-19.1
AB11E (Bezanson mammoth)					
1	-10.8	15.4	7.2	-24.9	-17.6
2	-10.6	14.1	6.9	-24.7	-19.0
3	-10.4	13.6	7.3	-24.5	-19.4
4	-10.2	13.9	5.9	-24.3	-19.1
5	-10.3	12.5	7.2	-24.4	-20.6
6	-10.7	11.4	5.0	-24.9	-21.7
7	-10.4	12.4	7.5	-24.6	-20.8
8	-10.6	12.2	7.2	-24.8	-20.9
9	-10.8	12.5	6.2	-24.9	-20.6
10	-11.0	13.3	6.2	-25.1	-19.7
11	-10.9	13.2	6.7	-25.0	-19.9
12	-11.1	13.2	6.0	-25.2	-19.9
13	-10.5	13.2	6.3	-24.6	-19.9
14	-10.9	13.7	6.5	-25.1	-19.4
15	-10.8	14.0	6.2	-24.9	-19.0
16	-10.8	14.0	7.1	-24.9	-19.0
17	-10.4	13.0	6.0	-24.5	-20.1
18	-10.4	14.0	5.9	-24.6	-19.0
19	-10.4	12.9	5.8	-24.5	-20.1

Table 7.4 cont.

Position (mm)	Structural Carbonate			Diet	Water
	$\delta^{13}\text{C}$	$\delta^{18}\text{O}$	CO_3	$\delta^{13}\text{C}$	$\delta^{18}\text{O}$
	(‰)	(‰)	Wt %	(‰)	(‰)
20	-10.3	12.8	6.4	-24.5	-20.3
21	-10.3	12.7	7.1	-24.4	-20.4
22	-10.1	12.8	6.4	-24.2	-20.3
AB6E (Villeneuve area mammoth)					
1	-10.1	14.8	6.4	-24.3	-18.2
2	-10.3	13.8	6.5	-24.5	-19.2
3	-10.4	13.7	6.1	-24.5	-19.4
4	-10.4	13.1	5.9	-24.5	-20.0
5	-10.6	12.4	6.2	-24.8	-20.7
6	-10.4	13.4	6.0	-24.6	-19.6
7	-10.3	13.2	6.6	-24.5	-19.9
8	-10.5	13.1	5.3	-24.7	-20.0
9	-10.4	13.4	6.1	-24.6	-19.7
10	-10.3	14.7	6.5	-24.4	-18.3
11	-10.0	13.7	no data	-24.1	-19.3
12	-10.2	15.3	6.0	-24.3	-17.7
13	-10.2	16.6	6.9	-24.4	-16.3
14	-10.0	15.6	3.4	-24.1	-17.3
15	-10.0	15.1	6.6	-24.1	-17.9
16	-10.0	14.8	5.8	-24.1	-18.2
17	-9.1	15.0	6.8	-23.3	-18.0
18	-9.8	13.5	5.5	-23.9	-19.5
19	-9.8	13.2	5.5	-23.9	-19.9
20	-10.0	13.6	6.6	-24.2	-19.4
21	-9.8	13.5	6.4	-24.0	-19.6
22	-10.0	13.4	4.7	-24.2	-19.6
23	-10.2	13.5	6.4	-24.4	-19.6
AB10E (Villeneuve area mastodon)					
1	-9.1	13.0	6.5	-23.3	-20.1
2	-9.2	13.6	6.0	-23.3	-19.5
3	-9.3	12.6	5.1	-23.4	-20.5
4	-9.3	12.1	5.8	-23.5	-21.1
5	-9.2	11.7	5.1	-23.3	-21.4
6	-9.0	12.2	5.9	-23.2	-20.9
7	-8.8	13.8	5.1	-23.0	-19.3
8	-9.2	15.0	6.6	-23.3	-17.9
9	-10.0	14.9	6.7	-24.2	-18.1
10	-10.0	14.6	3.3	-24.2	-18.4
11	-9.8	14.9	6.0	-23.9	-18.1
12	-9.5	12.2	6.0	-23.6	-20.9
13	-9.2	11.1	3.8	-23.4	-22.1
14	-9.5	10.3	4.5	-23.6	-22.9
15	-9.5	10.6	5.6	-23.7	-22.6
16	-9.2	9.6	6.2	-23.4	-23.6
17	-9.0	9.7	6.4	-23.2	-23.6
18	-8.7	12.5	6.9	-22.9	-20.6

Table 7.4 cont.

Position (mm)	Structural Carbonate			Diet	Water
	$\delta^{13}\text{C}$ (‰)	$\delta^{18}\text{O}$ (‰)	CO_3 Wt %	$\delta^{13}\text{C}$ (‰)	$\delta^{18}\text{O}$ (‰)
19	-9.4	14.1	3.9	-23.6	-19.0
20	-9.2	13.4	6.7	-23.4	-19.7
21	-9.4	12.0	6.1	-23.6	-21.1
22	-9.2	11.1	5.6	-23.4	-22.1
23	-9.6	10.0	5.7	-23.7	-23.3
24	-9.4	9.3	5.1	-23.6	-23.9
25	-9.5	13.6	4.2	-23.7	-19.5
26	-9.7	12.7	5.9	-23.9	-20.4
27	-9.5	11.4	5.9	-23.6	-21.7
28	-9.5	10.9	5.9	-23.7	-22.3
29	-9.5	10.9	4.4	-23.6	-22.2
29.5	-9.4	15.0	6.4	-23.6	-18.0
30.5	-9.7	15.1	6.1	-23.9	-17.9
31	-9.5	13.3	5.8	-23.6	-19.7
32	-9.3	11.3	5.3	-23.5	-21.9
33	-9.4	10.4	5.5	-23.6	-22.8
34	-9.2	13.1	5.3	-23.4	-20.0
35	-9.3	12.1	5.1	-23.4	-21.0
36	-9.0	10.3	5.4	-23.2	-22.9
37	-8.9	11.9	5.0	-23.0	-21.2
YT8E (Old Crow mastodon)					
1	-10.4	9.5	6.4	-24.6	-23.8
2	-10.0	10.3	7.1	-24.1	-22.9
3	-10.0	11.2	6.3	-24.2	-22.0
4	-10.4	11.5	7.1	-24.5	-21.6
5	-10.2	12.6	6.1	-24.3	-20.5
6	-10.3	12.1	6.6	-24.4	-21.1
7	-9.6	13.0	5.9	-23.8	-20.1
8	-9.7	11.3	6.4	-23.8	-21.9
9	-10.2	10.5	6.5	-24.3	-22.7
10	-9.7	11.4	8.1	-23.8	-21.8
11	-9.5	10.5	5.7	-23.7	-22.7
12	-9.2	9.4	6.3	-23.4	-23.8
13	-9.5	11.2	7.0	-23.6	-22.0
14	-9.9	11.9	5.1	-24.0	-21.3
15	-10.0	12.0	4.8	-24.2	-21.1
16	-10.0	12.1	5.2	-24.2	-21.0
17	-10.1	10.8	5.3	-24.2	-22.4
18	-10.2	10.3	5.7	-24.4	-22.9
19	-10.2	11.2	5.4	-24.3	-21.9
20	-9.8	11.1	3.2	-23.9	-22.1
21	-9.9	10.6	4.7	-24.1	-22.6
22	-10.2	11.9	4.3	-24.4	-21.2
23	-10.2	11.6	4.9	-24.4	-21.5
24	-9.8	10.5	5.7	-24.0	-22.7

Table 7.4 cont.

Position (mm)	Structural Carbonate			Diet	Water
	$\delta^{13}\text{C}$	$\delta^{18}\text{O}$	CO_3	$\delta^{13}\text{C}$	$\delta^{18}\text{O}$
	(‰)	(‰)	Wt %	(‰)	(‰)
25	-9.7	9.4	6.2	-23.9	-23.8
26	-9.8	8.8	5.9	-24.0	-24.5
27	-9.7	9.2	5.2	-23.9	-24.1
28	-10.3	10.1	5.9	-24.4	-23.1
29	-10.8	10.3	6.0	-25.0	-22.9
30	-10.5	10.7	5.6	-24.6	-22.5
31	-10.6	9.3	5.2	-24.7	-24.0
32	-10.8	9.7	5.2	-24.9	-23.5
33	-10.5	10.7	5.5	-24.6	-22.5
YT7E - (Old Crow mammoth, developing cone)					
1	-8.8	7.9	7.5	-23.0	-25.4
2	-8.7	7.8	7.0	-22.8	-25.5
3	-8.6	7.6	6.1	-22.8	-25.7
4	-8.7	7.6	6.9	-22.9	-25.7
5	-8.8	8.3	6.8	-23.0	-25.0
6	-9.1	9.9	7.5	-23.2	-23.3
7	-9.2	9.8	6.0	-23.4	-23.4
8	-9.4	10.0	6.4	-23.5	-23.2
9	-9.1	9.0	6.6	-23.2	-24.3
10	-8.8	7.9	6.1	-23.0	-25.4
11	-8.7	7.6	6.4	-22.9	-25.7
12	-8.6	7.4	6.5	-22.8	-25.9
13	-8.7	7.7	6.9	-22.8	-25.6
14	-8.8	8.3	6.0	-22.9	-25.0
15	-9.1	9.7	6.3	-23.3	-23.6
16	-9.5	10.3	6.6	-23.7	-22.9
17	-9.4	9.9	5.5	-23.5	-23.3
18	-8.7	8.7	7.6	-22.9	-24.6
19	-8.4	7.7	6.7	-22.6	-25.6
20	-8.4	7.7	3.6	-22.6	-25.6
21	-8.8	9.0	7.3	-23.0	-24.3
22	-9.2	10.4	6.9	-23.3	-22.8
23	-8.5	8.7	6.2	-22.7	-24.6
24	-8.4	7.1	6.3	-22.6	-26.2
25	-8.5	7.4	6.1	-22.7	-25.9
26	-8.4	7.2	6.0	-22.6	-26.1
27	-8.6	7.9	5.9	-22.8	-25.4
28	-9.0	8.8	6.1	-23.2	-24.5
29	-8.9	9.7	6.7	-23.0	-23.5
30	-9.1	10.1	5.2	-23.3	-23.1
YT26E (Klondike mammoth)					
1	-12.4	13.6	7.1	-26.5	-19.4
2	-12.4	13.3	6.4	-26.5	-19.8
3	-12.5	12.6	6.3	-26.6	-20.5
4	-12.4	11.6	6.6	-26.5	-21.5
5	-12.5	11.2	6.8	-26.7	-21.9

Table 7.4 cont.

Position (mm)	Structural Carbonate			Diet	Water
	$\delta^{13}\text{C}$ (‰)	$\delta^{18}\text{O}$ (‰)	CO_3 Wt %	$\delta^{13}\text{C}$ (‰)	$\delta^{18}\text{O}$ (‰)
6	-12.5	11.9	6.5	-26.6	-21.3
7	-12.6	11.6	6.6	-26.7	-21.5
8	-12.4	10.9	7.1	-26.5	-22.3
9	-12.4	11.4	7.1	-26.5	-21.8
10	-12.4	11.2	7.2	-26.5	-22.0
11	-12.2	11.1	7.1	-26.3	-22.1
12	-12.3	10.7	7.0	-26.5	-22.4
YT35E (Klondike mastodon)					
1.00	-10.6	11.3	5.4	-24.8	-21.9
1.50	-10.8	11.4	4.0	-24.9	-21.7
2.00	-10.9	10.2	4.2	-25.1	-23.0
2.50	-10.9	9.7	4.6	-25.0	-23.6
3.00	-10.8	9.4	4.3	-25.0	-23.8
3.50	-10.6	8.4	4.3	-24.7	-24.9
4.00	-10.6	8.5	4.5	-24.8	-24.7
4.50	-10.8	8.5	4.3	-24.9	-24.8
5.00	-11.0	7.9	4.2	-25.2	-25.4
5.50	-10.8	7.8	4.0	-24.9	-25.5
6.25	-10.7	7.4	4.4	-24.9	-25.9
6.75	-11.3	7.5	4.0	-25.5	-25.8
7.25	-11.3	8.2	3.7	-25.4	-25.0
7.75	-11.4	9.1	4.5	-25.5	-24.2
8.25	-11.5	9.7	4.8	-25.6	-23.5
8.75	-11.6	10.2	4.2	-25.7	-23.0
9.25	-11.4	10.9	5.1	-25.5	-22.3
9.75	-11.9	9.5	4.2	-26.0	-23.7
10.25	-11.5	9.0	4.9	-25.6	-24.3

Values in **bold** are the results of duplicate analyses

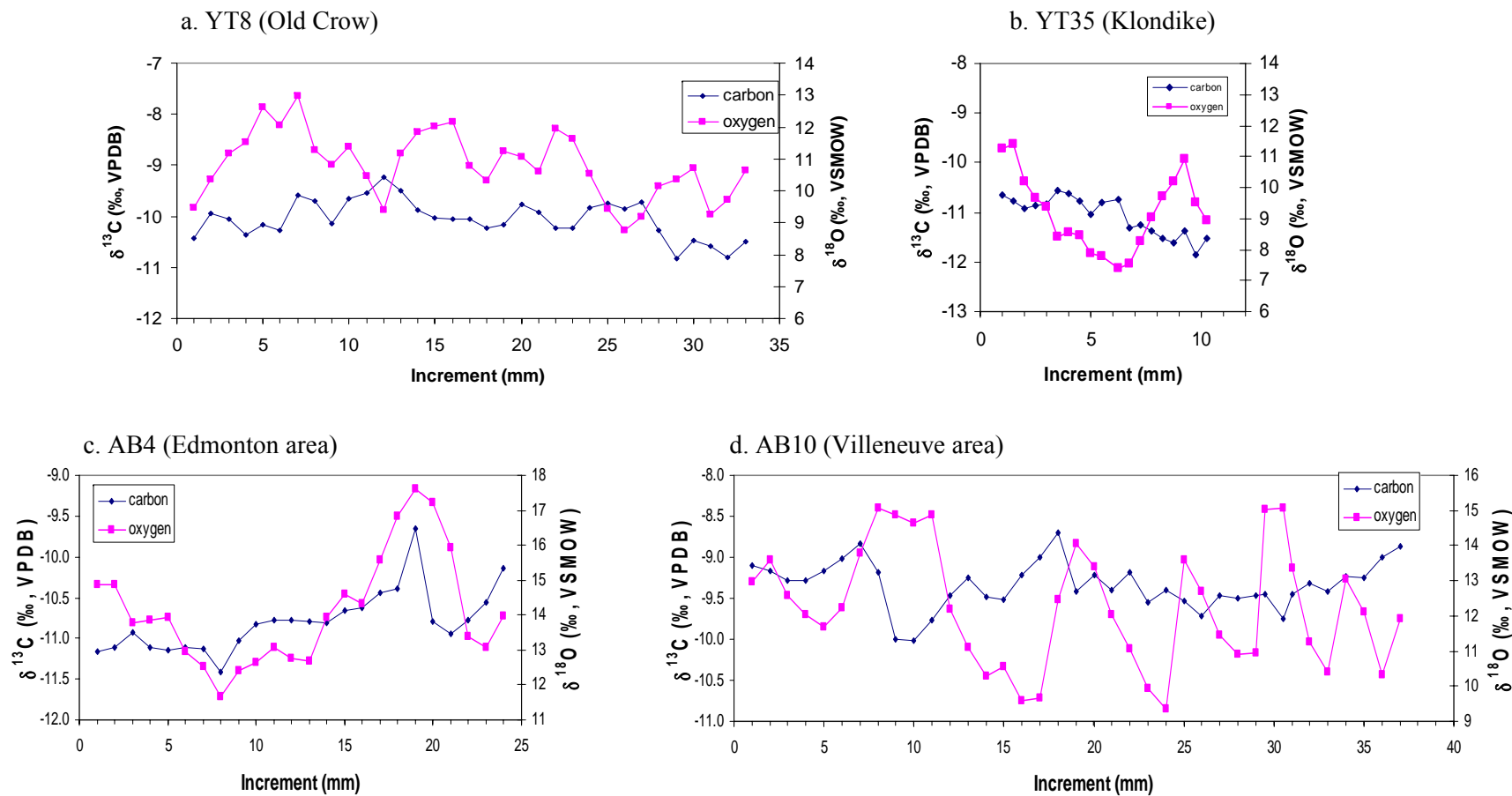


Figure 7.7 Carbon and oxygen isotope results for serial sampling of inner enamel from Western Canada mastodons. Higher increment numbers represent samples closer to the cervix.

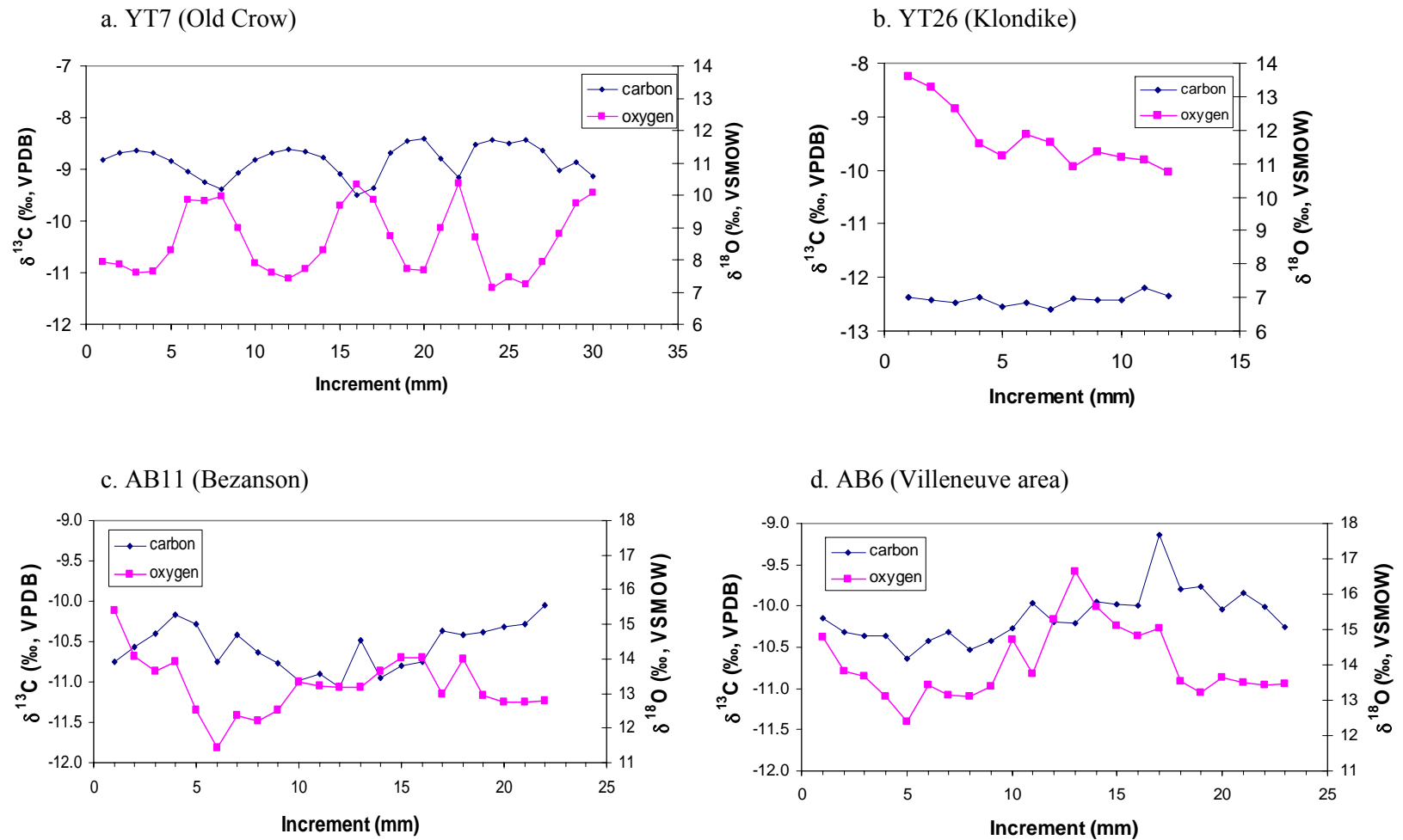


Figure 7.8 Carbon and oxygen isotope results for serial sampling of inner enamel from Western Canada mammoths. Higher increment numbers represent samples closer to the cervix.

Table 7.5 Summary of isotopic results for incrementally sampled Western Canada mastodons and mammoths.

Taxon	LSIS #	Location	n	$\delta^{13}\text{C}_{\text{sc}}$ (‰)				$\delta^{13}\text{C}_{\text{diet}}$ (‰)				$\delta^{18}\text{O}_{\text{sc}}$ (‰)				Period (mm)	No. **	$\delta^{18}\text{O}_{\text{water}}$ (‰)			
				Mean \pm SD	Min	Max	Range	Mean \pm SD	Min	Max	Range	Mean \pm SD	Min	Max	Range			Mean \pm SD	Min	Max	Range
Mastodon																					
	YT8	Old Crow	33	-10.1 \pm 0.4	-10.8	-9.2	1.6	-24.2 \pm 0.4	-25.0	-23.4	1.6	10.8 \pm 1.0	8.8	13.0	4.2	?	?	-22.4 \pm 1.1	-24.5	-20.1	4.4
	YT35	Klondike	19	-11.1 \pm 0.4	-11.9	-10.6	1.3	-25.2 \pm 0.4	-26.0	-24.7	1.3	9.2 \pm 1.2	7.4	11.4	4.0	8	1	-24.1 \pm 1.3	-25.9	-21.7	4.2
	AB4	Alberta	24	-10.8 \pm 0.4	-11.4	-9.7	1.8	-24.9 \pm 0.4	-25.5	-23.8	1.7	14.1 \pm 1.6	11.7	17.6	5.9	18? to 15*	>1	-18.9 \pm 1.7	-21.5	-15.3	6.2
	AB10	Alberta	38	-9.3 \pm 0.3	-10.0	-8.7	1.3	-23.5 \pm 0.3	-24.2	-22.9	1.3	12.3 \pm 1.7	9.3	15.1	5.7	11 to 3*	>5	-20.8 \pm 1.8	-23.9	-17.9	6.0
Mammoth																					
	YT7	Old Crow	30	-8.8 \pm 0.3	-9.5	-8.4	1.1	-23.0 \pm 0.3	-23.7	-22.6	1.1	8.6 \pm 1.1	7.1	10.4	3.3	9 to 6	>3	-24.7 \pm 1.1	-26.2	-22.8	3.4
	YT26	Klondike	12	-12.4 \pm 0.1	-12.6	-12.2	0.4	-26.5 \pm 0.1	-26.7	-26.3	0.4	11.8 \pm 0.9	10.7	13.6	2.9	>11?	<1	-21.4 \pm 1.0	-22.4	-19.4	3.0
	AB11	Alberta	22	-10.6 \pm 0.3	-11.1	-10.1	1.0	-24.7 \pm 0.3	-25.2	-24.2	1.0	13.2 \pm 0.8	11.4	15.4	3.9	14?	>1	-19.9 \pm 0.9	-21.7	-17.6	4.1
	AB6	Alberta	23	-10.1 \pm 0.3	-10.6	-9.1	1.5	-24.3 \pm 0.3	-24.8	-23.3	1.5	14.0 \pm 1.0	12.4	16.6	4.2	14	>1	-19.0 \pm 1.1	-20.7	-16.3	4.4

LSIS #: Sample ID used for Laboratory for Stable Isotope Science analyses, and referred to in this study

* Periods decrease closer to the cervix

** Number of periods recorded in isotope record (estimated)

7.3.11 Serially-Sampled Enamel: Seasonal Patterns

There is no consistent relationship between the $\delta^{13}\text{C}$ and $\delta^{18}\text{O}$ curves for mammoths or mastodons, or for Alberta or Yukon specimens (Figures 7.7, 7.8). Considering that the specimens may date to drastically different time periods, this lack of consistency is not unexpected. For two of the Alberta specimens (AB4 mastodon and AB6 mammoth), the $\delta^{13}\text{C}$ and $\delta^{18}\text{O}$ curves were similarly shaped, with high and low values for both curves occurring within the same increment or with a slight offset. This pattern is similar to that obtained for the Hiscock mastodon (Chapter 6). For one specimen (Old Crow mammoth, YT7), there is a very strong negative correlation between the $\delta^{13}\text{C}$ and $\delta^{18}\text{O}$ curves (Pearson's $r = -0.90$, $df = 28$, $p < 0.001$). A similar pattern (though without a statistical correlation) was observed for two Ontario mastodons (Chapter 6). There are numerous possible explanations for these two patterns, considering the many climatic, vegetational, and physiological factors that can affect seasonal changes in $\delta^{13}\text{C}$ (see Chapter 6 for more detailed discussion). The remaining five serially-sampled Western Canada proboscideans do not exhibit any simple relationship between their $\delta^{13}\text{C}$ and $\delta^{18}\text{O}$ curves.

7.3.12 Serially-sampled enamel: Isotopic composition of diet and drinking water

The calculated $\delta^{13}\text{C}_{\text{diet}}$ values reflect 100% C_3 plant consumption throughout the year for all individuals (range = -26.7 to -22.6‰) (Table 7.5). The calculated $\delta^{18}\text{O}_{\text{water}}$ values for Yukon range from -26.2 to -19.4‰ , and those for Alberta range from -23.9 to -15.3‰ (Table 7.5). The overlap between these ranges occurs because the values from “incremental” analysis represent seasonal extremes, whereas those from “bulk” analysis (which did not overlap; Figure 7.4) average a year or more of growth.

To directly compare serially-sampled isotope results for different specimens (which have different growth rates), the distance axis was converted to time using a simple anchor-point method, as described in Chapter 5 and demonstrated in Chapter 6. The $\delta^{18}\text{O}$ values of Yukon specimens are lower than those of Alberta specimens, whereas the $\delta^{13}\text{C}$ values overlap (Figure 7.9). This was also observed for “bulk” samples (Section 7.3.6). The amplitudes of the $\delta^{18}\text{O}$ curves tend to be larger in Alberta specimens than Yukon specimens (Figure 7.9, Table 7.5).

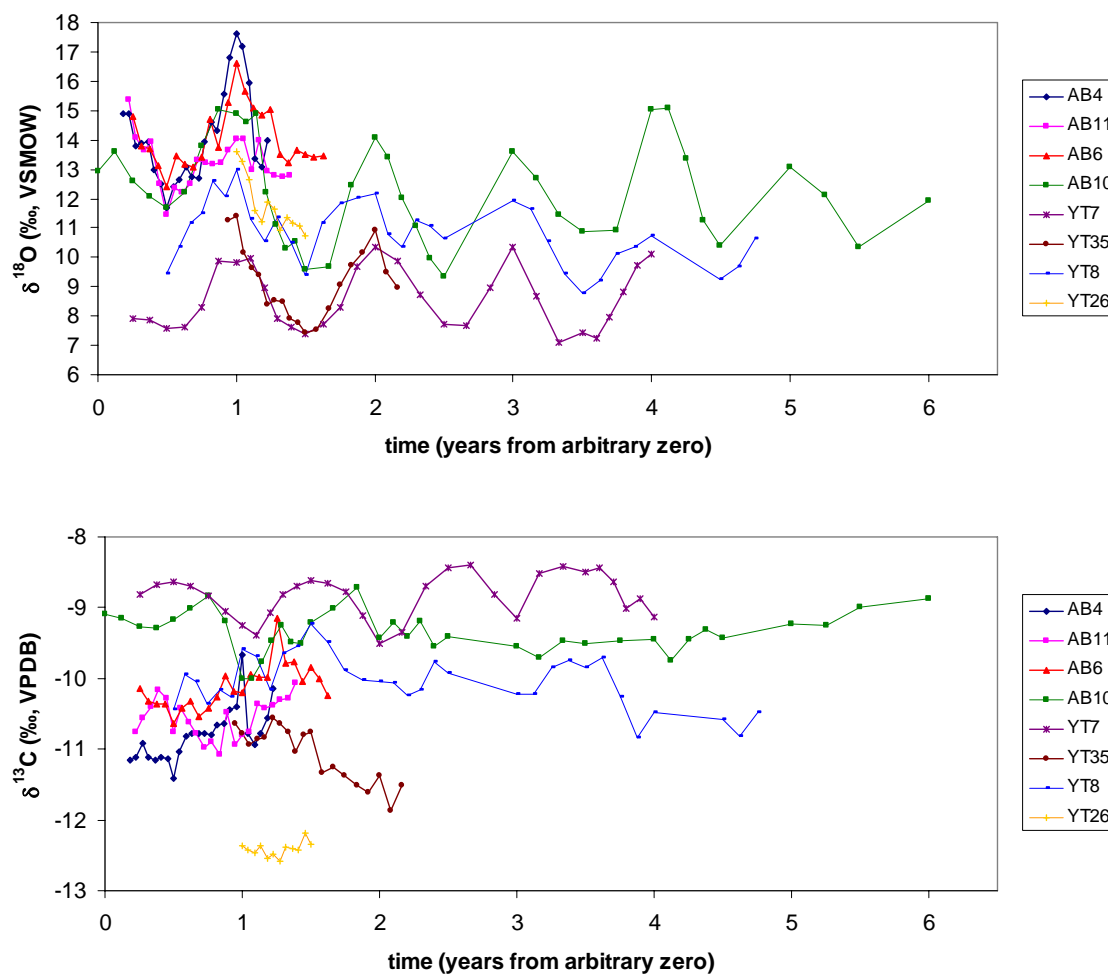


Figure 7.9 Comparison of carbon and oxygen isotope results for serial sampling of inner enamel from Western Canada proboscideans. The “distance” axis has been transformed to time, as described in the text. The reference point for time is arbitrary, so although the data are stacked for comparison of seasonal trends, the true age of each sample differs.

Table 7.3 lists the ranges of seasonal drinking water $\delta^{18}\text{O}$ values calculated from proboscidean tooth enamel in each region compared to the seasonal ranges of modern precipitation $\delta^{18}\text{O}$ values (monthly arithmetic means) at “nearby” locations. The data for Edmonton, Mayo, and Barrow were obtained from the IAEA database (IAEA/WMO, 2010). The data for Old Crow are the minimum and maximum $\delta^{18}\text{O}$ values for March snowpack and June to September rainfall that fall along the Global Meteoric Water Line (Turner et al., 2010). The seasonal $\delta^{18}\text{O}_{\text{water}}$ values calculated from proboscidean enamel fall within the ranges of modern precipitation from nearby stations, but the ranges calculated from enamel are much smaller than those of modern monthly precipitation. In part, this may result from the isotopic averaging that occurs during metabolism and tooth mineralization (Chapter 5). However, it also likely reflects consumption of groundwater, glacial meltwater, permafrost meltwater, and lake or river water, which have attenuated seasonal $\delta^{18}\text{O}$ variations relative to those of precipitation.

Seasonal variability in the $\delta^{18}\text{O}$ values of precipitation at mid- to high-latitudes is related to several factors, including seasonal changes in temperature, evapotranspiration flux, and changing vapour source areas (Rozanski et al., 1993). Typically, the highest $\delta^{18}\text{O}$ values in precipitation occur in summer and the lowest in winter. However, as previously suggested by Fox et al. (2007) for northern Siberia, a combination of factors (i.e., enhanced evaporation and low- ^{18}O ice-melting during summers, in combination with increased Arctic-derived precipitation in winter) could lead to the opposite of the typical meteoric water seasonal pattern in drinking waters (i.e., high values during winter and low values during summer). This causes a fundamental problem in determining which parts of the serially-sampled isotope curve represent summer versus winter growth.

Large regions of central Alberta, including the Edmonton area, only underwent a single late Wisconsin glaciation (with maximum ice-cover during and after the LGM, ca. 22,000 to 12,000 BP) (Catto et al., 1996; Hartman and Clague, 2008; Young et al., 1994). During the earlier Wisconsinan, when mammoths and mastodons were present in the region, the lack of glacial ice suggests that glacial meltwater did not contribute to drinking water in significant quantities (although some contribution from mountain glaciers may have occurred). Thus, for Alberta specimens, seasonal variations in the $\delta^{18}\text{O}$ values of drinking water were probably controlled by precipitation and evaporation

effects, and peaks in the $\delta^{18}\text{O}$ curves most likely represent summer growth, whereas valleys represent winter growth. Drinking water for mammoths and mastodons from Yukon may have had more input from glacial meltwater, snowmelt, and/or permafrost melt. The Old Crow region was never glaciated, but did receive meltwater drainage from the Laurentide Ice Sheet. However, major inundation and formation of glacial lakes only began after the primary period of proboscidean occupation, ca. 18,000 BP (Kennedy et al., 2010). The Klondike area was also unglaciated throughout the Pleistocene, but local montane ice melting (e.g., from the Ogilvie Mountains, the source of the modern Klondike River) could have contributed to summer drinking water. The $\delta^{18}\text{O}$ values of modern Yukon River waters, which include seasonal meltwater inputs, are lowest in late spring to early summer and most positive in late summer to early fall (Landwehr et al., 2010). Nevertheless, surface waters in modern Alaska are good proxies for precipitation, varying mainly with latitude and altitude (Sloat et al., 2010). Thus, it is less likely that glacial meltwater *controlled* seasonal $\delta^{18}\text{O}$ variations (reversing the typical meteoric water trend), than it is that ice-melt inputs caused *attenuation* in the seasonal variations controlled by precipitation and evaporation (weakening a pattern in which $\delta^{18}\text{O}$ peaks represent summer growth, and valleys, winter). The latter phenomenon would explain the lower amplitude of $\delta^{18}\text{O}$ curves for Yukon samples relative to Alberta specimens (Table 7.5). Furthermore, there is a larger difference in $\delta^{18}\text{O}$ maxima between Yukon and Alberta specimens than in $\delta^{18}\text{O}$ minima (Table 7.5), which can be explained by meltwater-induced decreases in summer (high) drinking water $\delta^{18}\text{O}$ values in Yukon, where $\delta^{18}\text{O}$ values are lower than in Alberta. However, it is not possible to definitively distinguish which portions of the oxygen isotope curve represent summer or winter using the currently available data. Furthermore, without this knowledge, it is not possible to interpret the seasonal trends in diet represented by the $\delta^{13}\text{C}$ curves.

7.3.13 Mammoth and Mastodon Seasonal Behaviour

Mastodon teeth tended to have larger seasonal variations in $\delta^{13}\text{C}$ and $\delta^{18}\text{O}$ values than mammoth teeth in both Yukon and Alberta (Table 7.5). It is possible, but unlikely, that this difference is related to sampling methodology. Since mammoth teeth have thinner enamel than mastodon teeth, samples drilled to identical depths encompass a

greater proportion of the total tooth thickness of the former specimens. That said, the growth rate of enamel perpendicular to the EDJ (i.e., “enamel thickness” growth rate) was estimated to be 0.8 to 1.5 mm/year for a Columbian mammoth (Chapter 4). Using the same methodology and histological measurements presented in Chapter 6 and above, this parameter is estimated at 0.7 to 1.8 mm/year for a Great Lakes mastodon (cervical vs. occlusal enamel, respectively) and 1.1 to 1.7 mm/year (mean = 1.4 mm/year) for an Alberta mastodon. Hence, there is little difference in growth rate perpendicular to the EDJ for mammoths and mastodons, which implies that there is little difference in the degree of isotopic averaging that occurs when drilling these teeth to the same depth. Because mastodon teeth often have lower extension rates than mammoth teeth (Chapter 6 and Table 7.5), more averaging would have occurred in the former as a result of the width of drill line (i.e., in the occlusal-basal direction, or “tooth height”). However, this difference should have decreased, not increased, the amplitude of the isotopic curves for mastodons. It remains possible that a difference in “isotopic averaging” could result from differing mineralization rates for inner enamel in mammoth versus mastodon teeth. However, no data are yet available on this process in proboscideans.

A more viable hypothesis is that the larger amplitudes of the $\delta^{13}\text{C}$ and $\delta^{18}\text{O}$ curves in mastodons relative to mammoths are the result of “real” differences in the degree to which the isotopic compositions of drinking water and diets varied seasonally. As described in Section 7.3.5, the mean oxygen isotope compositions of mammoth and mastodon drinking water did not differ. However, mastodons could have had larger seasonal variations in drinking water $\delta^{18}\text{O}$ values because they (1) relied on a water source (or sources) with larger seasonal changes in input (e.g., groundwater, precipitation, and meltwater), (2) migrated among water sources with very different $\delta^{18}\text{O}$ values, spending considerable time at each source, and/or (3) relied more heavily on precipitation-derived water sources than did mammoths. Given the lack of difference in mean $\delta^{18}\text{O}$ values between the taxa, and the extremely arid conditions in Beringia during the Pleistocene (Guthrie, 2001), possibility (3) has been eliminated from consideration. In contrast to mastodons, mammoths (1) relied on a water source (or sources) with a more stable isotopic composition, and/or (2) migrated frequently among numerous different water sources, thus averaging their isotopic compositions.

In the Great Lakes region, mammoths primarily inhabited well-drained upland areas near the shorelines of glacial lakes, whereas mastodons lived in wetter lowland plains (Chapter 6). In eastern Europe, mammoths are thought to have migrated between upland plains in summer and sheltered river valleys in winter (Velichko and Zelikson, 2005). Given their preference for wetter environments, mastodons might have remained in river valley environments all year round. Zazula et al. (2006a) document evidence for locally diverse habitats in the Klondike region (i.e., mesic valley bottoms, riparian meadows, and well-drained upland steppe-tundra) around 25,300 BP. There is no direct evidence for differences in mammoth and mastodon habitat preferences in Western Canada, but since the specimens were not discovered in primary contexts (see Section 7.2), the possibility remains. Thus, mastodon preference for river valley environments, and mammoth migration among different local habitats, is a viable explanation for the differences in the amplitudes of their $\delta^{18}\text{O}$ curves. Greater migration among microhabitats might also explain the slightly smaller amplitude of $\delta^{13}\text{C}$ values in mammoths (Table 7.5), which could result from more isotopic averaging of diverse plant species and plant parts. This possibility might be testable using an independent migration proxy, such as $^{87}\text{Sr}/^{86}\text{Sr}$ ratios.

An alternative scenario is that mammoths and mastodons lived during very different climatic periods (i.e., glacial vs. interglacial, respectively), and the differences in the amplitudes of their $\delta^{18}\text{O}$ curves is a result of changes in seasonal hydrological regimes between these periods. For example, increased precipitation or seasonal ice melting during warmer interglacial periods could lead to larger amplitudes of variation in drinking water $\delta^{18}\text{O}$ values for mastodons. As described in Section 7.3.5, the “average” drinking water $\delta^{18}\text{O}$ values of mammoths and mastodons calculated from bulk enamel do not support the hypothesis that there was a temporal difference between the taxa, but do not preclude the possibility either.

7.3.14 Use of Isotopes for Geographic Sourcing and Taxonomic Determination

The above results demonstrate that for Western Canada proboscidean fossils, isotopic analysis of structural carbonate in tooth enamel can be useful in determining the geographic origins. For example, Alberta specimens can clearly be distinguished from

Yukon specimens using “bulk” enamel $\delta^{18}\text{O}_{\text{sc}}$ values (Figure 7.4). Specimens from different regions of Yukon can also be distinguished using a combination of $\delta^{18}\text{O}_{\text{sc}}$ and $\delta^{13}\text{C}_{\text{sc}}$ values, which could be helpful in assigning provenance to isolated museum samples. In addition, $\delta^{15}\text{N}$ values of collagen can sometimes be used to distinguish between mammoth and mastodon specimens. For example, AB3 and AB12 were bone fragments that could only be identified as Proboscidea based on morphology (Table 7.1). However, the very high $\delta^{15}\text{N}$ value of AB3 (10.9‰) strongly suggests that it is a *Mammuthus* specimen, whereas the extremely low $\delta^{15}\text{N}$ value of AB12 (1.4‰) strongly suggests that it is *Mammot* (Table 7.2, Figure 7.3). It is worth noting that AB12 is the only known post-glacial Alberta specimen included in the present study (Table 7.1). Post-glacial occurrence of mastodon in central Alberta is consistent with the rapid expansion of spruce forests during the Terminal Pleistocene (MacDonald and McLeod, 1996). Spruce forests were preferred habitats for mastodons, but unfavourable to mammoths, who preferred open grasslands (see Chapter 6).

7.4 Conclusions

This study has shown that isotopic analyses (in particular, $\delta^{15}\text{N}$ values) can be useful in assigning taxonomic designations to proboscidean skeletal specimens (e.g., some mammoth and mastodon bones from Alberta). Unfortunately, this is not possible in all cases (e.g., proboscidean tusks from BC, which have $\delta^{15}\text{N}$ values intermediate to those of mammoths and mastodons in other regions).

We hypothesize that isotopic differences between mammoths and mastodons are primarily a result of paleoenvironmental conditions (habitat preferences), rather than physiological differences or nutritional stress. Spruce forest environments were relatively widespread in eastern Beringia during the last interglacial period (Harington, 1990; Matheus et al., 2003; Matthews et al., 1990; Reyes et al., 2010b; Schweger and Matthews Jr, 1991), and it has been argued that mastodon presence in the region was confined to that and earlier interglacials (Guthrie, 2001; Zazula et al., in prep). However, there is no evidence from $\delta^{18}\text{O}$ or $\delta^{13}\text{C}$ values that mastodons in Western Canada were restricted to warm interglacial periods. Spruce certainly persisted in valley bottom refugia between about 26,000 to 24,500 BP (Zazula et al., 2006c), and possibly during other glacial

periods as well. Thus, it is feasible that at least some mastodons in Yukon were contemporaneous with mammoths. Radiocarbon dates obtained for mammoths and mastodons in this study were consistent with previous studies, indicating that most specimens date to before the Last Glacial Maximum. Techniques capable of dating fossils older than ca. 40,000 BP are needed to further address the question of mammoth and mastodon contemporaneity.

Differences in $\delta^{18}\text{O}$ values among regions correspond to expectations based on modern latitudinal gradients in $\delta^{18}\text{O}$ compositions of precipitation, demonstrating the similarity of continental-scale processes (temperature gradients, movements of air masses) during the Pleistocene and today. In combination with $\delta^{13}\text{C}_{\text{sc}}$ values, these differences can be used to identify the geographic origins of samples with unknown provenance. The $\delta^{13}\text{C}_{\text{col}}$ and $\delta^{15}\text{N}$ values of proboscidean collagen in all of the regions overlapped, but on average, the results for Old Crow were significantly different from those of most other regions. Furthermore, differences between mammoths and mastodons were more pronounced in Old Crow than in any of the other regions. The environmental conditions that caused these differences between Old Crow and the other regions remain to be determined.

Temporal changes in the $\delta^{15}\text{N}$ and $\delta^{13}\text{C}_{\text{col}}$ values of proboscideans in Klondike were consistent with previous isotopic studies, and observations that the LGM in eastern Beringia was very cold and dry. Although the data are limited, $\delta^{18}\text{O}_{\text{sc}}$ and $\delta^{13}\text{C}_{\text{sc}}$ values further support this contention.

Proboscideans in Western Canada consumed 100% C_3 -plant diets throughout the year. “Seasonal” ranges of drinking water $\delta^{18}\text{O}$ values calculated from proboscidean enamel are smaller than the ranges of $\delta^{18}\text{O}$ values for modern monthly precipitation at nearby locations. This probably results both from the isotopic “averaging” that occurs during tooth formation and sampling, and from reliance on groundwater, glacial meltwater, lake water, and/or river water sources of drinking water instead of solely on precipitation.

Mastodons had larger “seasonal” variations in drinking water than mammoths. It remains possible that mammoths and mastodons lived during different temporal periods (i.e., glacials vs. interglacials). However, we argue that the most likely explanation for the

difference in $\delta^{18}\text{O}$ amplitudes for Western Canada proboscideans is that mastodons relied on water sources (likely in sheltered river valleys) with relatively large seasonal changes in source-water inputs (i.e., varying proportions of groundwater, precipitation, and meltwater), whereas mammoths migrated frequently among different water sources, thus averaging their isotopic compositions. The slightly smaller amplitudes in mammoth $\delta^{13}\text{C}$ values could likewise result from greater migration among microhabitats throughout the year, leading to greater averaging of plant isotopic compositions. This hypothesis fits with previous interpretations of mammoth and mastodon habitat preferences, and neither precludes nor requires temporal differences between mammoths and mastodons.

A major difficulty in interpreting serially-sampled isotope results for animals from regions with seasonally variable glacial meltwater input to drinking water is determining which portions of the $\delta^{18}\text{O}$ curve represent summer or winter growth. Ideally, independent evidence for summer versus winter growth periods would be obtained. Previous researchers have used increment thicknesses to determine which portions of the stable isotope curve in proboscidean tusk dentin correspond to summer or winter (e.g., Fisher and Fox, 2003; Fox et al., 2007; Koch et al., 1989). At some lower-latitude sites (southeastern Michigan and western New York), there is regular periodicity in proboscidean dentin $\delta^{18}\text{O}$ values, and low $\delta^{18}\text{O}$ values correspond to slow-growth periods (inferred winters), as expected when drinking water $\delta^{18}\text{O}$ values reflect the isotopic compositions of seasonal precipitation (Koch et al., 1989). At others (e.g., the Hiscock site in western New York) there is a lack of regular periodicity and no simple correspondence between slow-growth periods and the $\delta^{18}\text{O}$ curve (Fisher and Fox, 2003). At some higher-latitude sites (e.g., Chukotka, in eastern Siberia), $\delta^{18}\text{O}$ values are highest during inferred winters and lowest during spring/summer, which can be attributed at least in part to the contribution of winter snow melt (Fox et al., 2007). At other sites (e.g., Taimyr Peninsula in northern Russia), there are no coherent patterns of seasonal variation in $\delta^{18}\text{O}$ values (Fox et al., 2007). To our knowledge, comparison of growth increment thicknesses and stable isotope compositions has not yet been attempted for tooth enamel. However, since enamel growth increments form during the initial secretory stage of development, whereas stable isotope compositions reflect bioapatite growth during both the secretory and maturation stages, there may be an offset between increment formation

and the isotope curve (Smith and Tafforeau, 2008). Further study of enamel growth in relation to stable isotope compositions is needed to interpret the seasonal variations in serially-sampled enamel.

7.5 References

- Agenbroad, L.D., 2005. North American proboscideans: Mammoths - the state of knowledge, 2003. *Quaternary International*, 126-28: 73-92.
- Ambrose, S.H., 1990. Preparation and characterization of bone and tooth collagen for isotopic analysis. *Journal of Archaeological Science*, 17(4): 431-451.
- Ambrose, S.H. and Norr, L., 1993. Experimental evidence for the relationship of the carbon isotope ratios of whole diet and dietary protein to those of bone collagen and carbonate. In: J.B. Lambert and G. Grupe (Editors), *Prehistoric Human Bone: Archaeology at the Molecular Level*. Springer-Verlag, Berlin, pp. 1-37.
- Anderson, P.H. and Lozhkin, A.V., 2001. The Stage 3 interstadial complex (Karginskii/middle Wisconsinan interval) of Beringia: variations in paleoenvironments and implications for paleoclimatic interpretations. *Quaternary Science Reviews*, 20(1-3): 93-125.
- Armstrong, J.E. and Clague, J.J., 1977. Two major Wisconsin lithostratigraphic units in southwest British Columbia *Canadian Journal of Earth Sciences*, 14(7): 1471-1480.
- Arppe, L. and Karhu, J.A., 2006. Implications for the Late Pleistocene climate in Finland and adjacent areas from the isotopic composition of mammoth skeletal remains. *Palaeogeography Palaeoclimatology Palaeoecology*, 231(3-4): 322-330.
- Arppe, L. and Karhu, J.A., 2010. Oxygen isotope values of precipitation and the thermal climate in Europe during the middle to late Weichselian ice age. *Quaternary Science Reviews*, 29(9-10): 1263-1275.
- Ayliffe, L.K., Lister, A.M. and Chivas, A.R., 1992. The preservation of glacial-interglacial climatic signatures in the oxygen isotopes of elephant skeletal phosphate. *Palaeogeography Palaeoclimatology Palaeoecology*, 99(3-4): 179-191.
- Barnes, I., Shapiro, B., Lister, A., Kuznetsova, T., Sher, A., Guthrie, D. and Thomas, M.G., 2007. Genetic structure and extinction of the woolly mammoth, *Mammuthus primigenius*. *Current Biology*, 17(12): 1072-1075.
- Barnosky, A.D., Koch, P.L., Feranec, R.S., Wing, S.L. and Shabel, A.B., 2004. Assessing the causes of Late Pleistocene extinctions on the continents. *Science*, 306(5693): 70-75.
- Beaudoin, A.B. and Oetelaar, G.A., 2003. The changing ecophysical landscape of southern Alberta during the late Pleistocene and early Holocene. *Plains Anthropologist*, 48(187): 187-207.
- Beaudoin, A.B., Wright, M. and Ronaghan, B., 1996. Late Quaternary landscape history and archaeology in the 'ice-free corridor': Some recent results from Alberta. *Quaternary International*, 32: 113-126.
- Bigelow, N.H., Brubaker, L.B., Edwards, M.E., Harrison, S.P., Prentice, I.C., Anderson, P.M., Andreev, A.A., Bartlein, P.J., Christensen, T.R., Cramer, W., Kaplan, J.O., Lozhkin, A.V., Matveyeva, N.V., Murray, D.F., McGuire, A.D., Razzhivin, V.Y., Ritchie, J.C., Smith, B., Walker, D.A., Gajewski, K., Wolf, V., Holmqvist, B.H., Igarashi, Y., Kremenetskii, K., Paus, A., Pisaric, M.F.J. and Volkova, V.S., 2003. Climate change and Arctic ecosystems: 1. Vegetation changes north of 55 degrees

- N between the last glacial maximum, mid-Holocene, and present. *Journal of Geophysical Research - Atmospheres*, 108(D19): 25.
- Bocherens, H., 2003. Isotopic biogeochemistry and the paleoecology of the mammoth steppe fauna. *Deinsea*, 9: 57-71.
- Bocherens, H., Billiou, D., Patou-Mathis, M., Bonjean, D., Otte, M. and Mariotti, A., 1997. Paleobiological implications of the isotopic signatures (^{13}C , ^{15}N) of fossil mammal collagen in Scladina cave (Sclayn, Belgium). *Quaternary Research*, 48(3): 370-380.
- Bocherens, H., Pacaud, G., Lazarev, P.A. and Mariotti, A., 1996. Stable isotope abundances (^{13}C , ^{15}N) in collagen and soft tissues from Pleistocene mammals from Yakutia: Implications for the palaeobiology of the Mammoth Steppe. *Palaeogeography Palaeoclimatology Palaeoecology*, 126(1-2): 31-44.
- Bryant, J.D., Koch, P., Froelich, P.N., Showers, W.J. and Genna, B.J., 1996. Oxygen isotope partitioning between phosphate and carbonate in mammalian apatite. *Geochimica et Cosmochimica Acta*, 60(24): 5145-5148.
- Burns, J.A., 1996. Vertebrate paleontology and the alleged ice-free corridor: the meat of the matter. *Quaternary International*, 32: 107-112.
- Burns, J.A., 2010. Mammalian faunal dynamics in Late Pleistocene Alberta, Canada. *Quaternary International*, 217(1-2): 37-42.
- Burns, J.A., G., B.C. and Mol, D., 2003. An extraordinary woolly mammoth molar from Alberta, Canada. *Deinsea*, 9: 77-85.
- Burns, J.A. and Young, R.R., 1994. Pleistocene mammals of the Edmonton area, Alberta. Part I. The carnivores. *Canadian Journal of Earth Sciences*, 31(2): 393-400.
- Catto, N., Liverman, D.G.E., Bobrowsky, P.T. and Rutter, N., 1996. Laurentide, Cordilleran, and Montane glaciation in the western Peace River Grande Prairie Region, Alberta and British Columbia, Canada. *Quaternary International*, 32: 21-32.
- Cerling, T.E. and Harris, J.M., 1999. Carbon isotope fractionation between diet and bioapatite in ungulate mammals and implications for ecological and paleoecological studies. *Oecologia*, 120(3): 347-363.
- Churcher, C.S., 1968. Pleistocene ungulates from the Bow River gravels at Cochrane, Alberta. *Canadian Journal of Earth Sciences*, 5(6): 1467-1488.
- Clague, J.J., Froese, D., Hutchinson, I., James, T.S. and Simon, K.M., 2005. Early growth of the last Cordilleran ice sheet deduced from glacio-isostatic depression in southwest British Columbia, Canada. *Quaternary Research*, 63(1): 53-59.
- Clark, P.U., Dyke, A.S., Shakun, J.D., Carlson, A.E., Clark, J., Wohlfarth, B., Mitrovica, J.X., Hostetler, S.W. and McCabe, A.M., 2009. The Last Glacial Maximum. *Science*, 325(5941): 710-714.
- Clementz, M.T., Fox-Dobbs, K., Wheatley, P.V., Koch, P.L. and Doak, D.F., 2009. Revisiting old bones: coupled carbon isotope analysis of bioapatite and collagen as an ecological and palaeoecological tool. *Geological Journal*, 44(5): 605-620.
- Coltrain, J.B., Harris, J.M., Cerling, T.E., Ehleringer, J.R., Dearing, M.D., Ward, J. and Allen, J., 2004a. Rancho La Brea stable isotope biogeochemistry and its implications for the palaeoecology of late Pleistocene, coastal southern California. *Palaeogeography Palaeoclimatology Palaeoecology*, 205(3-4): 199-219.

- Coltrain, J.B., Hayes, M.G. and O'Rourke, D.H., 2004b. Sealing, whaling and caribou: the skeletal isotope chemistry of Eastern Arctic foragers. *Journal of Archaeological Science*, 31(1): 39-57.
- Coplen, T.B., 1994. Reporting stable hydrogen, carbon, and oxygen isotopic abundances. *Pure and Applied Chemistry*, 66: 271-276.
- Coplen, T.B., Brand, W.A., Gehre, M., Groning, M., Meijer, H.A.J., Toman, B. and Verkouteren, R.M., 2006. New guidelines for $\delta^{13}\text{C}$ measurements. *Analytical Chemistry*, 78(7): 2439-2441.
- Cowling, S.A., 1999. Perspectives: Paleoecology - Plants and temperature- CO_2 uncoupling. *Science*, 285(5433): 1500-1501.
- Cowling, S.A. and Sykes, M.T., 1999. Physiological significance of low atmospheric CO_2 for plant-climate interactions. *Quaternary Research*, 52(2): 237-242.
- Cummings, L.S. and Albert, R.M., 2007. Phytolith and starch analysis of Dent site mammoth teeth calculus: new evidence for Late Pleistocene mammoth diets and environments. In: R.H. Brunswig and B.L. Pitblado (Editors), *Frontiers in Colorado Paleoindian Archaeology: From the Dent Site to the Rocky Mountains*. University Press of Colorado, Boulder, pp. 185-192.
- Debruyne, R., Chu, G., King, C.E., Bos, K., Kuch, M., Schwarz, C., Szpak, P., Grocke, D.R., Matheus, P., Zazula, G., Guthrie, D., Froese, D., Buigues, B., de Marliave, C., Flemming, C., Poinar, D., Fisher, D., Southon, J., Tikhonov, A.N., MacPhee, R.D.E. and Poinar, H.N., 2008. Out of America: Ancient DNA evidence for a New World origin of Late Quaternary woolly mammoths. *Current Biology*, 18(17): 1320-1326.
- DeNiro, M.J., 1985. Post-mortem preservation and alteration of "in vivo" bone collagen ratios: implications for paleodietary analysis. *Nature*, 317: 806-809.
- Elias, S.A., Short, S.K. and Birks, H.H., 1997. Late Wisconsin environments of the Bering Land Bridge. *Palaeogeography Palaeoclimatology Palaeoecology*, 136(1-4): 293-308.
- Fedje, D.W. and Josenhans, H., 2000. Drowned forests and archaeology on the continental shelf of British Columbia, Canada. *Geology*, 28(2): 99-102.
- Fisher, D.C. and Fox, D.L., 2003. Season of death and terminal growth histories of Hiscock mastodons. In: R.S. Laub (Editor), *The Hiscock Site: Late Pleistocene and Holocene Paleoecology and Archaeology of Western New York State: Proceedings of the Second Smith Symposium, held at the Buffalo Museum of Science, October 14-15, 2001*. Buffalo Society of Natural Sciences, Buffalo, pp. 83-101.
- Fox-Dobbs, K., Leonard, J.A. and Koch, P.L., 2008. Pleistocene megafauna from eastern Beringia: Paleoecological and paleoenvironmental interpretations of stable carbon and nitrogen isotope and radiocarbon records. *Palaeogeography Palaeoclimatology Palaeoecology*, 261(1-2): 30-46.
- Fox, D.L., Fisher, D.C., Vartanyan, S., Tikhonov, A.N., Mol, D. and Buigues, B., 2007. Paleoclimatic implications of oxygen isotopic variation in late Pleistocene and Holocene tusks of *Mammuthus primigenius* from northern Eurasia. *Quaternary International*, 169: 154-165.
- France, C.A.M., Zelanko, P.M., Kaufman, A.J. and Holtz, T.R., 2007. Carbon and nitrogen isotopic analysis of Pleistocene mammals from the Saltville Quarry

- (Virginia, USA): Implications for trophic relationships. *Palaeogeography Palaeoclimatology Palaeoecology*, 249(3-4): 271-282.
- Fuller, B.T., Fuller, J.L., Sage, N.E., Harris, D.A., O'Connell, T.C. and Hedges, R.E.M., 2005. Nitrogen balance and $\delta^{15}\text{N}$: why you're not what you eat during nutritional stress. *Rapid Communications in Mass Spectrometry*, 19(18): 2497-2506.
- Garvie-Lok, S.J., Varney, T.L. and Katzenberg, M.A., 2004. Preparation of bone carbonate for stable isotope analysis: the effects of treatment time and acid concentration. *Journal of Archaeological Science*, 31(6): 763-776.
- Genoni, L., Iacumin, P., Nikolaev, V., Gribchenko, Y. and Longinelli, A., 1998. Oxygen isotope measurements of mammoth and reindeer skeletal remains: an archive of Late Pleistocene environmental conditions in Eurasian Arctic. *Earth and Planetary Science Letters*, 160(3-4): 587-592.
- Gobet, K.E. and Bozarth, S.R., 2001. Implications for late Pleistocene mastodon diet from opal phytoliths in tooth calculus. *Quaternary Research*, 55(2): 115-122.
- Guthrie, R.D., 1982. Mammals of the mammoth steppe as paleoenvironmental indicators. In: D.M. Hopkins, J.V. Matthews Jr., C.E. Schweger and S.B. Young (Editors), *Paleoecology of Beringia*. Academic Press Inc., New York, pp. 307-326.
- Guthrie, R.D., 1990. *Frozen fauna of the Mammoth Steppe: the story of Blue Babe*. University of Chicago Press, Chicago, 323 pp.
- Guthrie, R.D., 2001. Origin and causes of the mammoth steppe: a story of cloud cover, woolly mammal tooth pits, buckles, and inside-out Beringia. *Quaternary Science Reviews*, 20(1-3): 549-574.
- Guthrie, R.D., 2006. New carbon dates link climatic change with human colonization and Pleistocene extinctions. *Nature*, 441(7090): 207-209.
- Harington, C.R., 1975. Pleistocene muskoxen (*Symbos*) from Alberta and British Columbia. *Canadian Journal of Earth Sciences*, 12(6): 903-919.
- Harington, C.R., 1990. Vertebrates of the last interglaciation in Canada: a review, with new data. *Geographie Physique et Quaternaire*, 44(3): 375-387.
- Hartman, G.M.D. and Clague, J.J., 2008. Quaternary stratigraphy and glacial history of the Peace River valley, northeast British Columbia. *Canadian Journal of Earth Sciences*, 45(5): 549-564.
- Haynes, G., 1991. *Mammoths, mastodonts, and elephants: biology, behavior, and the fossil record*. Cambridge University Press, Cambridge New York, 413 pp.
- Haynes, G., 2009. Introduction to the volume. In: G. Haynes (Editor), *American megafaunal extinctions at the end of the Pleistocene*. Vertebrate Paleobiology and Paleoanthropology Series. Springer, Netherlands, pp. 1-20.
- Hedges, R.E.M., Stevens, R.E. and Richards, M.P., 2004. Bone as a stable isotope archive for local climatic information. *Quaternary Science Reviews*, 23(7-8): 959-965.
- Hetherington, R., Barrie, J.V., Reid, R.G.B., MacLeod, R. and Smith, D.J., 2004. Paleogeography, glacially induced crustal displacement, and Late Quaternary coastlines on the continental shelf of British Columbia, Canada. *Quaternary Science Reviews*, 23(3-4): 295-318.
- Hetherington, R., Barrie, J.V., Reid, R.G.B., MacLeod, R., Smith, D.J., James, T.S. and Kung, R., 2003. Late Pleistocene coastal paleogeography of the Queen Charlotte Islands, British Columbia, Canada, and its implications for terrestrial biogeography and early postglacial human occupation. *Canadian Journal of Earth Sciences*, 40(12): 1755-1766.

- Hillson, S., 1996. *Dental Anthropology*. Cambridge University Press, Cambridge, 373 pp.
- Hobson, K.A., Alisauskas, R.T. and Clark, R.G., 1993. Stable-isotope enrichment in avian tissues due to fasting and nutritional stress: Implications for isotopic analyses of diet *Condor*, 95(2): 388-394.
- Hoffecker, J.F. and Elias, S.A., 2003. Environment and archeology in Beringia. *Evolutionary Anthropology*, 12(1): 34-49.
- Iacumin, P., Bocherens, H., Mariotti, A. and Longinelli, A., 1996. Oxygen isotope analyses of co-existing carbonate and phosphate in biogenic apatite: a way to monitor diagenetic alteration of bone phosphate? *Earth and Planetary Science Letters*, 142: 1-6.
- Iacumin, P., Nikolaev, V. and Ramigni, M., 2000. C and N stable isotope measurements on Eurasian fossil mammals, 40 000 to 10 000 years BP: Herbivore physiologies and palaeoenvironmental reconstruction. *Palaeogeography Palaeoclimatology Palaeoecology*, 163(1-2): 33-47.
- IAEA/WMO, 2010. Global Network of Isotopes in Precipitation. The GNIP Database. Accessible at: <http://www.iaea.org/water>.
- Josenhans, H., Fedje, D., Pienitz, R. and Southon, J., 1997. Early humans and rapidly changing Holocene sea levels in the Queen Charlotte Islands Hecate Strait, British Columbia, Canada. *Science*, 277(5322): 71-74.
- Keddie, G., 1979. The Late Ice Age of southern Vancouver Island. *The Midden*, 11(4): 16-22.
- Kennedy, K.E., Froese, D.G., Zazula, G.D. and Lauriol, B., 2010. Last Glacial Maximum age for the northwest Laurentide maximum from the Eagle River spillway and delta complex, northern Yukon. *Quaternary Science Reviews*, 29(9-10): 1288-1300.
- Koch, P.L., 1991. The isotopic ecology of Pleistocene proboscideans. *Journal of Vertebrate Paleontology*, 11(Suppl. 3): 40A.
- Koch, P.L., 1998. Isotopic reconstruction of past continental environments. *Annual Review of Earth and Planetary Sciences*, 26: 573-613.
- Koch, P.L. and Barnosky, A.D., 2006. Late Quaternary extinctions: State of the debate. *Annual Review of Ecology Evolution and Systematics*, 37: 215-250.
- Koch, P.L., Fisher, D.C. and Dettman, D., 1989. Oxygen isotope variation in the tusks of extinct proboscideans: a measure of season of death and seasonality. *Geology*, 17: 515-519.
- Koch, P.L., Tuross, N. and Fogel, M.L., 1997. The effects of sample treatment and diagenesis on the isotopic integrity of carbonate in biogenic hydroxylapatite. *Journal of Archaeological Science*, 24(5): 417-429.
- Kohn, M.J., 1996. Predicting animal $\delta^{18}\text{O}$: Accounting for diet and physiological adaptation. *Geochimica et Cosmochimica Acta*, 60(23): 4811-4829.
- Kohn, M.J. and McKay, M., 2010. Stable isotopes of fossil teeth corroborate key general circulation model predictions for the Last Glacial Maximum in North America. *Geophysical Research Letters*, 37(22): L22702.
- Kohn, M.J., Schoeninger, M.J. and Valley, J.W., 1996. Herbivore tooth oxygen isotope compositions: Effects of diet and physiology. *Geochimica et Cosmochimica Acta*, 60(20): 3889-3896.

- Kuitens, M., 2010. Water and food stress: fatal blow for mammoths? Stable isotopes as indicators of water and food stress in large Pleistocene herbivores, 11th ICAZ (International Council for Archaeozoology) Conference, Paris, France.
- Kuzmin, Y.V., 2010. Extinction of the woolly mammoth (*Mammuthus primigenius*) and woolly rhinoceros (*Coelodonta antiquitatis*) in Eurasia: Review of chronological and environmental issues. *Boreas*, 39(2): 247-261.
- Lacourse, T., 2005. Late Quaternary dynamics of forest vegetation on northern Vancouver Island, British Columbia, Canada. *Quaternary Science Reviews*, 24(1-2): 105-121.
- Lacourse, T., Mathewes, R.W. and Fedje, D.W., 2005. Late-glacial vegetation dynamics of the Queen Charlotte Islands and adjacent continental shelf, British Columbia, Canada. *Palaeogeography Palaeoclimatology Palaeoecology*, 226(1-2): 36-57.
- Landwehr, J.M., Coplen, T.B. and Schuster, P.F., 2010. Decadal variation in stable isotopes ($\delta^2\text{H}$, $\delta^{18}\text{O}$) of water in the Yukon River system during an extended period of warming air temperatures, AGU Fall Meeting, 13-17 December, San Francisco, California.
- Lyons, S.K., Smith, F.A., Wagner, P.J., White, E.P. and Brown, J.H., 2004. Was a 'hyperdisease' responsible for the late Pleistocene megafaunal extinction? *Ecology Letters*, 7(9): 859-868.
- MacDonald, G.M. and McLeod, T.K., 1996. The Holocene closing of the 'ice-free' corridor: A biogeographical perspective. *Quaternary International*, 32: 87-95.
- MacPhee, R.D.E. and Marx, P.A., 1997. The 40,000-year plague: humans, hyperdisease, and first-contact extinctions. In: S.M. Goodman and B.D. Patterson (Editors), *Natural change and human impact in Madagascar*. Smithsonian Institution Press, Washington, D.C., pp. 169-217.
- MacPhee, R.D.E., Tikhonov, A.N., Mol, D., Maliave, C.D., Van der Plicht, H., Greenwood, A.D., Flemming, C. and Agenbroad, L., 2002. Radiocarbon chronologies and extinction dynamics of the Late Quaternary mammalian megafauna of the Taimyr Peninsula, Russian Federation. *Journal of Archaeological Science*, 29(9): 1017-1042.
- Mandryk, C.A.S., 1996. Late-glacial vegetation and environment on the eastern slope foothills of the Rocky Mountains, Alberta, Canada. *Journal of Paleolimnology*, 16(1): 37-57.
- Mariotti, A., 1983. Atmospheric nitrogen is a reliable standard for natural ^{15}N abundance measurements. *Nature*, 303: 685-687.
- Martin, P.S., 1984. Prehistoric overkill: the global model. In: P.S. Martin and R.G. Klein (Editors), *Quaternary extinctions: a prehistoric revolution*. University of Arizona Press, Tucson, pp. 345-403.
- Matheus, P., Beget, J., Mason, O. and Gelvin-Reymiller, C., 2003. Late Pliocene to late Pleistocene environments preserved at the Palisades Site, central Yukon River, Alaska. *Quaternary Research*, 60(1): 33-43.
- Matheus, P., Burns, J., Weinstock, J. and Hofreiter, M., 2004. Pleistocene brown bears in the mid-continent of North America. *Science*, 306(5699): 1150-1150.
- Matthews, J.V., Schweger, C.E. and Janssens, J.A., 1990. The last (Koy-Yukon) interglaciation in the northern Yukon: evidence from Unit 4 at Ch'ijees Bluff, Bluefish Basin. *Geographie Physique et Quaternaire*, 44(3): 341-362.

- McCue, M.D. and Pollock, E.D., 2008. Stable isotopes may provide evidence for starvation in reptiles. *Rapid Communications in Mass Spectrometry*, 22(15): 2307-2314.
- McNeil, P., Hills, L.V., Kooyman, B. and Tolman, S.M., 2005. Mammoth tracks indicate a declining Late Pleistocene population in southwestern Alberta, Canada. *Quaternary Science Reviews*, 24(10-11): 1253-1259.
- Mekota, A.M., Grupe, G., Ufer, S. and Cuntz, U., 2006. Serial analysis of stable nitrogen and carbon isotopes in hair: monitoring starvation and recovery phases of patients suffering from anorexia nervosa. *Rapid Communications in Mass Spectrometry*, 20(10): 1604-1610.
- Menounos, B., Osborn, G., Clague, J.J. and Luckman, B.H., 2009. Latest Pleistocene and Holocene glacier fluctuations in western Canada. *Quaternary Science Reviews*, 28(21-22): 2049-2074.
- Metcalfe, J.Z., Longstaffe, F.J. and Zazula, G.D., 2010. Nursing, weaning, and tooth development in woolly mammoths from Old Crow, Yukon, Canada: Implications for Pleistocene extinctions. *Palaeogeography Palaeoclimatology Palaeoecology*, 298: 257-270.
- Murphy, B.P. and Bowman, D., 2009. The carbon and nitrogen isotope composition of Australian grasses in relation to climate. *Functional Ecology*, 23(6): 1040-1049.
- Petersen, K.L., Mehringer, P.J. and Gustafson, C.E., 1983. Late-Glacial vegetation and climate at the Manis Mastodon Site, Olympic Peninsula, Washington. *Quaternary Research*, 20(2): 215-231.
- Reyes, A.V., Froese, D.G. and Jensen, B.J.L., 2010a. Permafrost response to last interglacial warming: field evidence from non-glaciated Yukon and Alaska. *Quaternary Science Reviews*, 29(23-24): 3256-3274.
- Reyes, A.V., Jensen, B.J.L., Zazula, G.D., Ager, T.A., Kuzmina, S., La Farge, C. and Froese, D.G., 2010b. A late-Middle Pleistocene (Marine Isotope Stage 6) vegetated surface buried by Old Crow tephra at the Palisades, interior Alaska. *Quaternary Science Reviews*, 29(5-6): 801-811.
- Richards, M.P. and Hedges, R.E.M., 2003. Variations in bone collagen $\delta^{13}\text{C}$ and $\delta^{15}\text{N}$ values of fauna from Northwest Europe over the last 40 000 years. *Palaeogeography Palaeoclimatology Palaeoecology*, 193(2): 261-267.
- Roche, D., Segalen, L., Balan, E. and Delattre, S., 2010. Preservation assessment of Miocene-Pliocene tooth enamel from Tugen Hills (Kenyan Rift Valley) through FTIR, chemical and stable-isotope analyses. *Journal of Archaeological Science*, 37(7): 1690-1699.
- Rothschild, B.M. and Laub, R., 2006. Hyperdisease in the late Pleistocene: validation of an early 20th century hypothesis. *Naturwissenschaften*, 93(11): 557-564.
- Rozanski, K., Araguas-Araguas, L. and Gonfiantini, R., 1993. Isotopic patterns in modern global precipitation. In: P.K. Swart, J. McKenzie, K.C. Lohmann and S. Savin (Editors), *Climate Change in Continental Isotope Records*. AGU Geophysical Monograph. American Geophysical Union, Washington, DC, pp. 1-36.
- Saunders, J.J., Grimm, E.C., Widga, C.C., Campbell, G.D., Curry, B.B., Grimley, D.A., Hanson, P.R., McCullum, J.P., Oliver, J.S. and Treworgy, J.D., 2010. Paradigms and proboscideans in the southern Great Lakes region, USA. *Quaternary International*, 217(1-2): 175-187.

- Schweger, C.E. and Matthews Jr, J.V., 1991. The last (Koy-Yukon) interglaciation in the Yukon: Comparisons with Holocene and interstadial pollen records. *Quaternary International*, 10-12: 85-94.
- Shapiro, B., Drummond, A.J., Rambaut, A., Wilson, M.C., Matheus, P.E., Sher, A.V., Pybus, O.G., Gilbert, M.T.P., Barnes, I., Binladen, J., Willerslev, E., Hansen, A.J., Baryshnikov, G.F., Burns, J.A., Davydov, S., Driver, J.C., Froese, D.G., Harington, C.R., Keddie, G., Kosintsev, P., Kunz, M.L., Martin, L.D., Stephenson, R.O., Storer, J., Tedford, R., Zimov, S. and Cooper, A., 2004. Rise and fall of the Beringian steppe bison. *Science*, 306(5701): 1561-1565.
- Shellis, R.P., 1984. Variations in growth of the enamel crown in human teeth and a possible relationship between growth and enamel structure *Archives of Oral Biology*, 29(9): 697-705.
- Sloat, A.R., Lachniet, M.S. and Lawson, D.E., 2010. A surface water Isoscape for Alaska reveals the climate, moisture source, and physiographic controls on $\delta^{18}\text{O}$, δD , and deuterium excess, AGU Fall Meeting, 13-17 December, San Francisco, California.
- Smith, T.M. and Tafforeau, P., 2008. New visions of dental tissue research: Tooth development, chemistry, and structure. *Evolutionary Anthropology*, 17(5): 213-226.
- Stalker, A.M., 1968. Geology of the terraces at Cochrane, Alberta. *Canadian Journal of Earth Sciences*, 5(6): 1455-1466.
- Steffen, M.L. and Harington, C.R., 2010. Giant short-faced bear (*Arctodus simus*) from late Wisconsinan deposits at Cowichan Head, Vancouver Island, British Columbia. *Canadian Journal of Earth Sciences*, 47(8): 1029-1036.
- Stevens, R.E. and Hedges, R.E.M., 2004. Carbon and nitrogen stable isotope analysis of northwest European horse bone and tooth collagen, 40,000 BP-present: Palaeoclimatic interpretations. *Quaternary Science Reviews*, 23(7-8): 977-991.
- Stewart, G.R., Turnbull, M.H., Schmidt, S. and Erskine, P.D., 1995. ^{13}C natural abundance in plant communities along a rainfall gradient: A biological integrator of water availability *Australian Journal of Plant Physiology*, 22(1): 51-55.
- Swap, R.J., Aranibar, J.N., Dowty, P.R., Gilhooly, W.P. and Macko, S.A., 2004. Natural abundance of ^{13}C and ^{15}N in C_3 and C_4 vegetation of southern Africa: patterns and implications. *Global Change Biology*, 10(3): 350-358.
- Szpak, P., Grocke, D.R., Debruyne, R., MacPhee, R.D.E., Guthrie, R.D., Froese, D., Zazula, G.D., Patterson, W.P. and Poinar, H.N., 2010. Regional differences in bone collagen $\delta^{13}\text{C}$ and $\delta^{15}\text{N}$ of Pleistocene mammoths: Implications for paleoecology of the mammoth steppe. *Palaeogeography Palaeoclimatology Palaeoecology*, 286(1-2): 88-96.
- Tieszen, L.L., 1991. Natural variations in the carbon isotope values of plants: Implications for archaeology, ecology, and paleoecology. *Journal of Archaeological Science*, 18: 227-248.
- Turner, K.W., Wolfe, B.B. and Edwards, T.W.D., 2010. Characterizing the role of hydrological processes on lake water balances in the Old Crow Flats, Yukon Territory, Canada, using water isotope tracers. *Journal of Hydrology*, 386(1-4): 103-117.
- Tutken, T., Furrer, H. and Vennemann, T.W., 2007. Stable isotope compositions of mammoth teeth from Niederweningen, Switzerland: Implications for the Late

- Pleistocene climate, environment, and diet. *Quaternary International*, 164-65: 139-150.
- Ukkonen, P., Arppe, L., Houmark-Nielsen, M., Kjaer, K.H. and Karhu, J.A., 2007. MIS 3 mammoth remains from Sweden: implications for faunal history, palaeoclimate and glaciation chronology. *Quaternary Science Reviews*, 26(25-28): 3081-3098.
- van Geel, B., Aptroot, A., Baittinger, C., Birks, H.H., Bull, I.D., Cross, H.B., Evershed, R.P., Gravendeel, B., Kompanje, E.J.O., Kuperus, P., Mol, D., Nierop, K.G.J., Pals, J.P., Tikhonov, A.N., van Reenen, G. and van Tienderen, P.H., 2008. The ecological implications of a Yakutian mammoth's last meal. *Quaternary Research*, 69(3): 361-376.
- van Geel, B., Guthrie, R.D., Altmann, J.G., Broekens, P., Bull, I.D., Gill, F.L., Jansen, B., Nieman, A.M. and Gravendeel, B., 2010. Mycological evidence of coprophagy from the feces of an Alaskan Late Glacial mammoth. *Quaternary Science Reviews*, In Press, Corrected Proof.
- van Klinken, G.J., 1999. Bone collagen quality indicators for paleodietary and radiocarbon measurements. *Journal of Archaeological Science*, 26(687-695).
- Velichko, A.A. and Zelikson, E.M., 2005. Landscape, climate and mammoth food resources in the East European Plain during the Late Paleolithic epoch. *Quaternary International*, 126-28: 137-151.
- Warinner, C. and Tuross, N., 2010. Brief communication: Tissue isotopic enrichment associated with growth depression in a pig: Implications for archaeology and ecology. *American Journal of Physical Anthropology*, 141(3): 486-493.
- Waters, M.R. and Stafford, T.W., 2007. Redefining the age of Clovis: Implications for the peopling of the Americas. *Science*, 315(5815): 1122-1126.
- Wilson, M.C., Kenady, S.M. and Schalk, R.F., 2009. Late Pleistocene *Bison antiquus* from Orcas Island, Washington, and the biogeographic importance of an early postglacial land mammal dispersal corridor from the mainland to Vancouver Island. *Quaternary Research*, 71(1): 49-61.
- Wooller, M.J., Zazula, G.D., Edwards, M., Froese, D.G., Boone, R.D., Parker, C. and Bennett, B., 2007. Stable carbon isotope compositions of Eastern Beringian grasses and sedges: Investigating their potential as paleoenvironmental indicators. *Arctic, Antarctic and Alpine Research*, 39(2): 318-331.
- Young, R.R., Burns, J.A., Smith, D.G., Arnold, L.D. and Rains, R.B., 1994. A single, late Wisconsin, Laurentide Glaciation, Edmonton area and southwestern Alberta. *Geology*, 22(8): 683-686.
- Zazula, G.D., Froese, D.G., Elias, S.A., Kuzmina, S., La Farge, C., Reyes, A.V., Sanborn, P.T., Schweger, C.E., Smith, C.A.S. and Mathewes, R.W., 2006a. Vegetation buried under Dawson tephra (25,300 C-14 years BP) and locally diverse late Pleistocene paleoenvironments of Goldbottom Creek, Yukon, Canada. *Palaeogeography Palaeoclimatology Palaeoecology*, 242(3-4): 253-286.
- Zazula, G.D., Froese, D.G., Elias, S.A., Kuzmina, S. and Mathewes, R.W., 2007. Arctic ground squirrels of the mammoth-steppe: paleoecology of Late Pleistocene middens (similar to 24000-29450 C-14 yr BP), Yukon Territory, Canada. *Quaternary Science Reviews*, 26(7-8): 979-1003.
- Zazula, G.D., Froese, D.G., Schweger, C.E., Mathewes, R.W., Beaudoin, A.B., Telka, A.M., Harington, C.R. and Westgate, J.A., 2003. Ice-age steppe vegetation in east

- Beringia: Tiny plant fossils indicate how this frozen region once sustained huge herds of mammals. *Nature*, 423(6940): 603-603.
- Zazula, G.D., Hare, P.G. and Storer, J.E., 2009. New radiocarbon-dated vertebrate fossils from Herschel Island: Implications for the palaeoenvironments and glacial chronology of the Beaufort Sea coastlines. *Arctic*, 62(3): 273-280.
- Zazula, G.D., Metcalfe, J.Z., Hodgins, G., Southon, J. and Harington, C.R., in prep. Local mastodon extirpation in Beringia predates human colonization and terminal Pleistocene climate change.
- Zazula, G.D., Schweger, C.E., Beaudoin, A.B. and McCourt, G.H., 2006b. Macrofossil and pollen evidence for full-glacial steppe within an ecological mosaic along the Bluefish River, eastern Beringia. *Quaternary International*, 142: 2-19.
- Zazula, G.D., Telka, A.M., Harington, C.R., Schweger, C.E. and Mathewes, R.W., 2006c. New spruce (*Picea* spp.) macrofossils from Yukon Territory: Implications for Late Pleistocene refugia in Eastern Beringia. *Arctic*, 59(4): 391-400.
- Zimov, S.A., Chuprynin, V.I., Oreshko, A.P., Chapin, F.S., Reynolds, J.F. and Chapin, M.C., 1995. Steppe-tundra transition: a herbivore-driven biome shift at the end of the Pleistocene. *American Naturalist*, 146(5): 765-794.

Chapter 8

General Discussion and Conclusions

This thesis explored the isotopic paleoecology of proboscideans (mammoth, *Mammuthus*, and mastodon, *Mammot*) in North America (Arizona, the Great Lakes, and Western Canada) during the Late Pleistocene. Several themes have emerged from this research, including (1) methodological developments and challenges, (2) mammoth and mastodon environmental adaptations and niche partitioning, (3) seasonality of proboscidean drinking water and diet, and (4) use of mammoths and mastodons as paleoclimate proxies. This chapter summarizes the results presented in this thesis, discusses their implications (particularly in relation to proboscidean extinction), and suggests pertinent avenues of future research.

8.1 Methodological Developments and Challenges

8.1.1 Analysis of Structural Carbonate in Bioapatite

The carbon and oxygen isotope compositions of structural carbonate in bioapatite can provide records of diet and drinking water isotope compositions, if reliable measurements can be obtained and significant post-mortem alteration has not occurred. Chapter 2 (Metcalf et al., 2009) demonstrated that when bioapatite is reacted with phosphoric acid at high temperatures (e.g., 90°C) and the reaction products are immediately frozen into a cryogenic trap, a contaminant gas can be transferred into the mass spectrometer, resulting in extremely low and erroneous $\delta^{18}\text{O}$ values. This problem can be prevented by reacting bioapatite under “sealed vessel” conditions (i.e., closing the connection with the cold trap for the duration of the reaction). The sealed vessel reaction has been shown to result in reproducible $\delta^{13}\text{C}$ and $\delta^{18}\text{O}$ measurements not only for bone bioapatite (Chapter 2), but also for enamel (Chapters 3, 5) (Metcalf et al., 2010), and is thus the configuration of choice for structural carbonate analysis.

Pretreatment of skeletal tissues is commonly employed to remove contaminants prior to analysis. However, pretreatment was generally unnecessary for proboscidean enamel, since pretreated and untreated aliquots of the same samples had $\delta^{13}\text{C}$ and $\delta^{18}\text{O}$

values that did not differ significantly from the range typical of analytical error (Chapters 5, 7). In contrast, pretreatment caused much larger changes in the $\delta^{13}\text{C}$ and $\delta^{18}\text{O}$ values of proboscidean bone, dentin, and cementum, and did not bring the values consistently closer to those of enamel (Chapter 7). We concluded that only enamel bioapatite can be reliably used for structural carbonate analysis in the present samples.

8.1.2 Enamel Growth Rate

Estimating the enamel growth rate is important for determining the temporal resolution of serially-sampled isotope results (Chapters 4-7), the degree of isotopic averaging in “bulk” samples, and the timing of formation of different teeth (Chapters 3, 5-7). Indeed, the main weakness of the weaning study (Chapter 3) (Metcalf et al., 2010) is the uncertainty in the timing and duration of formation of individual proboscidean teeth.

This thesis investigated aspects of proboscidean enamel formation using histological and isotopic measurements (Chapters 4-7) and inferences based on modern elephant tooth eruption patterns (Chapter 3). Histological measurements demonstrated that in both mammoths and mastodons, the growth rate through the enamel thickness (i.e., from the inner to outer enamel surface) is much slower than that along the height of the tooth (i.e., extension rate; from the occlusal surface to the cervix) (Chapters 4, 7). This implies that sequential sampling through the enamel thickness can be used to investigate shorter-term (e.g., weekly) variations in $\delta^{13}\text{C}$ and $\delta^{18}\text{O}$ values, whereas sequential sampling along the tooth height (especially on the inner enamel surface) can be used to investigate longer-term (i.e., monthly or yearly) variations. Stable isotope results obtained using these two methods confirm this difference in temporal resolution (Chapter 4). Histological measurements also demonstrated that there is significant variability in growth rates within teeth (e.g., slower near the cervix, particularly in mastodons), and among individuals (Chapters 5-7).

The results presented in this thesis can be used to design sampling strategies for future studies, and to refine interpretations presented in previous studies. For example, Feranec and MacFadden (2000) investigated seasonality in mammoths from Florida by drilling sample lines perpendicular to the tooth height, about 5 mm apart. Some of their specimens had regular periodicity, with a distance of about 10 to 20 mm between peaks or

valleys in the $\delta^{18}\text{O}$ curves. Results in this thesis suggest that mammoth tooth enamel grows at a rate of about 9 to 23 mm per year along the height of the tooth, which suggests that the results of Feranec and MacFadden (2000) do represent seasonal changes in drinking water $\delta^{18}\text{O}$ values. However, their “traditional” sampling strategy (i.e., drilling enamel from the outer enamel surface through much of the enamel thickness) likely resulted in greater signal attenuation than would drilling to very shallow depths, on the inner enamel surface (see Section 1.3).

Further study is needed to understand proboscidean tooth formation processes. Detailed study of proboscidean tusk dentin and molar enamel microstructure have been conducted (Dirks et al., 2010; Ferretti, 2003, 2008; Fisher, 1996; Fisher and Fox, 2006; Fisher et al., 1998), but to our knowledge the rate and geometry of proboscidean enamel maturation and its variability throughout the tooth remain unexplored, unlike the situation for some other species (e.g., Passey and Cerling, 2002; Tafforeau et al., 2007). Such information is crucial for estimating the isotopic compositions of body fluids from incrementally sampled tooth enamel (Passey et al., 2005).

8.1.3 Incremental Sampling of Proboscidean Enamel

To investigate “seasonal” changes in the isotopic compositions of diet and drinking water, this thesis employed serial sampling of the inner enamel surface (IES), along the height of the tooth. In all the study regions, there was a strong correlation between the mean isotope composition of serial samples and bulk analyses from the same individuals (Chapters 5-7). The mean $\delta^{18}\text{O}$ values of serial samples tended to be lower than bulk $\delta^{18}\text{O}$ values, but there was no systematic offset for $\delta^{13}\text{C}$. We suggest that the offset in $\delta^{18}\text{O}$ is a result of the more rapid mineralization rate of inner enamel relative to the rest of the tooth.

The IES isotope results often had regular periodicity, which likely reflect seasonal changes in diet and drinking water. The amplitudes of variation in diet and drinking water isotope compositions presented in this thesis represent minimum variations, since some signal attenuation occurs as a result of the mineralization process and sampling geometry. However, the presence of a rapidly-mineralized inner enamel layer in many species

suggests that the IES sampling strategy should result in less attenuation than traditional methods of sampling the outer enamel surface (penetrating most of the enamel thickness).

A fundamental problem with interpreting serially-sampled isotope results is determining which portions of the curve represent summer or winter growth. Ideally, independent evidence for summer versus winter growth periods would be obtained, such as the growth increment thicknesses that have previously been used for proboscidean tusk dentin (e.g., Fisher and Fox, 2003; Fox et al., 2007; Koch et al., 1989). Further study is needed to determine if this method is applicable to tooth enamel.

8.2 Mammoth and Mastodon Environmental Adaptations and Niche Partitioning

Stable isotope analyses support the contention that mammoths and mastodons occupied different environmental niches, both in the Great Lakes region and Western Canada. Nevertheless, both taxa consumed a wide range of resources and regional differences were evident.

In all study areas, mammoths had higher $\delta^{15}\text{N}$ values than mastodons. The possibility that low $\delta^{15}\text{N}$ values in mastodons was at least partially a result of their direct association with spruce forest environments was presented (Chapters 6-7). The potential relationship between high $\delta^{15}\text{N}$ values in mammoths and coprophagy, suggested by previous researchers (Clementz et al., 2009; van Geel et al., 2010), was discussed in relation to the apparent preference of mammoths for open, dry environments and of mastodons for more forested, wetter environments (Chapter 6-7). However, the possibility remains that this difference could also be related to physiological factors. These competing hypotheses could be explored through isotopic analysis of individual amino acids in mammoth and mastodon collagen, and isotopic study of animals and plants in modern analogue ecosystems.

There were no differences between mammoth and mastodon carbon isotope compositions within regions, with the exception of Old Crow (Chapters 6-7). The similar $\delta^{13}\text{C}$ values likely reflect the consumption of a wide variety of plant taxa by both mammoths and mastodons.

There was no difference between mammoth and mastodon $\delta^{18}\text{O}$ values in Old Crow, Klondike, or Alberta, but mammoths in southern Ontario had lower $\delta^{18}\text{O}$ values

than mastodons. Thus, it appears that in Western Canada either the isotopic compositions of waters were relatively homogeneous, or mammoths and mastodons consumed waters ultimately derived from the same sources. In contrast, mammoths in Ontario had lower $\delta^{18}\text{O}$ values, likely because of their geographic association with the “upland” shoreline of glacial Lake Iroquois, which received greater input from low- ^{18}O glacial meltwater. Mastodons in Ontario had higher $\delta^{18}\text{O}$ values because they inhabited the wetter, lowland Lake Warren plains, which likely received a greater proportion of input from local precipitation than did mammoth environments.

Saunders (2010) suggested that a high degree of environmental niche overlap between mammoths and mastodons in the American Midwest could have increased their susceptibility to regional extinction. This hypothesis can be rejected for southern Ontario, where geographic and isotopic differences are clearly evident for mammoths and mastodons. Although McAndrews and Jackson (1988) found no evidence that mammoths and mastodons in Ontario lived during distinct time periods, additional radiocarbon dates are needed to determine whether the specimens used in this study were contemporaneous. In Western Canada, there was isotopic evidence for dietary differences between mammoths and mastodons, but surprisingly no difference in the isotopic composition of their drinking water. Thus, the question of whether mammoths and mastodons occupied different temporal intervals, or coexisted in different microhabitats, remains unresolved.

Evidence from stable isotopes and trace elements indicated that mammoths in Old Crow delayed the initiation of weaning until 2 to 3 African elephant years (AEY) of age (Chapter 3) (Metcalf et al., 2010). This may have been a defensive adaptation to the increased predation risk and decreased food quality/quantity during the long hours of winter darkness at this high latitude location. Potential consequences of delayed weaning for Old Crow mammoths, such as longer inter-birth intervals, greater maternal energy investments, and decreased self-sufficiency in infants, may have increased the population's vulnerability to climatic stress or human hunting. Although these factors could have contributed to regional extinction, delayed weaning is unlikely to have been a major factor in the extinction of the species, since woolly mammoths living at lower latitudes would not have experienced the same adaptive pressures, and may thus have initiated weaning earlier.

8.3 Seasonality of Proboscidean Drinking Water and Diet

In the San Pedro Valley of Arizona, Clovis-age mammoths had regular, approximately sinusoidal variations in serially-sampled $\delta^{13}\text{C}$ and $\delta^{18}\text{O}$ values (Chapter 5). Based on the positive relationship between the isotope curves, it appears that Clovis mammoths consumed more C_4 plants in summer, probably seeking out C_4 grasslands that “greened up” as a result of summer rainfall. This predictable seasonal behavior may have increased their susceptibility to both human hunting and sudden climate change – in the first case, because they would have been relatively easy to locate, and in the second, because they would have had little previous experience to prepare them for a sudden, drastic change in climate. Study of additional Clovis and pre-Clovis specimens, particularly enamel cones that developed near the time of death, are needed to determine whether this pattern was unique to Clovis mammoths.

Seasonal variations in proboscidean teeth from C_3 -dominated environments in proximity to glacial meltwater sources are more difficult to interpret. Regular seasonal variations were observed for both mammoths and mastodons, but were not consistent among individuals or regions. Glacial meltwater inputs to drinking water have the potential to attenuate, reverse, or otherwise alter the seasonal variations in $\delta^{18}\text{O}$ values typical of meteoric water (i.e., high values in summer and low values in winter). Furthermore, isotopic results alone cannot be used to determine whether carbon isotope variations within individuals living in C_3 environments resulted from seasonal variations in the isotopic compositions or nutritional values of plants, consumption of different plant species or plant parts, or metabolic changes.

Seasonal amplitudes for $\delta^{18}\text{O}$ were larger at lower latitude locations (i.e., the largest ranges were in Ontario, followed by Alberta, and the smallest were in Yukon). The larger amplitudes for Ontario proboscideans, despite their relatively close proximity to major glacial meltwater sources, suggests that seasonal variations were not attenuated by increased meltwater input in summer. This implies that either meltwater input was the major control on seasonal variations in drinking water $\delta^{18}\text{O}$ values, or – in contrast – that it had a minimal effect. The discussion of seasonal variations for Ontario mastodons in Chapter 6 is based on evidence that proboscideans in nearby areas (southern Michigan

and western New York) had $\delta^{18}\text{O}$ patterns typical of seasonal meteoric water variations (Koch et al., 1989), implying minimal seasonal variations in glacial meltwater contributions to drinking water. This does not imply that glacial meltwater did not contribute at all to waters in the Great Lakes region, but rather that seasonal variations in the proportion of glacial meltwater were not the major determinants of seasonal variations in $\delta^{18}\text{O}$. However, direct evidence for the attribution of high versus low $\delta^{18}\text{O}$ values to summer versus winter in the specimens studied in this thesis is currently unavailable (see Section 8.1.3).

Seasonal amplitudes in $\delta^{13}\text{C}$ and $\delta^{18}\text{O}$ values were smaller for mammoths than mastodons, in both Yukon and Alberta (Chapter 7). The possibility that the smaller seasonal amplitudes for mammoths are a result of greater migration among microhabitats (and hence, greater isotopic averaging of plant $\delta^{13}\text{C}$ and drinking water $\delta^{18}\text{O}$ values), is potentially testable using independent migration proxies. For example, Hoppe et al. (1999) used inter-individual variability in bulk $^{87}\text{Sr}/^{86}\text{Sr}$ ratios to infer that Florida mastodons undertook long-distance migrations (from 120 to 700 km), whereas mammoths remained within a smaller geographic region (less than a few hundred km). Migration patterns among regions would likely differ as a result of different habitat availabilities. In Florida, open prairie habitats were confined to the southern and coastal regions, so mammoths remained within these preferred areas rather than venturing further north into the forested habitats frequented by mastodons. In contrast, the vast open steppe environment of Yukon during the Pleistocene would have provided mammoths with a much larger geographic range, in contrast to mastodons who may have been confined to river valleys, at least if they persisted during full glacial periods.

8.4 Mammoths and Mastodons as Paleoenvironmental Proxies

In mixed $\text{C}_3\text{-C}_4$ environments (i.e., Arizona), the higher $\delta^{13}\text{C}$ and $\delta^{18}\text{O}$ values for Clovis than pre-LGM mammoths support the contention that the former lived in a warmer, and probably drier, environment than the latter. However, comparison of isotope results for Clovis-associated and Clovis-age (possibly older) specimens revealed no evidence for severe drought. Rather, summer rainfall remained sufficient to support a large C_4 plant biomass. However, the presence of low $\delta^{18}\text{O}$ values during inferred

summers for the single “Clovis-age” (not Clovis-associated) specimen suggests that summer monsoon intensity may have been greater just prior to the Clovis period. Additional samples are needed to test this hypothesis.

The carbon isotope compositions of proboscideans living in C_3 -dominated environments (Great Lakes, Alberta, Yukon) were remarkably similar: about -21‰ for collagen and -11‰ for structural carbonate (Figure 8.1). Using tissue-diet fractionation factors of about 5‰ for collagen and 14‰ for structural carbonate, the average diet $\delta^{13}C$ values were about -26 or -25‰. This lack of difference among regions supports the contention that proboscideans consumed a wide variety of plant taxa, averaging their carbon isotope compositions. Further, it suggests that proboscidean tissues should be useful in determining climate-related changes in plant $\delta^{13}C$ values, as long as sufficiently large sample sets are obtained and climate-induced changes in $\delta^{13}C$ were widespread across various plant taxa.

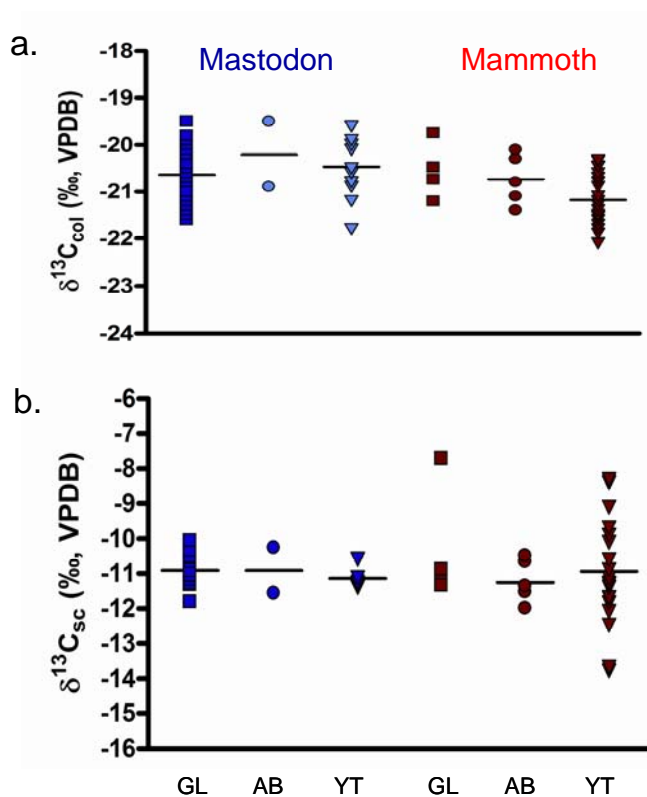


Figure 8.1 Carbon isotope compositions obtained from collagen (a) and structural carbonate (b) for mammoths and mastodons from the Great Lakes (GL), Alberta (AB), and Yukon Territory (YT). Horizontal lines represent means; the GL mammoth mean is not shown because the sample set includes a local outlier (Rostock mammoth).

The mean $\delta^{15}\text{N}$ values of mammoths living in C_3 -dominated environments were similar (about 8‰), but there was a large range of values from each region (Figure 8.2). The mean $\delta^{15}\text{N}$ values of mastodons differed more among regions, with the lowest $\delta^{15}\text{N}$ values in the Great Lakes and the highest in Yukon (Figure 8.2). Notably, the Great Lakes region also had the best evidence for spruce environments, lending support to the hypothesis that low $\delta^{15}\text{N}$ values may be related to associations with spruce trees (Chapters 6-7). Temporal trends in the $\delta^{15}\text{N}$ values of Klondike proboscideans and regional differences in mammoth $\delta^{15}\text{N}$ values within Yukon support the contention that higher $\delta^{15}\text{N}$ values in mammoths are associated with more arid time periods and geographical locations (Chapter 7).

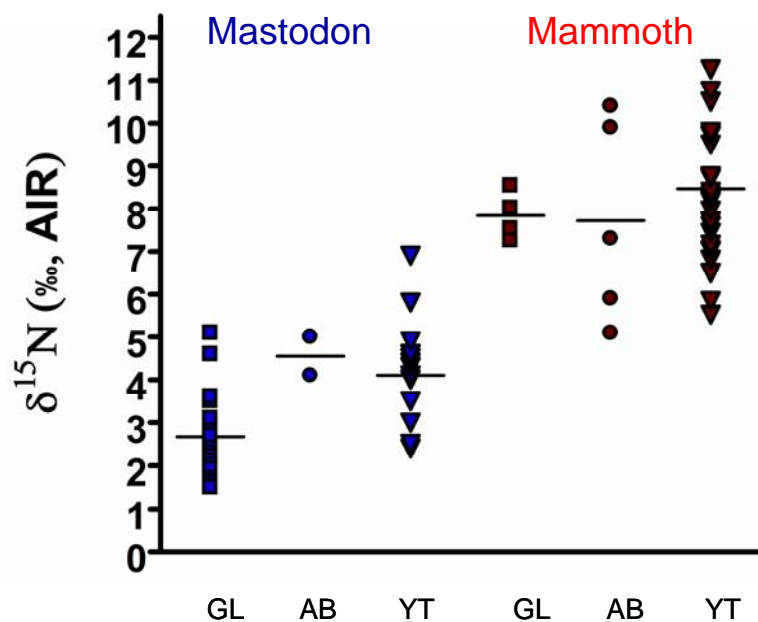


Figure 8.2 Nitrogen isotope compositions obtained from collagen for mammoths and mastodons from the Great Lakes (GL), Alberta (AB), and Yukon Territory (YT). Horizontal lines represent means.

Oxygen isotope compositions of proboscidean tissues varied with latitude. As expected based on the depletion of ^{18}O in meteoric water with latitude, $\delta^{18}\text{O}$ values were highest in the Great Lakes, intermediate in Alberta, and lowest in Yukon (Figure 8.3). In Chapter 7, a correlation between the $\delta^{18}\text{O}$ values of drinking water calculated from Western Canada proboscideans and the $\delta^{18}\text{O}$ values of modern meteoric water in nearby locations was presented. Here, we add the Great Lakes and Arizona data to that analysis (Figure 8.4). The modern meteoric water $\delta^{18}\text{O}$ value for the Great Lakes was obtained from a five-year IAEA record of precipitation for Simcoe, Ontario (IAEA/WMO, 2010). The modern meteoric water $\delta^{18}\text{O}$ value for the San Pedro Valley, Arizona was calculated using the $\delta^{18}\text{O}$ values of summer and winter precipitation/runoff for the San Pedro Valley ($-6.3 \pm 1.0\text{‰}$, $-11.2 \pm 2.8\text{‰}$, respectively) and the average amount of summer and winter precipitation (244 mm and 81 mm, respectively) (Baillie et al., 2007). This calculation excludes the 28 mm of precipitation that falls in other seasons, for which no isotopic data were available.

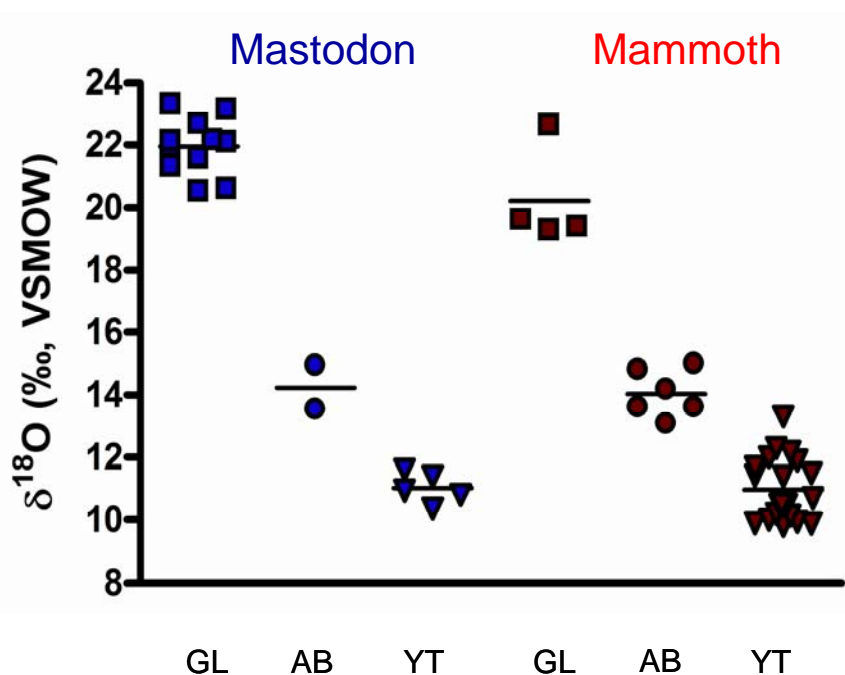


Figure 8.3 Oxygen isotope compositions obtained from enamel structural carbonate for mammoths and mastodons from the Great Lakes (GL), Alberta (AB), and Yukon Territory (YT). Horizontal lines represent means.

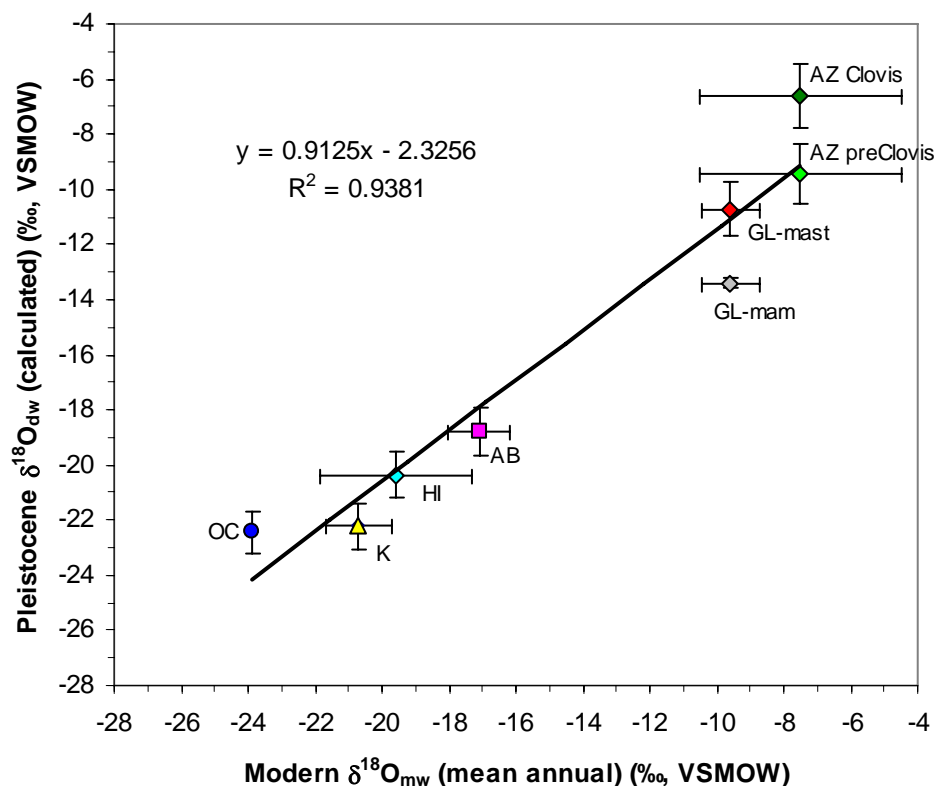


Figure 8.4 Comparison of the oxygen isotope compositions of Pleistocene drinking water (dw) calculated from proboscidean enamel (OC = Old Crow, K = Klondike, HI = Herschel Island, AB = Alberta, GL-mam = Great Lakes mammoths, GL-mast = Great Lakes mastodons, AZ = Arizona) and the weighted mean annual oxygen isotope compositions of precipitation (meteoric water, mw) from “nearby” locations (Old Crow, Mayo, Barrow, Edmonton, Simcoe, and the San Pedro Valley). Error bars represent 1 SD. The trend line and associated regression equation are derived from all of the data points.

There is a statistically significant correlation between Pleistocene and modern water $\delta^{18}\text{O}$ values (Pearson's $r = 0.97$, $df = 6$, $p < 0.001$). The slope of the regression line (0.91) indicates that the gradient in $\delta^{18}\text{O}$ values among regions during the Pleistocene was similar to that which exists today. That is, the degree of ^{18}O -depletion with latitude was similar in the Pleistocene and modern worlds. On a regional scale, mean annual $\delta^{18}\text{O}$ values of precipitation at different locations are correlated with mean annual surface air temperatures (Dansgaard, 1964). Thus, the data imply that temperature differences among the regions studied in this thesis were similar in the Pleistocene and today. However, the $\delta^{18}\text{O}$ values of Pleistocene drinking water tended to be lower than modern meteoric

waters, which might indicate lower temperatures at all the study locations. In theory, lower $\delta^{18}\text{O}$ values but similar latitudinal gradients could result from changes at or near the moisture source location (i.e., at low-latitude tropical locations). Cold periods in the northern hemisphere are associated with southern displacement of the inter-tropical convergence zone (ITCZ, the region where northern and southern air masses meet), which in turn is associated with increased rainfall in Central America (Lachniet et al., 2009). Since both increased rainfall amounts and longer distances travelled by air masses are associated with lower $\delta^{18}\text{O}$ values, these processes could have caused the lower $\delta^{18}\text{O}$ values at all the study locations.

The $\delta^{18}\text{O}$ values for some Pleistocene-modern water pairs deviate from the trend line. Clovis-age mammoths drank waters with higher $\delta^{18}\text{O}$ values than expected, probably because they lived during a warm and dry interval, with increased evaporation, increased precipitation during summer, and/or changes in source moisture locations (Chapter 5). Great Lakes mammoths had lower than expected $\delta^{18}\text{O}$ values, probably because of low- ^{18}O glacial meltwater input to their drinking water (Chapter 6). Great Lakes mastodons, in contrast, plot near the regression line, which supports the contention that they consumed primarily meteoric water (Chapter 6). Finally, Old Crow proboscideans had higher than expected $\delta^{18}\text{O}$ values, which could indicate a generally warmer temporal interval, a greater proportion of precipitation derived from Arctic moisture masses, or enhanced evaporation effects.

8.5 Concluding Remarks

The isotopic compositions of proboscidean skeletal tissues have significant potential for improving our understanding of paleoclimate and paleoecology. This thesis has shown that studying specimens using various techniques (i.e., bulk sampling, incremental sampling, stable isotopes, trace elements) and at various geographical scales (e.g., local, regional, or continental) can provide insights into diverse topics such as habitat preferences, weaning behaviour, seasonality, and climate change. This information not only helps us understand the extremely dynamic climatic fluctuations and ecosystem responses that occurred during the Pleistocene, but may also provide a baseline for understanding modern climatic and ecological changes (Hofreiter and Stewart, 2009).

8.6 References

- Baillie, M.N., Hogan, J.F., Ekwurzel, B., Wahi, A.K. and Eastoe, C.J., 2007. Quantifying water sources to a semiarid riparian ecosystem, San Pedro River, Arizona. *Journal of Geophysical Research: Biogeosciences*, 112(G3): G03S02, doi: 10.1029/2006JG000263
- Clementz, M.T., Fox-Dobbs, K., Wheatley, P.V., Koch, P.L. and Doak, D.F., 2009. Revisiting old bones: coupled carbon isotope analysis of bioapatite and collagen as an ecological and palaeoecological tool. *Geological Journal*, 44(5): 605-620.
- Dansgaard, W., 1964. Stable isotopes in precipitation. *Tellus*, 16: 436-468.
- Dirks, W., Bromage, T.G. and Agenbroad, L., 2010. The timing of molar lamellae formation in *Mammuthus columbi* and *Palaeoloxodon cypriotes* from dental histology, *The World of Mammoths: Vth International Conference on Mammoths and their Relatives*, Le Puy en Velay, France.
- Feranec, R.S. and MacFadden, K.B.J., 2000. Evolution of the grazing niche in Pleistocene mammals from Florida: evidence from stable isotopes. *Palaeogeography Palaeoclimatology Palaeoecology*, 162(1-2): 155-169.
- Ferretti, M.P., 2003. Structure and evolution of mammoth molar enamel. *Acta Palaeontologica Polonica*, 48(3): 383-396.
- Ferretti, M.P., 2008. Enamel structure of *Cuvieronius hyodon* (Proboscidea, Gomphotheriidae) with a discussion on enamel evolution in elephantoids. *Journal of Mammalian Evolution*, 15(1): 37-58.
- Fisher, D.C., 1996. Extinction of proboscideans in North America. In: J. Shoshani and P. Tassy (Editors), *The Proboscidea: Evolution and Palaeoecology of Elephants and Their Relatives*. Oxford University Press, Oxford, pp. 296-315.
- Fisher, D.C. and Fox, D.L., 2003. Season of death and terminal growth histories of Hiscock mastodons. In: R.S. Laub (Editor), *The Hiscock Site: Late Pleistocene and Holocene Paleocology and Archaeology of Western New York State: Proceedings of the Second Smith Symposium, held at the Buffalo Museum of Science, October 14-15, 2001*. Buffalo Society of Natural Sciences, Buffalo, pp. 83-101.
- Fisher, D.C. and Fox, D.L., 2006. Five years in the life of an Aucilla River mastodon. In: S.D. Webb (Editor), *First Floridians and Last Mastodons: The Page-Ladson site in the Aucilla River*. Springer, Netherlands, pp. 343-377.
- Fisher, D.C., Trapani, J., Shoshani, J. and Woodford, M.S., 1998. Schreger angles in mammoth and mastodon tusk dentin. *Current Research in the Pleistocene*, 15: 105-107.
- Fox, D.L., Fisher, D.C., Vartanyan, S., Tikhonov, A.N., Mol, D. and Buigues, B., 2007. Paleoclimatic implications of oxygen isotopic variation in late Pleistocene and Holocene tusks of *Mammuthus primigenius* from northern Eurasia. *Quaternary International*, 169: 154-165.
- Hofreiter, M. and Stewart, J., 2009. Ecological change, range fluctuations and population dynamics during the Pleistocene. *Current Biology*, 19(14): R584-R594.

- Hoppe, K.A., Koch, P.L., Carlson, R.W. and Webb, S.D., 1999. Tracking mammoths and mastodons: Reconstruction of migratory behavior using strontium isotope ratios. *Geology*, 27(5): 439-442.
- IAEA/WMO, 2010. Global Network of Isotopes in Precipitation. The GNIP Database. Accessible at: <http://www.iaea.org/water>.
- Koch, P.L., Fisher, D.C. and Dettman, D., 1989. Oxygen isotope variation in the tusks of extinct proboscideans: a measure of season of death and seasonality. *Geology*, 17: 515-519.
- Lachniet, M.S., Johnson, L., Asmerom, Y., Burns, S.J., Polyak, V., Patterson, W.P., Burt, L. and Azouz, A., 2009. Late Quaternary moisture export across Central America and to Greenland: evidence for tropical rainfall variability from Costa Rican stalagmites. *Quaternary Science Reviews*, 28(27-28): 3348-3360.
- McAndrews, J.H. and Jackson, L.J., 1988. Age and environment of Late Pleistocene mastodont and mammoth in southern Ontario. In: R.S. Laub, N.G. Miller and D.W. Steadman (Editors), *Late Pleistocene and Early Holocene Paleoecology and Archeology of the Eastern Great Lakes Region: Proceedings of the Smith Symposium*. Bulletin of the Buffalo Society of Natural Sciences. Buffalo Society of Natural Sciences, Buffalo, pp. 161-172.
- Metcalfe, J.Z., Longstaffe, F.J. and White, C.D., 2009. Method-dependent variations in stable isotope results for structural carbonate in bone bioapatite. *Journal of Archaeological Science*, 36(1): 110-121.
- Metcalfe, J.Z., Longstaffe, F.J. and Zazula, G.D., 2010. Nursing, weaning, and tooth development in woolly mammoths from Old Crow, Yukon, Canada: Implications for Pleistocene extinctions. *Palaeogeography Palaeoclimatology Palaeoecology*, 298: 257-270.
- Passey, B.H. and Cerling, T.E., 2002. Tooth enamel mineralization in ungulates: Implications for recovering a primary isotopic time-series. *Geochimica et Cosmochimica Acta*, 66(18): 3225-3234.
- Passey, B.H., Cerling, T.E., Schuster, G.T., Robinson, T.F., Roeder, B.L. and Krueger, S.K., 2005. Inverse methods for estimating primary input signals from time-averaged isotope profiles. *Geochimica et Cosmochimica Acta*, 69(16): 4101-4116.
- Saunders, J.J., Grimm, E.C., Widga, C.C., Campbell, G.D., Curry, B.B., Grimley, D.A., Hanson, P.R., McCullum, J.P., Oliver, J.S. and Treworgy, J.D., 2010. Paradigms and proboscideans in the southern Great Lakes region, USA. *Quaternary International*, 217(1-2): 175-187.
- Tafforeau, P., Bentaleb, I., Jaeger, J.J. and Martin, C., 2007. Nature of laminations and mineralization in rhinoceros enamel using histology and X-ray synchrotron microtomography: Potential implications for palaeoenvironmental isotopic studies. *Palaeogeography Palaeoclimatology Palaeoecology*, 246(2-4): 206-227.
- van Geel, B., Guthrie, R.D., Altmann, J.G., Broekens, P., Bull, I.D., Gill, F.L., Jansen, B., Nieman, A.M. and Gravendeel, B., 2010. Mycological evidence of coprophagy from the feces of an Alaskan Late Glacial mammoth. *Quaternary Science Reviews*, In Press, Corrected Proof.

Appendix A
Copyright Release

Chapters 2 and 3 were published in Elsevier journals (Journal of Archaeological Science; Palaeogeography, Palaeoclimatology, Palaeoecology).

The following excerpt is taken from the Elsevier website,
<http://www.elsevier.com/wps/find/authorsview.authors/copyright>
accessed January 17, 2011:

As a journal author, you retain rights for a large number of author uses, including use by your employing institute or company. These rights are retained and permitted without the need to obtain specific permission from Elsevier. These include:

the right to include the journal article, in full or in part, in a thesis or dissertation

Curriculum Vitae
Jessica Zoe Metcalfe

A. Post-Secondary Education

<i>Ph.D. (Geology & Environmental Science)</i>	2006-2011
The University of Western Ontario	
<i>M.A. (Anthropology)</i>	2003-2005
The University of Western Ontario	
<i>B.Sc. (Biological Psychology)</i>	1997-2001
The University of British Columbia	

B. Awards and Scholarships

NSERC Canada Graduate Scholarship – Doctoral, 2007-2010
 ÉGIDE French Embassy in Canada Travel Award, 2010
 Environment & Sustainability Graduate Student Award, UWO, 2010
 Environment & Sustainability Travel Award, UWO, 2010
 Arcangelo Rea Family Foundation Scholarship in Environmental Research, UWO, 2010
 Robert and Ruth Lumsden Graduate Fellowship in Science, UWO, 2007
 Environmental Research Western Entrance Scholarship, UWO, 2006
 Ontario Graduate Scholarship, 2004-2005
 SSHRC Canada Government Scholarship – Master’s, 2003-2004
 Graduate Tuition Scholarship, UWO, 2003-2005
 Outstanding Student Initiative Scholarship, UBC, 1997-2001
 Dean’s Honour List, UBC, 1997-2001
 Charles and Jane Banks Scholarship, UBC, 2001
 Science Scholar Award, UBC, 2000
 BC Provincial Scholarship, 1997-1998
 Passport to Education, BC, 1997-1998

C. Related Work Experience

Research Assistant/Technician

UWO Department of Earth Sciences	2005-2006
UWO Department of Anthropology	2004
UBC Department of Psychology	2001-2002

Teaching Assistant

UWO Department of Earth Sciences	2006-2007
UWO Department of Anthropology	2003-2005

D. Publications

1. Articles in refereed journals

- Metcalf, J.Z.**, Longstaffe, F.J. and Zazula, G.D. (2010). Nursing, weaning, and tooth development in woolly mammoths from Old Crow, Yukon, Canada: Implications for Pleistocene extinctions. *Palaeogeography Palaeoclimatology Palaeoecology* 298: 257-270.
- Metcalf, J. Z.**, White, C. D., Longstaffe, F. J., Wrobel, G., Cook, D. C., & Pyburn, K. A. (2009). Isotopic evidence for diet at Chau Hiix, Belize: Testing regional models of hierarchy and heterarchy. *Latin American Antiquity* 20(1): 15-36.
- Metcalf, J. Z.**, Longstaffe, F. J., & White, C. D. (2009). Method-dependent variations in stable isotope results for structural carbonate in bone bioapatite. *Journal of Archaeological Science* 36: 110-121.
- Metcalf, J. Z.** (2005). Multiple histories: the archaeology, ethnohistory, oral history, and national history of Iximche', Guatemala. *Totem: The UWO Journal of Anthropology* 13.

2. Articles in non-refereed journals

- Metcalf, J. Z.** (2009) Mammoths in the San Pedro Valley, Arizona. *Archaeology Southwest* 23(3):9.

3. Conference Presentations (Oral)

- Metcalf, J.Z.** & Longstaffe, F.J. (September 2010). Paleoenvironmental reconstruction from stable isotope analysis of North American mammoths and mastodons. Paper presented by J. Z. M. at The World of Mammoths: 4th International Conference on Mammoths and their Relatives, Le Puy en Velay, France.
- Metcalf, J.Z.** (April 2008). Nitrogen isotope compositions of mammoth and mastodon skeletal tissues as paleoenvironment proxies. Paper presented by J.Z.M. at the 5th Annual Environmental Research Western Earth Day Colloquium, London, Ontario.
- Metcalf, J.Z.** (April 2007). Mammoth and mastodon extinction in North America. Paper presented by J.Z.M. at the 4th Annual Environmental Research Western Earth Day Colloquium, London, Ontario.
- Metcalf, J.Z.** (February 2007). How low can they go? Anomalous $\delta^{18}\text{O}$ values from bone bioapatite. Paper presented at the Stable-Isotope Biogeochemistry Laboratory / Laboratory for Stable Isotope Science Symposium, Hamilton, Ontario.
- Law, K., Huang, L., Yau, G., Larson, T., Munro, L., Brady, A., **Metcalf, J.**, White, C., & Longstaffe, F. (June 2006). Structural carbonate in bone bioapatite: "You are what you eat and drink" \pm the pretreatment and extraction methods. Paper presented by K.L. at the 12th Canadian Continuous Flow Isotope Ratio Mass Spectrometry Workshop, Victoria, British Columbia.

- Metcalf, J. Z.**, White, C. D., & Longstaffe, F. J. (April 2006). Isotopic Anthropology at Chau Hiix, Belize: Comparisons with Lamanai. Paper presented by J.Z.M. at the Society for American Archaeology 71st Annual Meeting, San Juan, Puerto Rico.
- Metcalf, J. Z.**, White, C. D., & Longstaffe, F. J. (October 2004). Postclassic Maya socio-economic complexity and ideology at Chau Hiix, Belize: A stable isotope study. Paper presented by J.Z.M. at the Annual Meeting of the Canadian Association for Physical Anthropology, London, Ontario.

4. Poster Presentations

- Metcalf, J.Z.** & Longstaffe, F.J. (August 2010). Stable isotope records of seasonality in Clovis and pre-Clovis mammoths from the San Pedro Valley, Arizona. Poster presented by J.Z.M. at the International Council for Archaeozoology 11th International Conference, Paris, France.
- Metcalf, J.Z.** & Longstaffe, F.J. (March 2008). Identification of chemical consolidants and their effects on the stable isotope compositions of skeletal materials. Poster presented by J.Z.M. at the Society for American Archaeology 73rd Annual Meeting, Vancouver, British Columbia. Abstracts of the 73rd Annual Meeting, p. 384.
- Metcalf, J.Z.**, Longstaffe, F.J. & White, C.D. (December 2007). Method-dependent variations in oxygen isotope compositions obtained for structural carbonate in bone bioapatite. Poster presented by J.Z.M. at the AGU Fall Meeting, San Francisco, USA. EOS Transactions AGU 88(52), Fall Meeting Supplement, Abstract B13A-0888.
- Cross, A., Wheeler, S. M., Williams, L. J., Beauchesne, P., Marciano, L. D., & **Metcalf, J. Z.** (October 2004). The UWO mummy project: the students' perspective on multidisciplinary approaches to applied research. Poster presented at the Annual Meeting of the Canadian Association for Physical Anthropology, London, Ontario.
- The UWO Mummy Project Team (30 authors including **Metcalf, J.Z.**) (October 2004). Lady Hudson and mummy studies at UWO. Poster presented at the Annual Meeting of the Canadian Association for Physical Anthropology, London, Ontario.
- Badali, M. A., **Metcalf, J. Z.**, & Craig, K. D. (November 2000). Sex-type: A psychosocial contributor to sex differences in pain? Poster presented at the 19th Annual Scientific Meeting of the American Pain Society, Atlanta, Georgia.

5. Edited Volumes

- Beauschene, P., Colquhoun, I., Cross, A., Gardner, J., Longstaffe, F., Marciano, L., **Metcalf, J.**, Nelson, A., Pawlowski, A., Wheeler, S., White, C. D., & Williams, L. (2008). Lady Hudson and Mummy Studies at the University of Western Ontario. In: Mummies and Science: World Mummies Research. Proceedings of the VI World Congress on Mummy Studies (Teguise, Lanzarote, Spain. Feb 20-24, 2007). P.A. Pena, C.R. Martin, & M.A.R. Rodriguez, Eds.